THE UNIVERSITY OF HULL

Miniaturised Analytical Systems with Chemiluminescence Detection for
Environmental Applications.

being a Thesis submitted for the Degree of

Doctor of Philosophy

in the University of Hull

by

Leanne Marle MChem

University of Hull

March 2006

Declaration

The work described in this thesis was carried out in the Department of Chemistry, University of Hull under the supervision of Dr. G. M. Greenway between October 2002 and August 2005. Except where indicated by references, the work is original and has not been submitted for any other degree.

Leanne Marle

March 2006

Contents

ii

Abstract

This thesis details the use of microfluidic devices and chemiluminescence detection in order to develop a portable method of analysis for measuring chemical species in the environment.

Chapter 1 outlines microfluidic technology, including fabrication techniques, fluid manipulation and mixing within the devices. Their advantages for analytical environmental purposes are demonstrated along with a review of their uses in environmental applications. Chemiluminescence detection provides a sensitive method of analysis for measuring chemical species in the environment and chemiluminescence theory and reagents are addressed.

Chapter 2 details the development of a portable battery operated chemiluminescence detection system, which can be used in conjunction with microfluidic devices. The fabrication of the microfluidic devices used in this work is documented. Different microfluidic channel manifolds were investigated for chemiluminescence reactions and a serpentine design (200 μm width, 65 μm depth) with a channel length of 206 mm was selected as the most suitable design. Methods of fabrication for incorporating immobilised reagents on solid supports within a microfluidic device were also designed.

Chapter 3 documents the investigation of the luminol-cobalt(II) chemiluminescence reaction within a microfluidic device using the portable chemiluminescence detection system to produce a miniaturised analytical system for the determination of hydrogen peroxide in rainwater. Enhancement of the chemiluminescence signal by 132% was achieved by means of using the *mirror reaction* to apply a reflective surface directly

to the top of the microfluidic device. Immobilisation techniques for immobilising luminol using adsorption and covalent attachment onto a solid support were investigated as a means of producing a reagentless system, however poor sensitivity was observed and this was not progressed for the analytical system.

Using the luminol-cobalt(II) chemiluminescence reaction within a microfluidic device a method of measuring hydrogen peroxide in the low micromolar concentrations was achieved, producing a limit of detection of 4.7 nmol L^{-1} with a small sample volume (10 μL min^{-1}). A small reagent consumption size (1.2 mL per hour) and a low waste production size (2.4 mL per hour) were also achieved. This system was then used for the determination of hydrogen peroxide in rainwater samples during rainfall events showing the hydrogen peroxide concentration varied from 0.1 to 3.2 μmol L^{-1}. The method was also applied to the analysis of hydrogen peroxide in snow demonstrating the hydrogen peroxide concentration varied from 0.2 to 0.5 μmol L^{-1} in samples taken at ground level.

Chapter 4 details the development of a heterogeneous (two site) sandwich immunoassay within a microfluidic device to produce a miniaturised analytical system for the determination of *E. coli* bacteria in seawater. There is a need for rapid sensitive methods of analysis to measure *E. coli* in seawater as an indicator of faecal contamination. A review of traditional methods and current research on the area is presented. Immunological techniques based on using antibodies to specifically bind to their respective antigens were found to be the most amenable method of analysis for *E. coli* and an outline of how they work is shown. HRP was selected as the sensitive enzyme label for the antibody in the sandwich immunoassay. The chemiluminescence detection of HRP using the luminol-hydrogen peroxide

chemiluminescence reaction was investigated within a microfluidic device, the detection was optimised and p-iodophenol was selected as an enhancer for the reaction. The investigation into the immobilisation of *E. coli* specific antibodies using covalent attachment onto controlled pore glass is presented, an optimal loading of 1.5 µg g^{-1} was achieved. The development of an ELISA method for the purpose of screening the antibody for their specificity towards different isolates of *E. coli* and their non-specificity towards other bacteria is detailed. Finally, a microfluidic immunoassay was developed. Regeneration of the immobilised antibodies was achieved using 0.5 mol L^{-1} sodium hydroxide, allowing the immobilised antibodies to be reused. The microfluidic immunoassay provided a rapid method for the determination of *E. coli* with an analysis time of 13 min for each sample. The assay also used a low reagent consumption and waste production. This would enable the rapid testing of a number of small samples to provide high temporal and spatial resolution data. Sensitivity provided a problem with the immunoassay and ways to overcome this were addressed.

Acknowledgements

Many thanks must firstly go to my supervisor, Dr Gillian Greenway for all her support and continuous encouragement throughout my research.

I would also like to thank several people for their help during the work, without whom it would not have been possible, these include: Nigel Parkin (Workshop, Department of Chemistry) for construction of the portable chemiluminescence detection system, Dr Ian Bell (Department of Engineering) for work on the automated rainwater sampling system, Dr Tim Paget (Department of Biological Sciences) for general advice on microbiology and immunoassays, Cath Wadforth (Department of Biological Sciences) for showing me general microbiological laboratory procedures, and Dr Howard Snelling (Department of Physics) for the laser ablation work.

I would also like to thank all members of the Analytical Research Group at Hull University, past and present for making my time in the group both enjoyable and memorable, especially in Lab F326. A special mention must go to Ruth and Vicki for keeping me sane during those tough times.

I wish to dedicate this thesis to my family and all those who are special to me, especially the ones who cannot be with me to see the final result.

Abbreviations

APD	Avalanche Photodiode
APTS	3-Aminopropyltriethoxysilane
BSA	Bovine Serum Albumin
CCD	Charged Couple Device
CE	Capillary Electrophoresis
CFU	Colony Forming Units
CPG	Controlled Pore Glass
DMF	Dimethylformamide
DMSO	Dimethyl Sulfoxide
DRIE	Deep Reactive Ion Etching
ECL	Electrogenerated Chemiluminescence
ELISA	Enzyme Linked Immosorbent Assay
EOF	Electroosmotic Flow
FIA	Flow Injection Analysis
FPW	Flexural Plate Wave
GMBS	N-Succinimidyl 4- Maleimidobutyrate
HRP	Horseradish Peroxidase
LED	Light Emitting Diode
LOD	Limit of Detection
MEMS	Microelectromechanical Systems
μTAS	Miniaturised Total Analysis System
MF	Membrane Filter
MTF	Multiple-Tube Fermentation
MTS	(3-Mercaptopropyl) trimethoxysilane
PBS	Phosphate Buffered Saline
PDMS	Polydimethylsiloxane
PMMA	Polymethylmethacrylate
PMT	Photomultiplier Tube
SAMS	Self Assembled Monolayers
SAW	Surface Acoustic Wave
SIA	Sequential Injection Analysis
SPE	Solid Phase Extraction
TMB	(3,3',5,5'tetramethylbenzidine Dihydrochloride)

Chapter 1

Introduction

1.   Introduction

1.0   Aims

The ever-increasing demand for environmental monitoring creates a need for *in-situ* real time measurements. Microfluidic devices provide an advantageous approach to portable methods of analysis. An overview of microfluidic technology, including the concepts of microfluidic devices and background information with specific reference to environmental applications is detailed. Chemiluminescence detection is an ideal method for measuring chemical species in the environment due to its sensitivity and simple instrumental set up. The theory of chemiluminescence is documented to explain this and different chemiluminescence reagents are detailed for different applications.

1.1   Miniaturising Environmental Analysis

Environmental monitoring is used to investigate and gain knowledge of natural processes as well as to implement and regulate existing directives concerning chemical species in the environment. Portable robust accurate methods of analysis are needed to achieve environmental monitoring such that samples can be analysed in the field. This enables results to be available faster, at a low cost and to minimise the risk of contamination due to the elimination of transportation of samples. The information obtained must be of sufficient quantity as well as quality to give high temporal and spatial resolution data on environmental processes and portable systems provide a solution for this. One approach to portable systems for environmental monitoring is the use of chemical sensors, whereby chemical

information is transduced into electrical information. The advantages of this are their rapid analysis and cost effectiveness, however they are limited by their selectivity.[1] The development of automated flow injection analysis (FIA) systems has presented another solution for portable systems in the field.[2] FIA has the advantages of simple instrumentation, high sensitivity and good limits of detection. J. Růžička and E. H. Hansen first introduced FIA in 1975.[3] Their aim was to propose a system which consisted of a continuous flow analyser, where the sample was injected directly into a flowing system without disrupting it, and which was not segmented with air. The FIA instrumental design has lead towards the "total analysis system" (TAS), consisting of the entire analysis within the system. However, this approach to environmental monitoring produces several disadvantages including large sample volumes, high reagent consumption and therefore large waste production because of the high flow rates (mL min^{-1}) used within the system.[4] The use of sequential injection analysis (SIA) is one approach to resolve the disadvantages of FIA, in SIA the sample and reagent zones are sequentially aspirated into a holding coil by valves and reverse flow is used to stack the reagents and samples before detection.[5, 6] Another method to resolve these problems is by means of periodic measurements, but this is dependent on the application and not always a desirable approach. This has led to the miniaturisation of analytical techniques, which has been an area of much interest over the last few years. The "miniaturized total analysis system" (μTAS) concept was first introduced in the 1990's by Manz *et al.*[1] whereby sample pre-treatment, separation and detection is miniaturised into one system. This has led to terms such as "lab on a chip". Miniaturisation of analytical techniques using microfluidic devices provides many advantages for environmental monitoring applications. Their small dimensions allow for portability allowing measurements to

2

be taken in the field. The low flow rates used within the devices (μL min^{-1}) allow for low reagent consumption and small sample volumes, which leads to a reduction in waste production. This is a key issue for portable techniques as low reagent consumption reduces costs to the analysis and limits the amount of chemicals which are taken out into the field. Faster analysis times are achieved using microfluidic devices because of the reduced transport lengths and optimised mass transport for the chemical reaction, this allows for the real time analysis of chemical species in the field. Due to these ideal properties, microfluidic devices have been investigated in order to develop portable methods of analysis for environmental applications.

1.2 Microfluidic Devices

1.2.1 Substrates

Microfluidics is concerned with the control of small volumes of liquid (fL to μL) in microscopic channels. The devices used which contain the micron sized channels are known as microfluidic devices, microreactors or chips. Glass, silicon and quartz are widely used substrates in microfluidic devices,[7] because of their good chemical stability, good optical properties and the ease of fabricating channels within them. Silicon is a good substrate to use when there is a need for high precision small dimensions (<100 nm). Disadvantages of using silicon arise from its electrical conducting and hydrophobic properties, which make it incompatible with electro osmotic flow (EOF) (see section 1.2.3). Even with surface modifications, the EOF voltage range is still limited. Quartz possesses low thermal conductivity and does not absorb in the UV region, which is advantageous with optical detection methods. The disadvantage of quartz is the high temperature (1000 $^{\circ}$C) required for thermally

bonding substrates together (see section 2.2.2). Different glass substrates including sodalime, pyrex and crown have been used in microfluidic device fabrication. They are compatible with electroosmotic flow (EOF) (see section 1.2.3) and glass substrates can be sealed using a lower thermal bonding temperature (around 600 °C).

Polymers and plastic devices have also been widely used substrates in microfluidic devices due to their good optical properties (down to ≈ 300 nm) and good electrical properties.[8] They can sometimes provide a low cost alternative to glass devices (depending on choice of polymer and fabrication technique). These attributes along with the fact they can be disposable are attractive characteristics for environmental monitoring applications.[9] Examples of polymers used include polymethylmethacrylate (PMMA) and polydimethylsiloxane (PDMS). PDMS is a widely used polymer for microfluidics. It is a two part elastomer, consisting of 10 parts base elastomer and 1 part curing agent. EOF can be supported if the surface is oxidised. Disadvantages occur if there is a need to use organic solvents as they can adsorb to the channel and may cause swelling of the polymer.

The dimensions of the channels fabricated into the substrates are wide-ranging and cover a large span from depths (or widths) of ten to hundreds of micrometers. A schematic representation of a basic design for a microchannel with two inlets, called a T-shape (or T-mixer) microfluidic device is given in figure 1.1.
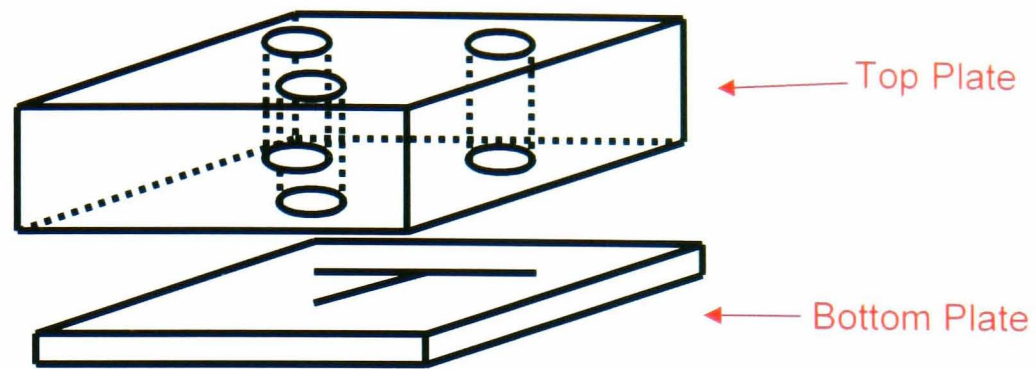
Figure 1.1 Schematic of a T-shape microfluidic device, with microchannels etched into the bottom plate and reservoirs for sample introduction drilled in the top plate.[10]

1.2.2 Device Fabrication

There are a variety of techniques available for fabricating microfluidic devices, each providing different channel characteristics. Considerations when identifying a technique to use include process costs, process time, accuracy and precision of the channels to be fabricated, reliability and reproducibility of the method, the device substrate and design as well as the availability of equipment.

1.2.2.1 Photolithography and Wet Etching

The most popular and earliest method used for silicon and glass device fabrication is photolithography and wet etching.[11, 12] The silicon or glass device is coated with a layer of metal with vapour deposition, followed by spin coating of a photoresist layer. The design of the channels is created in a mask form. The mask is placed above the photoresist layer and is exposed to UV light. This permits the photoresist to be removed from the exposed areas allowing the channel design to be transferred to the microfluidic device. The metal layer is then removed using a metal etchant and finally the channels are isotropically etched into the device using an appropriate etching solution. This is discussed in detail in section 2.2.1.

1.2.2.2 Dry Etching of Silicon

Dry etching processes utilising directed ions from a low pressure plasma (or ion) beam under high vacuum allow for the anisotropic removal of substrate. The advantage of this technique is there are fewer geometrical limitations with reference to the microchannels. Deep reactive ion etching (DRIE) can also be used, which produces deep structures with high aspect ratios.[13, 14]

1.2.2.3 LIGA

LIGA (German acronym Lithographie Galvanoformung Abformung) is based on a three step sequence combining lithography, electroforming and moulding for fabrication of microstructures within plastics.[15] The lithographic step utilises a thick photoresist layer exposed to a high-energy electron or ion beam (including UV and X-rays) to generate the microstructures. This is followed by electroforming of a complementary metal structure generated from the resist layer, which is used as a mould insert or embossing tool for injection moulding or embossing. This allows for the mass production of plastic devices.

Other Fabrication Techniques

Hot embossing incorporates a polymer heated to above its glass transition temperature under vacuum amalgamated to a master channel design template. The polymer is cooled and separated from the master producing imprinted microchannels in the polymer substrate.[16-18] Injection moulding is dependent on mould inserts generated from the LIGA process and other techniques including microerosion and precision engineering.

Other techniques for fabricating channels into substrates include surface cutting with diamond tools, milling, drilling and turning techniques and laser micromaching.[7, 19]

1.2.3 Fluid Manipulation

Fluid movement in a micro reactor requires low flow rates and minimal pulsation. Fluid manipulation is mainly achieved either by pressure driven flow or electroosmotic flow (EOF).[4, 11]

Pressure driven flow can be used for both aqueous and non-aqueous liquids. The flow is dependent on the viscosity of the fluid and the geometry of the channel and is predominantly laminar with a parabolic flow profile (figure 1.2). Conventional syringe or piston pumps can be utilised off chip to achieve pressure driven flow within the device by direct connection to the microfluidic device. Syringe pumps are selected over traditional peristaltic pumps used for flow injection analysis (FIA) due to the low flow rates required within the microfluidic devices.

EOF is the bulk flow of a solution produced as a result of an electric field on counter ions adjacent to the negatively charged channel wall. At pH >4 the silanol groups at the surface of the channel are deprotonated producing a negative charge, positive counter ions accumulate in the solution adjacent to the channel wall. When an electric field is applied, this layer of positive charge migrates towards the negative electrode, resulting in a bulk flow of the solution towards the negative electrode (figure 1.3).[20] This produces a flow profile, which is characteristically flat (figure 1.2). EOF has the advantages that it is pulse free, there is no backpressure as there is with mechanical pumps and it is amenable to miniaturisation. Disadvantages of using

7

EOF for environmental monitoring arise due to the need to maintain a stable high

voltage gradient over a long period of time.[21]

a)   b)

Profile for pressure driven   Profile for electroosmotic flow
flow (parabolic)   (flat)
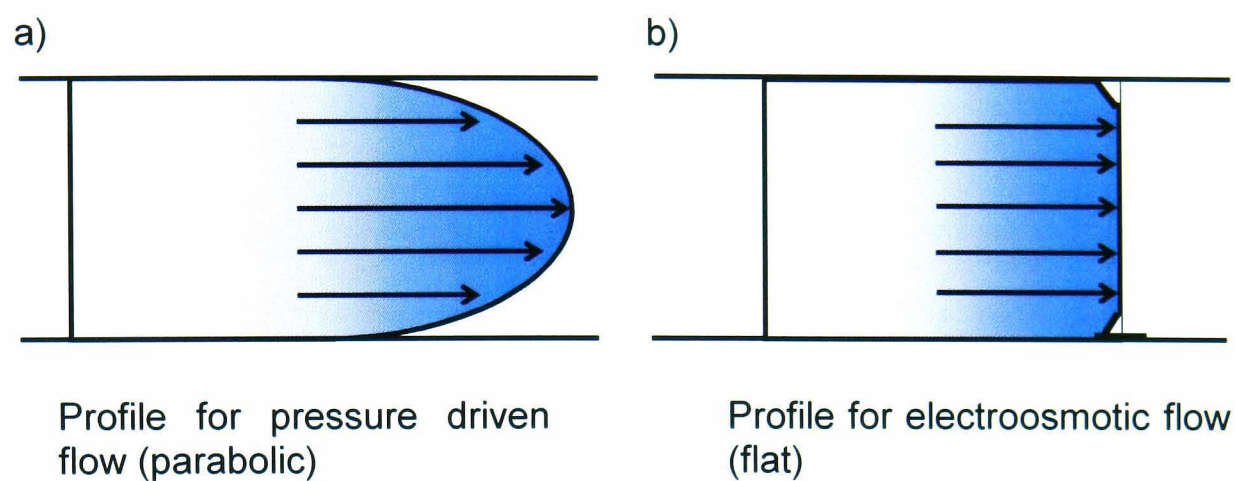
Figure 1.2 Flow profiles for a) pressure driven flow and b) electroosmotic flow (EOF).[10]

Bulk flow towards cathode

Positive counterions

Negatively
charged
channel wall
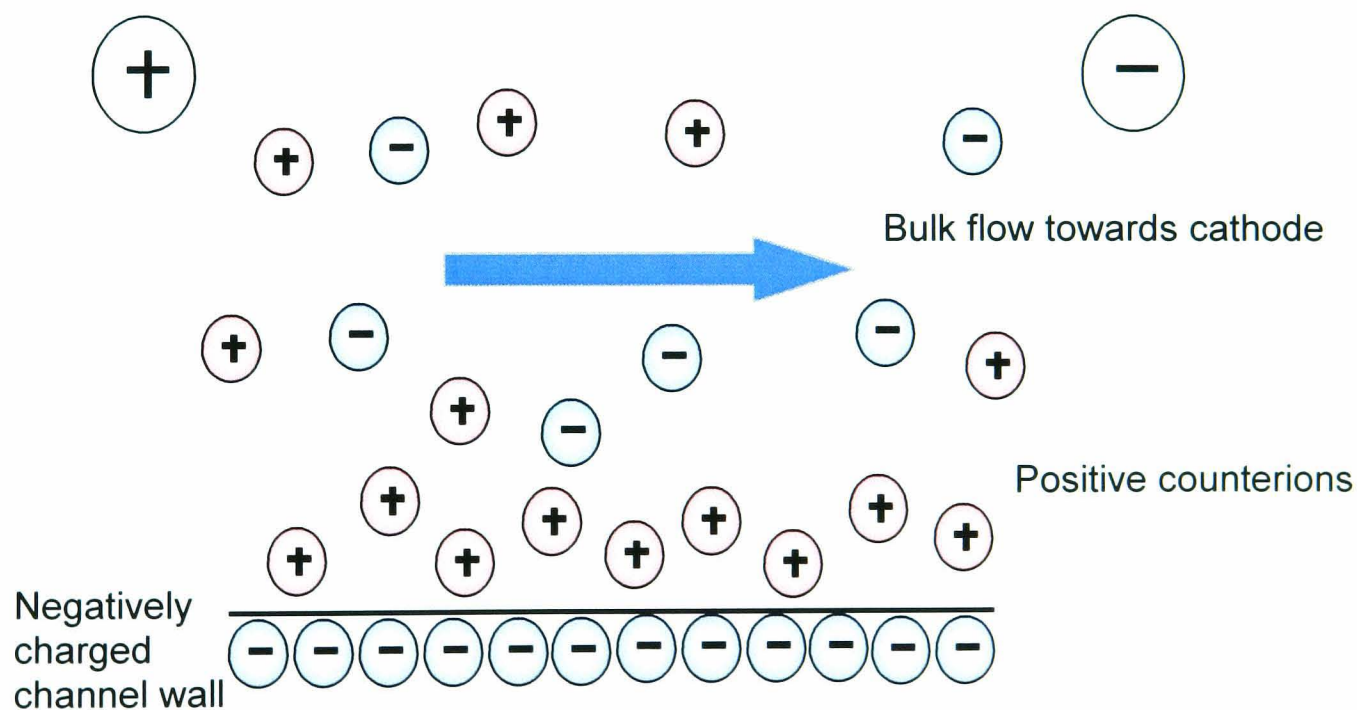
Figure 1.3 Schematic representation of electroosmotic flow (EOF), the bulk flow of a solution produced as a result of an electric field on counter ions adjacent to the negatively charged channel wall .[10]

When using electroosmotic pumping techniques the sample and reagents can be introduced into the channels by using open reservoirs as storage units. One way to achieve this is by using thick glass plates containing predrilled holes as the reservoirs (figure 1.1).[22] A disadvantage to this approach is the fact that if the liquids in the open reservoirs are not at the same level, the pressure difference will result in hydrodynamic flow, greatly affecting the electroosmotic flow causing irreproducibility. Christensen *et al.* overcame this problem by incorporating silica frits into the bottom of the reservoir.[23] Another problem with using the open reservoir approach is the positioning of the electrodes, which may become irreproducible.

Micropumps

To achieve a truly micro total analysis system several groups have developed micropumps such that flow can be accomplished from within the device.[21]

There are two types of micropumps: displacement pumps and dynamic pumps. Displacement pumps produce flow by exerting pressure on the fluid through moving boundaries. The majority of documented micropumps are reciprocating displacement pumps, consisting of a deformable plate (pump diaphragm), usually made of silicon, glass or plastic, as the moving surface that applies force. The device is made up of a pump chamber (one or more chambers can be utilised), with the pump diaphragm on one side, a driver (actuator mechanism) and two check valves (inlet and outlet). When in operation the driver controls the pump diaphragm to increase and decrease the volume in the pump chamber, forcing the fluid into and out of the chamber according to the check valves and thus generates flow. Drivers used for this include piezoelectric,[24-27] thermopneumatic,[28, 29] electrostatic,[25] and pneumatic.[30] Other

9

periodic displacement pumps detailed include rotary displacement pumps (micro gear pumps).[31] Aperiodic displacement pumps have also been documented.[32]

Dynamic micropumps generate flow by adding energy to the fluid in order to increase its momentum or its pressure. EOF is an example of dynamic pumping. The most common type of dynamic pump is a centrifugal pump, however effective miniaturised centrifugal pumps have not been achieved due to limitations of the technology.[21] Other types of dynamic pumping systems include magnetohydrodynamic pumps, based on the application of a magnetic field on current carrying ions in aqueous solutions to produce a Lorentz force on the flow to induce flow.[33-35]

Micropumps provide a miniaturised technique for fluid manipulation on chip, which is advantageous for microfluidic devices to be used in the field as it makes them portable. However, the limitations arise due to their robustness and reproducibility of low flow rates due to small moving parts. For an environmental application where the device is to be used in the field robustness of the pump is a key issue.

1.2.4 Sample Introduction

For flow injection analysis, samples are introduced into the system by means of injection, whereby a reproducible sample is injected into the flowing carrier stream without causing disturbance. There are two ways to inject a sample into the manifold (i) timed (or gated) injection and (ii) introducing a discreet volume.[4] The time-based method consists of the sample being introduced over a set period of time. This has the advantage that the sample volume can be controlled easily. However, irreproducible volumes may be a problem because of uncontrolled dispersion, unless

a constant flow rate is observed. A discreet volume can be introduced using a sample loop, usually incorporated into the flowing stream by a rotary or slide valve. This method of sample introduction provides a reproducible and precise injection volume, independent of flow rate. To vary the volume size the geometrical dimensions of the sample loop must be changed. It is these principles of sample introduction from traditional methods that have been applied to introducing samples into the channels of microfluidic devices.

Micro total analysis systems create a need for reproducible and representative small sample volumes. The problem with using conventional FIA rotary valves is the sample volume is too large for microfluidic devices (μl volumes). Alternative methods of sample introduction are therefore needed for microfluidic devices.[10, 36]

Electrokinetic injection within a microfluidic device can be utilised when using electrokinetic pumping techniques.[37] Time-based injection can easily be achieved by using EOF to pump the sample for a specific amount of time. Discreet volume based injection can be attained by designing the channel manifold in order to fill a channel with a defined volume that can be incorporated into the flow. Two injection geometries have been utilised, the x and z type junctions (figure 1.4). The sample injected can either be "floating" or "pinched" depending on the electrical field applied. "Floating" based injection has the advantages of using only two electrodes, allowing simple manipulation of the fluid, whilst "pinched" based injection requires more electrodes it has the advantage of allowing more control over sample volume and is less affected by diffusion.[4, 10, 38, 39]
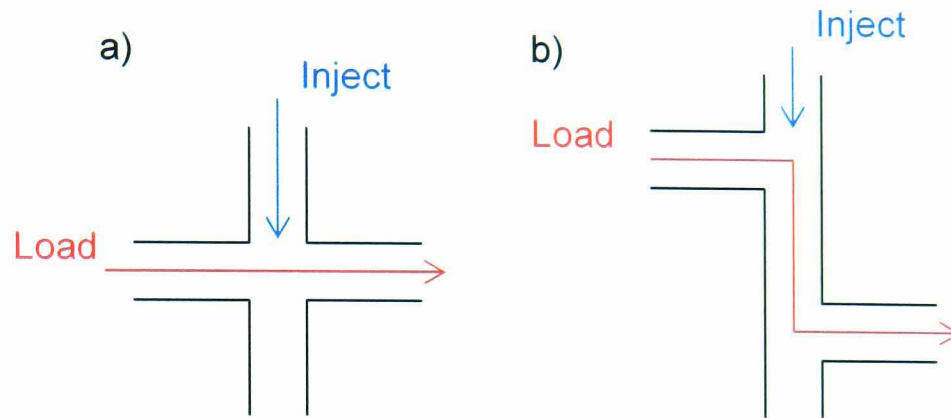
Figure 1.4 Channel manifolds for electrokinetic injection of the sample into a microfluidic device, where a) is an x type and b) is a z type geometry.[10]

A drawback to electrokinetic injection is electrokinetic sample biasing.[40] To overcome this problem hydrodynamic injection has been investigated. Baldock *et al.* demonstrated hydrodynamic flow for sample introduction using a wide bore sample channel connected to narrower separation channel *via* a short connection channel at 45°.[40] Lee *et al.* detailed a pressure injection technique utilising an air vent channel and passive valve system for introducing a sample into a microfluidic device.[41] O'Neill *et al.* demonstrated an on-chip pressure driven picolitre injection method. The sample was controlled on-chip using off chip valves to produce a sample plug, similar to that formed using electrokinetic injection. This method allows easy control over the sample length and volume.[42] Solignac *et al.* used hydrodynamic injection into a microfluidic device by using a pressure pulse.[43]

Gai *et al.* combined hydrostatic pressure and electrokinetic forces as a method for sample introduction. The liquid levels in different reservoirs were changed to generate the hydrostatic pressure without the need for additional pumping.[44] Backofen *et al.* utilised hydrodynamic injection with electrokinetic forces, the technique worked by switching off both high-voltage power supplies for a set

amount of time allowing the injector region to fill due to the hydrodynamic flow of the sample because of the higher electrolyte solution level in the sample reservoir.[45]

Micro rotary valves have also been used with microfluidic devices, Bai *et al.* used pressure driven flow with a two-way micro-8-port valve connected to a microchannel network.[46]

Optical gating sample introduction has been demonstrated as a method of sample introduction for microfluidic devices.[47-52] The technique utilises fluorescently labelled samples, which are continuously introduced into the microfluidic channel. A split laser beam is used and focused onto two points of the channel. One beam (gating beam) has a high power and is used to photobleach the fluorescent labels as they pass through the channel. Sample introduction is achieved by time discrimination of the photobleaching by blocking the gating beam for a set period of time creating a plug of non-photobleached sample, which can be detected by laser-induced fluorescence using the lower powered second beam (probe beam). This method provides a fast, reproducible small volume injection. The disadvantage is this technique is limited to fluorescence applications.

The need for very small and reproducible samples poses a challenge for sample introduction for microfluidic devices. Although progress has been made utilising both electrokinetic and hydrodynamic techniques, long term robustness and reproducibility present a problem for environmental applications.

1.2.5 Separation

Environmental samples comprise of a complicated matrix containing a mixture of chemical species. For multianalyte analysis some form of separation on chip is

13

required. The most popular method of separation on chip utilises electrokinetic methods such as zone electrophoresis and isotachophoresis.[53-56] The techniques utilise the migration of ions in an electric field and achieve separation due to the different mobilities of the ions. In zone electrophoresis the separation takes place in a continuous electrolyte, whereas isotachophoresis uses a discontinuous electrolyte system consisting of a leading and terminating electrolyte, creating zones in which the analyte separates. Chromatographic separation has also been demonstrated on chip utilising different supports for the separation such as porous polymer monoliths, sol-gels, packed beads with stationary phase coating and direct coating of the channels with the stationary phase.[7, 19, 57-59] Solid supports used within microfluidic devices are discussed in detail in section 2.3.2.

1.2.6 Mixing

Rapid mixing of the sample and reagents is essential for analytical purposes. The small channel size within a microfluidic device means that the flow of the liquid within this is predominantly laminar due to the dominant viscous forces. The dimensionless parameter, the Reynolds number (R_e) gives the ratio of viscous and inertial forces and is used to determine whether flow of the fluid is laminar or turbulent (equation 1.1).[60] At low Reynolds numbers (< 2000) laminar flow occurs, where fluid motion is smooth and constant. At high Reynolds numbers (> 2000), inertial forces are dominant generating eddies and turbulent flow.

$$R_e = D_e v \rho / \mu$$
(Equation 1.1)

Where D_e is the channel diameter (m), v is the velocity (m s^{-1}), ρ is the density of the fluid (kg m^{-3}) and μ is the viscosity of the fluid (Ns m^{-2}).

From equation 1.1, we can see that for microchannels (diameter < 500 μm) a low Reynolds number is obtained, e.g. for water (ρ = 1000 kg m^{-3} and μ = 0.001 Ns m^{-2}) flowing through a 100 μm channel at a velocity of 1 cm s^{-1} $R_e \approx$ 1. The dominant laminar flow means that mixing of the reagents within the microchannels is diffusion limited and mixing will occur at the interface of reagent and sample streams. Diffusion is the process whereby the molecules move from high-density regions to low-density regions thus dispersing. According to Fick's first law, the rate of diffusion (dn/dt) of a solute across an area, A, i.e. the amount of solute crossing area A in time t, is given by equation 1.2, where $\sigma c/\sigma x$ is the concentration gradient of the solute and D is the diffusion coefficient (cm^2 s^{-1}). [61]

$$dn/dt = -DA(\sigma c/\sigma x) \qquad \text{(Equation 1.2)}$$

From this the Einstein-Smoluchowski equation is derived (equation 1.3), where x is the distance travelled by the diffusing molecule (cm) in time t (s).[61]

$$X = \sqrt{2Dt} \qquad \text{(Equation 1.3)}$$

The diffusion times for a small molecule (D = 1 x 10^{-9} m^2 s^{-1}) over varying distances calculated using the Einstein-Smoluchowski equation (equation 1.3) are shown in table 1.1. The residence times for a fluid within a microchannel 150 μm wide x 50 μm deep x 20 mm long at various flow rates are given in table 1.2.

Table 1.1 Difussion times for a small molecule (D = 1 x 10⁻⁹ m² s⁻¹) over different distances.

Distance	Time to Diffuse
1 cm	13.9 h
1 mm	8 min
100 μm	5 s
10 μm	0.05 s
1 μm	0.5 ms

Table 1.2 Residence time for a fluid within a microchannel (150 μm x 50 μm x 20 mm) at different flow rates. Residence time calculated using: channel length (m) length/flow rate (m s⁻¹).

Volume Flow Rate (μL min⁻¹)	Velocity (m s⁻¹)	Residence Time (s)
1	0.002	9
2	0.004	4.5
5	0.01	1.8
10	0.02	0.9
15	0.03	0.6
20	0.04	0.5
25	0.06	0.4

From the calculated values in table 1.1 and 1.2 it can be seen that at high flow rates over short channel lengths there is not sufficient time for full difussional mixing to take place. To ensure complete mixing within the microchannels different mixing techniques are required.

1.2.6.1 Micromixers

To increase the mixing of reagents within microchannels a number of groups have utilised micromixers integrated within a microfluidic device. There are two types of micromixers, passive and active micromixers.[62]

Passive Mixers

For passive mixers there is no need for external energy, mixing is based on manipulating the laminar flow such that the surface contact between the fluids is increased and the diffusion path between them is decreased, improving molecular diffusion or by creating chaotic advection. Several groups have documented parallel lamination as a method of passive mixing. The device is designed such that multiple substreams of the fluids are created in parallel, therefore increasing the contact surface and improving mixing.[63-67] Hinsmann *et al.* utilised the lamination of two liquid sheets on top of one another producing complete mixing within 100 ms.[63] Bessoth *et al.* designed a 32 stream parallel mixing device with complete mixing within 15 ms.[65]

Hydrodynamic focusing is another example of parallel lamination.[68-70] The microfluidic device is designed with three inlets, with the sample as the middle flow and the two outer flows working as the sheath flows, which decrease the sample stream width, reducing the diffusional path and improves mixing. Knight *et al.* detailed a hydrodynamic focusing mixing device, which could achieve mixing in less than 10 µs.[69] Serial lamination is another type of passive micromixer and works by splitting and rejoining the flow streams.[66] Gray *et al.* used this technique to design a multilevel laminating device.[71] Similarly, Munsen *et al.* used a geometry, which

splits the fluid in the vertical plane and reunites it with another layer in the horizontal plane.[72] Multiple intersecting channels between meandering (serpentine) channels has also been used to achieve serial lamination. He *et al.* used intersecting channels of varying lengths at 45° angles,[73] whilst Melin *et al.* used intersecting channels at 90° to the meandering channels.[74] An injection mixer has also been documented as a passive mixer and work by splitting only one of the streams of fluid into substreams and reintroduces them into the bulk flow for mixing.[21] Droplet micromixers have also been documented to improve mixing.[75-77]

Advection (transport of something from one region to another) of the fluid within a microfluidic device is normally parallel to the flow direction. Using certain geometries, such that the fluid stream undergoes folding, stretching, splitting and breaking, chaotic advection can be produced to improve mixing. Several groups have used three-dimensional serpentines as a technique to create chaotic advection.[78-84] Lin *et al.* inserted obstacles into the channel as a means of creating chaotic advection.[85, 86] Another method to create chaotic advection is to apply grooves to the bottom of the channel.[87-89]

Active mixers

Active mixers use external force disturbance effects to cause mixing. Examples include pressure field disturbance, electrohydrodynamic disturbance, dielectrophoretic disturbance, magnetohydrodynamic disturbance and acoustic disturbance. Pressure field disturbance can be achieved by several methods including disrupting the flow (stopping) causing serial segmentation,[90] generating pulses,[91] or integrating magnetic stirrers.[92] Electrohydrodynamic disturbance is produced using electrodes to change the voltage and frequency.[93] Electrodes can also be used for

18

dielectrophoretic disturbance, whereby polarised particles are produced and moved between the electrodes.[21] EOF has also been applied to a pressure driven flow system to disturb the flow and improve mixing.[94, 95] Magnetohydrodynamic disturbance has been demonstrated, which uses dc voltages in the presence of an external magnetic field to generate Lorenz forces to improve mixing, a disadvantage of this technique is that it can only be used for an electrolyte solution.[96] Acoustic disturbance has also been presented as a technique to improve mixing using acoustic actuatators to generate vibrations.[97-101] Temperature affects the diffusion coefficient and as such thermal energy can be used to improve mixing as demonstrated by Mao *et al.* who used a linear temperature gradient across the channels.[102]

Several techniques have been demonstrated in order to improve mixing within microfluidic devices. Passive mixing is more amenable to environmental applications due to portability issues that active mixers may present by needing extra instrumentation as well as robustness and reproducibility of the active mixing method. However, certain passive mixing manifolds require complex device fabrication. For environmental applications the fabrication method should be as simple as possible to keep costs down and for long term mass production of the device.

1.2.7 Detection

Microfluidic devices have been used for a variety of analytical applications.[19, 59] Specific applications include bioanalysis,[103] pharmaceutical analysis,[104] clinical applications,[105-109] and forensic applications.[108] Microfluidic devices have also been used in the area of organic synthesis.[110-112] Electrochemical detection and spectrophotometric detection have been the main methods of detection used with

microfluidic devices.[113] These shall be discussed with specific reference to environmental applications.

1.2.7.1 Electrochemical Methods of Detection

The implementation of simple electrodes to measure a chemical signal is amenable to a miniaturised system. It provides a simple, low powered, cost effective method of detection, which is easily incorporated within a microfluidic device whilst maintaining sensitivity.[114, 115]

Amperometry

Amperometry produces good limits of detection (LODs) and is therefore ideal for µTAS for environmental monitoring, however it is limited to analytes, which are electroactive. For nonelectroactive analytes indirect amperometry can be achieved by using an electroactive compound in the background buffer.[116] Wang *et al.* integrated capillary electrophoresis with direct amperometric detection within a glass microfluidic device for the separation and detection of organic peroxides in water, including mixtures of hydrogen peroxide, peroxyheptanoic acid, peroxypropanoic acid, peroxyacetic acid and oxygen.[117] By adapting this method to utilise micellar electrokinetic chromatography (MEKC) it was applied to the analysis of cumene hydroperoxide and tert-butyl peroxide. LODs in the micromolar range were achieved. Wang *et al.* also produced a CE chip with a thick-film electrode for direct amperometric detection for the separation and detection of toxic hydrazine compounds, including hydrazine, methylhydrazine, dimethylhydrazine, and phenylhydrazine achieving an LOD of 1.5 µmol L^{-1} for toxic hydrazine compounds.[118] The system was also used for separating and detecting seven priority

toxic chlorophenolic pollutants in river water. LODs in the range 1 - 2 μmol L^{-1} were achieved using this method.[119] In addition, this system was adapted to separate and detect toxic organophosphate nerve agent compounds, including paraoxon, methyl parathion, fenitrothion, and ethyl parathion in river water samples and achieved LODs in the micromolar range.[120] Wang *et al.* also used this set up to analyse nonelectroactive analytes. Eight amino acids were detected utilizing precolumn derivatization with σ-phthaldialdehyde/2- mercaptoethanol to generate electroactive species, which could be detected.[121]

Hilmi *et al.* demonstrated a CE chip with direct amperometric detection for five nitroaromatic explosives including trinitrotoluene (TNT) in ground water and soil extracts. The microfluidic device achieved rapid separation and detection of explosive compounds with LODs of 0.4-0.9 μmol L^{-1}.[122, 123] There are limited applications for the use of microfluidic devices for the analysis of soil matrices. This is inherently due to the complexity of sampling and sample pre-treatment required of the matrix.

Voltammetry

Voltammetric micro sensors for trace–metal analysis in ground waters has been documented by Guenat *et al.* Thin film technology was used to fabricate an array of Iridium microdisc electrodes producing a micro system with LODs up to 1 mmol L^{-1} for trace-metals.[124] Guenat *et al.* also describe a coulometric nanotitrator as a micro total analysis system. This system was applied to the argentometric titrations of chloride and thiosulfate, the redox titration of iron(II) and to acid base titrations,

detecting nanomolar concentrations of analytes. Continuous-flow coulometric titrations were also presented.[124]

Conductivity

Prest *et al.* utilized isotachophoresis within a PMMA microfluidic device for the simultaneous determination of two inorganic selenium species, separation of selenium(IV) and selenium(VI) was achieved with conductivity detection to produce LODs of 6.6 μmol L^{-1} and 8.2 μmol L^{-1} respectively.[54] Prest *et al.* also demonstrated this approach to the analysis of inorganic arsenic species. LODs of 24 μmol L^{-1} and 64 μmol L^{-1} were achieved for arsenic(V) and arsenic(III) respectively.[55]

Tanyanyiwa *et al.* presented a device with contactless conductometric detection, utilising external electrodes independent from the electrophoretic separation part of the device.[8] The advantage of this technique is that construction of the device is simplified, electrode fouling is avoided and high sensitivity was observed when applied to the chip. The device was used for the multianalyte analysis of small inorganic ions including rubidium, potassium, sodium and lithium, producing LODs of around 1.5 μmol L^{-1}. This approach was also used for the analysis of iron(III), cadmium(II) and cobalt(II) with LODs of 3.5, 8 and 2 μmol L^{-1} respectively being achieved as well as for the species chloride, nitrate, and perchlorate, giving LODs of 2.5, 3 and 2.5 μmol L^{-1} respectively. The versatility of the device was also demonstrated by its application to the analysis of organic anions, specifically the carboxylates: oxalate, tartrate, succinate, acetate and lactate, the LODs were determined to be 4.4, 7, 10, 25 and 30 μmol L^{-1} respectively. The separation and detection of amino acids was also demonstrated for tryptophan, phenylalanine,

theonine and tyrosine, producing LODs of 50, 43, 45 and 32 μmol L^{-1} respectively. Pumera *et al.* have also demonstrated the use of contactless conductivity detection for a PMMA microchip capillary electrophoresis device.[117] Separation of potassium, sodium, barium and lithium cations and chloride, sulfate, fluoride, acetate and phosphate anions was achieved producing LODs of 2.8 μmol L^{-1} for potassium and 6.4 μmol L^{-1} for chloride. Contactless conductivity detection has also been used by Lichtenberg *et al.* for a glass microchip capillary electrophoresis device.[125] Potassium, sodium and lithium cations were separated using the device producing an LOD of 18 μmol L^{-1} for potassium. To improve this limit of detection field amplified sample stacking (FASS) is suggested as a sample preconcentration method to make the limit of detection comparable with other contact conductivity detection methods previously reported. The differences in limits of detection are attributed to the difference in geometrical parameters of the electrodes used in the device manifold.

Sample introduction for atmospheric samples into a microfluidic device is a complex process and different groups have addressed this in a variety of ways. Becker *et al.* used thin and thick film tin oxide gas sensing elements embedded into micro reaction chambers (270 μl) to produce a microanalysis system.[126, 127] They demonstrate an approach of using tin oxide systems to produce analytical signals for individual species. The analysis is based on the thin and thick films giving different responses to oxidising and reducing agents present in the gas mixtures. CO, NO_2, NO, O_3 and CH_4 were measured meeting the sensitivity requirements that would be shown in environmental samples. This provides an approach for continuous air monitoring.

Timmer *et al.* used a gas permeable membrane for gas sampling in a glass microfluidic device in order to analyse ammonia in air.[128] Enhanced selectivity was

achieved by removing interfering acid gases by using a second membrane and an alkaline solution followed by detection using an electrolyte conductivity sensor. This provided a method capable of measuring ammonia concentrations at less than 60 μmol L^{-1}. Although the set-up was used for the biomedical application of measuring breath ammonia levels, the analysis could be adapted to measure atmospheric levels of ammonia.

Ohira *et al.* demonstrated gas sampling *via* diffusion through a miniaturised planar porous polypropylene membrane coupled with a conductivity detector for the determination of atmospheric sulphur dioxide.[129] LODs of 0.7 – 1.0 ppbv (parts per billion by volume in the atmosphere) were achieved and ambient changes could be measured.

Korenaga *et al.* addressed the issue of gas sampling by utilising a porous glass plate for gas absorption into a microchip. This method was applied to the analysis of atmospheric NO_2 achieving detection in the 0.2-1.0 μmol L^{-1} range.[130]

Many electrochemical detection methods incorporated with microfluidic devices have been demonstrated for environmental applications achieving detection limits in the low micromolar range. For environmental applications good sensitivity is vital for the detection method and must be considered for the individual application. Limitations of electrochemical detection occur due to the robustness of the electrodes due to electrode fouling, this can be overcome by using contactless methods.

1.2.7.2 Spectroscopic Methods of Detection

Spectroscopic methods of detection, including spectrophotometry and luminescence techniques (fluorescence and chemiluminescence) have been documented for environmental applications.

Spectrophotometry

Spectrophotometric detection is common because there are a wide range of possible applications. Limitations arise when using spectrophotometric detection for microfluidic devices due to reduction in path length within the device. According to Beer's law a decrease in path length inherently causes a decrease in the sensitivity of the detection method (see equation 1.4).[131]

$$A = \varepsilon c l \qquad\qquad (Equation\ 1.4)$$

Where, A is the absorbance, ε is the molar absorption coefficient (L mol^{-1} cm^{-1}), c is the concentration of the solution (mol L^{-1}) and l is the pathlength (cm).[131]

Spectrophotometric detection also requires a light source, which increases the complexity of the detection technique as a method for microfluidic devices. The development of a wide range of intense light emitting diodes (LEDs) that can be coupled to fibre optics has however enabled the miniaturisation of spectrophotometers, which can be integrated with microfluidic devices to provide a method of on chip detection (figure 1.5). Several groups have applied this to environmental monitoring.

25
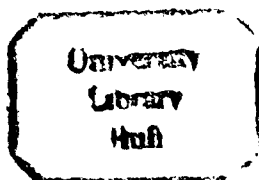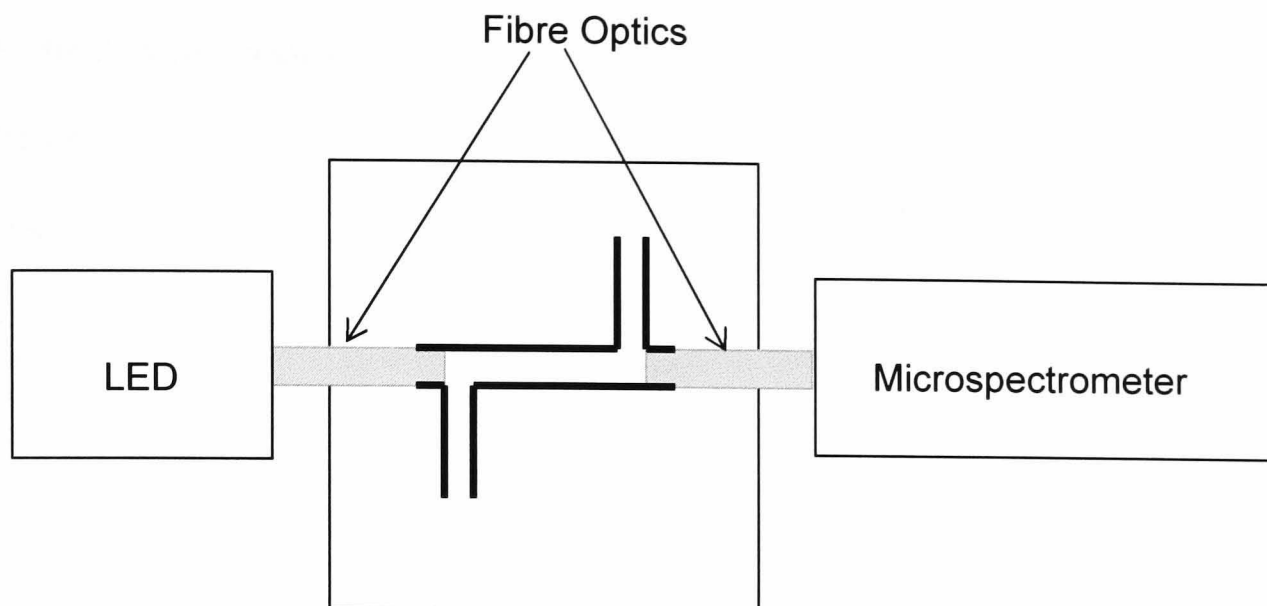
Figure 1.5 Scematic of a typical manifold for interfacing a microfluidic device with spectrophotometric detection using fibre optics.

Daykin *et al.* demonstrated an early example of the use of fibre optics coupled to a LED photodiode with a miniaturised device as a method of analysis of orthophosphate in water.[132] The detection of orthophosphate was based on the molybdenum blue spectrophotometric detection method. They successfully fabricated a μFIA manifold utilising EOF to mobilise the reagents within a glass micro reactor and to induce flow and therefore mixing within the device. They produced a method with LODs of 7.4 μmol L^{-1} of PO_4^{3-} in water with a path length of just 7mm. Doku *et al.* conducted a further study of this initial work producing a μFIA technique comparable to the conventional FIA determination of orthophosphate improving the LOD to 1.1 μmol L^{-1}.[133] The same set up as Daykin *et al.* was also used by Greenway *et al.* to produce a μFIA system for the spectrophotometric determination of nitrite in water.[22] The analysis was based on the Greiss reaction to form an azo dye. With this system an LOD of 0.2 μmol L^{-1} was

achieved and demonstrated the potential of a portable system that could be used in the field. A progression of this was to incorporate a cadmium reductor column within the device to use the same method for the analysis of nitrate in water producing an LOD of 0.51 μmol L^{-1}.[134]

Daridon *et al.* investigated the Berthelot reaction for the determination of ammonia in water utilising a microfluidic device consisting of a silicon chip between two glass plates.[135] Again the integrated system comprised of fibre optics coupled to a LED, using a path length of 400 μm. Reagent stability is a big limitation when considering methods for environmental monitoring. Devices ideally need to be left in the field for a certain period of time and give reproducible results during this time frame. Sequeira *et al.* address the stability of the reagents of this reaction for long term monitoring.[136]

Bowden *et al.* evaluated the yellow vanadophosphoric acid method as an analytical method for the determination of phosphorus in water within a microfluidic device using stopped flow with the aim of producing an automated device with a 1 year in field lifetime.[137-139] This method was selected in preference to the molybdenum blue method due to the greater stability of the reagents used in the analysis resulting in an assay with LOD of 2.1 μmol L^{-1} (orthophosphate) and a dynamic linear range of 0-500 μmo L^{-1}. The stability of this colorimetric analysis and long term reproducibility was validated for a one-year lifetime.

Lu *et al.* demonstrated a capillary electrophoresis (CE) microchip for the separation and spectrophotometric detection of three trinitroaromatic explosives: 1,3,5-trinitrotoluene (TNT), 1,3,5-trinitrobenzene (TNB) and 2,4,6-trinitrophenyl-N-

methylnitramine (tetryl) in seawater.[140] The analysis of explosives in seawater is required by the military for the identification of unexploded underwater mines. Detection was based on the chemical reaction of a base with trinitroaromatic compounds to form a product, which is red. Sensitivity of the method was improved by using solid phase extraction (SPE) to achieve LODs of 1.2 nmol L^{-1} for TNB, 1.5 nmol L^{-1} for TNT and 0.7 nmol L^{-1} for tetryl.

Ueno *et al.* utilised a microfluidic device for the determination of atmospheric benzene, toluene, ethyl benzene and xylenes (BTEX).[141-146] Gaseous samples were taken and preconcentrated using a commercially available adsorbent, silicon dioxide within the concentration cell unit of the device, the gas was desorbed by temperature elevation into the detection cell, where it was analysed using a fibre optic coupled to a UV spectrometer. Initial results gave results in the μmol L^{-1} range for toluene. This prototype was improved by employing an air-cooled cold trap after desorption, improving the LOD for toluene to 0.5 μmol L^{-1}. Separation of the gas mixture was addressed by using mesoporous silica as the adsorbent. In conclusion a portable system was devised enabling separate detection of benzene, toluene and *o*-xylene with an LOD of 0.1 μmol L^{-1} for toluene.

Spectrophotometric techniques provide a very sensitive method for environmental applications, however they also require a complex instrumental set up due to the need for a light source, this and path length reductions present limitations for environmental applications.

Fluorescence

Fluorescence is the property of some atoms and molecules (fluorophores) to absorb light at a particular wavelength and to subsequently emit light of longer wavelength. Fluorescence is a type of photoluminescence technique (along with phosphorescence). During the process a photon of energy is supplied to a fluorophore, sources include incandescent lamps (mercury discharge/xenon arc lamp) and lasers (laser induced fluorescence), this produces an electronically excited singlet state (S_1). In comparison to chemiluminescence, whereby a chemical reaction produces the excited state. When returning to the ground state a photon of energy is emitted. This is discussed in detail in section 1.3.1. This emission intensity is proportional to the concentration of emitting species and can be applied for analytical purposes as seen in equation 1.5.[131] Fluorescence as a detection technique has the advantage of being a very sensitive technique, as we can see from equation 1.5, the intensity is proportional to the radiant power of the incident light, which means laser induced fluorescence is highly sensitive.

$$I = kP_oC \hspace{3cm} \textit{(Equation 1.5)}$$

Where I is the emission intensity, P_o is the radiant power of the incident light and c is the concentration of the emitting species.

Broyles *et al.* demonstrated a quartz microfluidic device, which integrated sample filtration *via* an array of thin channels, solid phase extraction by a C18 coated channel, electrochromatographic separation and laser induced fluorescence detection using a He-Cd laser focused on the analysis channel of the microfluidic device. This was successfully applied to the determination of polycyclic aromatic hydrocarbons

(PAHs) in aqueous samples, including anthracene (LOD 3.1 nmol L^{-1}), pyrene (LOD 1.0 nmol L^{-1}), 1,2-benzofluorene (LOD 8.1 nmol L^{-1}) and benzo[a] pyrene (LOD 17 nmol L^{-1}).[147] Sensitivity can be enhanced utilising sample pre-treatment on chip.

The main application of fluorescence detection for environmental applications utilising microfluidic devices has been in the area of immunoassays, this is discussed in detail in section 4.1.2.6.

Fluorescence detection provides a highly sensitive detection method which is advantageous for environmental monitoring. Limitations to the technique arise due to the complicated instrumental set up of the detection method as an excitation source is required (the majority of fluorescence detection applications for microfluidic devices use a microscope set up).

Chemiluminescence

Chemiluminescence is defined as the emission of electromagnetic radiation by a chemical reaction and is discussed in more detail in section 1.3.1. The detection method has been used for several environmental applications.

The luminol chemiluminescence reaction has been applied to microfluidic devices for a number of applications (see section 1.3.3.1 for specific details of the reaction). The analysis of metal ions using the luminol-hydrogen peroxide system has been utilised by several groups for the determination of Co(II), Cu(II), Cr(III) and Ni(II). Nelstrop *et al.* investigated the luminol-hydrogen peroxide chemiluminescence detection of cobalt(II) in water within a microfluidic device, comparing both EOF and pressure pumping.[148] LODs for the pressure driven system of 30 pmol L^{-1} and 40 pmol L^{-1} for the EOF driven system were achieved. The slight differences in the

limits of detection are attributed to the different flow rates used in each pumping system. The luminol-hydrogen peroxide chemiluminescence was also used by Su *et al.* for the electrophoretic separation and detection of copper(II), cobalt(II) and nickel(II) within a glass microfluidic device.[149] The LODs determined were 5 nmol L^{-1} for copper(II), 5 pmol L^{-1} for cobalt(II) and 0.1 µmol L^{-1} for nickel(II). Xu *et al.* used a microfluidic device with luminol-hydrogen peroxide chemiluminescence detection for the analysis of chromium(III) in aqueous samples, producing an LOD of 0.1 µmol L^{-1}.[150] Liu *et al.* also utilized a electrophoretic separation of chromium(II), cobalt(II) and copper(II) within a microfluidic device using luminol-hydrogen peroxide detection, poorer LOD of 0.5 µmol L^{-1} for cobalt(II) was achieved.[151] Huang *et al.* analysed cobalt(II) and copper(II) using electrophoretic separation within a microfluidic device, accomplishing limits of detection of 12.5 nmol L^{-1} for cobalt(II) and 2.3 µmol L^{-1} for copper(II).[152] This was later optimised to 50 pmol L^{-1} for cobalt(II).[153]

Tyrrell *et al.* reported the determination of copper(II) using 1,10-phenanthroline chemiluminescence, achieving detection limits of 0.3 µmol L^{-1}.[154]

These methods utilized detection off chip by means of a photomultiplier tube (PMT), incorporation of chemiluminescence detection on chip was shown by Jorgensen *et al.* Back-side photodiodes were integrated with a microfluidic device for chemiluminescence detection.[155] The system was used for the determination of hydrogen peroxide using the luminol chemiluminescence reaction. Measurements in the range of 100 µmol L^{-1} to 1 mmol L^{-1} were demonstrated as an example of the working manifold. Although the application is for a fermentation process, it

demonstrates detection and analysis on chip, which is advantageous for the use of microfluidic devices for environmental monitoring.

Chemiluminescence as a method of detection for microfluidic devices has the advantage of high sensitivity. Comparing metal analysis with the chemiluminescence luminol reaction to contactless conductivity detection (section 1.2.7.1) much better LODs can be achieved using the chemiluminescence method. Chemiluminescence detection also has the advantage of only requiring a simple instrumental set up compared with spectrophotometric techniques due to the exclusion of an external light source. This is discussed in detail in section 1.3.1. A drawback of using chemiluminescence detection is the limited number of chemiluminescence reagents available.

1.2.8 Conclusions of Microfluidic Devices

The intrinsic advantages of microfluidic devices provide an approach to portable methods of analysis for environmental monitoring. These include the advantages of low reagent consumption, small sample volumes, low waste production, faster analysis times and portability due to their decreased size.

Sample introduction, small sample volumes, complexity of the sample matrix and low limits of detection of the chemical species in the environment present possible problems for the use of microfluidic devices for environmental analysis. These are the same problems encountered with sample introduction for other *in-situ* systems for environmental monitoring. Good filtration as well as a prevention of bio-organism growth in the sample introduction system is required. A good interface is required between the environment and the microfluidic device in order to achieve a robust,

reproducible sample introduction system. The microfluidic manifold has to be designed such that efficient mixing occurs. Small sample volumes could be unrepresentative; this can be addressed by taking more samples using the advantage of faster analysis. Another way to tackle this issue is to use a network of devices to gain high temporal and spatial data, avoiding the need for a representative sample. Matrix interferences need to be overcome and preconcentration and separation techniques within microfluidic devices can be used to resolve this problem.

The selected detection method is very important to achieve the sensitivity required, electrochemical and spectrophotometric detection for microfluidic devices have both been demonstrated. Electrochemical detection can readily be achieved using microfluidic devices; it provides the advantages of a simple, relatively sensitive, low powered, cost effective method of detection. However limitations arise due to the sensitivity required for environmental monitoring and the robustness of the electrodes. Spectrophotometric detection is frequently used due to its sensitivity and the wide range of applications available. Limitations arise when using spectrophotometric detection for microfluidic devices due to reduction in path length within the device which reduces the sensitivity and the complexity of the instrumental set-up because of the requirement of a light source. Fluorescence detection also provides a highly sensitive method of detection and again limitations arise due to the need for an excitation source which adds complexity to the instrumentation. Chemiluminescence detection has the advantage of high sensitivity and with the added advantage of simple instrumentation compared with other spectrophotometric techniques. Considering these factors, chemiluminescence has been chosen as the detection method to use for the microfluidic devices in order to

develop a portable method of analysis for environmental monitoring. Chemiluminescence reagents have been investigated in order to determine suitable reagents for the applications.

1.3 Chemiluminescence

1.3.1 Theory of Chemiluminescence

Chemiluminescence is defined as the emission of electromagnetic radiation by a chemical reaction. Chemiluminescence reactions usually produce a product in an electronic excited state, which produces light on returning to the ground state (S_o).[156] The route of light emission in chemiluminescence is the same as in photoluminescence (fluorescence, phosphorescence) except for the production of the excited state. In fluorescence and phosphorescence an excited state is produced as a result of the absorption of ultraviolet or visible light. In fluorescence, emission is from a singlet electronically excited state (S_1) and phosphorescence emission is from a triplet electronically excited state (T_1) (figure 1.6).[156]
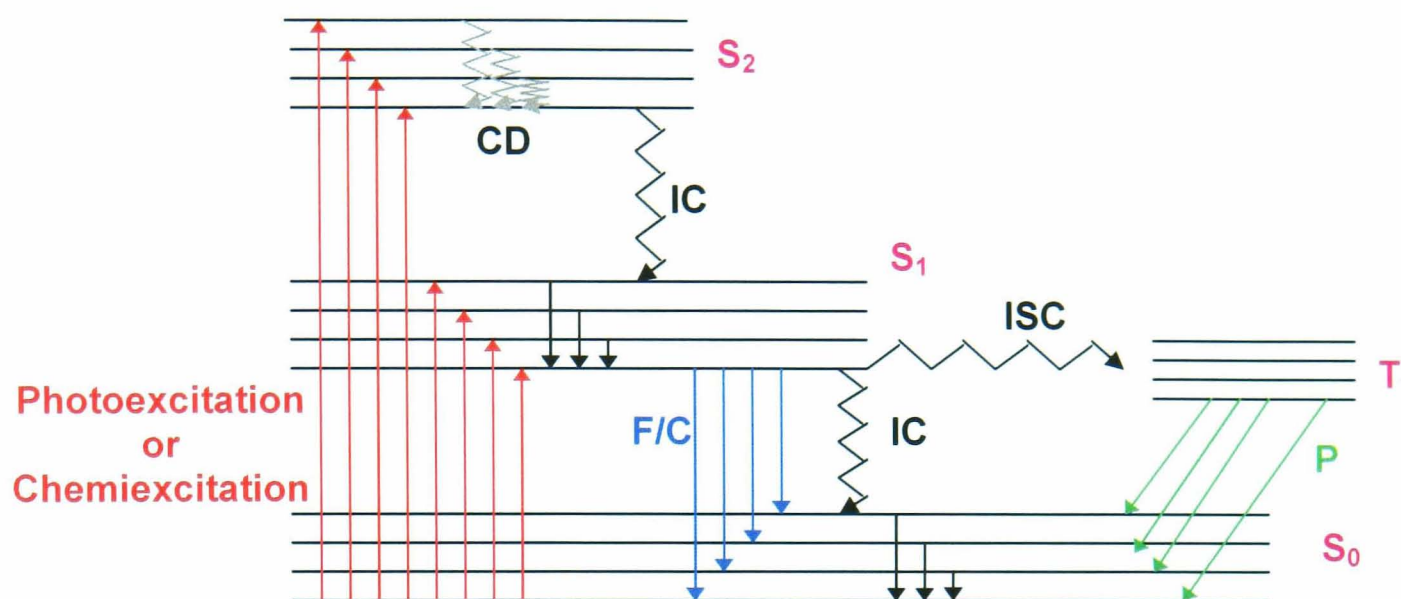
Figure 1.6 Jablonski diagram to show electronic states of a molecule absorbing and emitting light. Where S_0: Ground singlet state, S_1, S_2: Excited singlet states, T_1: excited triplet state, CD: Collisional deactivation, IC: Internal conversion, ISC: Intersystem crossing, F: Fluorescence, C: Chemiluminescence, P: Phosphorescence.[156]

Generally, a chemiluminescence reaction can be generated by two mechanisms, direct or indirect (sensitised or energy transfer) chemiluminescence (figure 1.7). Direct chemiluminescence involves two reagents, a substrate, usually a chemiluminescence precursor (a reductant) and an oxidant in the presence of cofactors to give a product (or intermediate) in an electronically excited state, which returns to the ground state emitting a photon. Indirect chemiluminescence is based on the initial interaction between an oxidant and reductant to generate an intermediate excited species, followed by a transfer of energy from this excited species to a fluorophore, which itself becomes excited and releases a photon upon returning to the ground state.

A + B

(Chemiluminescence precursor)   (Oxidant)

(Cofactors)

Intermediate or Product

P*

Direct Chemiluminescence   Indirect Chemiluminescence

Fluorophore (F)

P + $h\nu$ P + F*

F + $h\nu$

Figure 1.7 Scematic showing the different chemiluminescence reaction mechanisms (direct and indirect chemiluminescence).[156]

For a chemical reaction to produce light, certain criteria must be met. An exothermic reaction is required to generate enough energy to produce an electronically excited state (40-70 kcal mol^{-1}).[157] The reaction pathway has to be such that it favours the energy to be channelled into producing an electronically excited state. The deactivation process of the excited state must favour photon emission over other non-radiative processes such as molecular dissociation, reactions with other species, intramolecular energy transfer (indirect chemiluminescence), isomerisation and physical quenching. Chemiluminescence reagents are usually reduced species that can be easily oxidised, such as molecules containing amino and hydroxy groups, and polycyclic aromatic ring systems. Strongly alkaline arylamino groups deprotonate making them more susceptible to oxidation.

The intensity of the light emitted is dependent on the efficiency of producing electronically excited molecules, characterised by the quantum efficiency (quantum yield) and the rate of the reaction, see equation 1.6.

$$I_{CL} = \Phi_{CL} -dA/dt \qquad \textit{(Equation 1.6)}$$

Where, I_{CL} = *emission intensity (photons/second)*

Φ_{CL} = *quantum yield (efficiency of chemiluminescence reaction (ratio of number of photons emitted to the number of reactant molecules reacting))*

$-dA/dt$ = *rate at which chemiluminescence precursor A is consumed*

For direct chemiluminescence, Φ_{CL} is defined in equation 1.7.

$$\Phi_{CL} = \Phi_C \times \Phi_E \times \Phi_F \qquad \textit{(Equation 1.7)}$$

Where, Φ_C = *chemical yield (ratio of number of molecules that react via the reaction pathway to the total number of molecules reacted)*

Φ_E = *excitation yield (ratio of the number of molecules that form an electronically excited product to the number of molecules that react via the chemiluminescence pathway)*

Φ_F = *quantum yield of fluorescence of the light emitting species.*

For indirect chemiluminescence, Φ_{CL} is defined in equation 1.8.

$$\Phi_{CL} = \Phi_C \times \Phi_E \times \Phi_F \times \Phi_{ET} \qquad \textit{(Equation 1.8)}$$

Where, Φ_C, Φ_E *and* Φ_F *are defined above and* Φ_{ET} = *Efficiency of energy transfer between the initial excited species and the secondary product.*

Under defined experimental conditions Φ_{CL} is the constant of proportionality between the observed intensity of chemiluminescence (I_{CL}) and the rate of consumption of the initial chemiluminescence precursor (A) (equation 1.6). Therefore, on rapid mixing a direct chemiluminescence reaction will produce an emission with intensity I_{CL}, which can be measured as a function of time. If the reaction is first order with respect to analyte A with rate constant k_r, then equation 1.6 can be rearranged to give equation 1.9. So the measurement of the maximum intensity can be related to the concentration.

$$I_{CL} = \Phi_{CL}k_r[A] \qquad \text{(Equation 1.9)}$$

Several factors affect the chemiluminescence intensity, these include the chemical structure of the chemiluminescence precursor, the nature and concentration of other species that may affect the chemiluminescence pathway, the presence of a catalyst, temperature, pH and ionic strength, hydrophobicity of the solvent and solution composition and the presence of energy transfer acceptors.

As it has been demonstrated, chemiluminescence can be utilised for quantitative analysis because the reaction rate is a function of the chemical concentration. The advantages of using chemiluminescence as a detection method are:

1. No external light source is required unlike other photoluminescence and spectrophotometric techniques, which gives chemiluminescence the advantage of having a decreased background signal and a reduction in scattering, producing high sensitivity with wide dynamic ranges.

2. The instrumentation required for chemiluminescence detection is relatively simple and consists of a reaction cell, light-tight housing, a method of introducing reagents and sample (static or flowing stream), a light detector and a method of collecting the data. This is discussed in detail in section 2.1.

3. The technique is applicable to a wide variety of species that can participate in chemiluminescence reactions such as chemiluminescence substrates, chemiluminescence precursors, oxidants and reagents needed for the reaction, as well as species that affect the rate of the chemiluminescence reaction including activators, catalysts and inhibitors.

Chemiluminescence reactions can also be used as a detection technique for chromatography, capillary electrophoresis and immunoassays.[157] Problems associated with chemiluminescence detection include (i) the need of good mixing of the sample and reagents (ii) the fact that different reactions have different kinetics, which leads to the problem of where the light is being emitted and (iii) light scattering. These can be overcome by using a microfluidic device and are discussed in detail in section 2.1.2.

1.3.2 Gas Phase Chemiluminescence Reactions

There are a number of efficient gas phase chemiluminescence reactions, which can be used for analytical purposes. Ozone is the most widely used gas phase chemiluminescence reagent, undergoing reactions with NO, SO and hydrocarbons to produce chemiluminescence.[156] Gas phase chemiluminescence has not been investigated in this work and will not be discussed further.

1.3.3 Liquid-Phase Chemiluminescence Reactions

1.3.3.1 Acylhydrazides

The luminol (3-aminophthalahydrazide) reaction has become one of the most well-known chemiluminescence reactions since it was first reported in 1928 by Albrecht.[158] The reaction consists of the oxidation of luminol usually in the presence of a cooxidant in alkaline conditions. This reaction will be discussed in detail in section 3.1.4.

In comparison to the luminol molecule, changing the heterocyclic part of the hydrazide system blocks chemiluminescence emission and the unsubstituted phthalic acid hydrazide and a number of nonaromatic cyclic hydrazides e.g. maleic acid hydrazide also show weak or no chemiluminescence. Conversely, the 6-amino isomer of luminol, isoluminol (figure 1.8) is chemiluminescent to the same amount as luminol. Isoluminol is more expensive than luminol, however it is advantageous for chemiluminescence labelling due to the less steric hindrance of the amino group.[156, 157]

Luminol   Isoluminol
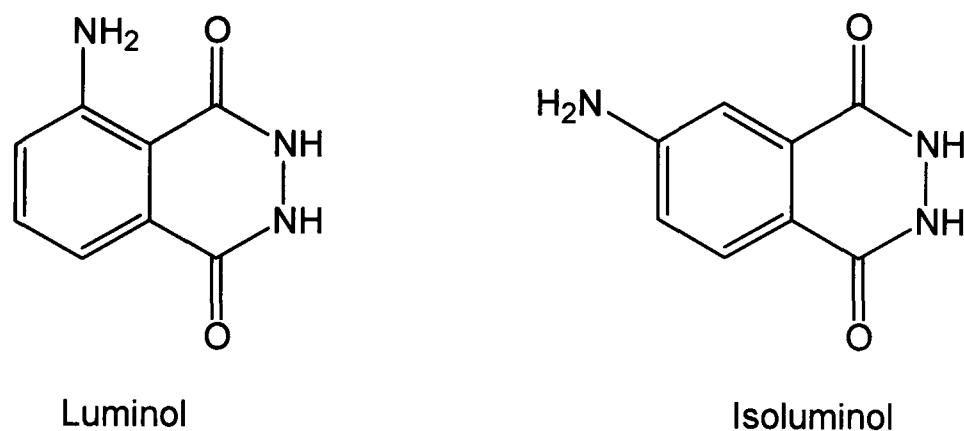
Figure 1.8 Structures of the luminol and isoluminol molecule.[156]

1.3.3.2 Imidazoles

Lophine (2,4,5-triphenylinidazole) (figure 1.9) undergoes oxidation in aqueous alkaline conditions to produce yellow light (525nm), *via* the formation of a hydroperoxide. Hydrogen peroxide can be used as the oxidant in the presence of cooxidants such as transition metal ions e.g. cobalt(II). Derivatives of lophine have also exhibited chemiluminescence properties e.g. 3-methylindole.[156, 157]
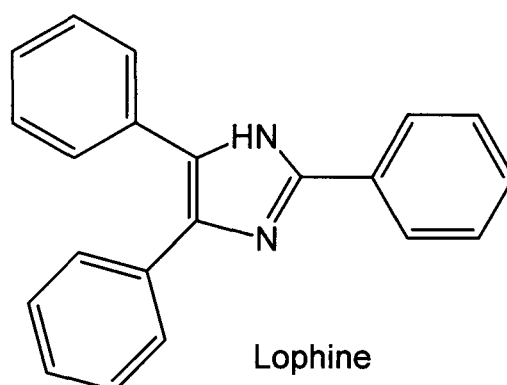
Lophine

Figure 1.9 Structure of the lophine molecule.[156]

1.3.3.3 Lucigenin and Acridinium Esters

Lucigenin (10,10'-dimethyl-9,9'bisacridinium dinitrate) (figure 1.10) undergoes oxidation by hydrogen peroxide or oxygen in the presence of cooxidants, with a

more intense chemiluminescence emission observed with transition metal ions e.g. Co(II), under alkaline conditions to yield blue-green light (440nm). Oxidation proceeds through a dioxetane intermediate producing the light emitting species N-methylacridone (10-methylacridan-9one), which is water insoluble.[156, 157]
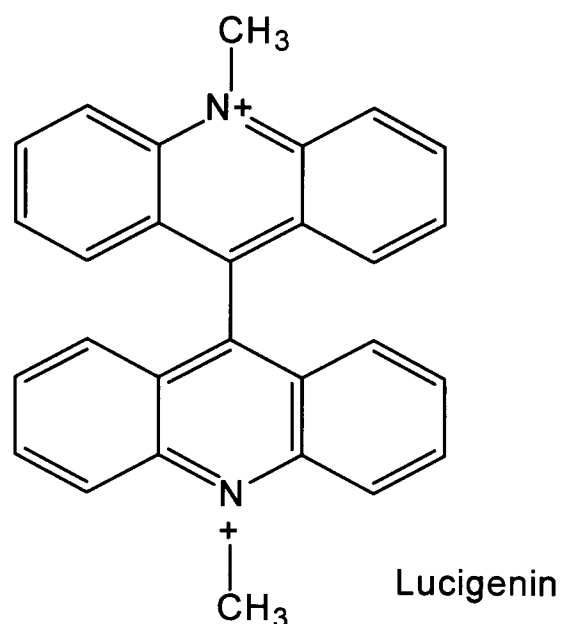
Figure 1.10 Structure of the lucigenin molecule.[156]

A number of acridinium esters related to lucigenin also produce chemiluminescence emission *via* oxidation with hydrogen peroxide or oxygen in alkaline conditions to form N-methylacridone (figure 1.11). The main advantage of acridinium ester chemiluminescence is that no catalyst or cooxidant is required, which provides a lower chemical blank and enables very high sensitivity. The main use of acridinium esters is as a label in immunoassays. The major disadvantage of acridinium ester chemiluminescence is the strongly alkaline solution (pH 12-13) required for efficient chemiluminescence and at this pH acridinium esters undergo reversible conversion to the non-chemiluminescence pseudo base form. This means sequential addition of the reagents is required to generate chemiluminescence.[156, 157]
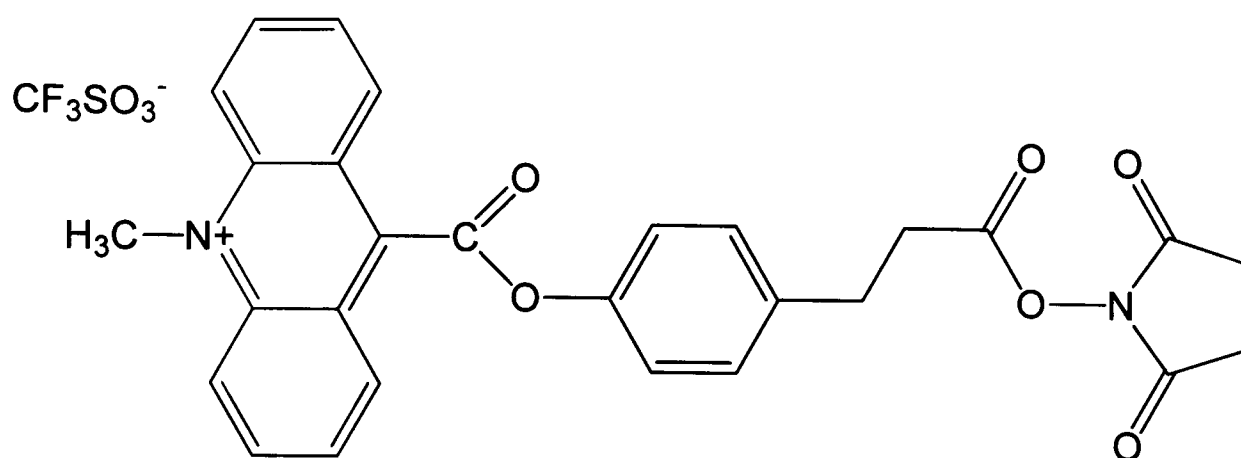
Acridinium NHS Ester

Figure 1.11 Structure of an acridinium NHS ester molecule, 4-(2-succinimidyl-oxycarbonylethyl)phenyl-10-acridinium-9-carboxylatetrifluoromethyl sulphonate.[156]

1.3.3.4 Peroxylates

The peroxylate reaction is an example of an indirect chemiluminescence reaction as the reaction incorporates an energy transfer step. Certain oxalic acid derivatives undergo oxidation, usually by hydrogen peroxide, to yield an energy rich intermediate, suggested to be 1,2-dioxetanedione, the energy is then transferred to a fluorophore producing an excited state, which produces light emission.

The two major oxayl derivatives used include *bis* (2,4,6-trichlorophenyl) oxalate (TCPO) and *bis* (2,4-dinitrophenyl) oxalate (DNPO). The fluorophore determines the wavelength of the emission of light examples include rhodamines, heterocyclic compounds (benzoxazoles) and polycyclic aromatic hydrocarbons (anthracenes, perylenes). The disadvantage of the peroxylate chemiluminescence reaction is the requirement of organic solvent for optimal solubility and chemiluminescence yields.[156, 157]

1.3.4 Electrogenerated Chemiluminescence (ECL)

ECL is the resulting process of electrochemical reactions, which directly or indirectly produce chemiluminescence emission. The process incorporates the diffusion of electrically generated reactants from one (or more) electrodes, which undergo high energy electron transfer reactions either with chemicals in solution or one another, producing excited state molecules which yield chemiluminescence emission. Conventional chemiluminescence reactions can be initiated electrochemically e.g. the luminol reaction. The main reagent used in ECL applications is tris(2,2'-bipyridine) ruthenium(II) ($Ru(bpy)_3^{2+}$). The compound undergoes one-electron redox reactions, which are fully reversible, to produce stable reduced or oxidised species, which go on to participate in a variety of ECL reactions, which ultimately produce light from the $Ru(bpy)_3^{2+}$ in the excited state, regenerating the chemiluminescence reagent. The advantage of ECL reactions is that the location of where the reaction occurs can be controlled. The disadvantages of ECL include the fact that it adds complexity to the instrumentation and methodology and electrode fouling can occur. ECL has not been investigated in this work, as conventional liquid phase chemiluminescence is more amenable to microfluidic devices for the application of environmental monitoring.

1.3.5 Chemiluminescence Detection for Microfluidic Devices

Chemiluminescence has been incorporated within microfluidic devices for several applications in addition to the environmental applications previously discussed (see section 1.2.7.2).

Su *et al.* utilised the permanganate chemiluminescence system within a microfluidic device for the analysis of dopamine and catechol, producing an LOD of 20 mmol L^{-1} and 10 mmol L^{-1} respectively.[159] Hashimoto *et al.* demonstrated the peroxylate chemiluminescent reaction within a microfluidic device for the determination of dansyl-lysine and glycine producing an LOD of 11 mmol L^{-1} for dansyl-lysine.[160] Greenwood *et al.* determined atropine and pethidine within a microfluidic system using chemically oxidised tris (2,2'-bipyridine)ruthenium(II) chemiluminescence to produce LODs of 3.8 and 77 nmol L^{-1} for atropine and pethidine respectively.[161]

The chemiluminescence analysis of glucose has been demonstrated within microfluidic devices based on the enzymatically-produced hydrogen peroxide using glucose oxidase. Xu *et al.* used the luminol-hexacyanoferrate system to detect the hydrogen peroxide, producing an LOD of 10 µmol L^{-1} for glucose.[162] Lv *et al.* also used this chemiluminescence system with the chemiluminescence reagents immobilised electrostatically to ion exchange resin for the determination of glucose, achieving a poorer LOD of 0.1 mmol L^{-1}.[163] This can also be applied to other systems which enzymatically generate hydrogen peroxide. Lv *et al.* demonstrated the analysis of uric acid within a microfluidic device utilising the enzymatically-produced hydrogen peroxide from uricase. The hydrogen peroxide was detected using the luminol-HRP reaction immobilised within a sol-gel with an LOD of 2.9 µmol L^{-1}.[164]

1.3.6 Conclusions of Chemiluminescence

Chemiluminescence can be employed for quantitative analytical techniques. It has the advantage of high sensitivity and simple instrumentation, which are ideal properties for detection techniques for environmental applications. The technique can be applied to a wide range of species including chemiluminescence substrates, chemiluminescence precursors, oxidants and cofactors needed for the reaction, as well as species that affect the rate of the chemiluminescence reaction including activators, catalysts and inhibitors. There are a number of chemiluminescence reactions available, which are relevant for environmental applications. Solubility, stability, cost-effectiveness and availability of the reagents are all factors to take into consideration when selecting a reagent to use with microfluidic devices for environmental applications. Luminol is commercially available at a cost effective price and can be used in aqueous conditions, as is lophine. Lucigenin generates a water insoluble product making it incompatible with microfluidic devices as precipitations can cause blockages. Peroxylates require an organic solvent, which would be preferable to avoid for field use applications. Acridinium esters require a high pH sequential addition which could cause problems for microfluidic devices. The choice of chemiluminescence reagent will be discussed in the individual chapters relating to the specific applications.

1.4 Conclusions

The advantages of microfluidic devices, which include reduced reagent consumption, small sample volumes, reduced waste production, faster analysis times and portability, are ideal properties for the *in-situ* measurement of chemical species in the environment. Sample introduction, fabrication methods, fluid manipulation and mixing for microfluidic devices have been explored in order to design a simple and cost effective channel manifold for a microfluidic device for environmental applications. Different detection methods for environmental applications have been investigated and chemiluminescence detection has been selected as an ideal method of portable analysis due to its high sensitivity and simple instrumentation. Chemiluminescence theory has been addressed and suitable chemiluminescence reagents identified and compared for future applications in this work.

Chapter 2

Instrumentation

2. Instrumentation

2.0 Aims

The aim was to design and develope a portable chemiluminescence detection system that could be used with microfluidic devices for the purpose of environmental applications. Mixing within the microfluidic devices was investigated in order to design a suitable microchannel manifold which could be used with chemiluminescence reactions. Details of the channel manifold designs are presented along with the fabrication techniques used to produce the devices. Immobilisation techniques are detailed as an approach to producing a reagentless system. Solid supports used within microfluidic devices have been explored as a means of improving the surface area within the device in order to increase the loading of immobilised reagents. Finally, a device designed to be used in conjunction with packed reagents is detailed. Specific experimental procedures for the different applications are given in the individual chapters, due to their varying nature.

2.1 Development of a Portable Chemiluminescence Detection System

2.1.1 Chemiluminescence Detection

Chemiluminescence can be detected using any instrumentation that is sensitive to changes in light intensity. The critical requirements for the detector are (i) it should detect light over a large range of intensities, (ii) it should be highly sensitive over the 400 – 600 nm spectrum range, (iii) the signal output should be directly related to the light sensitivity and (iv) the speed of the response of the detector must be greater

than the rate of the chemiluminescence reaction to give a true signal.[165] In general photon transducers are used to detect photons of light and convert them into electrical signals. There are two groups of photon transducers, solid state devices and vacuum tubes.[166]

2.1.1.1 Solid State Photon Transducers

A simple type of solid-state device is the silicon diode. The silicon comprises of a *p-n* junction. A reverse bias is applied to the diode, electrons and holes are drawn away from the junction causing a depletion area, enabling the junction to act as a capacitor. When radiation strikes the diode, free electrons and holes are produced and move to oppositely charged regions producing a current that can be monitored, allowing detection of the radiation.[166] A photodiode is made up of an array of silicon diodes. The advantages of silicon diodes for chemiluminescence detection are that they can simultaneously measure over a large spectral response (190 – 1100 nm) and that they are low cost, small and compact making them suitable for portable applications. However their main disadvantage is their lack of sensitivity. A progression of the silicon diode is the avalanche photodiode (APD),[166] which combines the advantages of solid-state devices with those of photomultipliers discussed in section 2.1.1.2. APDs work by applying a high reverse bias voltage to the *p-n* junction, which produces an internal gain effect. This is because at a certain level of the electric field strength (around 2×10^5 V cm^{-1}) collision of the electron hole pairs with the crystal lattice in the depletion area is likely to occur causing ionisation and producing new electron hole pairs, which then can go on to produce more electron-hole pairs, thus creating an avalanche effect. This produces a highly sensitive solid-state device. Another type of solid-state device is a charged couple device (CCD).[156] The CCD

consists of a two-dimensional array of pixels containing an n-doped and p-doped silicon substrate, which is covered by an insulating silicon dioxide layer, above the silicon dioxide layer the electrodes are positioned. Charge is generated and stored due to the radiation absorbed by the p-doped region introducing an electron into the conductance band leaving a hole in the valence band. The electron migrates to the positive electrode where it is stored, while the hole migrates to the n-doped substrate. The stored charge is then transferred by electrodes to a serial register and read out.[166] CCDs have the advantage of very high sensitivity and the ability to acquire the full chemiluminescence spectrum of the reaction, as opposed to the total chemiluminescence output provided by PMTs (see section 2.1.1.2). This enables information about the reaction to be obtained and more than one chemiluminescence reaction can be monitored at the same time.[167, 168] However, due to their increased size CCDs are less amenable to portability.

2.1.1.2 Vacuum Tube Photon Transducers

The most common detection device employed in chemiluminescence is the photomultiplier tube (PMT).[166] A PMT consists of a photosensitive negatively biased cathode and a collection anode separated by dynodes (electrical electrodes), which provide electron multiplication or gain. When radiation strikes the cathode it ejects an electron, which strikes the first dynode this then releases two to five secondary electrons. The field between the first and second dynodes causes the secondary electrons to accelerate and strike the next dynode with sufficient energy to release more electrons. This process is repeated with each dynode being biased with a greater positive potential than the previous allowing the multiplication process to continue producing approximately 10^4 - 10^7 electrons for each photon when the

electrons reach the anode (figure 2.1). The gain (average number of electrons per anode pulse) is dependent on the power supply. There are two main types of detection used with PMTs, these are photon-counting and analog. In the photon-counting mode, when the electrons reach the anode the lower-intensity noise pulses are filtered out using a discriminator and amplified to give a working output. In the analog mode, the resulting analog signal output is the sum of all the pulses. The main advantage of the photon-counting mode is that the signal-to-noise ratio of the data is higher than that of the analog mode. However the major disadvantage to this detection technique is the added cost compared to the analog mode.

In the absence of light a "background" signal is produced (unwanted output signal) because of the thermal emission of electrons at the photocathode and the dynodes.

The configuration of the PMT with respect to the reaction cell can occur in two ways, the "side-on" configuration and "end-on" configuration. The "side-on" configuration consists of the PMT positioned to the side of the reaction cell; this is a more economical set up, which requires less space. The "end-on" configuration consists of the PMT positioned beneath the reaction cell, this set up allows for a greater uniformity of light collection and of the response with a larger photocathode area.
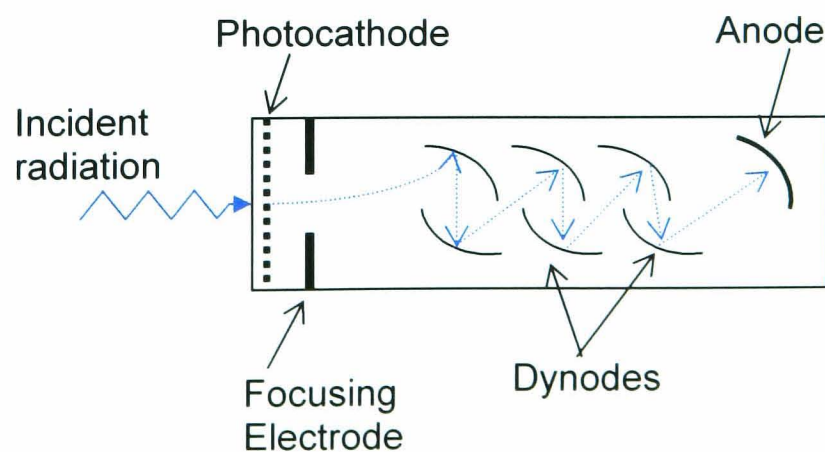

Figure 2.1 Schematic diagram of a photomultiplier tube (PMT).[156]

In order to choose a suitable photodetector several factors must be considered: the detectors active area, the signal to noise ratio, the wavelength of light to be detected and its intensity. For portability of the detector, the size and cost of the photodetector are also important. PMTs operate at very low light levels and come in a variety of active area sizes. Photodiodes tend to operate at higher light level, whilst APDs operate at light levels in between those detected by PMTs and photodiodes and tend not to be suitable for rapid measurements. CCDs have high sensitivity but are less portable. Taking into account these factors a cost effective, commercially available, small and compact PMT (analog mode) was selected as the photodetector for the portable chemiluminescence detector and is discussed in section 2.1.2.1.

2.1.2 Design of In-House Chemiluminescence Detector

2.1.2.1 Selection of Photodetector

The low power consumption photosensor module (H5784) was obtained from Hamamatsu Photonics Ltd. (Hertfordshire, UK). The photosensor module combines a "Head-on" PMT (Part number R7400U) with a high voltage supply and signal processing electronics in a metal package (dimensions 22 x 22 x 60 mm). The PMT active area is 8mm in diameter, providing a spectral response of 300 – 650 nm, with a peak wavelength of 420 nm. The system was designed with a variable gain dial, allowing the gain of the PMT and therefore the sensitivity of the PMT to be adjusted. A 15 V power supply is required for the PMT, allowing it to be battery operated (four 9 V batteries). Using this set up the system could be run for up to 20 hours continuously before the batteries required replacing; indicating a shutdown time is required when using the system in the field when data is not required to preserve the

batteries. The system could also be powered from the mains supply when operated in the laboratory; this was used during method development stages of the research to reduce costs. For development purposes in the laboratory a chart recorder was utilised to record the chemiluminescence signal (Chessel Ltd.., Worthing, Sussex, UK). The height of the chemiluminescence response was measured on the chart recorder, which represents the maximum chemiluminescence emission.

2.1.2.2 Design of Light Tight Housing

The portable chemiluminescence detection system was encased in a light-tight steel box with external and internal dimensions of 182 mm x 167 mm x 105 mm and 168 mm x 140 mm x 98 mm, respectively (RS Components, Corby, Northamptonshire, UK). In the absence of light a "background" signal was produced (unwanted output signal) because of thermal emission of electrons at the photocathode and the dynodes. For the chemiluminescence detector this was 3 mV. The steel box provides a light tight housing for the PMT to be situated in and removes interference from external light. The box also contains the miniaturised peristaltic pump discussed in section 2.1.2.3.1 and the reagents, sample and waste holder for the reaction situated in blackened containers. In the base of the steel box the five 9V batteries are located, which are required to power the system (PMT and pump). The portable chemiluminescence detector is shown in figure 2.2.

To make the system portable and amenable to field use, the system was designed with a protective shutter for the PMT. This allows access to the samples and the microfluidic device whilst preventing it from being exposed to external light. A shutter mechanism was constructed in-house and was designed such that it could only be opened when the box is properly shut and sealed from external light due to

the position and configuration of the thread on the closing mechanism which turns the direction of the shutter, likewise when the box is open the shutter remains closed.

2.1.2.3 Position of Microfluidic Device

The reaction cell must be positioned as close as possible to the detector to maximise optical efficiency. By using a microfluidic device this is achievable by placing the device directly on top of the shutter system containing the PMT. The base plate of the microfluidic devices are 3 mm as seen in section 2.2.3. This method was chosen as opposed to using a fibre optic system to detect the light intensity because by placing the entire microfluidic device above the PMT the entire chemiluminescence reaction and therefore light emission is taking place in front of the PMT active area. When using a fibre optic the area where chemiluminescence emission is observed is limited. If light guiding occurs along the channels a fibre optic connection would miss this emission and reduce the sensitivity of the detection. To improve the optical efficiency, reflective surfaces for the microfluidic devices have also been investigated and are discussed in detail in section 3.3.3.
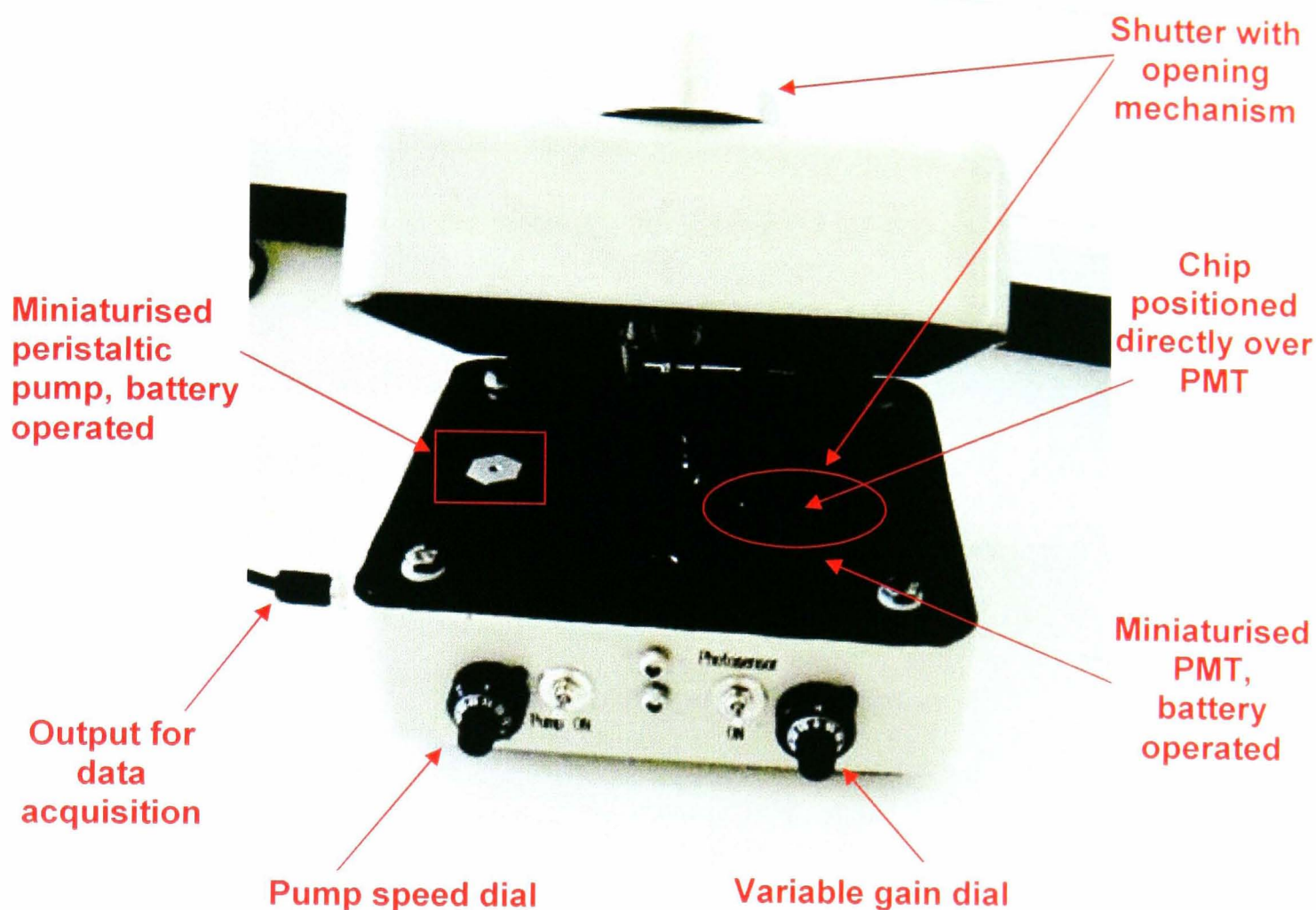
Figure 2.2 Photograph showing the portable chemiluminescence detection system designed in-house.

2.1.2.3 Design of Fluid Manipulation

2.1.2.3.1 Pumping

A miniaturised peristaltic pump (dimensions 27 x 32 x 54 mm (53g)), was used to introduce the sample and chemiluminescence reagent continuously into the device. It requires an 8 V power supply allowing it to be battery operated and was purchased from Camlab (Cambridge, UK). Two different connection manifolds for the tubing to the device were used. The first system utilised silicone peristaltic pump tubing (i.d.

250 μm) (Elkay Laboratory Products (UK) Ltd., Basingstoke, Hampshire) connected to PEEK tubing (150 μm i.d., Anachem Ltd., Bedfordshire) directly sealed onto the device using *Torr seal* (Varian Vacuum Technologies, USA). The PEEK tubing connection was required as the prototype devices contained 360 μm holes in the top plate for connection purposes. The second system directly connected the peristaltic pump tubing to the device using 2 mm holes in the top plate (see section 2.2.3). A schematic of the system manifold can be seen in section 3.3.2. The portable chemiluminescence detection system containing the microfluidic device and microfluidic connections to sample/reagent holders can be seen in figure 2.3.

Figure 2.3 Photograph showing the portable chemiluminescence detection system designed in-house. The microfluidic connections can be seen with peristaltic pump tubing connected directly from the sample/reagent containers to the microfluidic device located above the PMT. Further peristaltic pump tubing connects the microfluidic channels to the waste container. The reagent, sample and waste containers are covered with black tape when the box is operational to reduce interference.

2.1.2.3.2 Sample Introduction

There are two different configurations for introducing the sample and reagent for chemiluminescence detection, static or flowing stream. The advantage of using a static method is that it allows the chemiluminescence reaction time profile to be measured. When using a flow stream it is essential that maximum intensity is reached while the "stream" is in front of the detector, this can be accomplished simply when using a microfluidic device with the correct channel manifold (see section 2.2.3). A disadvantage of using a flow system is the large reagent consumption and waste production generated from the technique; this is overcome by using a microfluidic device as the low volume flow rates generate minimal reagent consumption and waste production.

As previously discussed in section 1.2.4, sample introduction into a microfluidic device creates a need for reproducible and representative small sample volumes. It was therefore decided to continuously introduce the sample and reagents. This continuous introduction of the plentiful sample reduces errors that may occur by introducing very small volumes of sample into the manifold and allows a simple interface to the environment.

A portable chemiluminescence detector has been developed to be used in conjunction with microfluidic devices. The system comprises of a battery operated miniature PMT with a protective shutter and a battery operated miniature pump, which allows the simple set up of continuous introduction of samples and reagents.

2.2 Design of Microfluidic Device

2.2.1 Device Fabrication

2.2.1.1 Photolithography and Wet Etching

The base plates containing the etched channels were fabricated by MCS (Micro Chemical Systems, Hull, UK) and prepared using photolithography and wet etching. The process is outlined in figure 2.4.[4, 11] A thin layer of metal (e.g. chromium) is coated onto the glass by vapour deposition, onto this a photoresist layer is spin coated. The manifold required for the microchannels is prepared in mask form and placed on top of the photoresist layer. The substrate is exposed to UV light for photoresist development followed by chrome etching to remove the metal layer. This way the channel manifold is transferred to the substrate. The channels are then chemically etched using a solution of 1% HF and 5% NH$_4$F in water (70°C), producing an etch rate of approximately 0.3–0.5 μm min^{-1}.[4]

1) Photoresist coated on glass with Cr mask layer

2) UV light exposure to substrate with design mask

3) Developed photoresist

4) Chemical etching of metal

5) Chemical etching of glass

6) Removal of metal and photoresist layer

7) Top glass layer bonded to form channel

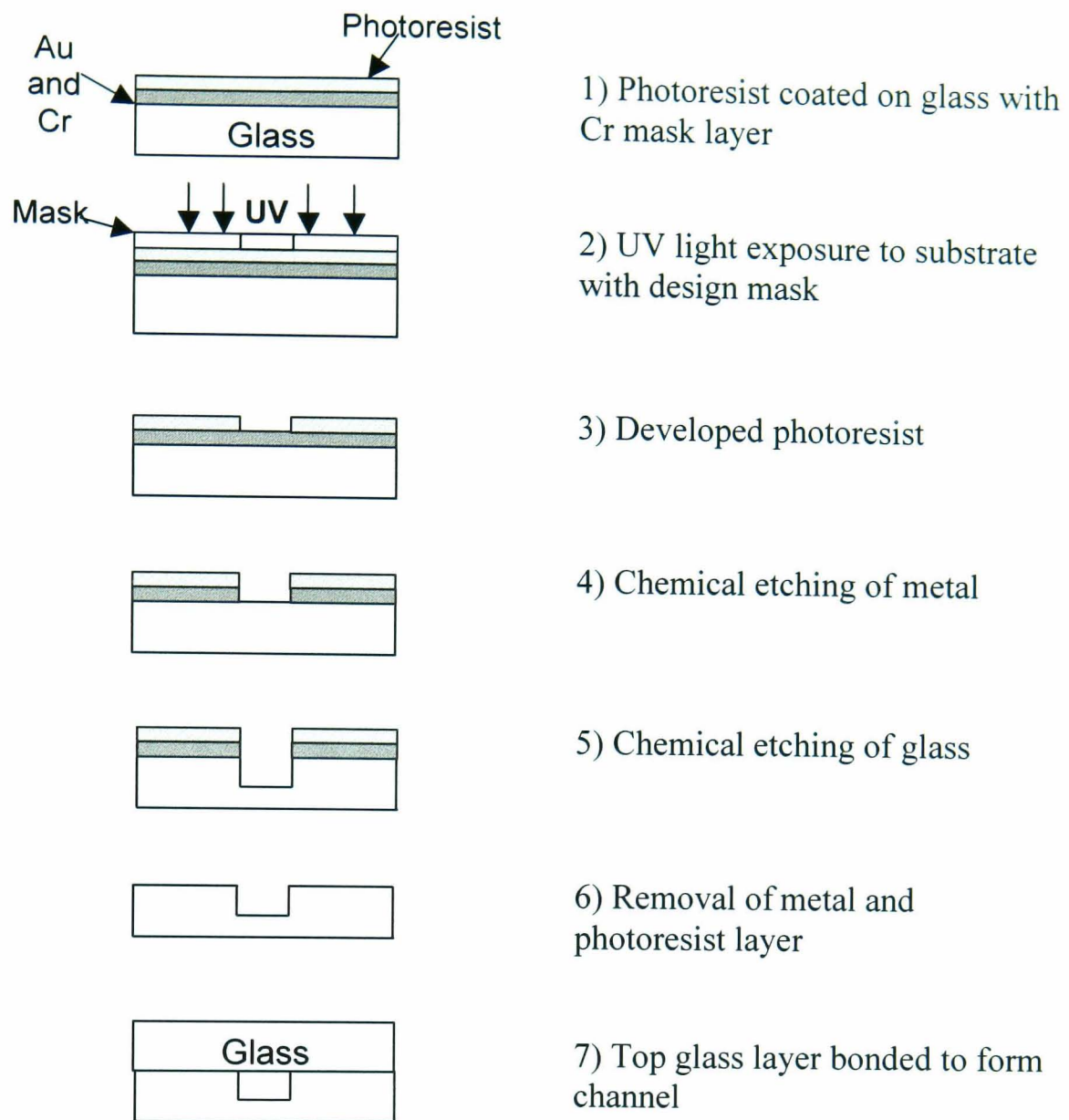*Figure 2.4 Schematic demonstrating channel fabrication using photolithography and wet etching in a glass substrate.[4, 11]*

The channels are isotropically etched into the glass substrate as outlined in figure 2.5.

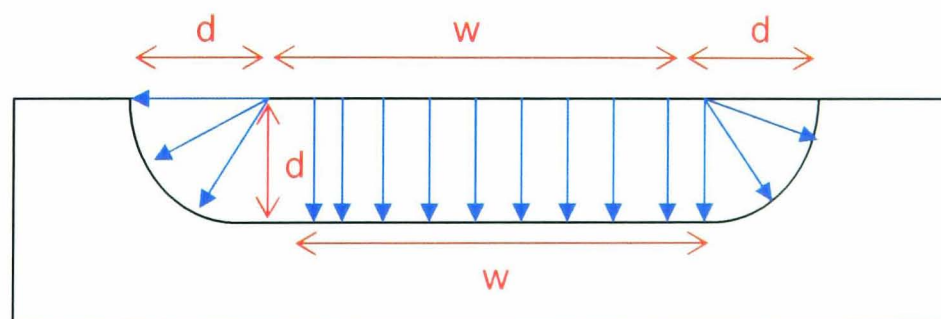The cross sectional area of the channel is calculated using equation 2.1.

Figure 2.5 Isotropic etching of a glass substrate, where w is the mask width and d is the channel depth.

$$A = (w \times d) + \frac{\pi d^2}{2} \qquad\qquad \textit{(Equation 2.1)}$$

Where A is the cross sectional area (m^2), w is the mask width (m) and d is the channel depth (m).

2.2.2 Thermal Bonding of Glass

The base plates containing the etched channels had to be bonded to a top plate (figure 2.3, stage 7). Thermal bonding was selected as the method to achieve this and was carried out in-house. Before the bonding took place, the top plate was drilled with holes for tubing connection. The two types of glass must be similar, with expansion coefficients within 0.02 $\mu m/^{\circ}C$ for successful thermal bonding to occur. The procedure consisted of the base and top plates being cleaned thoroughly with surfactant and rinsed with water and air dried. The two plates were then taped into position, lining up the channels with the connection holes. The device was then placed between metal plates and placed in a furnace for 3 hours at $560^{\circ}C$.

2.2.3 Design of Channel Manifold

The simplest form of design for a microchannel with two inlets is called a T-shape (or T-mixer) microfluidic device (figure 2.6). A T-shape device was fabricated with channel dimensions 200 μm wide and 60 μm deep (using approximately a 50 μm mask width (based on manufacturer's guidelines) with a channel mixing length of 20 mm.
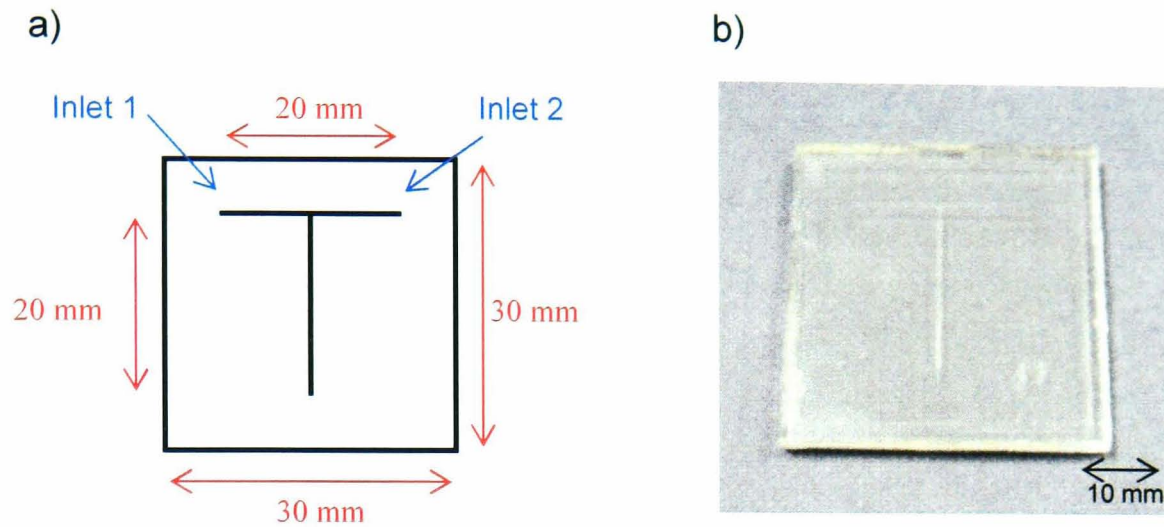
Figure 2.6 a) Schematic of a T-shape mixing microfluidic device and b) T-shape etched channels in a glass substrate.

As previously discussed in section 1.2.6, mixing within the channels is diffusion limited. For chemiluminescence reactions efficient mixing of the reagents are essential for sensitive detection. Using water as a model fluid (Diffusion coefficient $= 2.62 \times 10^{-9}$ m^2 s^{-1}), Fick's first law and the Einstein-Smoluchowski equation (see section 1.2.6) can be used to estimate that the time required for complete diffusion to occur across a 200 μm channel is 7.6 s. Taking into consideration the flow rate of the fluid and the cross sectional area of the channel, the distance required for complete mixing to occur can also be estimated (see table 2.1).[169] The cross sectional area is calculated using equation 2.1 (see section 2.2.1).

Table 2.1 Effect of flow rate on the length of channel required for complete mixing using water as a model. Calculation for the distance required (m) = velocity (m s⁻¹) x time to diffuse (s).

Volume Flow Rate (μL min^{-1})	Velocity (m s^{-1})	Channel Distance Required (cm)
1.0	0.002	1.2
2.0	0.003	2.4
5.0	0.008	6.1
10.0	0.016	12.1
15.0	0.024	18.2
20.0	0.032	24.2
25.0	0.040	30.3

From table 2.1, it can be seen that for a slower flow rate mixing occurs at a shorter channel distance. This lead to the design of microfluidic manifolds with longer channel lengths. In order to achieve this, the channel length had to be in the shape of a serpentine in order to fit the microchannels within an area that would sit above the PMT for detection. A serpentine was chosen over a coiled design, which has traditionally been used for flow cells for FIA chemiluminescence detection, because of the requirement of the length of channel required for mixing.

Two different serpentine devices were designed (figure 2.7 and figure 2.8) as this allows for a longer residence time and better mixing of the reagents. By using a serpentine the device can be designed such that the entire channel manifold can sit directly above the PMT for detection. This eliminates the problem of where the chemiluminescence reaction is occurring within the chip. Design 1 of the serpentine contained channel dimensions 200 μm wide and 60 μm deep with a channel length of approximately 116 mm with 10 meanders (figure 2.7). Design 2 of the serpentine

contained channel dimensions 200 µm wide and 65 µm deep with a channel length of approximately 206 mm with 21 meanders (figure 2.8).

Figure 2.6 Schematic of a T-shape serpentine channel manifold microfluidic device (Design 1 - 116 mm length, 10 meanders).

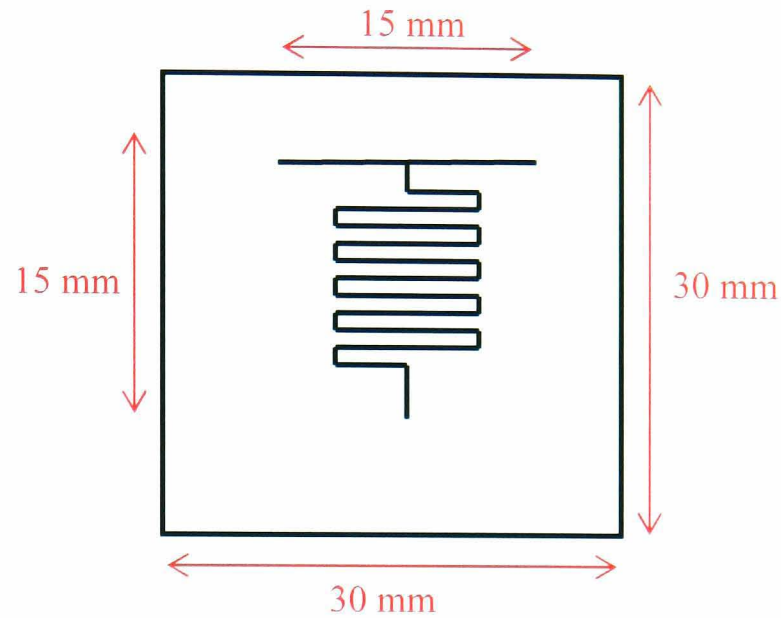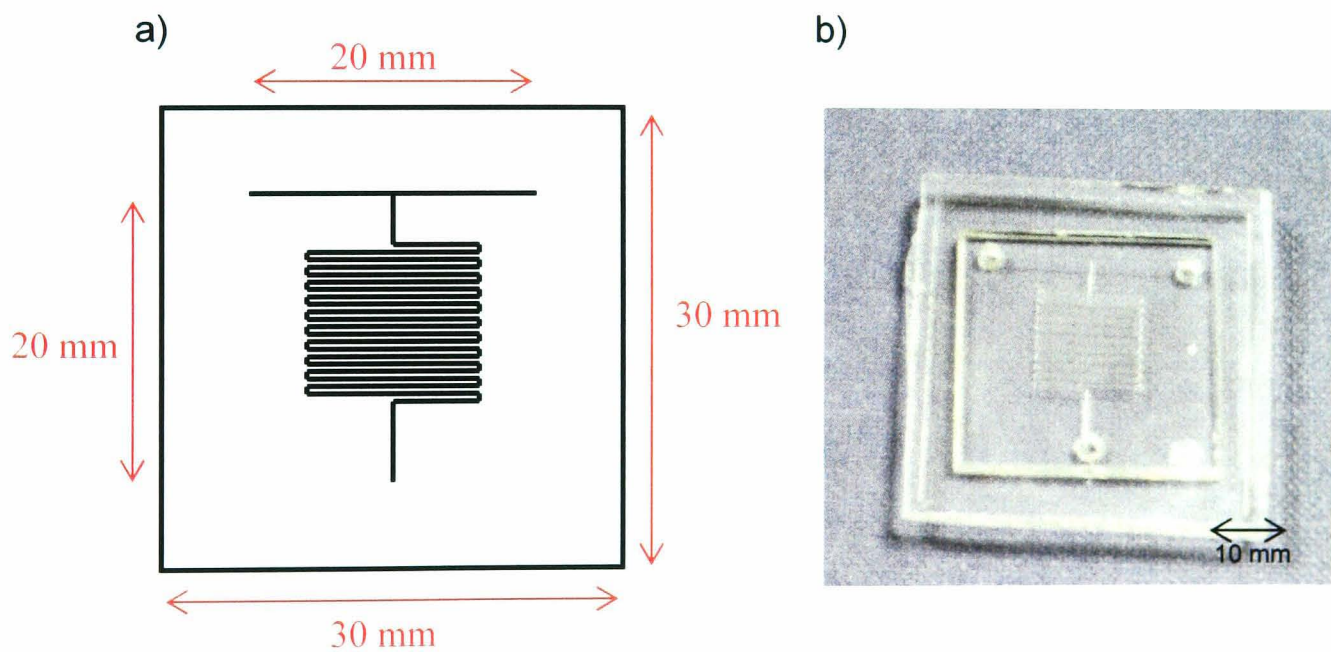*Figure 2.7 a) Schematic of a T-shape serpentine channel manifold microfluidic device (Design 2 - 206 mm length, 21 meanders) and b) Photograph of the etched channels in the serpentine device (Design 2 - 206 mm length, 21 meanders) complete with the top block containing the holes for fluidic connections.*

Taking into consideration the flow rate of the fluid and the cross sectional area of the channel, the residence time of the fluid over the channel lengths for the different manifolds can be estimated (see table 2.2).

Table 2.2 Estimated residence times for water within the different channel manifolds at different flow rates. Calculation for the residence time (s) = channel length (m)/flow rate (m s^{-1}).

		Residence Time (s)		
Flow Rate (µL min^{-1})	Velocity (m s^{-1})	T-shape (length 20 mm)	Serpentine 1 (length 116 mm)	Serpentine 2 (length (206 mm)
1	0.002	12.6	72.8	138.3
2	0.003	6.3	36.3	69.1
5	0.008	2.5	14.6	27.7
10	0.016	1.3	7.3	13.8
15	0.024	0.8	4.9	9.2
20	0.032	0.6	3.6	6.9
25	0.040	0.5	2.9	5.5

The different channel designs were investigated using the luminol-cobalt-hydrogen peroxide chemiluminescence reaction (This is discussed in detail in section 3.3). The chemiluminescence reagent consisted of 3 x 10^{-5} mol L^{-1} cobalt(II) and 5 x 10^{-4} mol L^{-1} luminol in 0.1 mol L^{-1} sodium carbonate, the pH was adjusted to pH 10.6 with 2 mol L^{-1} hydrochloric acid. The sample consisted of 1 µmol L^{-1} hydrogen peroxide. The chemiluminescence reagent was passed through one channel of the T-piece (inlet 1) and the sample was passed through the other channel (inlet 2). The chemiluminescence intensity was determined using the portable chemiluminescence detection system. The flow rates were varied to investigate the mixing within the microfluidic device (figure 2.9).
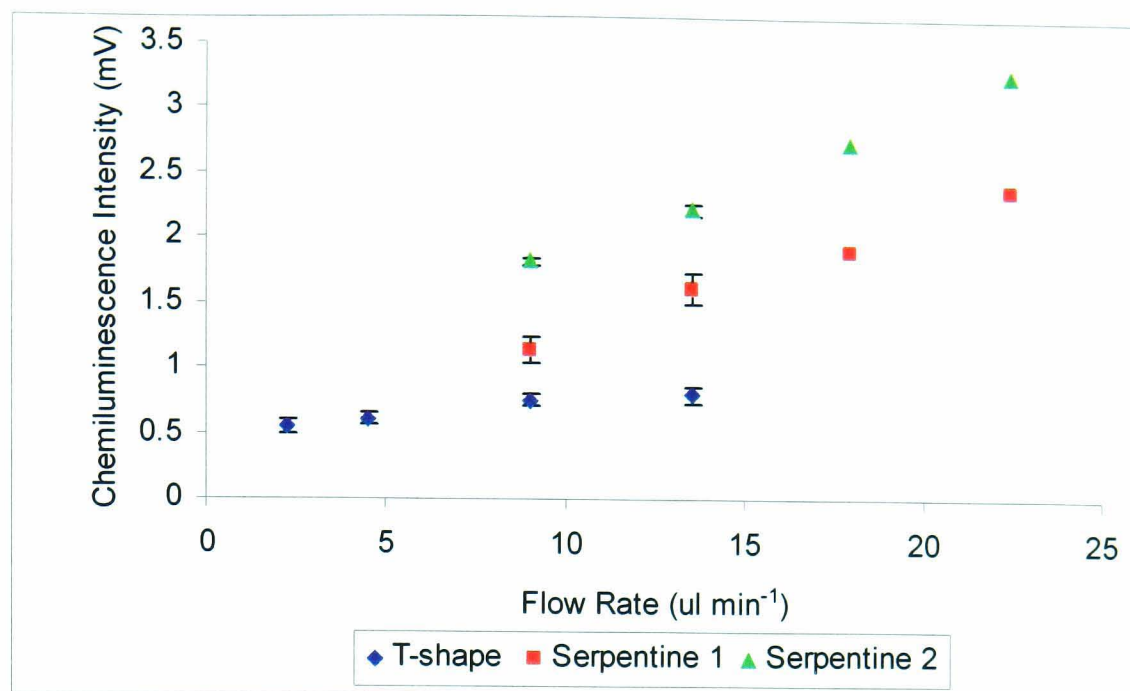
Figure 2.9 Effect of the flow rate on the chemiluminescence intensity of the luminol reaction using different channel geometries. Error bars: one standard deviation (n=5).

As expected the T-shape manifold gave the lowest chemiluminescence intensity due to the short channel length. The design with the longest channel length gave the best result (highlighted in figure 2.10). The improvement in chemiluminescence intensity within the serpentine manifolds can also be attributed to an improvement in mixing due to the meanders of the channels. As discussed in section 1.2.6, an improvement in mixing is achieved by increasing the surface contact between the fluids and decreasing the diffusion path between them. At the turns of the meander in the serpentine the diffusion path is decreased for one of the fluids allowing for an increase in molecular diffusion, producing an increase in mixing. The meanders do not produce turbulent flow as low Reynolds numbers are still predominant due to the low flow rates.

From the calculations in table 2.1, a slower flow rate is expected to improve mixing and therefore improve the chemiluminescence signal, however this is not observed from the experimental data (figure 2.9). From the results it can be seen that an increase in flow rate improves the chemiluminescence signal. This is probably related to the fast kinetics of the chemiluminescence reaction as discussed in more detail in section 3.3.2.
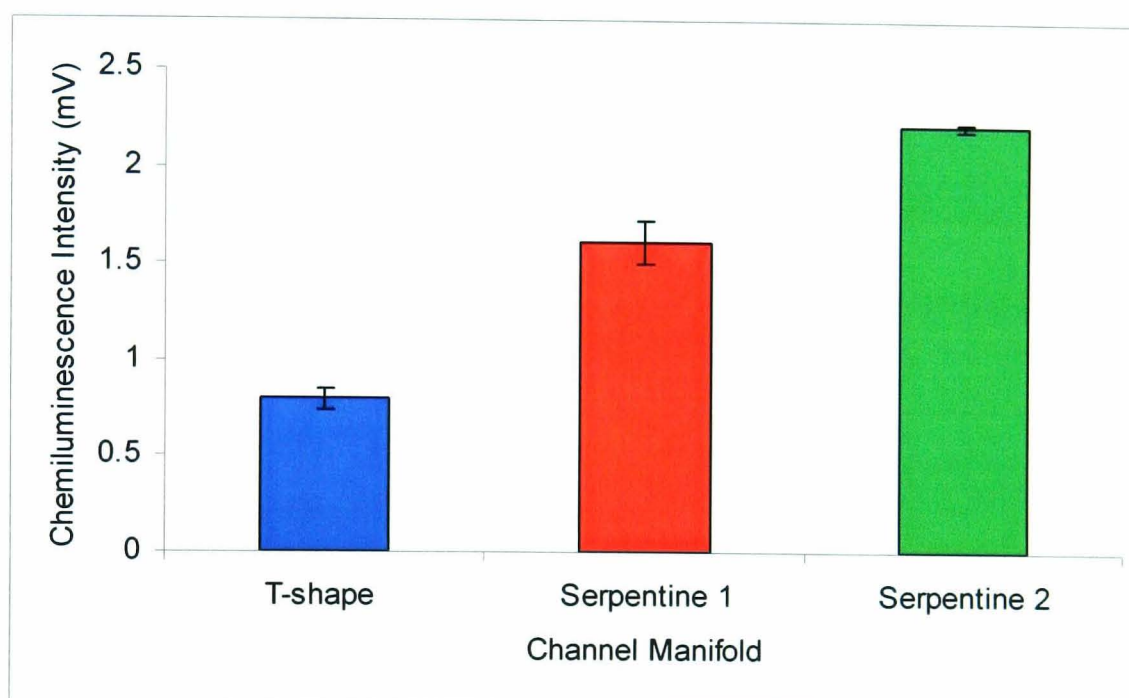
Figure 2.10 Comparison of the chemiluminescence intensity of the luminol reaction at a flow rate of 14 μl min⁻¹ using different channel geometries. Error bars: one standard deviation (n=5).

Different channel manifolds were explored and the mixing of the luminol chemiluminescence reagents was investigated in order to determine a suitable microfluidic design for chemiluminescence reactions. A serpentine configuration with a channel length of 206 mm and 21 meanaders was selected as the most suitable set up for further applications.

2.3 Design of Microfluidic Device for Packed Reagents

The immobilisation of chemical reagents can produce reagentless systems. The advantage of having a reagentless system is that it further simplifies the instrumental set up for the analysis, which is of benefit to portable systems because it reduces the amount of chemicals stored in the field. Immobilisation also has the benefits of cost advantages, for example if expensive catalysts such as enzymes are required in the reaction immobilising them enables them to be reused. Immobilisation can also improve the stability of certain biomolecules. There is also more control of where the reaction is occurring as the reagents are localised within the device, therefore you can direct the chemiluminescence reaction to occur directly over the active area of the PMT.

2.3.1 Immobilisation Techniques

Immobilisation techniques have been investigated and are discussed in general terms relating to biomolecules, but this can also apply to chemical reagents. Specific immobilisation protocols are given in the individual chapters relating to the immobilisation of specific species.

2.3.1.1 Methods of Immobilisation

In solution, biomolecules have complete freedom of movement for interactions to occur. Immobilisation of the biomolecule restricts this movement by providing a physical support. There is no ideal solid support or standard method of immobilisation; these must be considered to take into account the application of the immobilised product. There are five main methods of immobilising biomolecules,

these are adsorption, covalent bonding, entrapment, encapsulation and cross linking (see figure 2.11).[170]

A) Adsorption
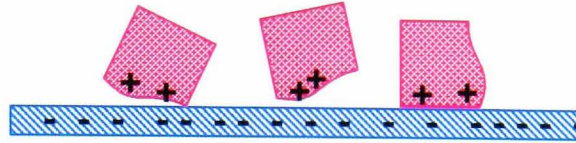
B) Covalent Bonding
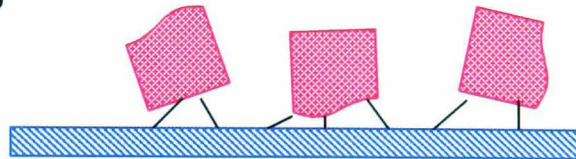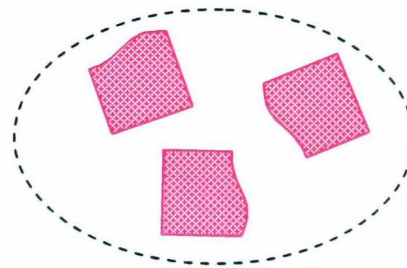
C) Entrapment
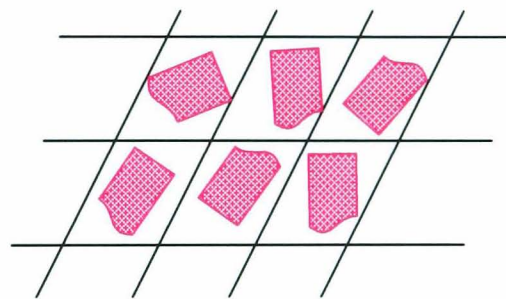
D) Encapsulation

E) Crosslinking
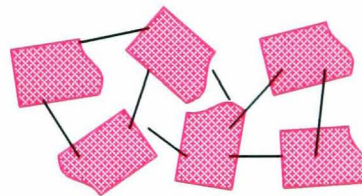
Figure 2.11 Illustration to show the five main methods of immobilising reagents: a) adsorption, b) covalent bonding, c) entrapment, d) encapsulation and e) crosslinking.

Adsorption

This is the simplest method and consists of surface interactions between the biomolecule and the solid support such as van der Waals, ionic and hydrogen bonding and is therefore reversible (see figure 2.11 - A).[170] These are weak forces but large enough in number to provide sufficient binding. The advantages of adsorption as an immobilisation technique include that there is little or no harm to the immobilised biomolecule, it is a simple, inexpensive and fast method of immobilisation, there are no chemical modifications to the support or biomolecule, and the reversibility allows for regeneration. The disadvantages of this method include leaching of the biomolecule from the support (desorption), non-specific binding of other species to the support, support overloading and steric hindrance caused by the support.

Covalent Bonding

The immobilisation is based on the formation of a covalent bond between functional groups on the biomolecule and functional groups on the support (see figure 2.11 - B).[170] These functional groups are normally amino, carboxylic, hydroxyl and thiol groups. The functional groups on the support are usually activated and this is followed by a coupling reaction to form the covalent bond. Most covalent bonding techniques fall under the following reactions: formation of an iso-urea linkage, diazo linkage, formation of a peptide bond and an alkylation reaction. Supports for covalent bonding immobilisation include polysaccharide polymers (cellulose, agarose), porous silica and porous glass.

Entrapment

Entrapment methods are different from adsorption/covalent binding techniques, as the biomolecule is free in solution but restricted by the lattice structure of a gel (see figure 2.11 - C).[170] The porosity of the lattice is controlled to prevent leaching of the entrapped biomolecules, but allows transfer of species to interact with the biomolecule, therefore protecting the entrapped biomolecule from external interferences. Methods of entrapment include: ionotropic gelation of macromolecules with multivalent cations (alginate), temperature induced gelation (agarose, gelatin), organic polymerisation by chemical/photochemical reaction (polyacrylamide), precipitation from immiscible solvent (polystyrene) and sol-gels.

Encapsulation

This is achieved by enveloping the biomolecule within a semi-permeable membrane (see figure 2.11 - D).[170] Like entrapment, the biomolecules are free in solution, but restricted in movement. The semi-permeable membrane allows the passing of small species to interact with the encapsulated larger biomolecule, which cannot pass through the membrane. Common materials used include nylon and cellulose nitrate. The advantage of this approach is the fact that one or more biomolecules can be incorporated into the encapsulated system (co-immobilisation). Disadvantages arise due the problems associated with diffusion; the immobilised species may have the same density as the bulk solution. Rupturing of the membrane may occur if there is a rapid accumulation of species undergoing interaction.

Crosslinking

Crosslinking provides a support free method of immobilisation and incorporates the amalgamation of the biomolecules to each other to form a large complex structure this is achieved by chemical or physical methods (see figure 2.11 - E).[170] Chemical crosslinking involves the formation of a covalent bond between the biomolecules utilising bi/multifunctional reagents (e.g. glutaraldehyde), therefore providing disadvantages from the toxicity of such reagents. Physical crosslinking can be achieved using flocculating reagents (e.g. polyamines, polystyrene sulfonates). Disadvantages of crosslinking as an immobilisation technique arise due to the non-existence of mechanical properties and poor stability.

Covalent attachment to a solid support as a method of immobilisation is preferable due to its increased sensitivity and robustness. This is accomplished due to the optimal presentation of the immobilised species to the reaction, which enhances the sensitivity of the reaction. Robustness is realised due to the conservation of the activity of the immobilised species and by reducing the physical loss of the immobilised species. Therefore solid supports for incorporating within a microfluidic device have been investigated as a support for covalent attachment of reagents.

2.3.2 Solid Supports

Characteristics to consider when choosing a support include:

- The physical properties of the support such as its strength, available surface area, shape and porosity.

- The support's chemical properties such as its inertness towards the biomolecule, available functional groups and its ability to be regenerated or recycled.

- The mechanical stability of the support.

- The resistance of the support towards chemicals, microorganisms (bacteria/fungi), pH, temperature and solvents.

- The biocompatibility of the support.

- The expense of the support.

2.3.2.1 Solid Supports for Microfluidic Devices

Open microchannels do offer a large surface to volume ratio for immobilisation, however in order to achieve high loadings solid supports can be introduced into a microfluidic device to improve this surface to volume ratio. This means that there is an increase in the binding surface allowing for a higher loading of reagent and an improvement in transport to the reactive surfaces because of the decrease in diffusion distances which improves the surface interaction efficiency. Several methods of incorporating solid structures within microfluidic devices have been demonstrated, including packing devices with beads, using membranes, producing supports through

microfabrication techniques and creating gels and polymer monoliths within the channels.[57, 58]

Beads have commonly been employed in FIA to immobilise reagents, they are relatively inexpensive and provide a high surface to volume ratio.[57, 58] The beads can be made from a variety of different materials including synthetic organic polymers such as polystyrene and polyacrylamide, organic biopolymers such as dextran and chitin, and synthetic inorganic materials such as glass (controlled pore) and silica. The problem associated with using beads is the requirement to keep the beads within the channels, this can be achieved two ways (i) trapping the beads or (ii) immobilising the beads.

Different geometries of microfluidic devices have been presented in order to trap beads within a channel. Andersson *et al.* detailed that a series of pillars could be used to contain beads (< 5.5 μm) within a microfluidic device.[171] Sato *et al.* demonstrated the formation of "dams" by restricting the height of the channels to constrain the beads (45.6 μm).[172] Oleshuk *et al.* produced a chamber within a microfluidic device in which the beads were packed in one direction and the system flow was from a different direction thereby trapping the beads.[173] Ceriotti *et al.* utilised a tapered channel geometry whereby the "keystone effect" is used to draw a slurry of beads into a narrower taper in order to trap them.[174] Packing beads within a microfluidic device provides a simple and relatively inexpensive method of incorporating solid supports. The alternative to packing beads is to immobilise the beads within the channels. Andersson *et al.* modified the surface of a channel by microcontact printing with a biotin labelled bovine serum albumin and used beads coated with the

complimentary protein streptavidin forming a self assembled monolayer within the channel.[175]

Magnetic particles have been utilised within a microfluidic devices, the main application of these is in the area of microimmunoassays (see section 4). Nomura *et al.* also used magnetic particles as a solid support for the immobilisation of enzymes within a microfluidic device.[176] Magnet particles offer the simple manipulation of the particles through the channel by use of a magnet; however the major drawback is the expense of the beads.

Membranes also provide an approach to incorporating solid supports into microfluidic devices. The easiest way to achieve this is to sandwich the membrane between the plates of the microfluidic device as shown by Xiang *et al.*[177]An alternative is to fabricate the membrane within the channel, which proves more difficult as documented by Park *et al.*[178] The disadvantage of using membranes as a solid support is their limitations to applications.

Microlithographic techniques have also been demonstrated as a method of fabricating solid supports within microfluidic devices. He *et al.* fabricated an LC column within a microfluidic device by producing many pillars within the channel that can be coated with the stationary phase.[179] This approach is advantageous for large-scale production as it provides an inexpensive and reproducible method for mass produced devices. However, on a smaller scale this approach can prove expensive.

More recently hydrogels (gels which contain high levels of water) and sol-gels (siloxane monolith structures) have become more commonly used in analytical

applications. Biomolecules can be encapsulated within a gel within a microfluidic device as demonstrated by several groups.[180-182] Limitations to this technique are due to the difficulty of preparing the gels within a device, this is partly overcome using photoinitiated polymerisation methods. Another disadvantage of this approach is the poor reproducibility between batches.

Porous polymer monoliths provide a method of incorporating a solid support within a device and are produced by UV initiated polymerisation of monomers in the presence of a progen. The UV initiation allows the monoliths to be formed in specific areas of the channels. Peterson *et al.* used this approach to produce a dual function microfluidic device containing a solid-phase extractor and an enzyme reactor.[57] A chip based solid phase extractor was also demonstrated by Tan *et al.*[183] and Yu *et al.*[184] Throckmorton *et al.* used porous polymer monoliths to produce a microfluidic device for reverse phase electrochromatography.[185] Again as with hydrogels and sol gels a disadvantage to this technique is the problem of irreproducibility between batches.

2.3.2.2 Selection of Solid Support and Manifold for Packed Reagents

Beads provide an attractive cost effective approach to incorporating solid supports within a microfluidic device for immobilising reagents, with good reproducibility between batches compared to other techniques, therefore a microfluidic device for packed beads with the keystone effect for bead trapping has been designed. Applications for this are discussed in the individual chapters.

2.3.3 Design of Channel Manifold

A tapered design has been created due to ease of fabrication, and the "keystone effect" is used to pack the device with the beads (figure 2.12). Again, the base plate containing the etched channels were fabricated by MCS (Micro Chemical Systems, Hull, UK) and the top plate, including the inlet holes was thermally bonded in-house (see section 2.2.2).
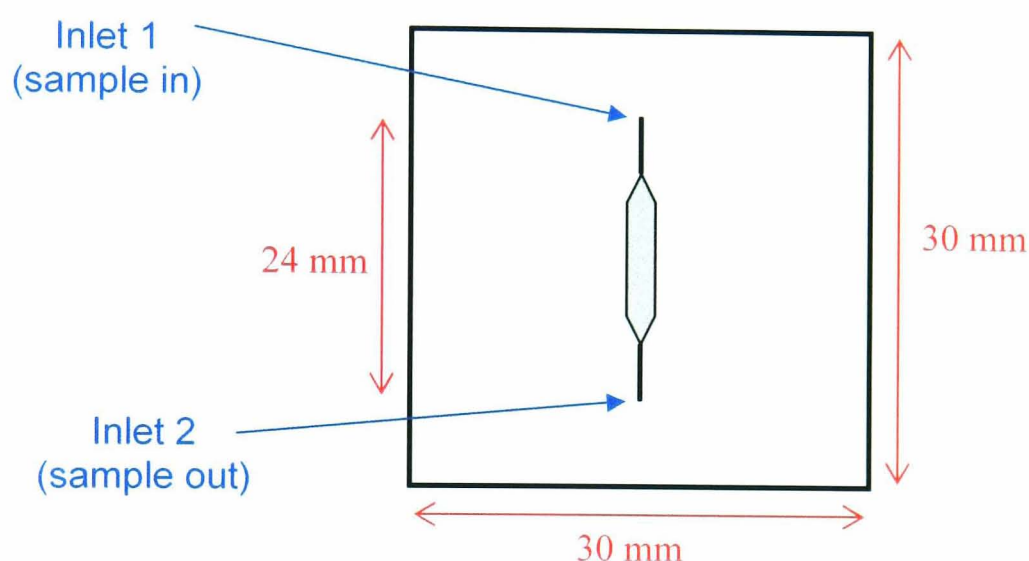
Figure 2.12 Design manifold for a microfluidic device for packing beads using the keystone effect.

2.3.3.1 Laser Ablation for Channel Deepening

The original base plates containing the channel manifold for the packed reagents provided by MCS (Micro Chemical Systems, Hull) contained a channel depth of 60 μm. The CPG obtained from Sigma (Poole, Dorset, UK) has a particle size ranging from 37 – 125 μm. Therefore a section of the channel had to be deepened in order to incorporate the beads. Further etching of the designated area cannot be easily achieved due to the non-discriminating nature of the etching solution; therefore an alternative method was required. Laser ablation has the advantage of creating

channels in specific areas of the device and was investigated as a method for deepening the channel. Before the top plate was thermally bonded to the channels, laser ablation was used to deepen a specific section of the packing area using an argon fluoride excimer laser (λ = 193 nm), a filter was used to direct the laser to the required section. Channel depth profiling using white light inteferometry (VEECO, WYKO NT1100 optical profiling system) shows that the depth of the deepened channel in the packing area has been increased to124 μm (figure 2.13 and 2.14).
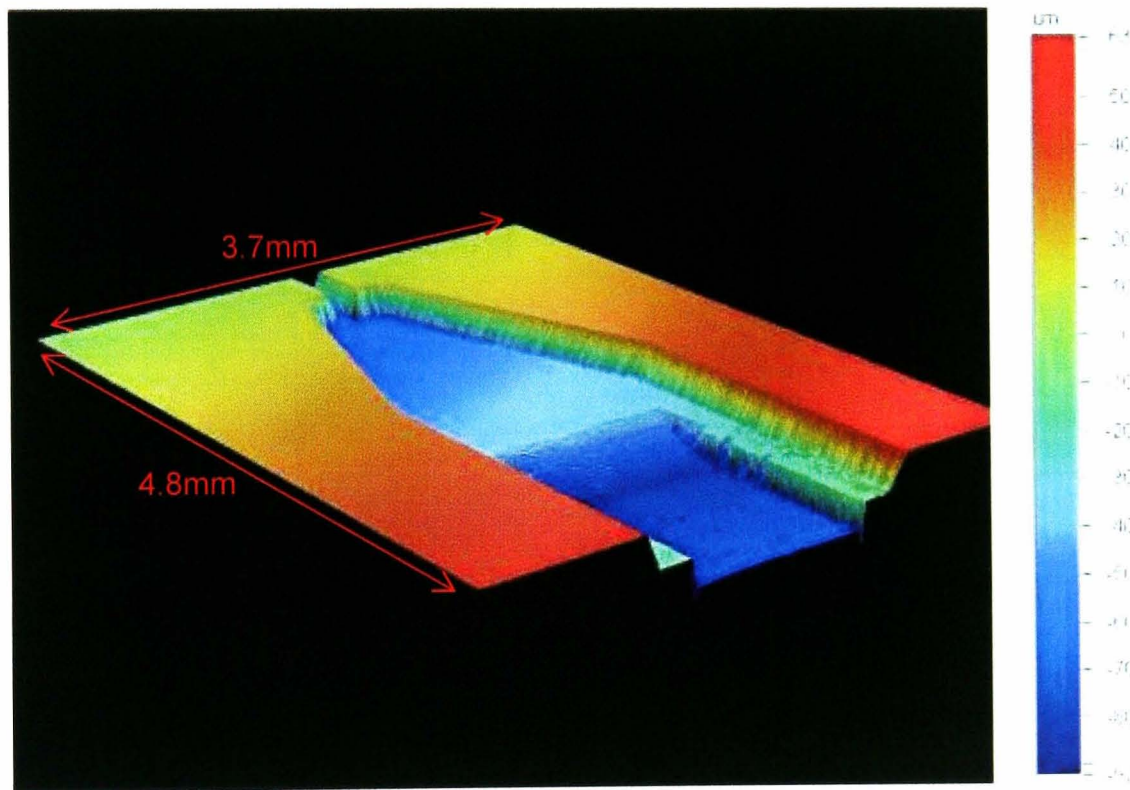
Figure 2.13 3D profile showing where laser ablation was used to deepen the microchannel (x 12.5), taken using whitelight interferometry.
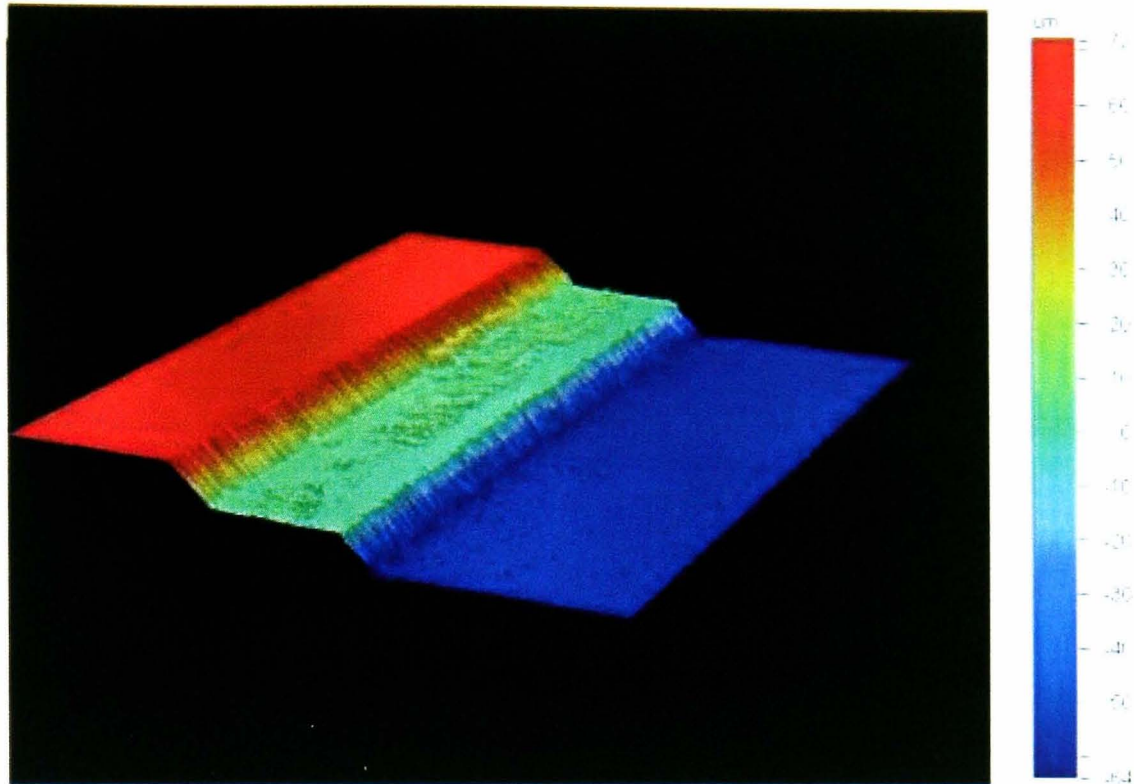
Figure 2.14 3D cross sectional profile showing where laser ablation was used to deepen the micrchannel (x 12.5), taken using whitelight interferometry. Where the red section is the surface of the device, the green area is the etched channel area and the blue area is the deepened laser ablated channel.

Laser ablated area

10 mm
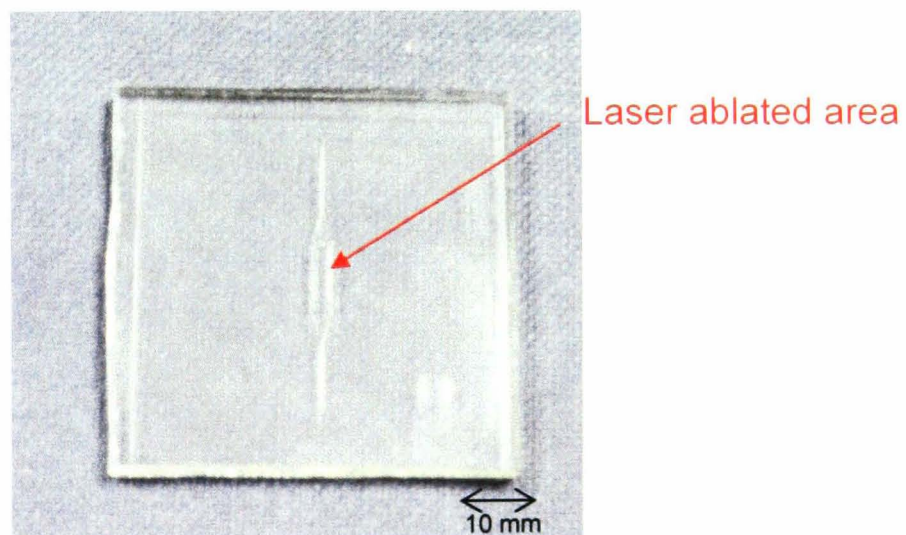
Figure 2.15 Photograph showing the chemically etched channels and laser ablated deepened channel for the packed microfluidic device.

The effect of the laser ablation on the surface of the channel was investigated by measuring the surface roughness (VEECO, WYKO NT1100 optical profiling system). Roughness is the measure of closely spaced irregularities or texture of a surface, the arithmetic mean of the absolute values of the surface departures from the mean of the plane. The Ra values (roughness average) are given in table 2.3. It can be seen that the laser ablation has produced a surface 70 times rougher than the original surface (figure 2.16).

Table 2.3 Ra values for the surfaces of the microfluidic device.

Surface	Roughness (Ra) (nm)
Glass	5.4
Chemical Etched	12.7
Laser ablation	388.8
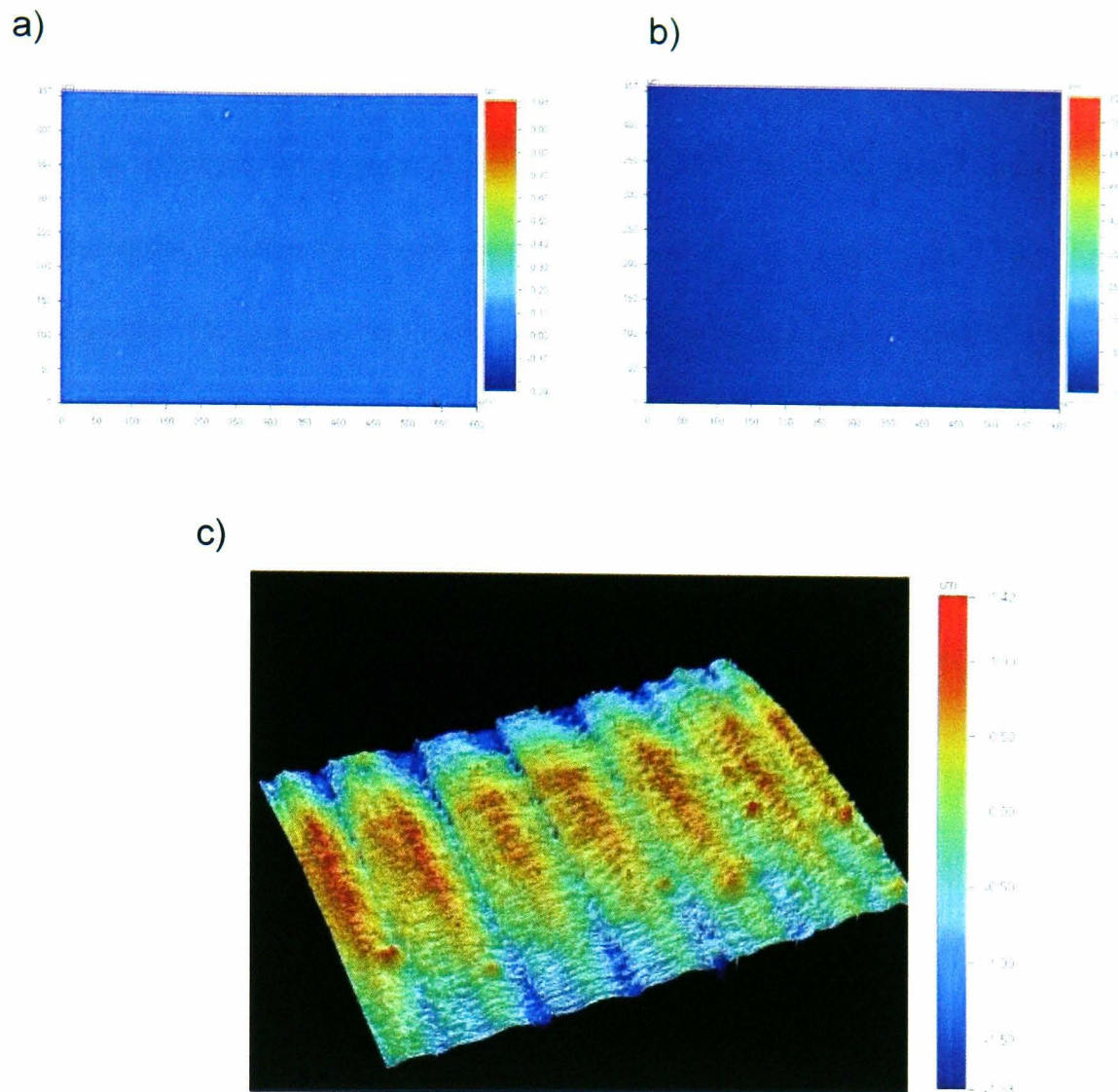
Figure 2.16 Profiles of the different microchannel surfaces a) untreated glass b) chemically etched glass and c) laser ablated glass.

The roughening of the channel surface can be advantageous for two reasons, firstly by roughening the surface mixing within a microfluidic device can be improved as the laminar flow is manoeuvred in order to create chaotic advection, as discussed in section 1.2.6. Secondly, it increases the surface area of the channels, which is of advantage for immobilising reagents in order to achieve high loadings.

The beads can be slurry packed into the device through a central inlet (figure 2.17) and the packed area can sit above the PMT for detection. Photographs of the microfluidic device for bead packing are given in figure 2.18. The specific beads chosen for the support are controlled porosity glass beads (CPG). CPG is a micro-porous glass powder, with a majority composition of pure silica. CPG has a particularly rigid structure and is very chemically inert. It has very high specific surface area, which provides many sites for chemical attachment or adsorption. The pore structures are precisely controlled and uniform which allows for good spatial distribution of immobilised species. A wide range of particle sizes and porosity are available and must be optimised for the application. CPG is free from swelling thus making it an ideal packing media for microfluidic devices.
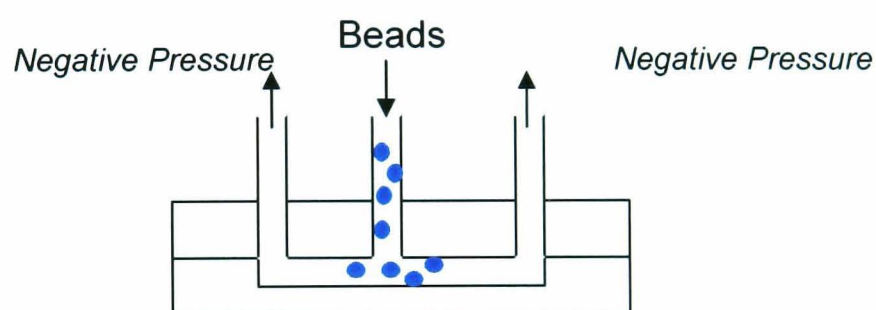
Figure 2.17 Procedure for slurry packing beads within a microfluidic device using a central inlet.
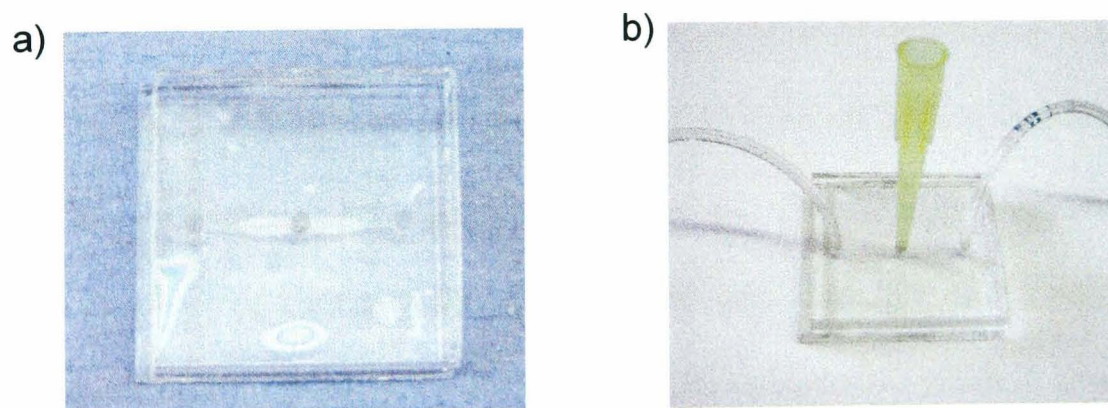
Figure 2.18 Photographs of the packed reactor microfluidic device where a) shows the etched channels with a top block with three holes for slurry packing the beads through a central inlet and b) shows the fluidic connections to the channels.

A device has been developed to enable beads to be packed within it. Laser ablation was used to deepen a certain area of the packing area to give a depth of 124 μm to enable amenable packing of the beads.

2.4 Conclusions

A portable chemiluminescence detection system was developed to provide a detection system for chemiluminescence reactions within microfluidic devices. A miniaturised peristaltic pump was used to continuously introduce samples and reagents into a microfluidic device situated above a miniaturised PMT, protected by a shutter. This was all contained within a light tight housing to prevent interference from external light.

Photolithography and wet etching was discussed as the fabrication process used for channel etching for the microfluidic devices supplied for the work and thermal bonding is described as the procedure to bond the glass plates together. Investigation into mixing showed a serpentine manifold gave improved mixing over a T-shape design and so has been selected for future work in this thesis (see chapter 3).

Immobilisation techniques were assessed for the purpose of developing a reagentless assay. Covalent bonding was identified as a suitable immobilisation technique, which lead to the investigation of solid supports for their compatibility with microfluidic devices in order to increase the surface area and therefore the loading of the immobilised species. Packed beads presented an inexpensive method of increasing the surface area within the channels, based on this a device was designed and fabricated utilising a tapered design to se the keystone effect to pack the beads within the device. The original channel depth was 60 μm, laser ablation was used to deepen

part of the packing area to 120 μm to improve packing. This provided a working device which can be used with reagents immobilised onto beads (see chapter 4).

Future work is to automate the system and incorporate a data logger in order to make the system more amenable to being used in the field. This is discussed in more detail in section 3.4.

Chapter 3

Determination of Hydrogen Peroxide in Rainwater in

a Miniaturised Analytical System.

3. Determination of Hydrogen Peroxide in Rainwater in a Miniaturised Analytical System

3.0 Aims

The hydrogen peroxide present in rainwater is an efficient oxidiser of sulphur dioxide to produce sulphuric acid, an important compound in acid rain formation. A portable, sensitive method of analysis is required to measure real time hydrogen peroxide levels in rainwater during a rainfall event. The aim of this work was to develop a system that could be taken and left in the field in order to analyse at least one entire rainfall event. Hydrogen peroxide levels in rainwater are at the micromolar level and therefore the method used had to be sensitive enough to measure this range. A fast sample analysis time is essential to enable rapid sampling of the rainwater, with the aim of sampling at least every 5 minutes depending on the rainfall rate.

The luminol-cobalt(II) chemiluminescence reaction is a sensitive method for hydrogen peroxide detection. This was investigated within a microfluidic device using a portable chemiluminescence detection system in order to produce a field deployable miniaturised analytical system for the determination of hydrogen peroxide in rainwater. Immobilisation of luminol onto a solid support was also explored in order to develop a reagentless system, which would make the instrumental set up even simpler for field use.

3.1 Introduction

3.1.1 Hydrogen Peroxide in Rainwater

Gas phase hydrogen peroxide is mainly formed in the troposphere from hydroperoxyl radicals (HOO·), products of photochemical chain reactions of atmospheric gases such as ozone and volatile organic compounds (equation 3.1). [186-189] Hydrogen peroxide in the gas phase is removed by several mechanisms including, photolysis, hydroxyl radical reaction and heterogeneous processes including rainout, washout and dry deposition. [188]

$$HOO· + HOO· \longrightarrow H_2O_2 + O_2 \qquad \textit{(Equation 3.1)}$$

Hydrogen peroxide has a high Henry's law constant (2×10^5 mol L^{-1} atm^{-1} at 15°C); therefore hydrogen peroxide is highly soluble and can dissolve in cloud and rain droplets. The main source of hydrogen peroxide in water is from gas phase hydrogen peroxide, although in-cloud processes can also contribute to the formation of hydrogen peroxide in the liquid phase including the disproportionation of scavenged peroxy radicals and photochemical reactions of dissolved organic substances in-cloud. The concentration of hydrogen peroxide varies from $10^{-4} - 10^{-7}$ mol L^{-1} in rainwater.

Hydrogen peroxide is an efficient oxidiser of sulphur dioxide to produce sulphuric acid, the main compound in acid rain formation. In atmospheric droplets, sulphur dioxide (SO_2) is hydrated and ionised to give the bisulphite ion (HSO_3^-) (equation 3.2 and 3.3).

$$SO_2 + H_2O \rightleftharpoons H^+ + HSO_3^- \qquad \textit{(Equation 3.2)}$$

$$HSO_3^- \rightleftharpoons H^+ + SO_3^{2-} \qquad \text{(Equation 3.3)}$$

Hydrogen peroxide oxidation is particularly important in that the oxidation of sulphur dioxide by H_2O_2 is fast even at pH's less than 5, whereas oxidation by other compounds, e.g. oxygen or ozone, is slow.[188] Equation 3.4 shows the oxidation.

$$HSO_3^- + H_2O_2 \longrightarrow SO_4^{2-} + H_2O + H^+ \qquad \text{(Equation 3.4)}$$

It has been found that there is a seasonal variation of hydrogen peroxide concentrations, with highest concentrations occurring during the summer months, this evidence suggests that photochemistry is a key factor in the formation of hydrogen peroxide. Hydrogen peroxide is also present in sea water at subnanomolar levels, where it is also thought to be involved in redox reactions in particular the speciation of trace metals and oxidation reactions of organic compounds.[190]

3.1.2 Hydrogen Peroxide Detection

Hydrogen peroxide in rainwater has been analysed by several different methods. A fluorometric method was demonstrated by Ortiz *et al.* based on the oxidation of *p*-hydroxyphenylacetic acid (POPHA). It was used in the analysis of rainwater samples taken from Santiago of Chile City, which showed an average hydrogen peroxide concentration of 5.5 μmol L^{-1}.[191] Tanner *et al.* utilised a spectrophotometric determination using the formation of the stable orange-red complex oxo-peroxo-pyridine-2,6-dicarboxylatovanadate (V) (OPDV) in acid media from hydrogen peroxide with pyridine-2,6-dicarboxylic acid and vanadate in acid. This method showed an LOD of 5.8 nmol L^{-1} for a 20 cm^3 sample size. Samples taken from Kowloon, Hong Kong showed an average hydrogen peroxide concentration of 15.9 μmol L^{-1}.[192] Lvovich *et al.* detailed an amperometric hydrogen peroxide sensor based

on a glassy carbon microelectrode with an electrodeposited polypyrrole/horseradish peroxidase membrane with a working range of 0.1 - 100 μmol L^{-1}.[193] Zhang *et al.* analysed hydrogen peroxide in rainwater using square wave voltammetry which produced a dynamic range of 0.5 – 1000 μmol L^{-1}.[194]

Chemiluminescence detection coupled with Flow Injection Analysis (FIA) has been a popular method of analysis for hydrogen peroxide. Price *et al.* developed a FIA with chemiluminescence for the determination of hydrogen peroxide in seawater.[195-197] This was based on the luminol-cobalt-hydrogen peroxide system and achieved an LOD of 5 nmol L^{-1} in seawater for a 100 μL sample size. A luminol chemiluminescence method with cobalt(II) as the cooxidant for FIA with reagent injection was detailed by Yuan and Shiller for the determination of hydrogen peroxide in sea water in the subnanomolar concentration range.[198] The method documented pre-mixing of the chemiluminescence reagents i.e. cobalt and luminol in an alkaline solution, prior to analysis, with the advantages that this system is simpler and easier to use and it purifies the reagents prior to analysis by removing the hydrogen peroxide from the buffer. This method gave an LOD of 0.42 nmol L^{-1} for a 60 μL sample volume. Cobalt was chosen as the catalyst as it has been found from the literature to be the most efficient catalyst for this reaction. Yuan *et al.* also applied this method to the analysis of rainwater collected from over the South and Central Atlantic Ocean showing levels varied from 3.5 to 71 μmol L^{-1}.[199] Escobar *et al.* reported using Cr(III) as a catalyst in the luminol reaction for the application of determining hydrogen peroxide in cultures of microalgae.[200] Zhou *et al.* presented a luminol–KIO_4–H_2O_2 CL system for the determination of hydrogen peroxide, based on the hydrogen peroxide having a co-oxidative effect on the oxidation of luminol by

KIO$_4$, producing a method with an LOD of 30 nmol L^{-1} for a 30 μL sample.[201] Ma *et al.* synthesized the novel chemiluminescence reagent 7-(4,6-Dichloro-1,3,5-triazinylamino)-4-methylcoumarin (DTMC) for the determination of hydrogen peroxide in snow water in a static system, achieving an LOD of 40 nmol L^{-1} for a sample volume of 100 μL.[202] Lin *et al.* also determined hydrogen peroxide in snow water, using the chemiluminescence reaction of periodate with hydrogen peroxide in an aqueous alkaline solution, with potassium carbonate as an enhancer, producing a method with an LOD of 5 nmol L^{-1} for a sample volume of 90 μL.[203]

Chemiluminescence sensors have been discussed by several groups, incorporating the immobilisation of reagents to produce reagentless systems. Reagentless systems are advantageous for portable systems, as it makes the instrumentation even simpler. Therefore immobilisation techniques of luminol have been investigated. The luminol reaction is irreversible as the luminol is used up in the reaction, thus limiting its use as a sensor. A high loading would be required to enhance the sensor lifetime. A chemiluminometric hydrogen peroxide sensor for flow injection analysis was described by Janasek *et al.*, hydrogen peroxide was detected chemiluminometrically in the presence of luminol at either cobalt or copper foils, achieving an LOD of 0.1 μmol L^{-1} for a 2.2 μL sample size.[204] Qin *et al.* reported a flow injection chemiluminescence sensor utilizing the electrostatic immobilisation of luminol and copper ions on an anion exchange resin and a cation exchange resin, respectively. The reagents were eluted under alkaline conditions to react with hydrogen peroxide in rainwater samples. An LOD of 32 nmol L^{-1} was achieved.[205] Qin *et al.* went on to detail a similar sensor with cobalt(II) immobilised onto cation exchange resin, which

slightly improved the LOD to 12 nmol L^{-1}.[206] Hanaoka *et al.* utilised a cobalt(II)

ethanolamine complex immobilised onto an anion exchange resin incorportated

within a flow injection system with luminol chemiluminescence, which produced an

LOD of 0.1 µmol L^{-1}.[207] Díaz *et al.* utilised the horseradish peroxidase (HRP)

catalysed luminol hydrogen peroxide reaction and immobilised HRP in sol gel

crystals *via* microencapsulation to produce a sol gel HRP biosensor. The

disadvantages of this system were that the LOD was only in the 10^{-4} mol L^{-1} range

and the biosensor had a single use lifetime.[208] Li *et al.* also developed a flow

biosensor based on the immobilisation of HRP with sol gel, incorporating luminol

immobilisation on anion exchange resin to produce a precise, rapid, sensitive

response from the sol gel positioned in front of the PMT with LODs in the 10^{-7} mol

L^{-1} range.[209] Li *et al.* went on to immobilise haemoglobin as the catalyst in the

system by the sol gel method, achieving similar limits of detection.[209] Zhou *et al.*

also used luminol on ion exchange resin and incorporated the HRP catalyst on to a

biocompatible chitosan membrane on the flow cell to produce a reagentless system

with an LOD of 10 nmol L^{-1}.[210] Controlled pore glass has also been used a support

for luminol immobilisation *via* a (aminoalkyl) silane-glutaraldehyde linkage as

demonstrated by Nieman *et al.*. Luminol was eluted from the support by hydrolysis

and an LOD of 1-2 µmol L^{-1} was achieved using this technique coupled with

cobalt(II) as the cooxidant.[211-213]

3.1.3 Hydrogen Peroxide Detection Within a Microfluidic Device

The determination of hydrogen peroxide demonstrated previously using microfluidic devices (section 1.2.7.2 and 1.3.5, which is summarised in table 3.1) are not amenable for the analysis of rainwater as the limits of detection are too high to cover the micromolar levels of hydrogen peroxide in rainwater.

Table 3.1 Comparison of chemiluminescence detection methods of hydrogen peroxide within microfluidic devices.

Chemiluminescence Reaction	Application	LOD (μmol L^{-1})	Reference
Luminol-Co(II)-H_2O_2	H_2O_2	100	155
Luminol-hexacyanoferrate-H_2O_2	Glucose	10	162
Luminol-ferricyanide- H_2O_2 (immobilised reagents on ion exchange resin)	Glucose	100	163
Luminol-HRP- H_2O_2	Uric acid	3	164

In this work the luminol-hydrogen peroxide reaction with cobalt as a cooxidant within a microfluidic device was investigated to produce a miniaturised analytical system for the determination of hydrogen peroxide in rainwater at the low micromolar level.

3.1.4 Theory of Luminol Chemiluminescence

As previously discussed in section 1.3.3.1, the chemiluminescence reaction of luminol consists of the oxidation of the luminol in alkaline conditions, usually in the presence of a cooxidant to produce the 3-aminophthalate ion in the excited singlet state, which emits light on returning to the ground state. Nitrogen and water are also produced from the reaction (figure 3.1).[158]
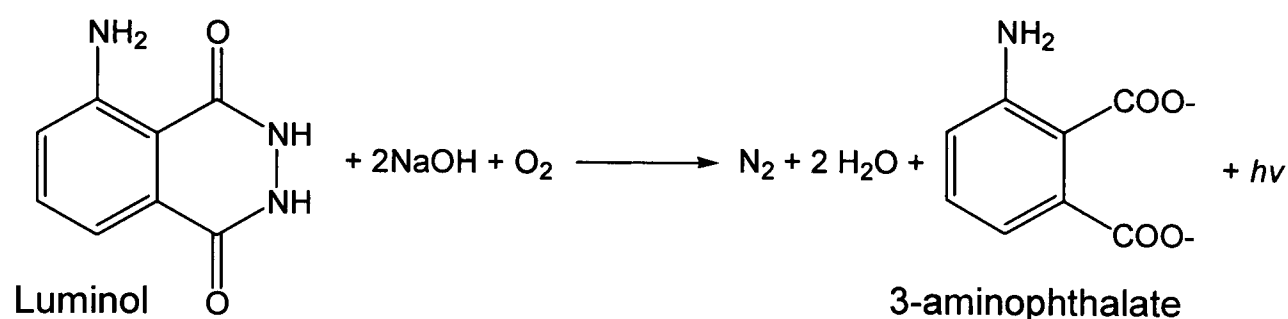
Figure 3.1 The luminol reaction, where luminol is oxidised in alkaline conditions to produce the 3-aminophthalate ion.[156]

Several oxidising agents can be utilised for the oxidation of luminol including hydrogen peroxide, hypochlorite, permanganate, oxygen, iodine and nitrogen dioxide. If hydrogen peroxide or oxygen is used as the oxidant, an initiator or cooxidant is required, these typically include persulfate, hypochlorite, peroxidase, ferricyanide, heme compounds, and transition metal ions including cobalt(II), chromium(III), copper(II), nickel(II), and iron(II). Cobalt(II) has been reported as the most efficient cooxidant as opposed to enzymes, which are expensive and produce solutions that are unstable.[156] The cooxidant horseradish peroxidase (HRP) is discussed separately in section 4.1.2.3.

The reaction can be carried out in protic media (water) or aprotic media (dimethysulphoxide (DMSO) or dimethylformamide (DMF)). In aqueous media emission occurs at 425 nm producing blue light and in aprotic media the reaction occurs at the longer wavelength of 510 nm producing green light. The shift in frequency is due to the presence of the quininoid tautomer, which can be formed in the aprotic media (figure 3.2). This species is not present in aqueous media because of the reduced basicity of the carboxylate groups hydrogen bonded to water molecules. The luminol reaction is one of the most efficient chemiluminescence reactions with a quantum yield of 0.01 in water and 0.05 in DMSO.[214]

3-aminophthalate   Quininoid tautomer
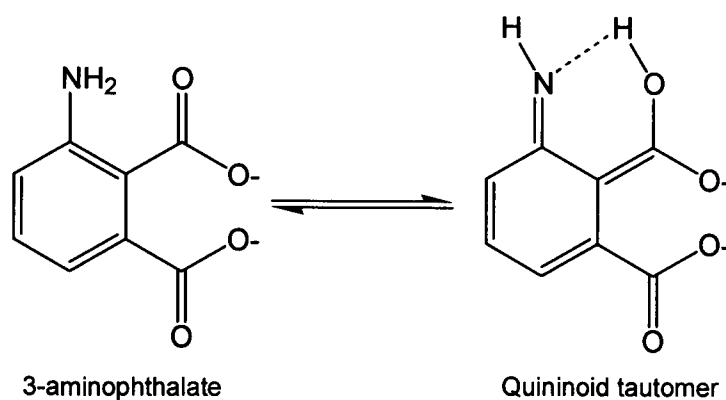
Figure 3.2 Formation of the quininoid tautomer from the 3-aminophthalate ion.[214]

The mechanism for the oxidation of luminol is still not fully understood. In aprotic media it has been shown that the reaction consists of the formation of the critical intermediate, a dinegative ion, following equilibrium with the base, which is then oxidised to give the 3-aminophthalate ion, and that this reaction is first order with respect to all the reactants,[215, 216] as shown in figure 3.3 taken from reference 160.
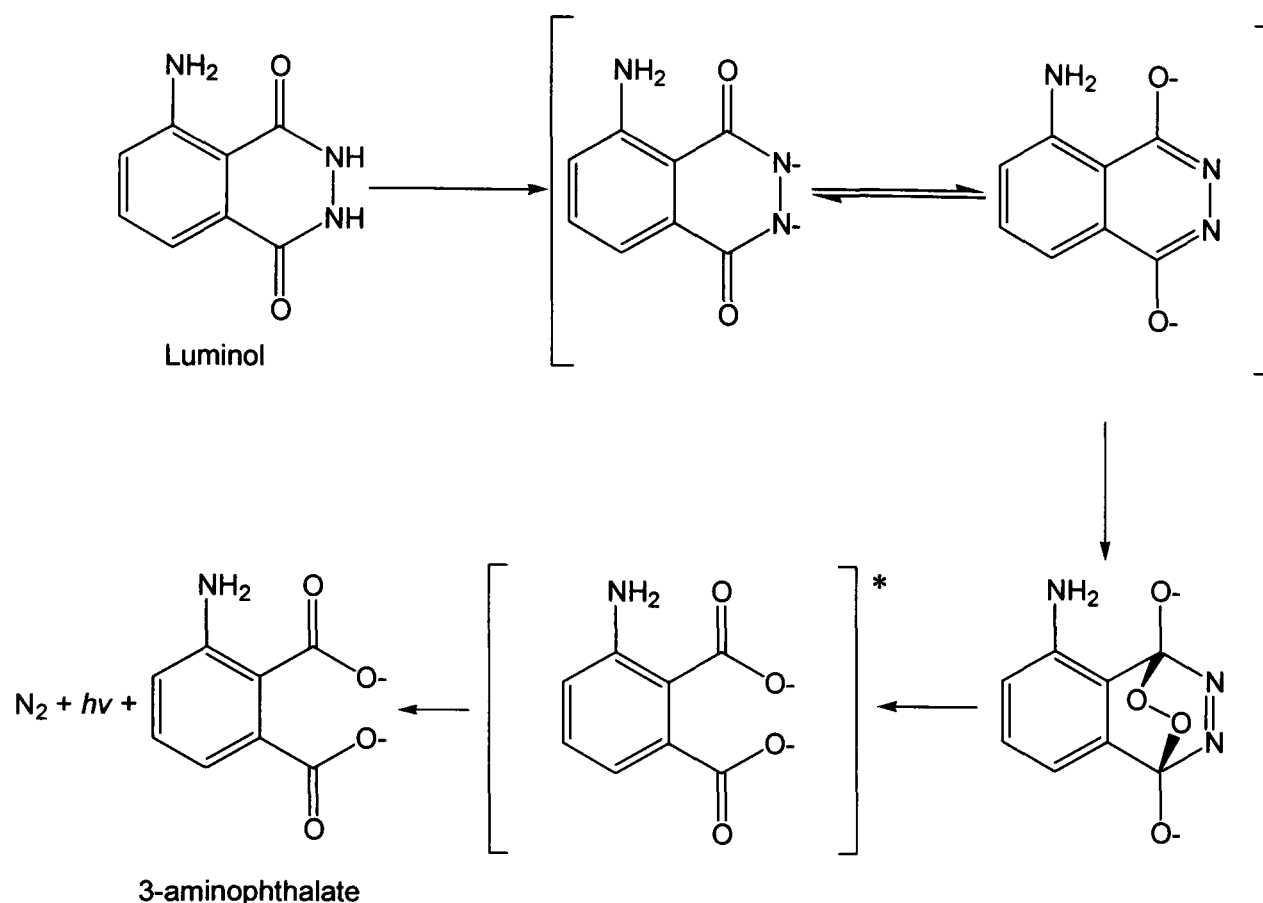
Figure 3.3 Proposed mechanism for the oxidation of luminol in aprotic media.[160]

For aqueous media the chemiluminescence producing mechanism for the oxidation of luminol has been suggested by Merenyi *et al.* to occur in three basic steps and to include (i) the oxidation of luminol to produce a luminol radical, (ii) the oxidation of the luminol radical to produce the key intermediate, α-hydroxyhydroperoxide, (iii) the decomposition of α-hydroxyhydroperoxide.[217-221] This is summarised in figure 3.4.[222]

In step one, the luminol undergoes a one electron oxidation to form the luminol radical, when using a transition metal and hydrogen peroxide, the primary oxidant is likely to be OH· (see equation 3.5). Superoxide (O_2^-) has been proved to be an unsuccessful primary oxidant.[219]

$$M^{2+} + H_2O_2 \longrightarrow M^{3+} + OH^- + OH^·$$ *(Equation 3.5)*

93

In step two, the luminol radical undergoes secondary oxidation to produce what is thought to be the key intermediate, α-hydroxyhydroperoxide. This can be formed *via* one of two pathways: one pathway incorporates the direct oxidation of the luminol radical by superoxide to produce α-hydroxyhydroperoxide, this can only occur if the monoanion form of the luminol radical (L^-) is present. The other pathway incorporates the formation of another intermediate, diazaquinone (L), which is then oxidised by monodissociated hydrogen peroxide (HO_2^-) to produce α-hydroxyhydroperoxide and occurs when the monoanion (L^-) or undissociated (LH^-) form of the luminol radical is present. Diazaquinone can be produced either by the recombination of the luminol radical (fast reaction 2.5×10^9 mol L^{-1} s^{-1}) or by the reaction of molecular oxygen with the luminol radical (slower reaction 5.5×10^{-2} mol L^{-1} s^{-1}). A by-product from this oxidation is superoxide, which can then be used in the alternative pathway reaction.

Finally in step three, the α-hydroxyhydroperoxide decomposes to produce 3-aminophthlate and nitrogen. The α-hydroxyhydroperoxide deprotonates in aqueous solution and depending on the pH may be present in the monoanion or undissociated form, only decomposition of the monoanion produces an excited state and therefore chemiluminescence emission, indicating the chemiluminescence yield is dependent on the pH. The chemiluminescence efficiency is observed to amplify towards approximately 10.5 due to the increase in monoanion production.
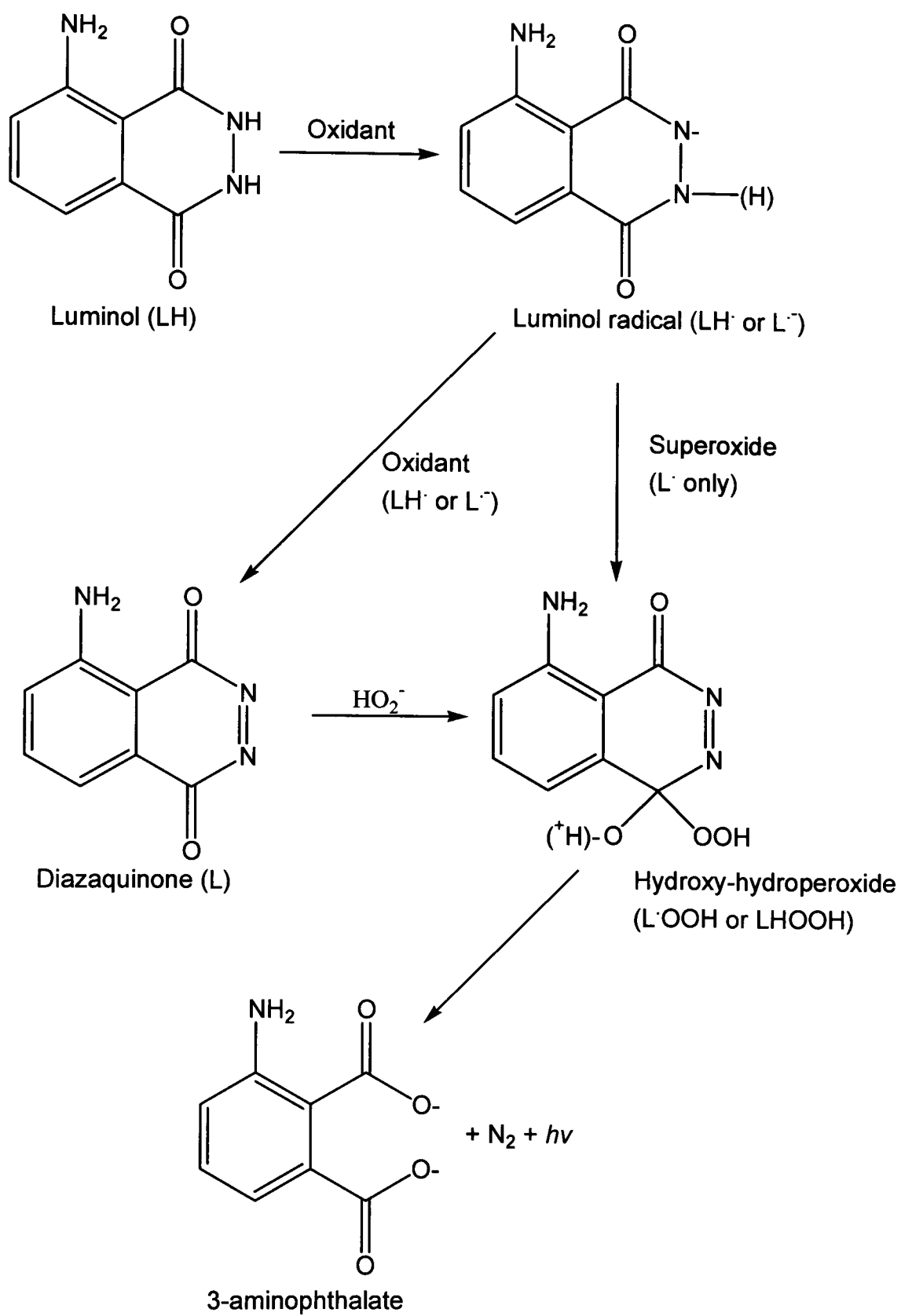
Figure 3.4 The three major steps in the oxidation of luminol in aqueous solution.[227]

3.2 Experimental

The luminol reaction using cobalt(II) as a cooxidant was investigated to determine its potential within a micro reactor for the determination of hydrogen peroxide. This reaction was chosen as it had been widely used previously, and provided a sensitive method to use for hydrogen peroxide detection. Cobalt was used as the cooxidant in the reaction because it had previously been identified as a stable, robust and efficient cooxidant in this reaction.[197, 198] Enhancement of the chemiluminescence signal was investigated by means of applying a reflective surface to the microfluidic device. Immobilisation of the luminol onto CPG was also investigated in order to produce a reagentless system.

The portable chemiluminescence detection system used for this experiment is described in detail in section 2.1.2.

3.2.1 Reagents and Standards

Luminol Chemiluminescence Reaction for the Determination of Hydrogen Peroxide

All reagents were analytical grade and prepared from high purity deionised water ((18 MΩcm) resistivity, Elgastat UHQ PS, Elga, High Wycombe). To reduce the background chemiluminescence of the blank samples, hydrogen peroxide was removed from the water used in the preparation of all of the solutions using a method detailed by Price *et al.*[197] MnO_2 is immobilised onto Amberlite XAD7 (Fluka) a non-ionic macroreticular polymeric resin, which is packed into a column. Hydrogen peroxide in the water passing the column is removed according to the reaction shown in equation 3.6. The column was prepared as follows: potassium permanganate was

heated, and the amberlite XAD7 resin was added and maintained for 15 minutes. The resin was washed and filtered and packed into a glass column.

$$MnO_2 + H_2O_2 + 2H^+ \rightleftharpoons Mn^{2+} + O_2 + 2H_2O \qquad (Equation\ 3.6)$$
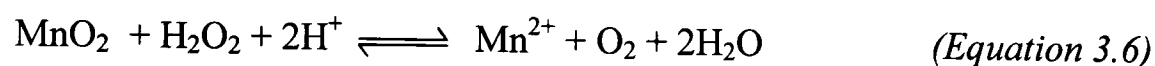
For the chemiluminescence reaction, sodium carbonate, luminol, and 30 %v/v hydrogen peroxide were obtained from Fluka (Poole, Dorset, UK). Cobalt(II) nitrate hexahydrate and hydrochloric acid were obtained from Fisher Scientific UK (Loughborough, UK) and potassium permanganate was obtained from BDH Chemicals Ltd. (Poole, Dorset, UK). The luminol stock and working solutions were prepared in 0.1 mol L^{-1} sodium carbonate and the pH was adjusted with 2 mol L^{-1} hydrochloric acid using a Hanna Instruments pH meter. Pre-mixing of the chemiluminescence reagents (cobalt and luminol in an alkaline solution) prior to analysis has the advantages of producing a simple manifold and it purifies the reagents prior to the chemiluminescence occurring by removing hydrogen peroxide from the buffer allowing for improved limits of detection for the analysis.[198] The final chemiluminescence reagent working solution was prepared by serial dilution of the luminol stock solution and spiking with cobalt(II) to the required concentration (see section 3.3.1). It has been reported that luminol solutions are at their most active approximately 24 h after preparation and stable for 2 months,[197] therefore the luminol solution was left for 24 h before use. The stock solution of hydrogen peroxide was prepared daily and standardised using 0.02 mol L^{-1} potassium permanganate according to the method adapted from Vogel,[223] utilising the reaction shown in equation 3.7. The standards were prepared by serial dilution of the stock solution.

$$2MnO_4^- + 5H_2O_2 + 6H^+ \rightleftharpoons 2Mn^{2+} + 5O_2 + 8H_2O \qquad (Equation\ 3.7)$$
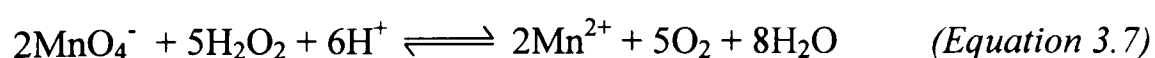
Preparation of a Reflective Surface

The *mirror reaction* was used to apply a reflective surface to the microfluidic device.[224] Potassium hydroxide, silver nitrate, glucose, ammonia and methanol were all obtained from Fisher Scientific UK (Loughborough, UK). To prepare the silver surface, 3.2 % m/m potassium hydroxide was added dropwise to 3 mL of 2 % m/m silver nitrate until the silver oxide precipitate was formed. To this, 30 % m/m ammonia solution was added dropwise until the precipitate dissolved completely to form $[Ag(NH_3)_2]^-$. This was followed by the dropwise addition of 6% m/m silver nitrate until a pale yellow brown solution was produced. 6 % m/m ammonia was then added until this solution became clear. The clear solution was mixed with 1mL 35 % m/m glucose and 0.5 mL methanol to produce a black solution. The upper surface of the microfluidic device was coated with this black solution and left for an hour at 50 °C. The surface was cleaned with water and sealed using grey primer spray paint.

Immobilisation of Luminol

For the immobilisation of luminol onto different solid supports, the strongly basic anion exchange resin (Ambersep 900 (OH)) and sodium hydroxide were obtained from Fluka (Gillingham, Dorset, UK). Controlled pore glass (CPG) (different specifications), 3-aminopropyltriethoxysilane (APTS), (3-mercaptopropyl) trimethoxysilane (MTS), N-succinimidyl 4- maleimidobutyrate (GMBS) and glutaraldehyde (25%) were obtained from Sigma (Poole, Dorset, UK). Ethanol, sodium hydroxide, nitric acid and toluene were purchased from Fisher Scientific UK (Loughborough, UK). Dimethyl sulfoxide (DMSO) was obtained from Avocado (Heysham, Lancashire, UK). Individual immobilisation procedures are discussed in the results section.

3.3   Results and Discussion

3.3.1 Cobalt Precipitation

The cobalt solutions were originally prepared in sodium carbonate buffer, however a blue and occasionally pink precipitate was produced. After investigating the literature, this precipitate is believed to be the basic salt $Co(OH)NO_3$ (equation 3.8). A pink cobalt(II) hydroxide precipitate is formed either by heating the basic salt or in excess alkali (equation 3.9).

$$Co^{2+} + OH^- + NO_3^- \longrightarrow Co(OH)NO_3\downarrow \qquad \textit{(Equation 3.8)}$$

$$Co(OH)NO_3\downarrow + OH^- \longrightarrow Co(OH)_2\downarrow + NO_3^- \qquad \textit{(Equation 3.9)}$$
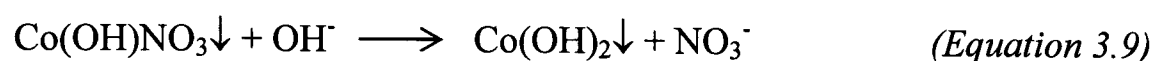
Cobaltous carbonate $CoCO_3$ could also be responsible for the precipitation, however this normally only forms on boiling of the carbonate solution (equation 3.10).

$$CO_3^{2-} + Co(NO_3)_2 \longrightarrow 2NO_3^- + CoCO_3 \qquad \textit{(Equation 3.10)}$$
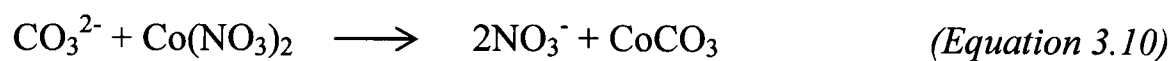
To avoid this problem, the cobalt stock solutions were prepared in high purity deionised water and an aliquot spiked into the working solution.

Preliminary investigations into the chemiluminescence reaction showed that a high cobalt concentration also produced a precipitate in the buffer, which is not desirable within a microfluidic device as it can cause blockages. The most suitable cobalt(II) concentration that did not produce a precipitate was found to be 3×10^{-5} mol L^{-1}.

3.3.2 Improvement of the Chemiluminescence Signal

Preliminary studies of the luminol-Co(II)-hydrogen peroxide chemiluminescence reaction were conducted using a FIA system. The FIA system comprised of a peristaltic pump (Gilson, Minipuls 2) with silicone peristaltic pump tubing (Elkay Laboratory Products (UK) Ltd., Basingstoke, Hampshire), a rotary (six-port) valve injector with a Teflon tubing sample loop (100µl), a chemiluminescence detector (Camspec) and a chart recorder (Chessel Ltd., Worthing, Sussex). The system was connected with Teflon tubing (0.5mm i.d.) using commercial connectors and fittings. The sample was injected directly into a single manifold containing the pre-mixed chemiluminescence reagents. The chemical constituents of the chemiluminescence reaction, which includes the luminol concentration, the cobalt concentration and the pH were investigated. The flow rate was not investigated at this point as it will greatly differ for the microfluidic device. A two level factorial design of experiment was produced and eight experiments were conducted. Yates' algorithm was used to determine if any of the factors were significant in altering the chemiluminescence response.[225] None of the variables were found to have a significant effect on the chemiluminescence response over the ranges investigated as their variance ratios were below the P=0.05 F-test critical value (F=7.7089, for 1 degree of freedom and 3 variables).[230] From this it was decided to individually investigate the effect of the luminol concentration, the pH and the flow rate on the chemiluminescence intensity within the microfluidic device in order to obtain optimal values for each variable.

The effects of pH, luminol concentration and flow rate were investigated using the microfluidic manifold shown in section 2.2.3 (figure 2.6), which consisted of a glass device with a serpentine manifold (206 mm length) with a channel width of 200 µm

100

and depth of 65 µm (Micro Chemical Systems, Hull). Reagents and sample were continuously introduced into the device (hydrogen peroxide in one inlet and the chemiluminescence reagent through the other) which was contained within the portable chemiluminescence detector detailed in section 2.1.2. A schematic of the manifold can be seen in figure 3.5.
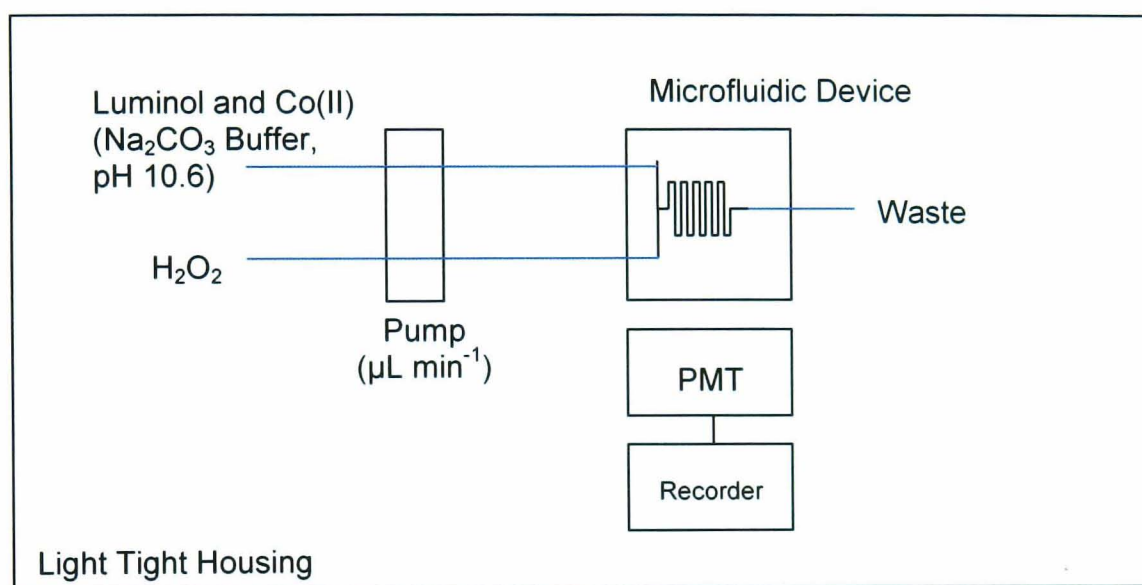
Figure 3.5 Manifold for the portable chemiluminescence detection system for microfluidic decives used in the determination of hydrogen peroxide in rainwater.

Hydrogen peroxide levels in rainwater are typically in the micro-molar range therefore the system had to be optimised to cover this range. All optimisation experiments were carried out using a 1 µmol L^{-1} hydrogen peroxide standard. Even with the hydrogen peroxide removed, the blank water sample still gave a slight signal, therefore the blank was subtracted from the standard to give a true value for the hydrogen peroxide concentration in the standards.

The effect of pH was investigated over the range 9.8-11.1, as this is the optimum range for the luminol reaction, discussed in section 3.1.4. The luminol concentration was 3×10^{-5} mol L^{-1} used by Price *et al.*.[197] The cobalt(II) concentration was 3×10^{-5} mol L^{-1} and the flow rate was $10\mu L$ min^{-1}. The results are presented in figure 3.6.

Figure 3.6 Effect of pH on the luminol chemiluminescence emission within a microfluidic device. Error bars: one standard deviation (n=5).

The highest chemiluminescence intensity was observed at pH 11.1, however at pH 10.6 a high response was also obtained with better reproducibility. This is consistent with the findings of Merenyi *et al.*.[220] The reaction is pH dependent because it is only the decomposition of the monoanion form of the α-hydroxyhydroperoxide that yields an excited state. The chemiluminescence efficiency is observed to increase towards approximately 10.5 due to the increase in monoanion production as discussed in section 3.1.4. A pH of 10.6 was therefore selected for all future use in the investigation.

Effect of Luminol Concentration

The effect of luminol concentration on the chemiluminescence signal was investigated over the range $1 \times 10^{-5} - 1.5 \times 10^{-3}$ mol L^{-1}. A pH of 10.6 was used, again the cobalt concentration was 3×10^{-5} mol L^{-1} with a flow rate of $10\mu L$ min^{-1}. The results are given in figure 3.7.

Figure 3.7 Effect of the luminol concentration on the chemiluminescence emission within a microfluidic device. Error bars: one standard deviation (n=5).

An optimal signal was obtained at a luminol concentration of 5×10^{-4} mol L^{-1}.

Flow Rate

It is necessary to optimise the flow rate to ensure efficient mixing of the reagents and sample within the microchannels in order to achieve an optimal chemiluminescence signal for the reaction. Mixing has previously been investigated and is detailed in section 2.2.3. The flow rate was again investigated using a larger number of different flow rates within the range 8 and 27 μL min^{-1} as can be seen in figure 3.8. The

luminol concentration was 5×10^{-4} mol L^{-1}, the cobalt(II) concentration was 3×10^{-5} mol L^{-1} and the pH was 10.6.
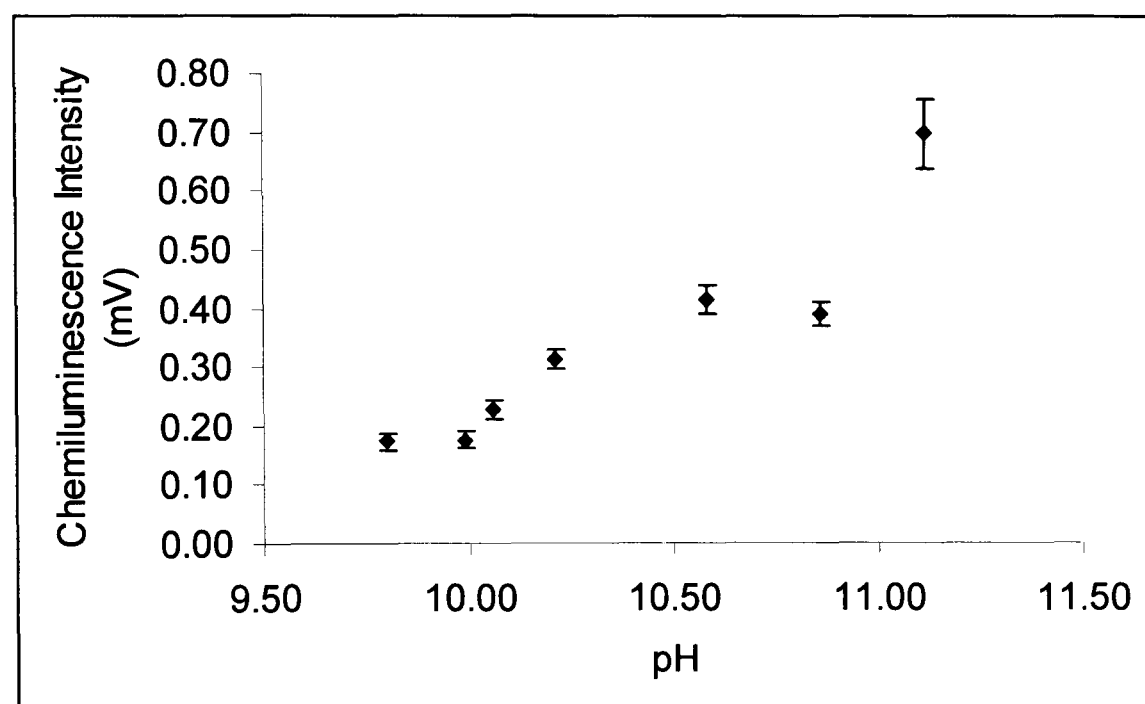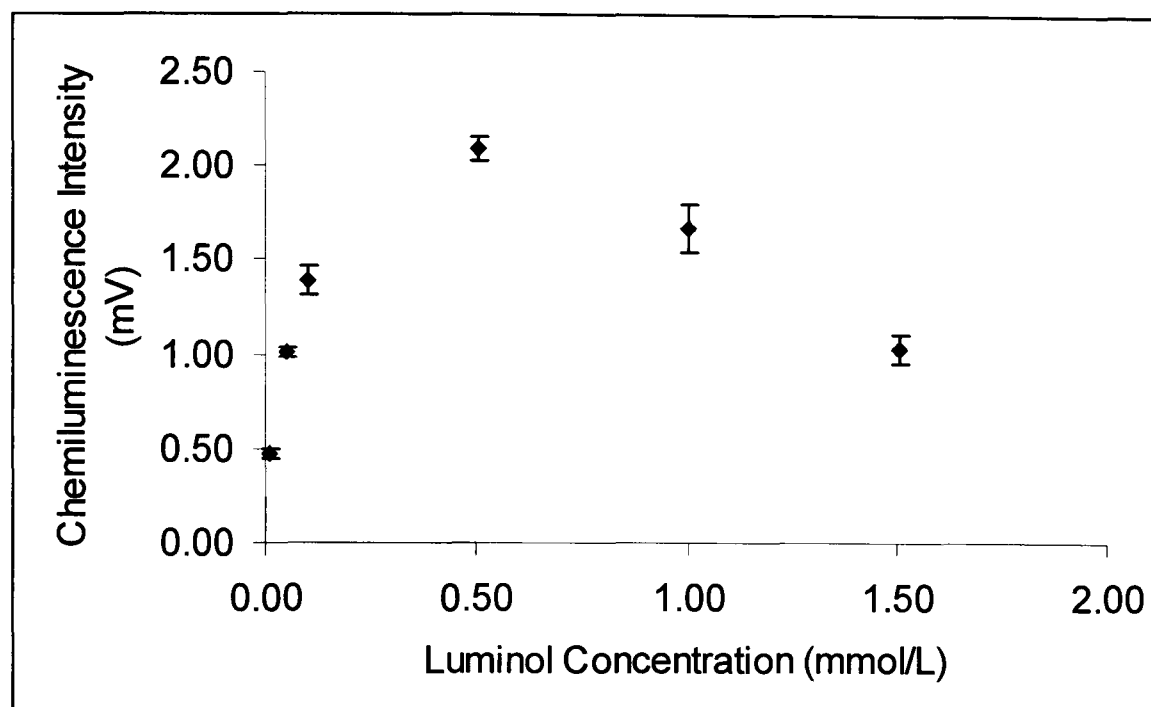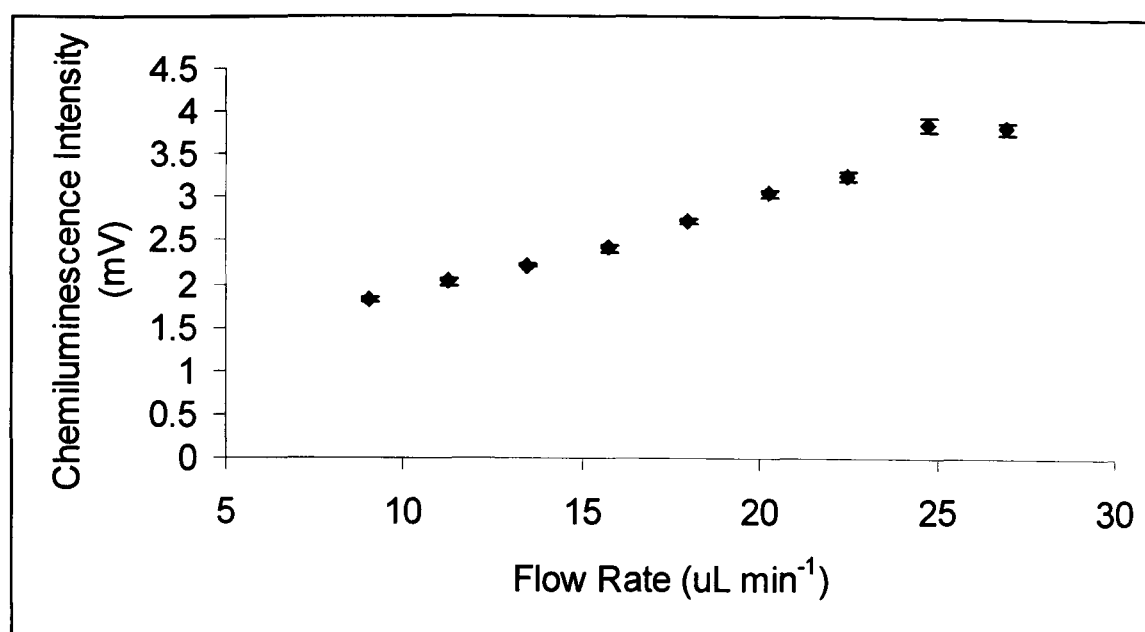

Figure 3.8 Effect of the flow rate on the luminol chemiluminescence emission within a microfluidic device. Error bars: one standard deviation (n=5).

An optimal flow rate of 25 µl min^{-1} was observed. However this produced a high backpressure and so a flow rate of 20 µl min^{-1} was adopted (RSD 1.5% (n=5)). As previously discussed, mixing within the channels of the microfluidic device is diffusion limited and a higher signal for a slower flow rate is expected, however this is not observed from the experimental data. The reaction kinetics is also involved in the process. The luminol reaction is a fast reaction, it has been reported that maximum peak intensity occurs after 500 ms in a stopped flow system.[156] The fast reaction kinetics is responsible for the increase in chemiluminescence intensity at the higher flow rates.

The working parameters found for the constituents of the luminol reaction for the determination of hydrogen peroxide are summarised in table 3.2.

Table 3.2 Optimal parameters for the luminol-cobalt(II) chemiluminescence reaction for the determination of hydrogen peroxide within a microfluidic device.

Luminol Concentration (mol L^{-1})	5×10^{-4}
Cobalt(II) Concentration (mol L^{-1})	3×10^{-5}
pH	10.6
Flow Rate (μL min^{-1})	20

In comparison with other luminol-cobalt(II) chemiluminescence methods used for the determination of hydrogen peroxide, Price *et al.* used a lower luminol concentration of 3×10^{-5} mol L^{-1}, a higher cobalt(II) concentration of 5×10^{-4} and a higher pH of 10.8.[197] Yuan *et al.* used a similar luminol concentration of 6.5×10^{-4} mol L^{-1}, a similar cobalt(II) concentration of 6×10^{-5} and a lower pH of 10.15.[198] These differences in optimal parameters with those obtained for the chemiluminescence reaction within the microfluidic devices are attributed to the nature of mixing of the reagents within the microfluidic channels. There is an improvement in the efficiency of mass transport and diffusional flux per unit volume (unit area) of the reagents within the microfluidic channels and the small fluid thickness permits rapid mixing times. Therefore the channels allow for the improved efficiency of mass transport of the luminol to the sample where it can be oxidised to produce the luminol radical, mass transport of this is also efficient enabling it to be further oxidised to produce the α-hydroxyhydroperoxide intermediate.

3.3.3 Enhancement of the Chemiluminescence Signal

To enhance the response and therefore the sensitivity, the effect of a reflectiv

surface applied to the top of the chip was investigated. It was essential that th

surface gave a reproducible response. An initial study using aluminium foil showe

the signal could be enhanced by 32.5% (1.33 fold) (figure 3.9). The material gav

reproducible results during an analysis run; however, this kind of material did nc

give reproducible results in between runs due to movement of the material, indicatin

a more permanent reflective surface was required. A thin silver film was forme

directly to the top layer of the glass microfluidic device using a method described b

Saito *et al.* based on the *mirror reaction.*[224] Partial coverage of the serpentine of th

chip (2 x 2 cm) and complete coverage of the chip (3 x 3 cm) with the silver mirrc

was investigated (figure 3.8) and the results can be seen in figure 3.9.
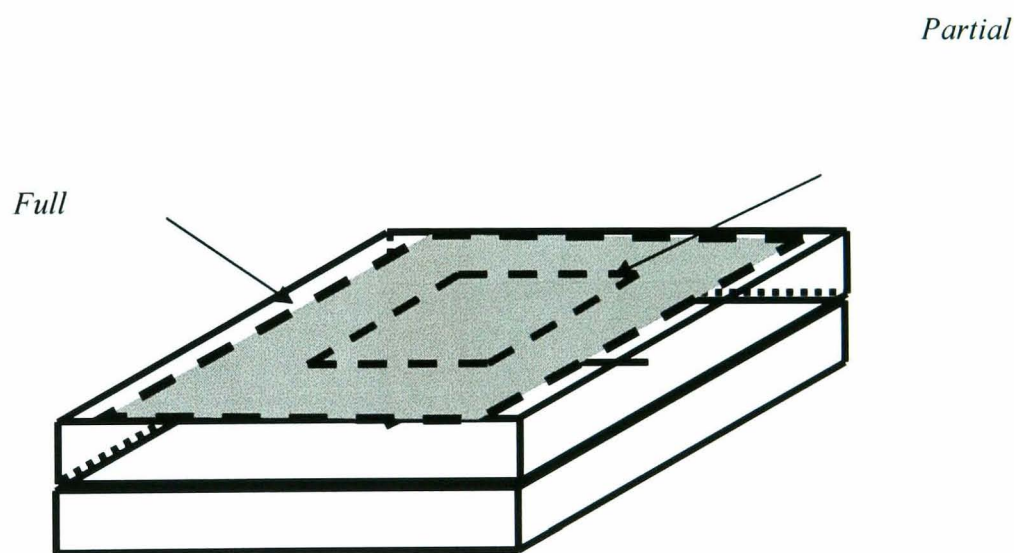
Partial

Full

Figure 3.8 Schematic showing reflective surface on microfluidic device.

a)

b)
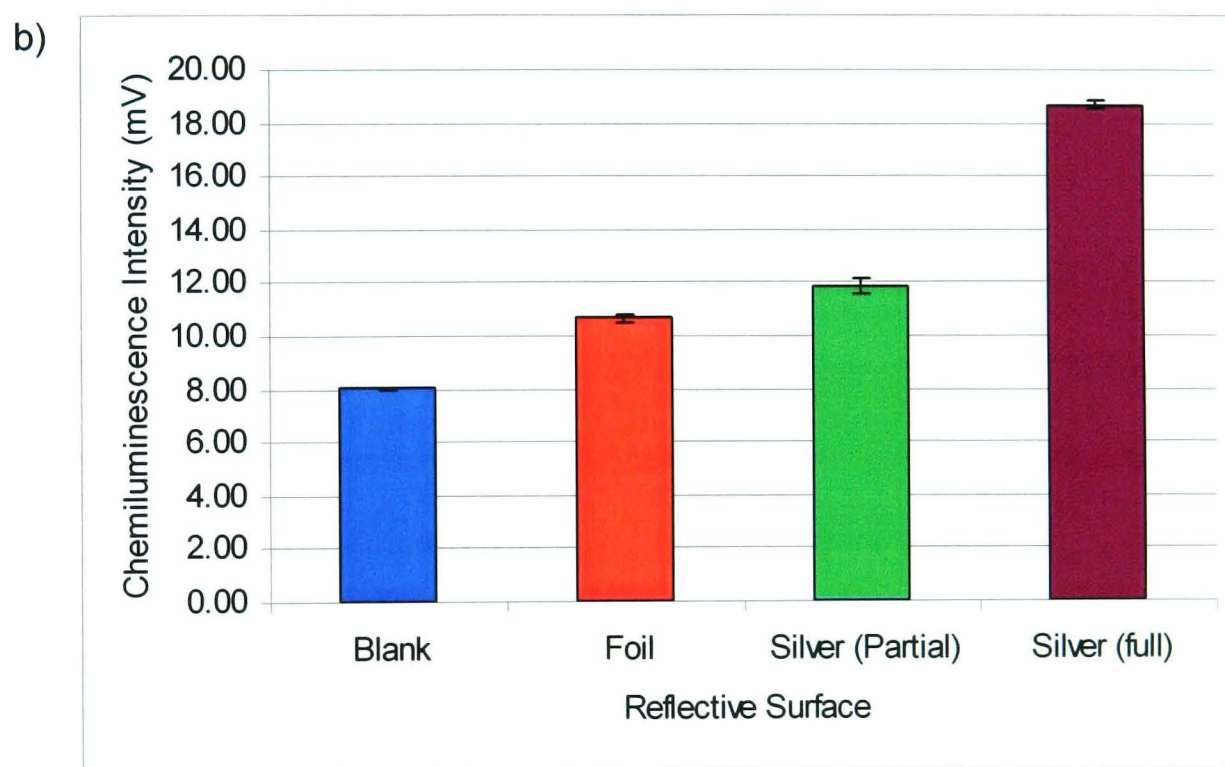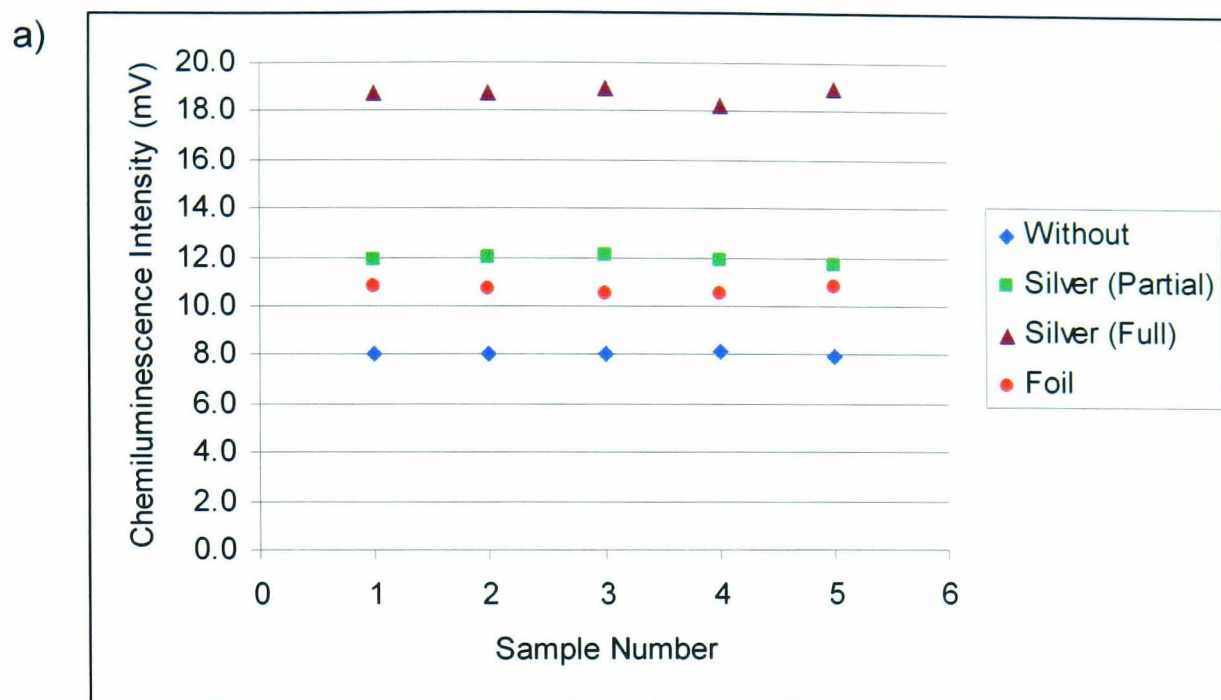
Figure 3.9 Enhancement of Chemiluminescence Signal with Reflective Surfaces or
Microfluidic Device: a) Reproducibility during analysis run b) Average enhancemen
of reflective surfaces. Error bars: one standard deviation (n=3).

Partial coverage of the chip gave an enhancement of 47.8% (1.47 fold) but this was improved by completely covering the surface of the top of the microfluidic device and a 132.3% (2.32 fold) enhancement was achieved (figure 3.9). As discussed in section 2.2.3, light piping of the chemiluminescence emission down the channels of the microfluidic device may occur, by using a reflective surface it increases the amount of light reaching the detector and therefore the chemiluminescence signal. The amount of light reaching the detector can also be increased by increasing the amount of reflective surface, which is why a greater enhancement for the full coverage of the microfluidic device with a reflective surface gave a greater enhancement.

3.3.4 Calibration

A calibration using the optimal conditions given in section 3.3.2 and using the serpentine chip with the mirror completely covering the top surface of the device was conducted in the range $0.1 - 7.5$ µmol L^{-1} hydrogen peroxide. The reagents and standards were continuously introduced into the microfluidic device and the response continuously measured over a 5 minute interval, with an average of 5 readings taken during this. A curve was fitted to the calibration data over this range ($y = 1.9323x^2 + 11.439x^2 - 4.2785$ (n=7), $R^2 = 0.9955$), where y is the response (mV) and x is the concentration of hydrogen peroxide (µmol L^{-1}) (figure 3.10). A linear response is observed over the range $0.1 - 1.0$ µmol L^{-1} ($y = 44.655x - 3.0085$ (n=5), $R^2 = .9905$) (figure 3.10). Good reproducibility was achieved with RSD values less than 2.7%. Good sensitivity was achieved and the limit of detection was determined to be 4.7 nmol L^{-1}. This was calculated using the linear portion of the curve and was based on three times the deviation of the y-residuals.[225] A log plot of the calibration curve

provides a linear response and can be used for the quantitative determination of hydrogen peroxide in real samples ($y = 1.6565x + 11.157$, $R^2 = 0.9906$).
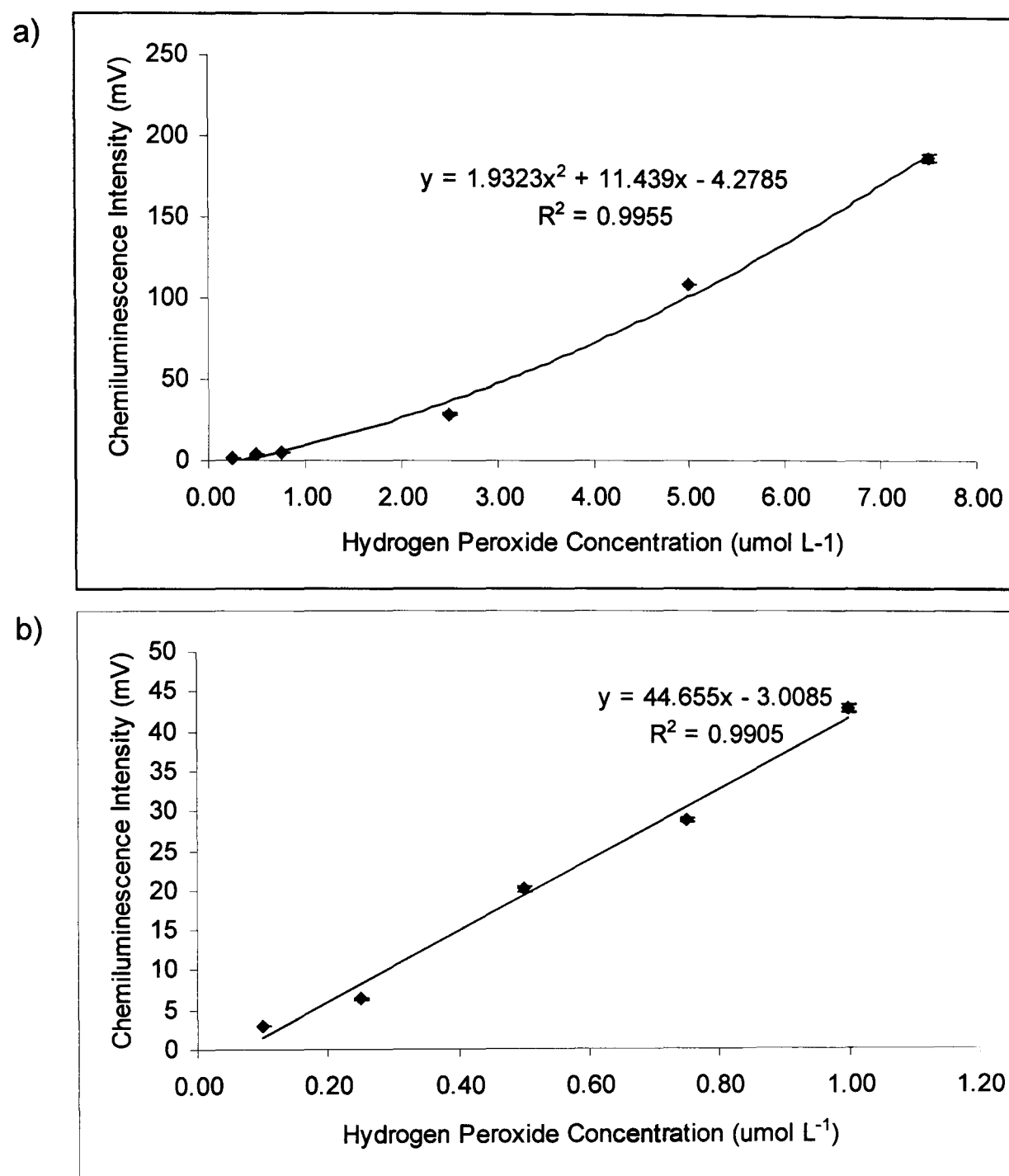
Figure 3.10 Calibrations for the determination of hydrogen peroxide using the luminol-cobalt(II) chemiluminescence reaction, where a) is the curved response over the range 0.1 – 7.5 μmol L^{-1} hydrogen peroxide, and b) is the linear response over the range 0.1 – 1.0 μmol L^{-1} hydrogen peroxide. Error bars: one standard deviation (n=3).

3.3.5 Immobilisation of Chemiluminescence Reagents

Luminol can be immobilised onto small support particles and packed into a reactor/detector cell incorporated into a flowing system. The advantage of immobilising reagents is that it produces a reagentless system making the analysis simpler (see section 2.3).

3.3.5.1 Ion Exchange Resin

Ion exchange resin as a support has been a popular choice in the literature due to the ease of the immobilisation procedure (see section 3.1.2). Luminol is immobilised onto the strongly basic anion exchange resin (Ambersep 900 (OH)) by electrostatic attraction, and eluted from the support to mix with the sample prior to detection (figure 3.11). As the luminol is used up in the reaction a very high loading is required.
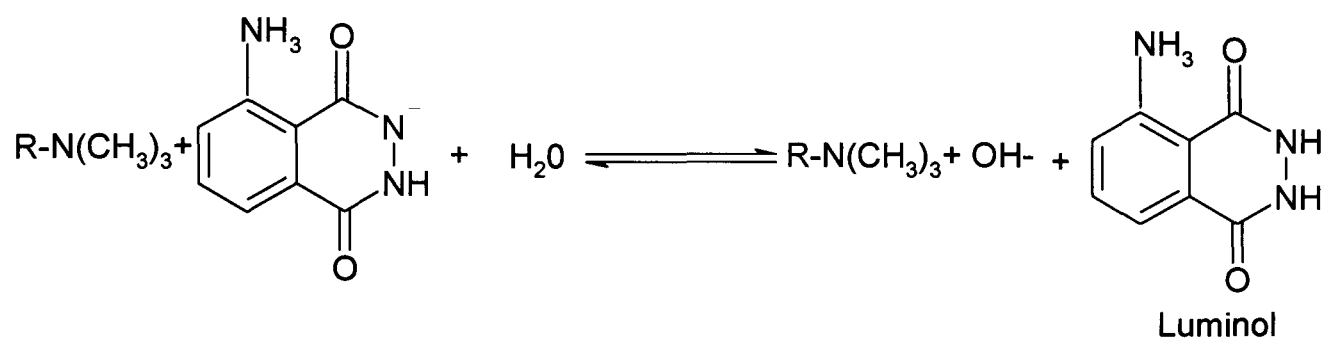
Figure 3.11 Immobilisation of luminol onto strongly basic anion exchange resin.[206]

The resin has a large particle size, however and swells when in liquid and so cannot easily be packed into a microfluidic device. Ion exchange resin has recently been incorporated into a micro reactor by utilising the reservoirs as shown by Lv *et al..* [163]

The procedure detailed by Qin *et al.* for the immobilisation of luminol anion exchange resin has been investigated to compare loadings for the covalent attachment of luminol onto solid supports.[206]

Immobilisation Procedure

The immobilisation procedure required 0.25 mol L^{-1} luminol prepared in 0.5 mol L^{-1} sodium hydroxide using high purity deionised water. 0.5 g of ion exchange resin was stirred for 15 hours with a 25 mL aliquot of the luminol solution. The resin was filtered, washed and dried. The success of the immobilisation procedure was assayed using a UV-VIS spectrometer (Perkin Elmer UV/VIS spectrometer, Lambda Bio 10). The absorbance of the luminol solution was measured prior and post immobilisation at 360 nm (figure 3.12) and a calibration was constructed in order to obtain the concentration of luminol in the solutions before and after immobilisation.[206] The loading of luminol onto the strongly basic anion exchange resin was determined by using the change in concentration of luminol in the immobilisation solution before and after the immobilisation procedure, and assuming all of this has been bound to the support can be calculated using equation 3.11. An average value of 1.94 mmol g^{-1} was obtained, which compliments that achieved by Qin *et al.* who reported a loading of 2.05 mmol g^{-1}.[206]

$$L = \frac{(CL_B - CL_A) \times V}{m}$$
(Equation 3.11)

Where L is the loading of the luminol on the solid support (mol g^{-1}), CL_B is the concentration of luminol before immobilisation (mol L^{-1}), CL_A is the concentration of luminol after immobilisation (mol L^{-1}), V is the volume of solution used in the immobilisation and m is the mass of the solid support used in the immobilisation (g).
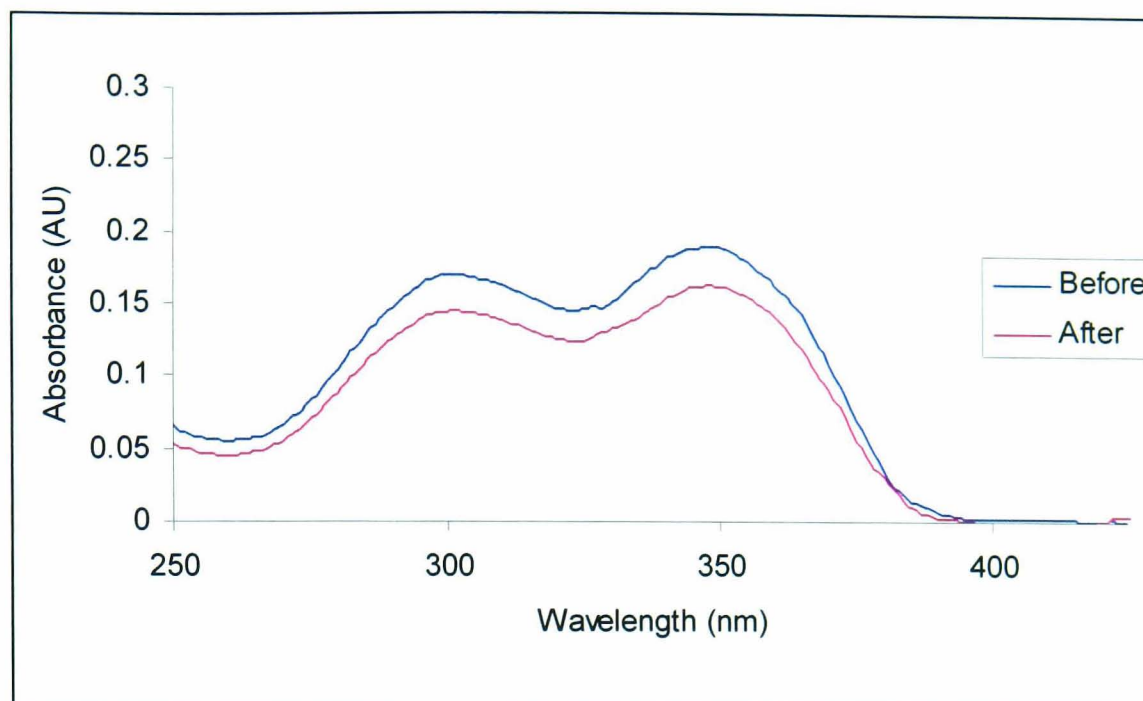
Figure 3.12 Absorption spectra for the luminol solution before and after adsorption with strongly basic anion exchange resin (Ambersep 900 (OH)). Absorption maxima at 360 nm.

3.3.5.2 Controlled Pore Glass

The immobilisation of luminol onto controlled pore glass has also been investigated. CPG has the advantage over ion exchange resin in that it does not swell and the particle size is small enough to pack directly into microfluidic channels (see section 2.3). Two different specifications of CPG were investigated (see table 3.3) as well as two different methods of immobilisation: glutaraldehyde linkage and GMBS linkage. Previous work by Hool *et al.* details that immobilised isoluminol gave a reduced signal in comparison with immobilised luminol and it has therefore not been investigated.[211]

Table 3.3 Size and pore specifications for the CPG used in the covalent attachment of luminol.

Name	Mesh	Particle size (μm)	Particle Pore Size (Å)
1	200-400	37-74	240
2	80-120	74-125	250

For the glutaraldehyde method, an (aminoalkyl)silane was used to modify the surface of the CPG, the glutaraldehyde was used as a cross linker to bridge the amino group from the silane to an amino group on the luminol (Schiff base reaction), resulting in the formation of two imine bonds which can be hydrolysed with base (figure 3.13).[211] For the GMBS method an amide bond was formed between the amino group on the silane to an amino group on the luminol, which was less susceptible to hydrolysis with base and so acts as a sensor rather than being eluted from the support (figure 3.14).[226]

113
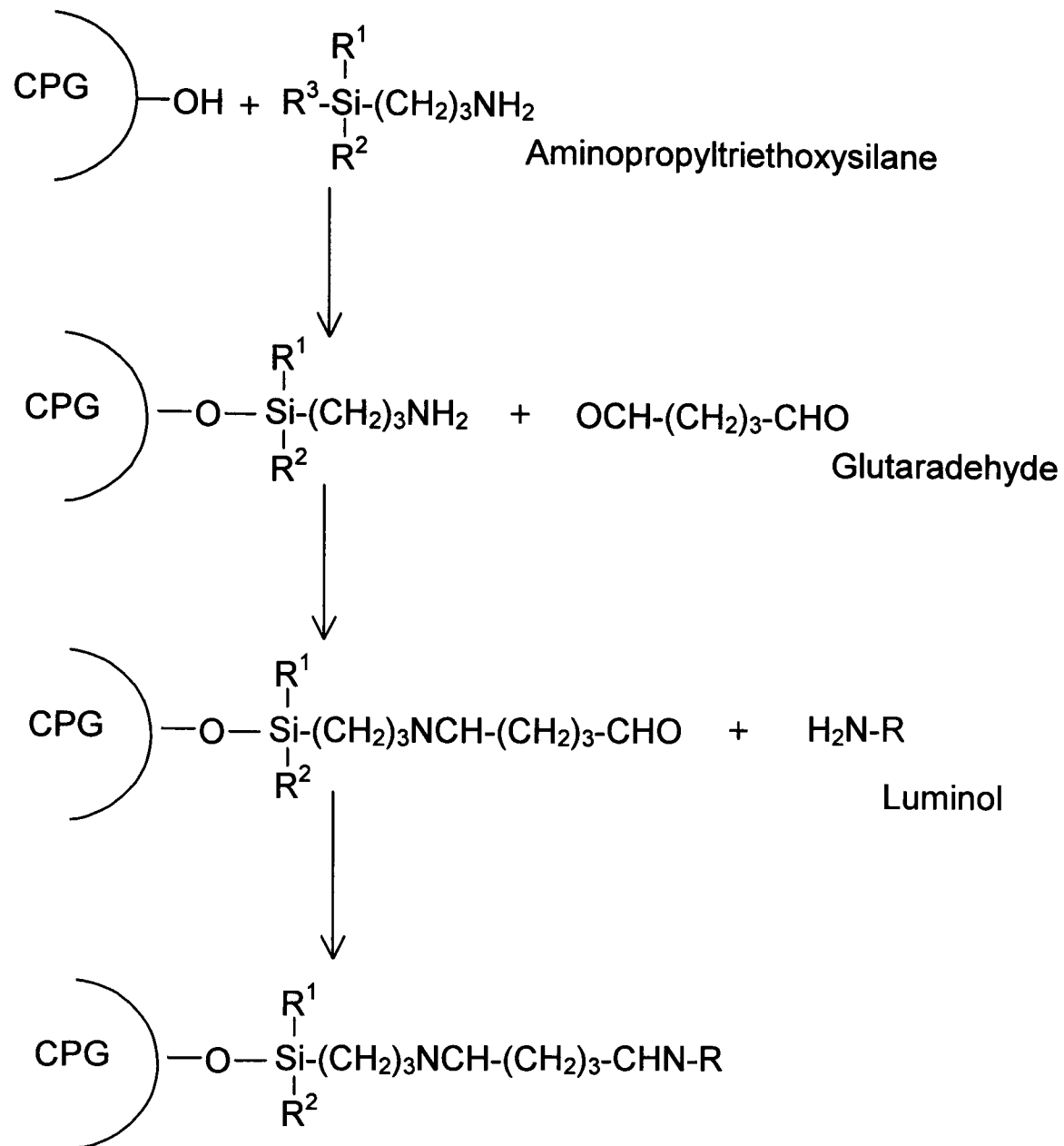
Figure 3.13 Schematic for the immobilisation procedure of luminol onto CPG using APTS and glutaraldehyde.

114
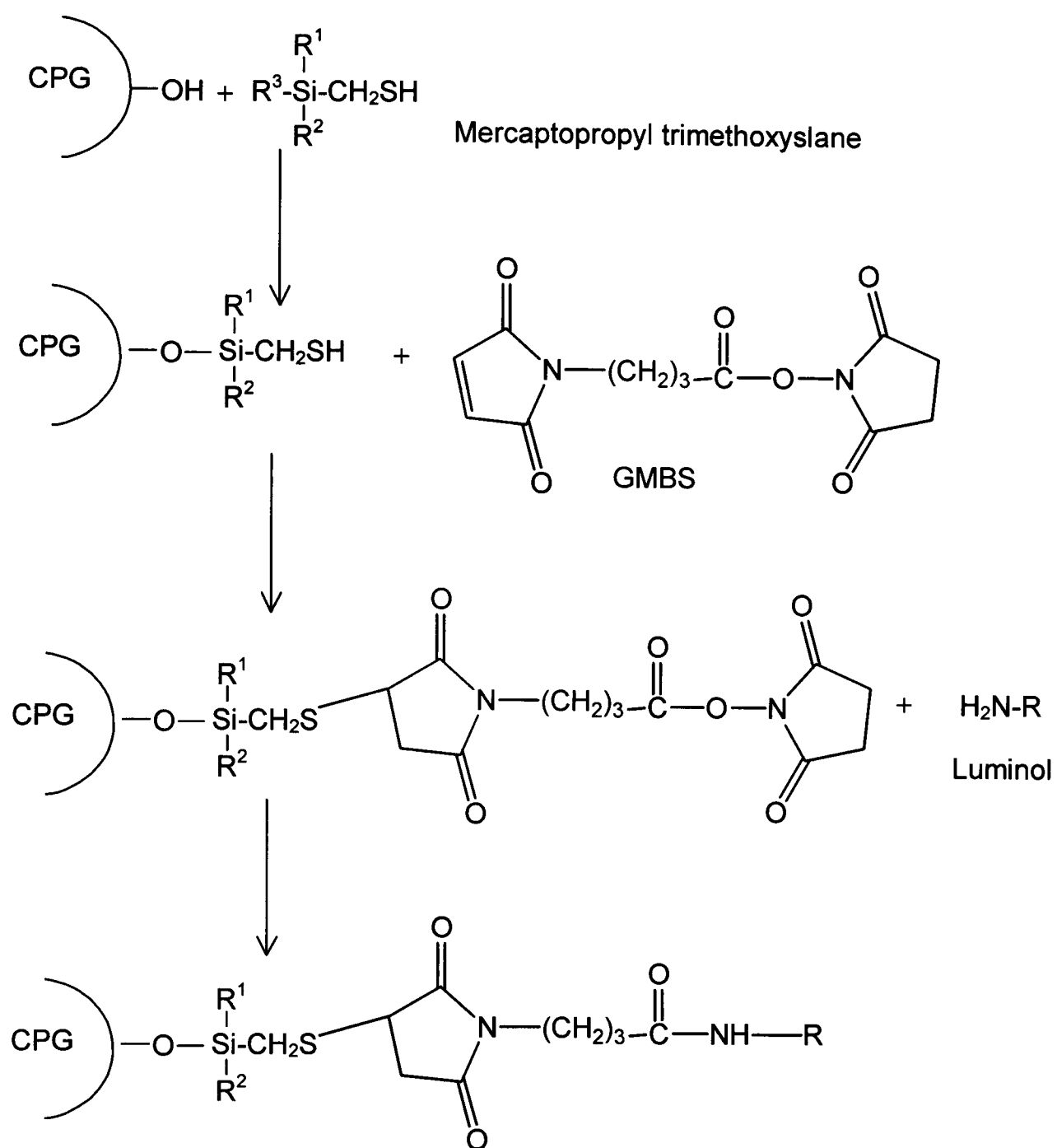
Figure 3.14 Schematic for the immobilisation procedure of luminol onto CPG using MTS nd GMBS.

Immobilisation Procedure

For the glutaraldehyde immobilisation, 2g CPG was boiled in 5% nitric acid (30 min), filtered, washed with deionised water and dried (100 °C). The cleaned CPG was immersed in 5 mL 10% APTS in toluene with shaking overnight. It was then filtered, washed with ethanol and water and dried (100 °C). The silanised CPG was immersed in 5ml 10% glutaraldehyde in water for 2 h with shaking. It was then filtered and washed with water and air dried. 0.5g of the CPG was placed in 5 mL of 0.02 mol L^{-1} luminol in DMSO, left overnight with stirring. It was then filtered and washed with water.[211, 212, 226]

For the GMBS immobilisation, 2g CPG is boiled in 5% nitric acid (30 min). It was then filtered, washed with deionised water and dried (100 °C). The cleaned CPG is immersed in 1 mL 4% MTS in toluene for 1 h with shaking. It was then filtered, washed with toluene and air dried under suction. The silanised CPG is immersed in 2 mmol L^{-1} GMBS in ethanol for 1 h with shaking. It was then filtered and washed with ethanol and water and air dried. 0.5g of the CPG is placed in 20 mL of 0.02 mol L^{-1} luminol in DMSO, left overnight with stirring. It was then filtered and washed with water.[211, 212, 226]

The immobilisation solution was assayed using UV-VIS spectroscopy at 360 nm, on the solution prior and post immobilisation to assess the success of the immobilisation technique and determine the loading for the immobilisation of luminol onto CPG as with the anion exchange resin method (see section 3.3.5.1).

3.3.5.3 Comparison of Loadings of Luminol
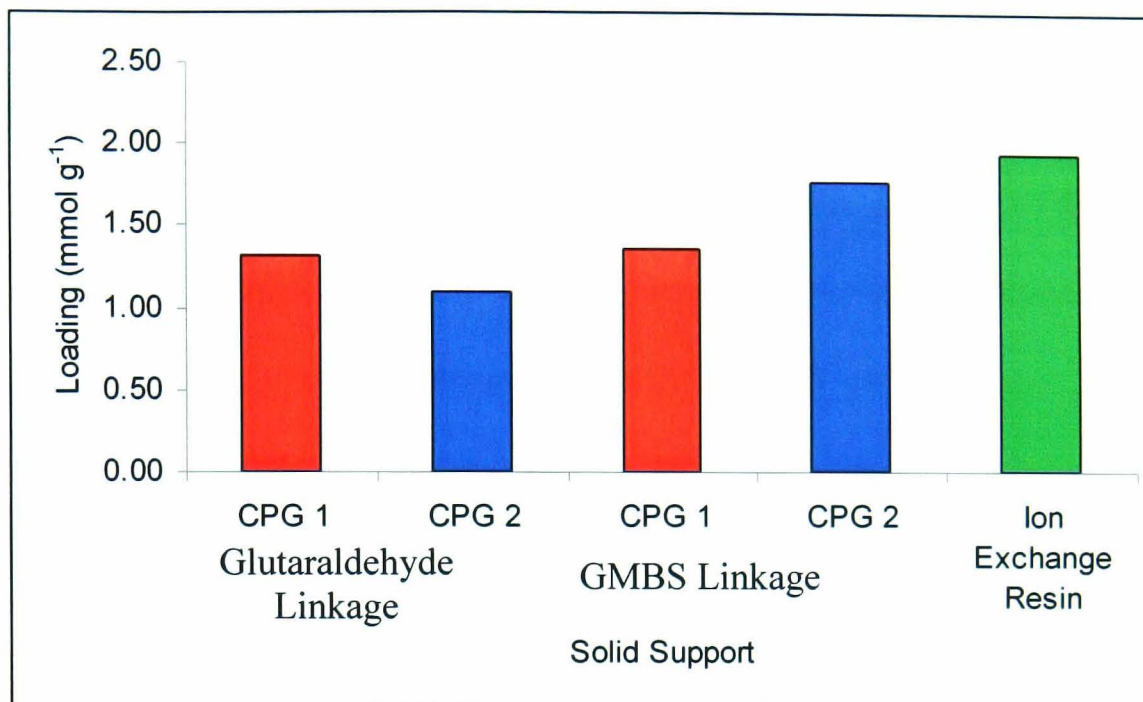
Figure 3.15 Comparisson of the different loading capacities of luminol onto CPG and ion exchange resin using different immobilisation techniques. Error bars: one standard deviation (n=2).

The results are shown in figure 3.15. A higher loading was achieved than that documented by Hool *et al.* for the immobilisation of luminol (29 μmol per g).[211, 212] Slightly higher loadings were achieved with the larger CPG particle size, however the smaller size is more amenable to packing in a microfluidic device. Higher loadings were achieved using the GMBS linkage rather than the glutaraldehyde linkage. Higher loadings can be achieved with the ion exchange resin, but can not be practically used with a microfluidic device.

3.3.5.4 Determination of Hydrogen Peroxide using Immobilised Luminol.

The different immobilisation procedures of the luminol on to the CPG, which allow for the elucidation or retention of the compound, were compared by their ability to

detect hydrogen peroxide. The CPG was packed into a borosilicate column (30 mm long, 500 μm i.d.) and sealed with glass wool.

For the glutaraldehyde method, the column was incorporated into the flow manifold used previously prior to mixing in the serpentine device (see figure 3.16). Co(II) in sodium carbonate buffer (pH 10.6) was passed through one inlet of the microfluidic device and the hydrogen peroxide sample passed through the other inlet. The results can be seen in table 3.3.
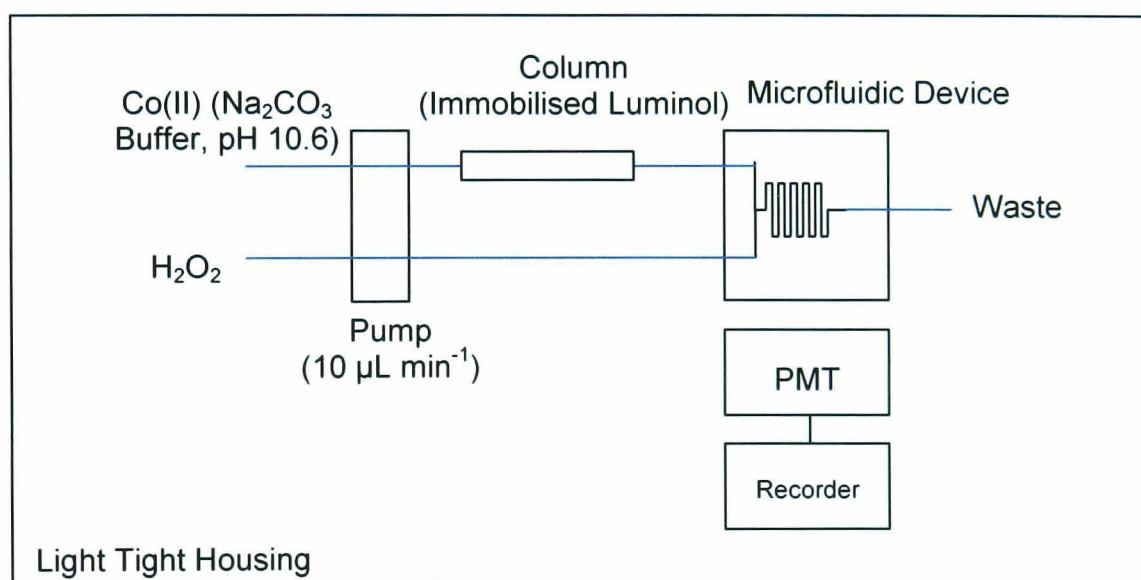
Figure 3.16 Manifold for the portable chemiluminescence detection system using a microfluidic decive used in the determination of hydrogen peroxide in rainwater, incorporating a packed column containg luminol immobilised onto CPG via glutaraldehyde attachment.

For the GMBS column, the column was directly placed above the PMT with mixing of the sample and cobalt reagents prior to this (figure 3.17). Again, Co(II) in sodium carbonate buffer (pH 10.6) was passed through one inlet of the microfluidic device and the hydrogen peroxide sample passed through the other inlet. The results can be seen in table 3.3.
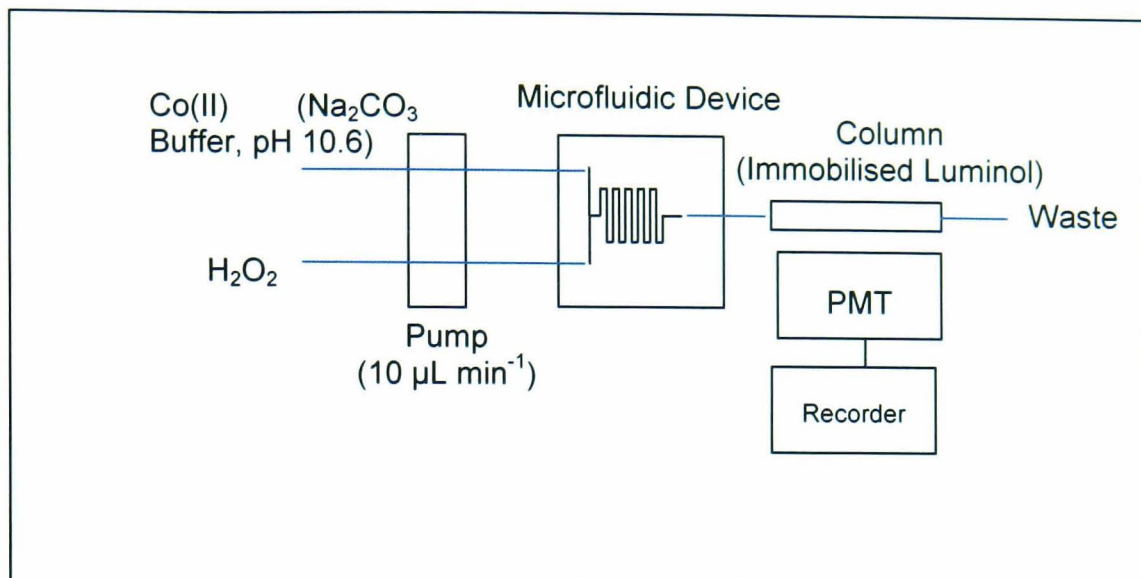
Figure 3.17 Manifold for the portable chemiluminescence detection system using a microfluidic decive used in the determination of hydrogen peroxide in rainwater, incorporating a packed column containg luminol immobilised onto CPG via a GMBS attachment.

Table 3.4 Results for the determination of hydriogen peroxide using luminol immobilised .

Immobilisation Method	Minimum Hydrogen Peroxide Concentration Detected	Chemiluminescence Intensity (mV)
GMBS	1 mmol L-1	1.09 ±0.03
Glutaraldehyde	0.1 mol L-1	1.63±0.03

From table 3.4 it can be seen that there is a great reduction in sensitivity using the immobilised reagents compared with luminol in solution. A decrease in the signal was observed after approximately 10 minutes, indicating a high enough loading of luminol has not been achieved. A very high loading of the luminol is required for long term analysis and this is not amenable for long term monitoring in the field. A simple system with good limits of detection can be achieved using luminol and cobalt in solution as discussed in section 3.3.2 and this has been used in further work for real sample analysis.

119

3.3.6 Rainwater Analysis

Rainwater was collected directly as it landed using a polythene funnel (15 cm diameter), samples were taken manually at specified intervals using micro polypropylene centrifuge tubes (0.5 mL). The samples were collected on the roof of the chemistry building at the University of Hull. The samples were collected and stored on ice and analysed within an hour. The sampling rate for the event was dependent on the extent of the sample available from the rainfall. Two rainfall events were studied (event 1 and event 2) and collection parameters are given in table 3.5.

Table 3.5 Parameters for the collection of rainfall for event 1 and 2.

Rainfall Event	Date of collection	Temperature(^{o}C)	Description of event	Time period of collection (min)	Sampling interval rate (min)
1	09/08/04	22	Light shower	45	6
2	10/08/04	23	Heavy continuous rain	50	5

The samples were analysed using the conditions detailed in section 3.3.2. The overall analysis time for one sample was 5 minutes using a total sample volume of 50 μL and total reagent volume of 50 μL for each analysis. A large sample analysis time was used for development purposes to ensure the stability and reproducibility of the chemiluminescence signal. This produced a total reagent and sample consumption of 1.2 mL per hour for each and a total waste production of 2.4 mL per hour. The signal was measured over 5 minutes, but this could be reduced to 1 minute as a steady signal is reached by this point, this would mean only 10 μL of sample is used. Results for event 1 are given in figure 3.18 and for event 2 in figure 3.19.
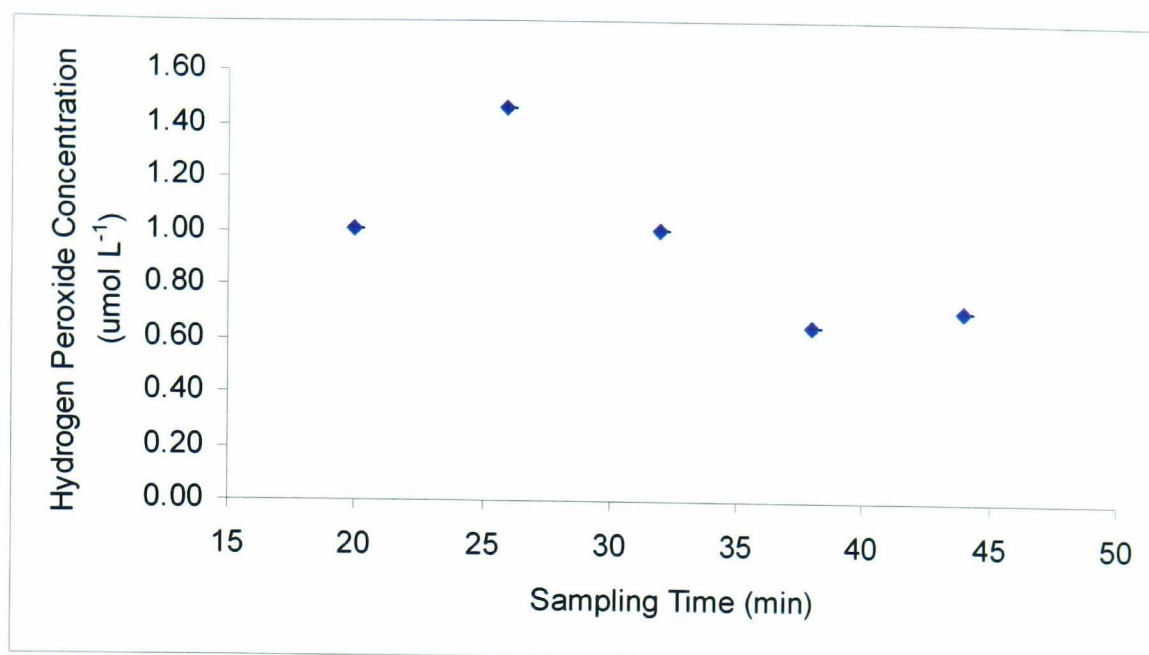
Figure 3.18 Hydogen peroxide levels for rainfull event 1. Error bars: one standard deviation (n=3).
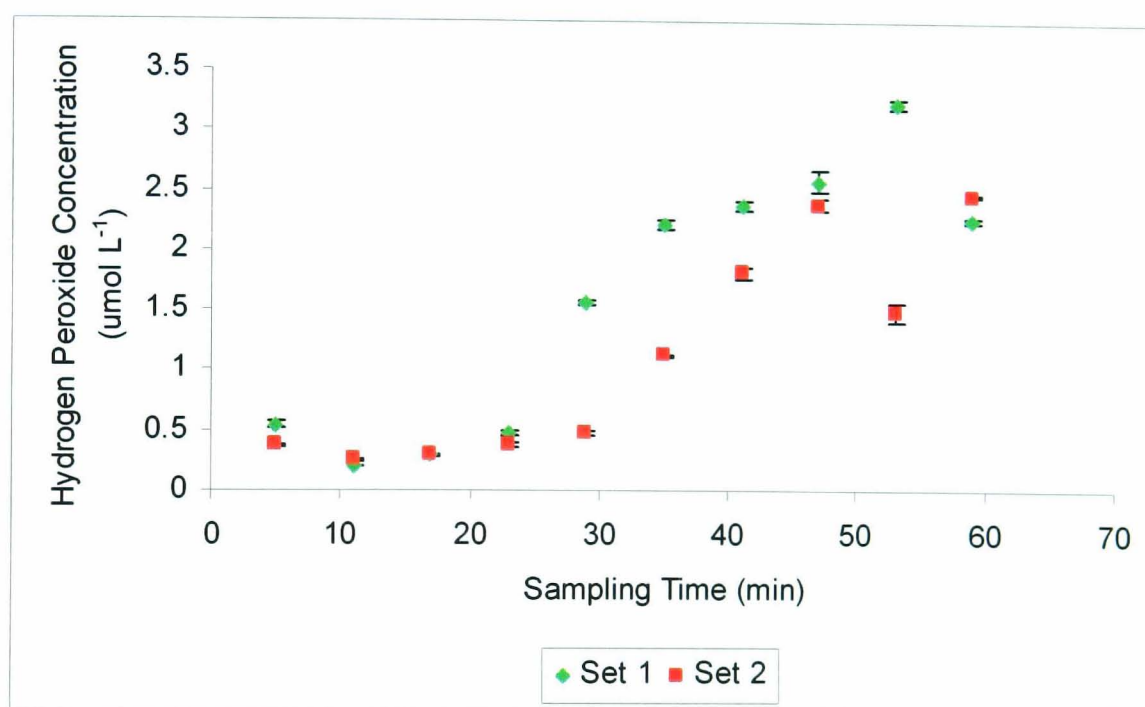
Figure 3.19 Hydogen peroxide levels for rainfull event 2. Error bars: one standard deviation (n=3).

The hydrogen peroxide concentration in the rainwater collected for rainfall event 1 varied from $0.1 - 1.8$ μmol L^{-1} (RSD < 5.6% n=5) (figure 3.18) and for rainfall event 2 it can be seen that the hydrogen peroxide concentration varied from $0.2 - 3.2$ μmol L^{-1} (RSD<6%) (figure 3.19). Variations in hydrogen peroxide levels are attributed to several factors. Slight elevations are due to an increase in the photochemical

121

production of the precursor hydroperoxyl radicals that form hydrogen peroxide in the troposphere. Decreases in hydrogen peroxide levels are due to washing and dilution effects of the rainwater. Influences from other meteorological factors such as wind speed and direction as well as chemical factors can also affect the concentration of hydrogen peroxide in the atmosphere.

During rainfall event 2, two bulk samples of the entire rainfall event over the sampling period were also collected in high density polythene containers. The average concentration of hydrogen peroxide for the set 1 sample was determined to be 0.278 μmol L^{-1}, and for set 2 samples 0.314 μmol L^{-1}. Each sample was spiked with 0.2 μmol L^{-1} hydrogen peroxide in order to determine the recovery of the hydrogen peroxide. For set 1 sample the recovery was 101.8% and for set 2 the recovery was 108.2% (Summarised in table 3.6). The recoveries suggest there is negligible interference from the sample matrix on the chemiluminescence signal. A detailed study of interferences can be seen in section 3.3.9.

Table 3.6 Recovery values for the determination of hydrogen peroxide using the bulk samples, set 1 and 2.

Sample	Average Concentration (μmol L^{-1})	Recovery (%)
Set 1	0.278±0.006	101.8
Set 2	0.314±0.004	108.2

3.3.7 Snow Analysis

Snow was collected from the roof of the chemistry building at the University of Hull using micro polypropylene centrifuge tubes (0.5 mL). Parameters for snow collection are given in table 3.7. Samples were taken from the ground at two different locations (5 samples from a 1 m^2 sampling area). Collection was also made during the snow event using a polythene funnel (15 cm diameter) and collected over a period of 30 minutes. The samples were collected and stored on ice and analysed as a liquid. The same analysis of the rainwater was performed on the snow samples.

Table 3.7 Parameters for the collection of snow for event 1 and 2.

Snow Event	Date of collection	Temperature(^{o}C)	Description of event	Collection
1	21/02/05	4	2 cm deep	Ground samples
2	23/02/05	5	1 cm deep	Ground samples

The hydrogen peroxide levels for event 1 snow samples varied from 0.2 - 0.5 μmol L^{-1} (RSD < 4%, n=5) and for event 2 0.3 – 0.4 μmol L^{-1} (RSD < 4%, n=5). The samples collected during the snow event show much higher concentrations of hydrogen peroxide than those collected from the ground, 0.6 μmol L^{-1} for event 1 and 1.0 μmol L^{-1} for event 2 (figure 3.20). This highlights the importance of sampling *in-situ* before sample degradation can occur.
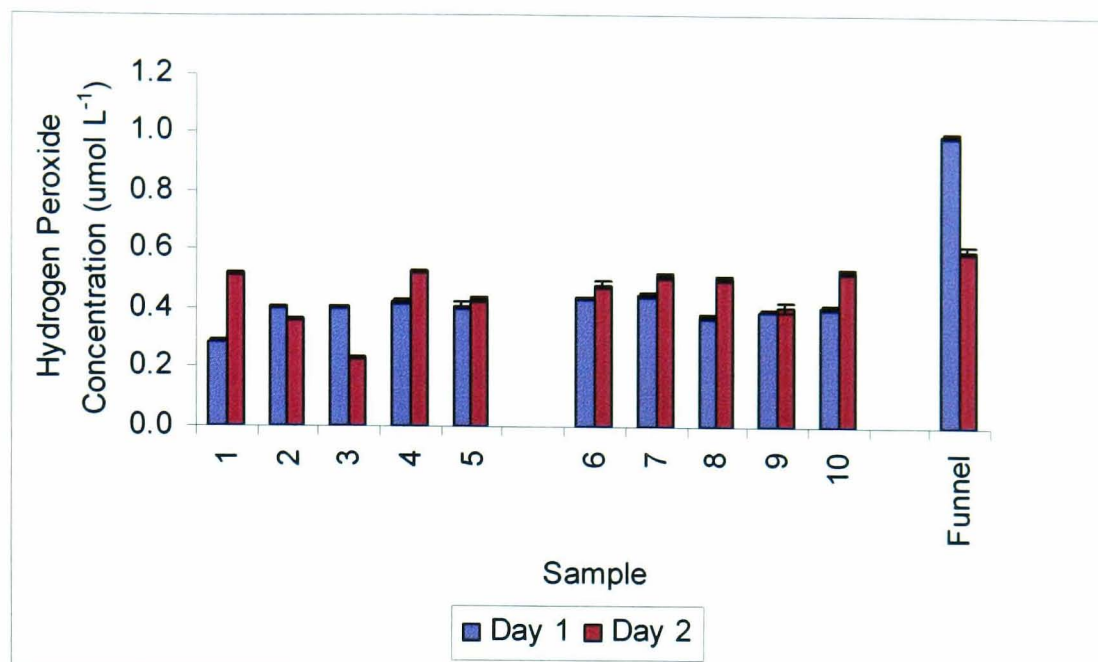
Figure 3.20 Hydogen peroxide levels for rainfull event 2. Error bars: one standard deviation (n=3).

3.3.8 Interferences

From a survey of the literature the following compounds present in rainwater samples were considered to be possible interferences in the luminol reaction: Co(II), Cd(II), Cu(II), Cr(III), Cr(VI), and Fe(II).[198] A quantitative ICP-MS analysis of theses metals in the rainwater and snow collected from the roof of the chemistry building, the University of Hull, was performed (Perkin Elmer, ELAN DRC II ICP-MS). The results are presented in figure 3.21 and 3.22.
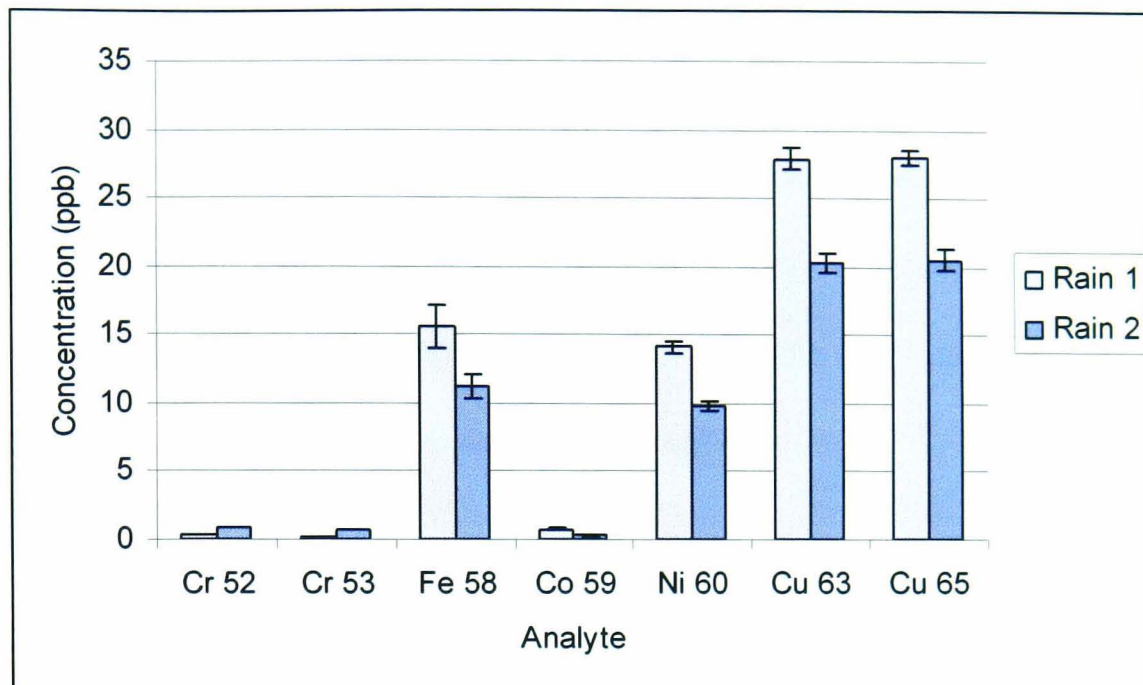
Figure 3.21 ICP-MS analysis of various metals (Cr, Fe, Co, Ni and Cu) in the rain water samples. Error bars: one standard deviation (n=2).
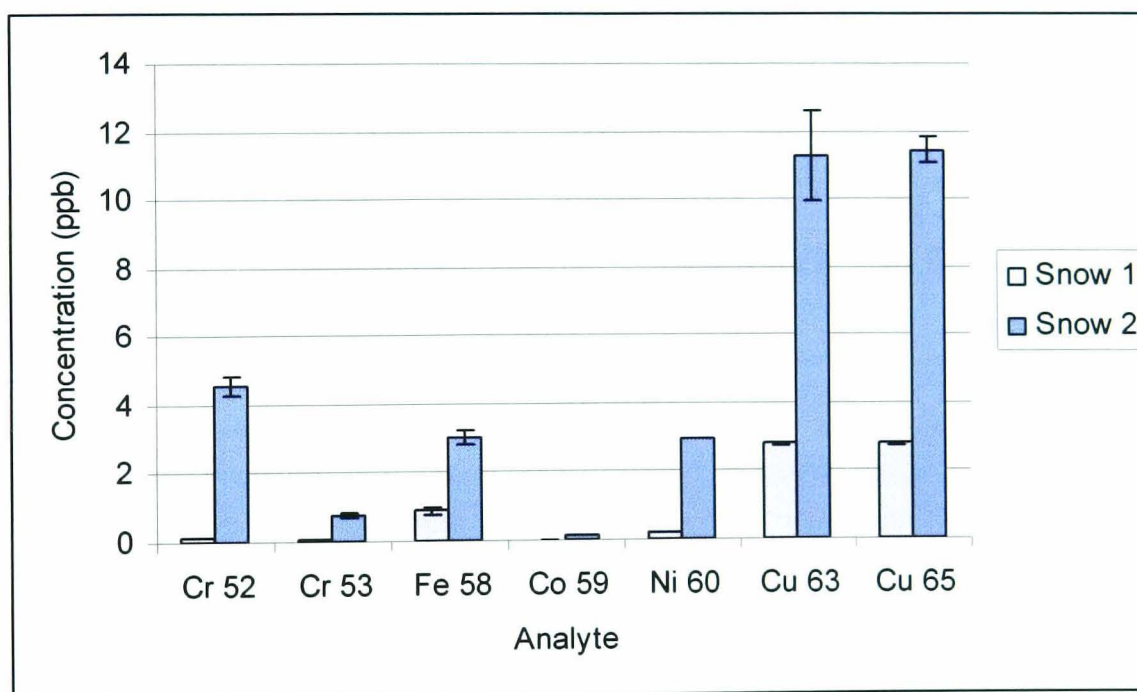
Figure 3.22 ICP-MS analysis of various metals (Cr, Fe, Co, Ni and Cu) in the snow samples. Error bars: one standard deviation (n=2).

The ICP analysis showed that these elements were present at a low ppb level (sub micromolar) in the rainwater and snow samples, and therefore will not provide interference.

Organic peroxides in the atmosphere could also provide a potential source of interference on the luminol reaction. The effect of t-butyl hydroperoxide (figure 3.23) and cumene hydroperoxide (figure 3.24) on the chemiluminescence signal was investigated by spiking a 1 μmol L^{-1} hydrogen peroxide standard. The percentage recoveries of the spiked samples are given in table 3.8 and 3.9 for t-butyl hydroperoxide and cumene hydroperoxide respectively.
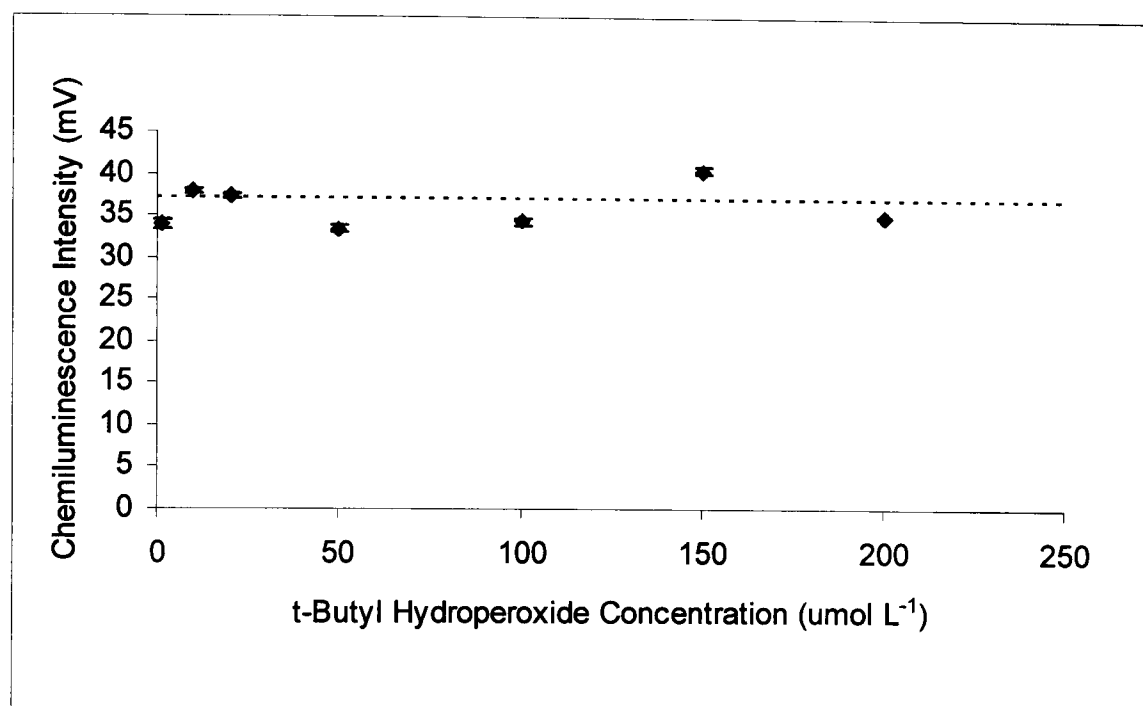
Figure 3.23 The effect of t-butyl hydroperoxide on the determination of hydrogen peroxide (1 μmol L^{-1}) using the luminol-Co(II) chemiliminescence reaction. The dashed line shows the response for hydrogen peroxide in the absence of any interfering species. Error bars: one standard deviation (n=3).

Table 3.8 Recovery values for hydrogen peroxide (1 μmol L^{-1}) in the presence of varying concentrations of the interferent t-butyl hydroperoxide.

t-Butyl hydroperoxide concentration (μmol L^{-1})	Hydrogen peroxide recovery (%)
5	90.6
20	99.5
50	89.1
100	91.8
200	93.7
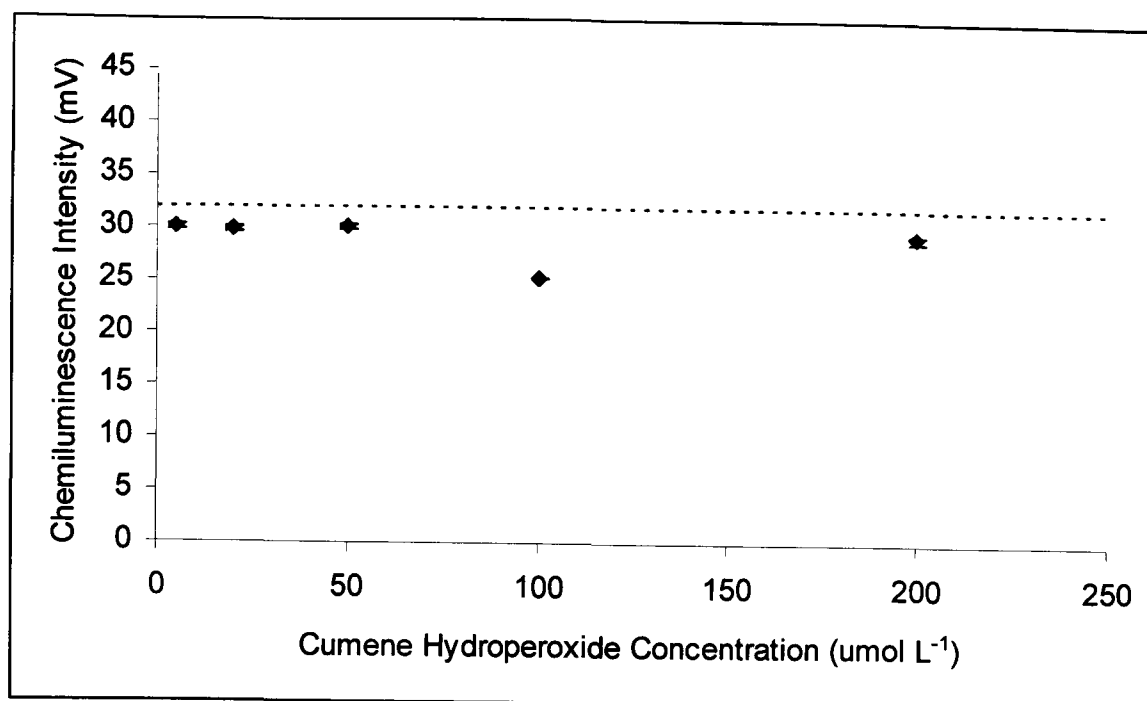
Figure 3.24 The effect of cumene hydroperoxide on the determination of hydrogen peroxide (1 μmol L⁻¹) using the luminol-Co(II) chemiliminescence reaction. The dashed line shows the response for hydrogen peroxide in the absence of any interfering species. Error bars: one standard deviation (n=3).

Table 3.9 Recovery values for hydrogen peroxide (1 μmol L⁻¹) in the presence of varying concentrations of the interferent cumene hydroperoxide.

Cumene hydroperoxide concentration (μmol L^{-1})	Hydrogen peroxide recovery (%)
5	98.6
20	98.1
50	98.5
100	82.6
200	96.1

The maximum molar tolerance ratio of t-butyl hydroperoxide and cumene hydroperoxide was determined to be >200 (i.e. 200 times greater than the concentration of hydrogen peroxide). This is much higher than the reported concentrations of organic peroxides present in rainwater and due to organic peroxides having a lower solubility in water it is unlikely to cause interference on the chemiluminescence response.[189]

127

Oxides of nitrogen in the atmosphere may also interfere with the luminol reaction. The effect of nitric acid on the reaction was investigated by spiking a 1 μmol L^{-1} hydrogen peroxide standard (figure 3.25). The percentage recoveries of the spiked samples are given in table 3.10.
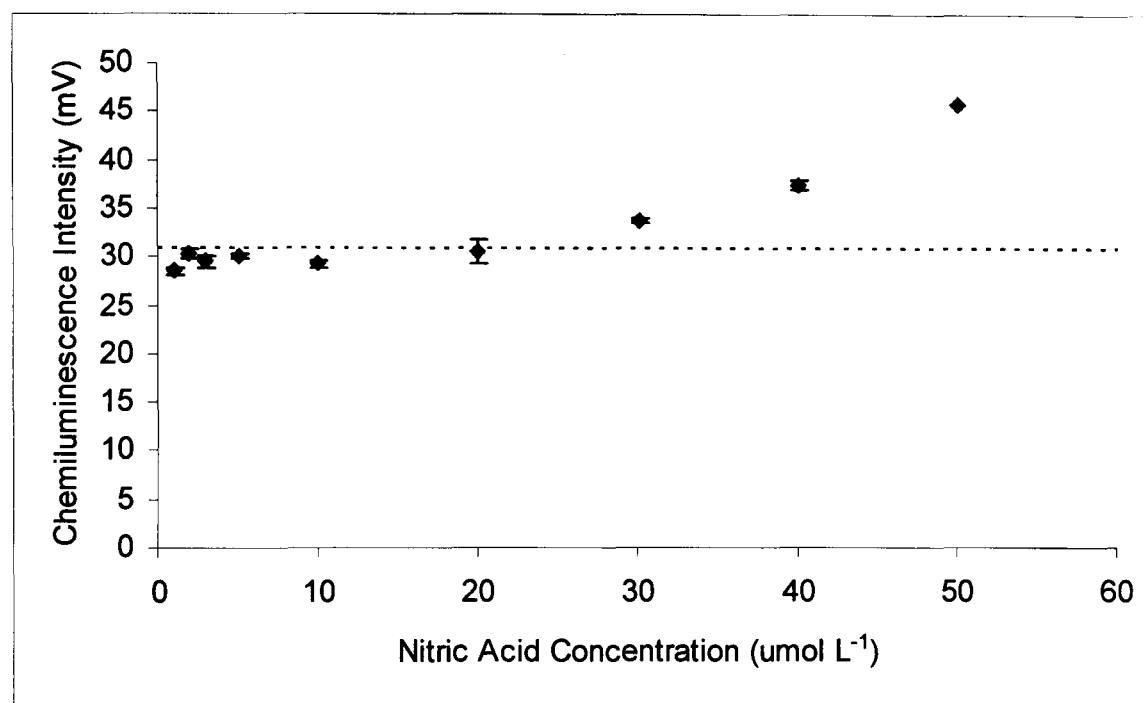
Figure 3.25 The effect of nitric acid on the determination of hydrogen peroxide (1 μmol L^{-1}) using the luminol-Co(II) chemiliminescence reaction. The dashed line shows the response for hydrogen peroxide in the absence of any interfering species. Error bars: one standard deviation (n=3).

128

Table 3.9 Recovery values for hydrogen peroxide (1 µmol L^{-1}) in the presence of varying concentrations of the interferent nitric acid.

Nitric acid concentration (µmol L^{-1})	Hydrogen peroxide recovery (%)
1	89.2
2	91.8
5	95.6
10	91.7
20	88.4
30	106.2
40	117.5
50	137.7

The maximum molar tolerance ratio of nitric acid was determined to be 30 and therefore unlikely to cause significant interference.

The bulk samples of rainwater (set 1 and 2) were analysed in the absence of the cobalt(II) co oxidant, which is necessary for the oxidation of luminol by hydrogen peroxide to occur in order to investigate other oxidising species in the rainwater (figure 3.26). The percentage response for hydrogen peroxide without the cobalt(II) present is given in table 3.11.
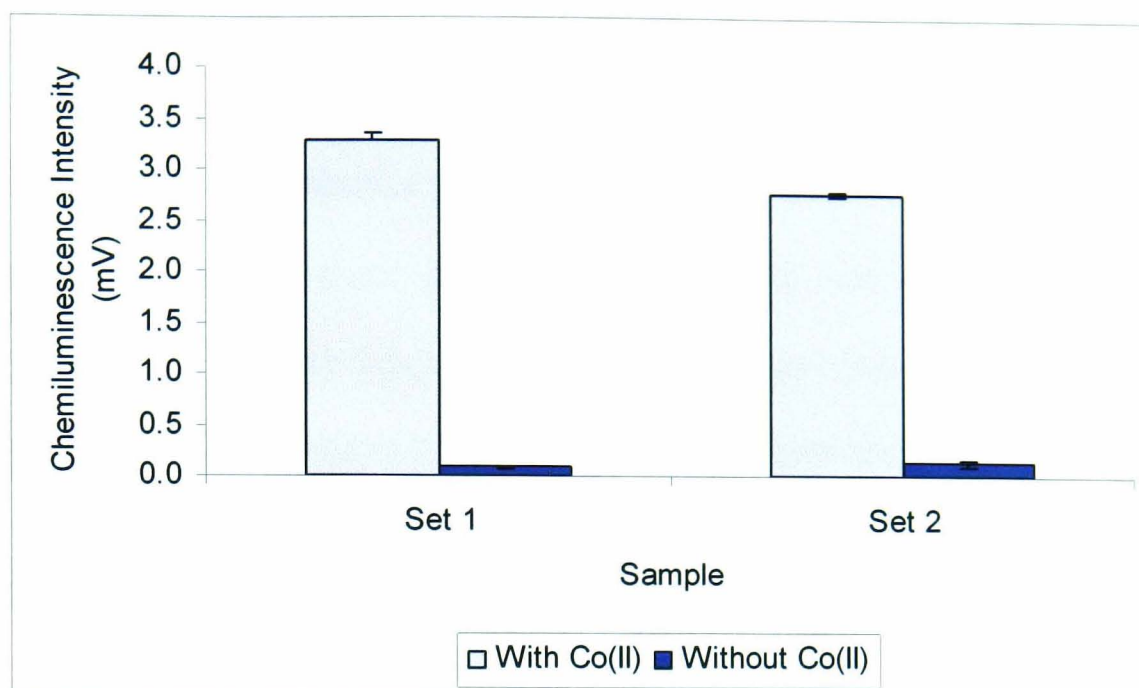
Figure 3.26 The effect of the presence of Co(II) on the determination of hydrogen peroxide in the bulk rainwater samples (set 1 and 2) using the luminol chemiliminescence reaction.

Table 3.11 Percentage response for the determination of hydrogen peroxide in the absence of Co(II) using the luminol chemiluminescence reaction.

Set	Chemiluminescence response with no Co(II) (%)
1	2.6
2	4.7

A negligible response was observed showing minimal interference from oxidising species in the sample matrix.

3.4 Conclusions and Future Work

A portable, sensitive method of analysis for the determination of real time hydrogen peroxide levels in rainwater during a rainfall event was developed. This was achieved using the luminol–cobalt(II) chemiluminescence reaction within a microfluidic device situated in the portable chemiluminescence detection system.

Enhancement of the chemiluminescence signal by 132.3% was achieved using the mirror reaction to directly apply a reflective surface to the top of the microfluidic device, this enable sensitivity to be achieved in the desired micromolar range with a limit of detection of 4.7 nmol L^{-1}. A small sample volume size of 10 µL min^{-1}, reagent consumption size (1.2 mL per hour) and waste production size (2.4 mL per hour) was also achieved. Comparing this with other chemiluminescence methods for the determination of hydrogen peroxide, high sensitivity has been maintained for a small sample volume. A comparison is given in table 3.12. Immobilisation techniques for immobilising luminol onto a solid support were investigated, however poor sensitivity was observed and this approach was not progressed.

Table 3.12 LODs and sample volume sizes for different chemiluminescence techniques used in the determination of hydrogen peroxide in comparison to the portable chemiluminescence detection system.

Chemiluminescence Reaction	LOD (nmol L^{-1})	Sample Volume (μL)	Reference
Luminol-Co(II)- H_2O_2	5 (seawater)	100	197
Luminol-Co(II)- H_2O_2 (reagent injection)	0.42^a	60	198
Luminol-Co(II)- H_2O_2 (immobilised reagents on ion exchange resin)	12	200	206
Luminol-Co(II) ethanolamine complex-H_2O_2 (immobilised reagents on ion exchange resin)	100	90	207
Luminol-KIO_4- H_2O_2	30	30	201
KIO_4-K_2CO_3-H_2O_2	5	90	203
DMTC-H_2O_2	40	100	202
Luminol-Co(II)- H_2O_2 (Microfluidic device)	4.7	10 μL min^{-1}	-

^{a} This detection limit was not calculated in the usual manner and is therefore not directly comparable with the other data listed.

Using this system two rainfall events were analysed achieving the desired sampling rate of every 5 minutes. The analysis showed the hydrogen peroxide concentration varied from 0.1-3.2 μmol L^{-1} in the rainwater collected. The system was also applied to the analysis of snow showing the levels of hydrogen peroxide varied from 0.2-0.5 μmol L^{-1} at ground level.

The system was not fully field deployable and to achieve this, the next step will be to fully automate the system by incorporating a sample introduction system and a data

logger. This can be accomplished using suitable switching valves, which can be used with microfluidic tubing connections. For the valves in use in this system, three way solenoid valves (Y valve configuration B (062 ministac ports)) have been obtained from Lee Valves (Lee Products Ltd., Buckinghamshire). The switching valves will enable the continuous introduction of the sample in order to monitor rapid changes of hydrogen peroxide levels during the rainfall event. A schematic of the system is given in figure 3.27. Valve 1 is closed, enabling the sample to be collected using a funnel and a float switch is used to indicate whether or not enough sample is present. When enough sample is present, the pump and PMT are switched on and the reactor is flushed with water (introduced through valve 2). During the analysis of the rain water, valve 1 and 2 are both open to allow the sample into the system and valve 3 is open to allow the chemiluminescence reagents into the system. At the end of the analysis, water is passed through valve 3 to flush the system (this prevents the carbonate buffer precipitating in the channels, which may cause a blockage) and the waste valve is open to allow collection of the new sample. When no sample is present the PMT and pump are switched off to conserve battery power. The exterior housing to the box will have to be redesigned such that it is water resistant so that the electrical components of the PMT, pump and data collection device are protected. One problem is with the calibration of the system as a hydrogen peroxide standard cannot be used in the field as it will degrade, therefore the chemiluminescence reagent will have to be checked against a hydrogen peroxide standard before field deployment. It may be possible to overcome this by producing the hydrogen peroxide electrochemically *in-situ*. Further stability testing of the reagent in the field will be necessary as well as an investigation into the lifetime the batteries in the system in

order to achieve a system that could be left in the field to analyse the hydrogen peroxide levels in an entire rainfall event.
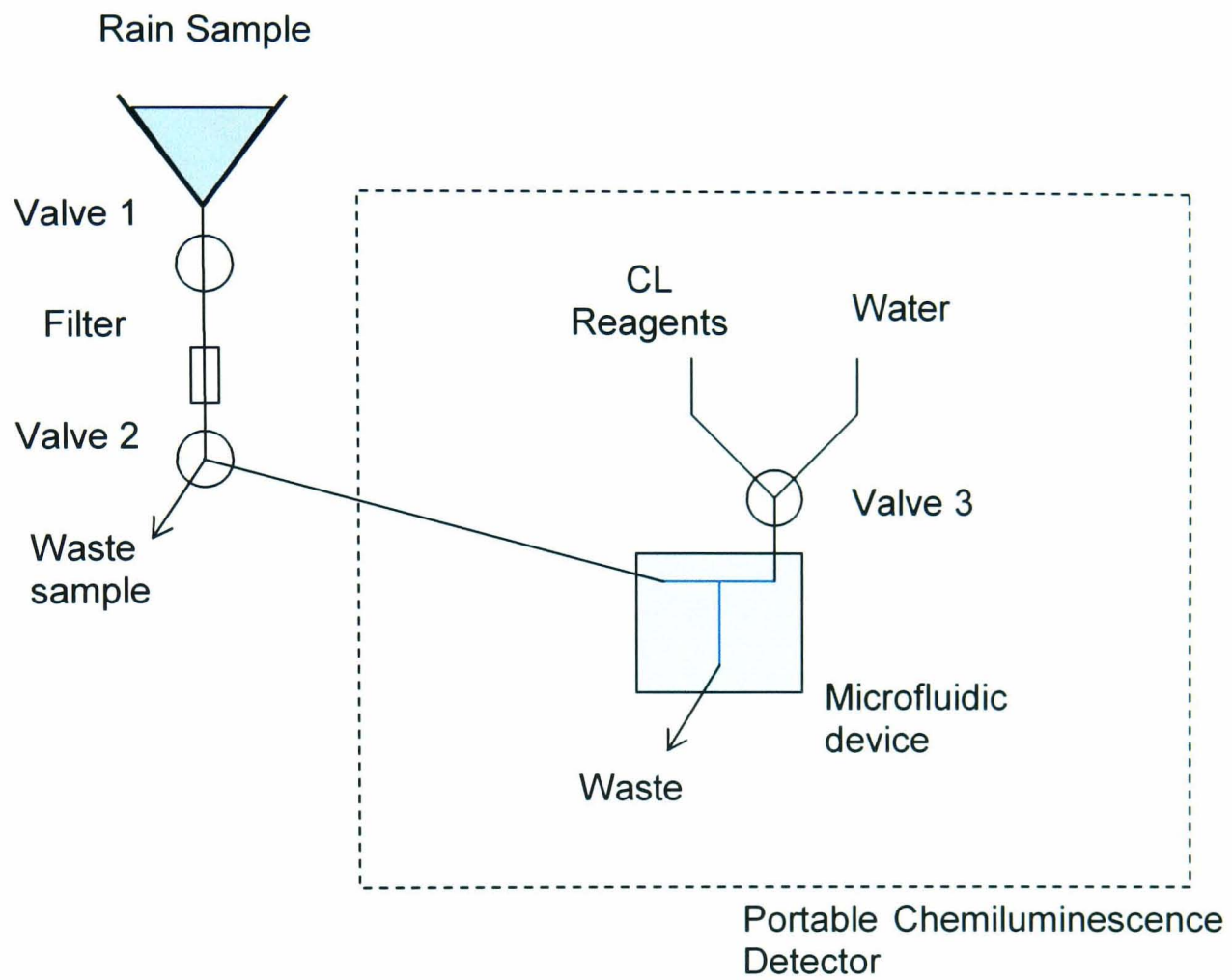
Figure 3.27 Schematic of the automated portable rainwater analyser, showing sample collection via a funnel and the valves for fluid manipulation.

Chapter 4

Analysis of *Escherichia coli* in Seawater

4. Analysis of *Escherichia coli* in Seawater

4.0 Aims

Escherichia coli (*E. coli*) bacteria present in seawater are an indicator for faecal contamination. Traditional methods of *E. coli* analysis are time consuming and must be carried out in a laboratory. Therefore a portable, fast and sensitive method of analysis is required to measure low levels of *E. coli* in seawater. The aim of this work was to develop a system that could detect *E. coli* in seawater in a rapid analysis time of less than 20 minutes. The system had to be specific enough to detect *E. coli* in the presence of other bacteria found in seawater and sensitive enough to detect less than 100 cells per mL of seawater. The system had to be portable enough to be taken into the field for on-site analysis.

A non-competitive (reagent excess) heterogeneous two step sandwich immunoassay with chemiluminescence detection of a HRP enzyme label was selected as specific and sensitive method for the detection of *E. coli*. This was investigated within a microfluidic device using a portable chemiluminescence detection system in order to produce a field deployable miniaturised analytical system for the determination of *E. coli* in seawater.

4.1 Introduction

4.1.1 *Escherichia Coli*

Bacteria are small (<1μm - 50μm) single celled microorganisms and are a form of prokaryotic cells (DNA not within a nuclear membrane).[227] *Escherichia coli* (*E. coli*) is a member of the eubacteria, it is a rod shaped gram-negative bacteria i.e. the cell

surface structure consists of a thin peptidoglycon (1-3 nm) layer with an outer membrane. *E. coli* is found within the gastrointestinal tract of all warm-blooded animals. An *E. coli* cell is between 0.4-0.7 µm diameter and 1.0-1.3µm long. There are over 200 specific serological types of *E. coli* based on their somatic (O), surface (K) and flagellar (H) antigens. *E. coli* is usually non pathogenic, it is only certain strains that are potentially harmful. One specific serotype of *E. coli*, which most people are familiar with is *E. coli* O157:H7, an enterohemorrhagic *E. coli*. This strain produces two toxins (verotoxins I and II) closely related to the *shigella dysenteriae* producing toxin. Illnesses associated with O157:H7 include cramping and severe diarrhoea, some victims can develop renal failure and haemolytic anaemia. Most of the outbreaks of *E. coli* O157:H7 are associated with undercooked/raw beef. The determination of *E. coli* O157:H7 is not covered in this work, but the methodology is applicable to *E. coli* in the environment and so has been included.

4.1.1.1 E. coli in the Environment

Faecal contamination of water is measured by the determination of the bacterial groups: total coliforms, faecal coliforms, and *E. coli*. Coliform bacteria are a group of bacteria, which are defined as rod-shaped Gram-negative organisms which ferment lactose with the production of gas when incubated at 35 °C, *E. coli* is a member of the coliform group.[227] Of these measurements *E. coli* is thought of as the most reliable measurement, because its presence directly indicates the presence of enteric pathogens. It is also difficult to detect most enteric bacteria and viral pathogens due to their low numbers; therefore the determination of *E. coli* is used as an indicator microorganism for the presence of traces of faecal contamination and therefore enteric pathogens.[227]

There are risks associated with pathogens present in sewage and marine sewage outfalls contaminating bathing beaches. Bathing water quality of designated beaches is monitored by the Environment Agency in England and Wales against the bathing water regulations (SI1991/1597) under the EC bathing water directive (76/160/EEC). The standards that should not be exceeded are 10,000 total coliforms per 100 mL of water and 2,000 faecal coliforms per 100 mL of water. 95% of samples must meet these standards to comply with the directive.[228]

4.1.1.2 Traditional Methods for E. coli Determination

E. coli in water samples are normally enumerated with culture-based methods that need a long time (18–72 h) to complete.[229] Standard techniques include multiple-tube fermentation (MTF) and membrane filter (MF) techniques. MTF is based on inoculating a number of tubes with specific dilutions of the water sample within a specific media (e.g. lactose). A positive presumptive test is achieved if there is either production of gas, acid formation during fermentation with lactose or abundant growth in the sample after 48 h at 35°C. All positive results then undergo confirmation tests. Numerical results are expressed in terms of most probable number (MPN) of microorganisims present, i.e. a statistical estimation based on the average number of coliforms in the sample. Therefore this is only a semi-quantitative method. Disadvantages associated with this approach include interferences from high numbers of non-coliform bacteria and inhibition effects from the chosen media and the long analysis time, which is tedious and labour intensive. Advantages of this approach include the fact it can be used for complex samples such as coloured or turbid samples, the method is easy and requires no expert skills or complicated equipment and it is inexpensive. The MF technique is based on the filtration of water

samples through a 0.45 µm pore size filter. This retains the bacteria and is then incubated on a specific media, which produces coliform bacteria of a certain colour, and then the colonies can be counted on the filter. Non-coliform bacteria can cause interferences and stressed or injured coliforms may not be detected. There are a number of media to use depending on the coliform under investigation and the environment from which the sample was taken, there is no universal media. Advantages include the fact that large numbers of water samples can be tested, which improves sensitivity and reliability. The method gives a quantitative result and is relatively simple. Disadvantages include the analysis time of 24 h for initial results and a further 24 h for confirmation tests. Therefore there is a need for fast, sensitive (low limits of detection) and accurate methods (prevention of false negatives and positives) for determining faecal contamination of water.

Immunological techniques based on the binding properties of antibodies and antigens are amenable for the species-specific detection of pathogenic bacteria. Selective identification is required as there may be low numbers of the specific bacteria coexisting with large numbers of different bacteria in a complex environmental sample. The advantages of using immunological approach are their specificity, rapid analysis time and the fact that the whole cell is detected. Immunological methods do not necessitate a cell/spore lysis step, which is required for the extraction of DNA/RNA. For the DNA analysis, the polymerase chain reaction (PCR) is used to amplify the target gene providing the method with the advantage of high sensitivity and selectivity, however it has the disadvantage of being quite complex and expensive to set up and requires expertise in molecular biology as well as being time consuming. The DNA primer must be unique for target bacteria and PCR is highly

susceptible to contamination compared with other techniques such as ELISA.[230, 231] Because of this PCR based techniques are not amenable to field use. Therefore immunological techniques have been selected as an appropriate approach for determining *E. coli* in seawater and will be investigated in order to develop a rapid and portable method of analysis.

4.1.2 Immunological Techniques

4.1.2.1 Antibodies

An immunoassay is a measurement system that uses antibodies as specific binding reagents. Antibodies are used by the immune system to specifically recognise target antigens. Immunoglobulins (Ig) are glycoproteins that function as antibodies. Immunoglobulins have a basic monomer unit consisting of two identical heavy (H) polypeptide chains and two identical light (L) polypeptide chains, linked together *via* a disulphide bond. The chains fold into discrete regions known as domains and within the chains there are constant and variable regions. The structure of the heavy chain determines the class and subclass of the immunoglobulin. There are five classes of immuoglobulins: IgG, IgA, IgM, IgD and IgE, which differ in size, charge, amino acid composition and carbohydrate content, and therefore specialise in different functions. IgG, IgE and IgD are monomers, IgA is dimeric and IgM is pentameric. The antibody class commonly used in immunoassays is IgG, which are a 150,000 Da glycoprotein consisting of two identical heavy (H) polypeptide chains ($\approx$ 420 residues) and two identical light (L) polypeptide chains ($\approx$ 215 residues). (See figure 4.1).[232, 233]
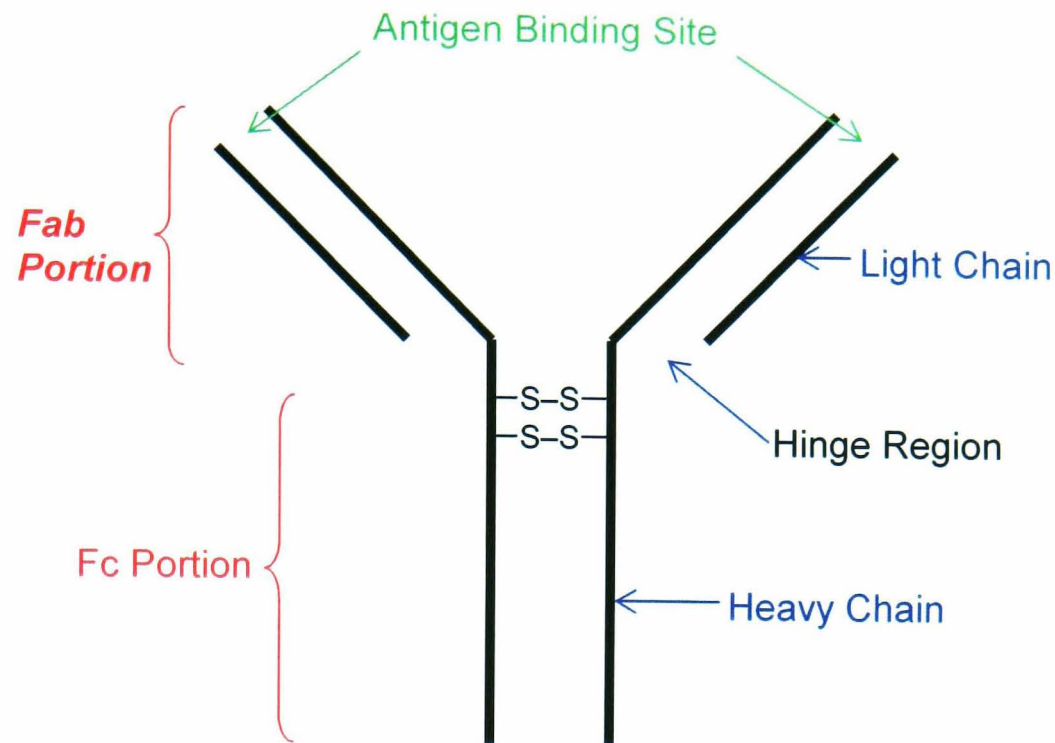
Figure 4.1 Schematic of IgG antibody structure.[232]

Each heavy chain has a constant region, which is the same for all the immunoglobulins of the same class and forms the –COOH end of the molecule, as well as a variable region. Light chains have two distinct forms, kappa (κ) and lambda (λ), and each antibody will have one of these forms. For IgG, each heavy chain has a constant region of three domains and one variable domain, and each light chain has one constant domain and one variable domain. The monomer can be separated into fragments forming the *Fab* (*f*ragment *b*inding *a*ntigen) fragments composed of one constant and one variable domain of each the heavy and the light chain and an *Fc* (*f*ragment *c*rystallisable) fragment composed from two heavy chains that each contribute two to three constant domains (depending on the class of the antibody) (see figure 4.1).[232, 233]

The hypervariable regions (or Complementary Determining Regions (CDR)) of the heavy and light chains form the antigen binding sites at the amino terminal end of the

molecule. Therefore for IgG, each molecule has two antigen binding sites. The variability of antibodies to bind to different antigens arises due to events known as somatic recombination. This is when genes are selected (variable (V), diversity (D) and joining (J) for heavy chains, and only V and J for light chains) to form innumerable combinations.[232, 233]

Antigen – antibody interactions are reversible. The binding occurs in two phases, phase one requires repulsive forces to be overcome; the second is the collision and formation of intermolecular attractive forces including hydrogen bonding, ionic and van der Waals forces between the antigen and antibody. The rate at which the collisions occur is dependent on diffusion rates, influenced by mass, shape, temperature and mobility of the reactants. This suggests that using a microfluidic device will improve the time of analysis because of the decreased diffusional paths within the channels. When the antibody or antigen is immobilised equilibrium is reached more slowly. Other physiochemical conditions of the aqueous environment apart from temperature which influence binding include pH, ionic strength and the presence of ionic species. The appropriate pH is required (usually around pH 7) to ensure dissociation/association of the acidic and basic groups on both the antibody and antigen.[232, 233]

4.1.2.2 Immunoassay Classification

There are a wide variety of formats that can be implemented for immunoassays and can be separated into four groups: Label free assays, reagent excess assays, reagent limited assays and ambient analyte assays, these are summarised in table 4.1 and a schematic representation can be seen in figure 4.2.[232, 233] In general immunoassays are carried out in 96 well microtitre plates.

Table 4.1 Comparison of the four groups of immunoassay types: label free, reagent excess, reagent limited and ambient analyte.

Immunoassay	Details	Examples		
Label Free	Complexes formed by antibody-antigen interaction can be detected visibly by naked eye or measured by their ability to scatter light.	Agglutination Precipitation Immunosensors		
Reagent Excess	Uses an excess concentration of labelled antibody/antigen.	One Site	Immunostaining Western Blotting	
		Two Site	ELISA (Enzyme Linked ImmunoSorbent Assay) Immunofluorometric Assay Immunoradiometric assay	
Reagent Limited (Competitive Assays)	Uses a limited concentration of labelled antibody/antigen. Less sensitive than reagent excess techniques.	Radioimmunoassay Enzymimmunoassay Fluoroimmunoassay		
Ambient Analyte	Low concentrations of capture antibodies/antigen.	Microarray/microchip		

Figure 4.2 Schematic representation of the range of different designs of immunoassays, Where A and B are label free assays, C-E are reagent excess assays and F and G are reagent limited competitive assays.[232]
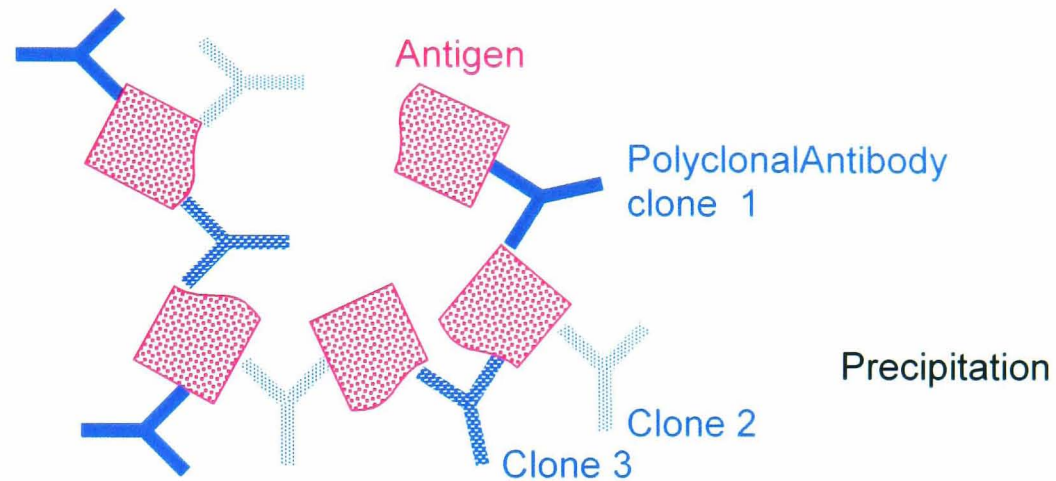
A. Precipitation occurs if there are sufficient concentrations of the immunocomplexes formed by the antibody-antigen interactions. These may be visible for a quantitative assay or measured by light scattering for quantitative analysis. If the antibody concentration is constant then the antigen concentration can be determined (and vice versa). Reagents can also be used to promote precipitation e.g. polyethylene glycol.
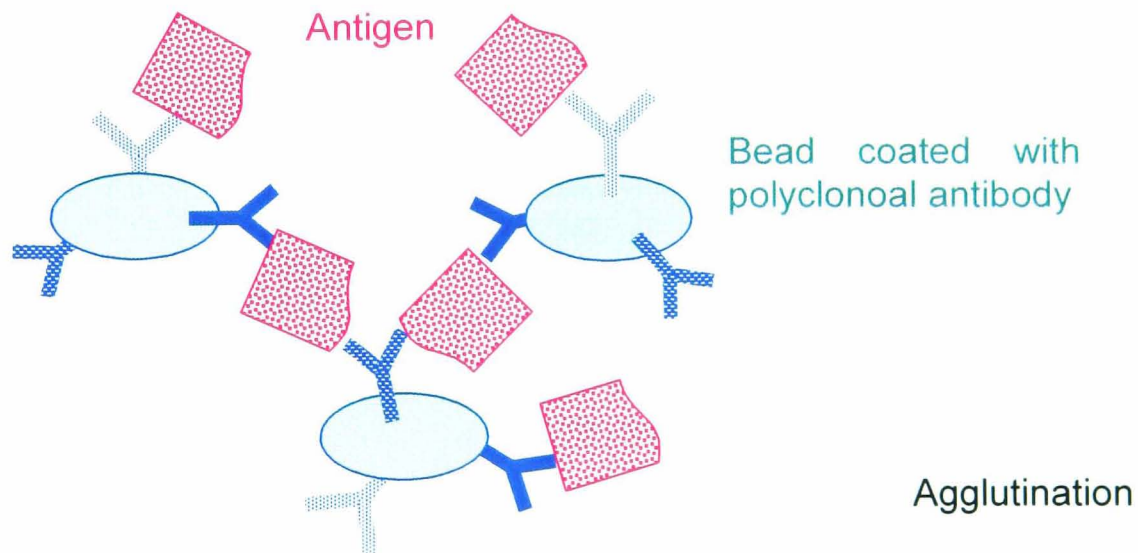
B. Agglutination incorporates the use of antibody coated latex beads. Specific antigen binding causes the suspension of beads to clump producing detectable agglutination.
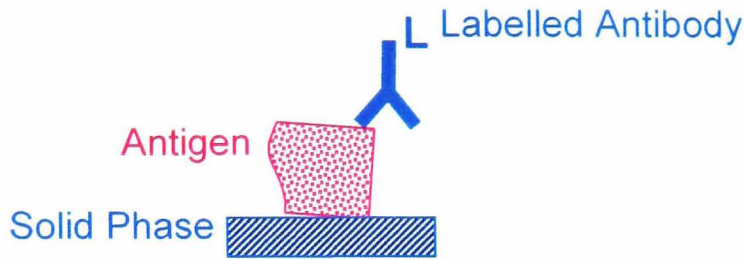
Simple immunoassay complex – immobilised antigen with labelled antibody

C. *The immobilised antigen with labelled antibody represents the final immunocomplex obtained after simple immunoassay e.g. western blotting and immunostaining.*
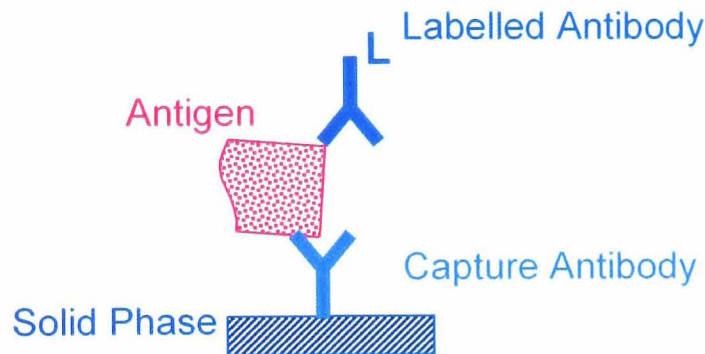
Two site assay. Capture antibody immobilised to a solid phase, directly labelled detection antibody.

D. *Common arrangement for reagent-excess sandwich immunoassay.*
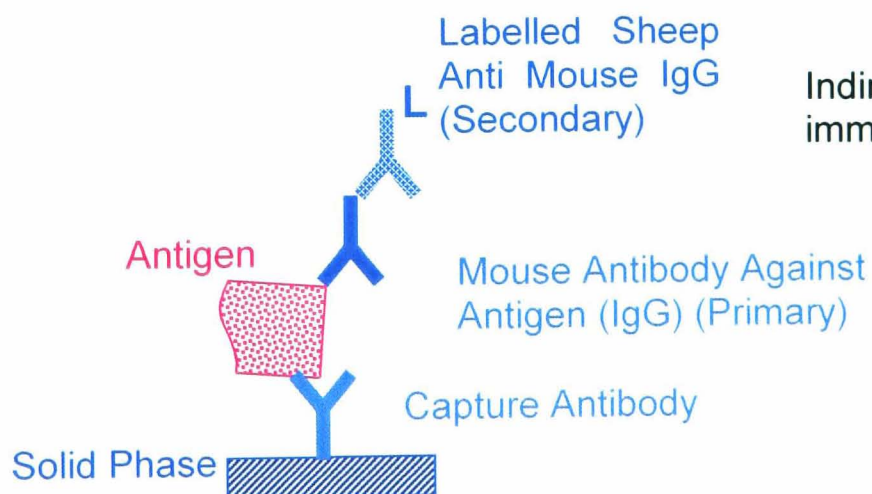
Indirect labelling of sandwich immunoassay

E. *As D, but with use of secondary antibody for indirect labelling (see section 4.5 for details)*
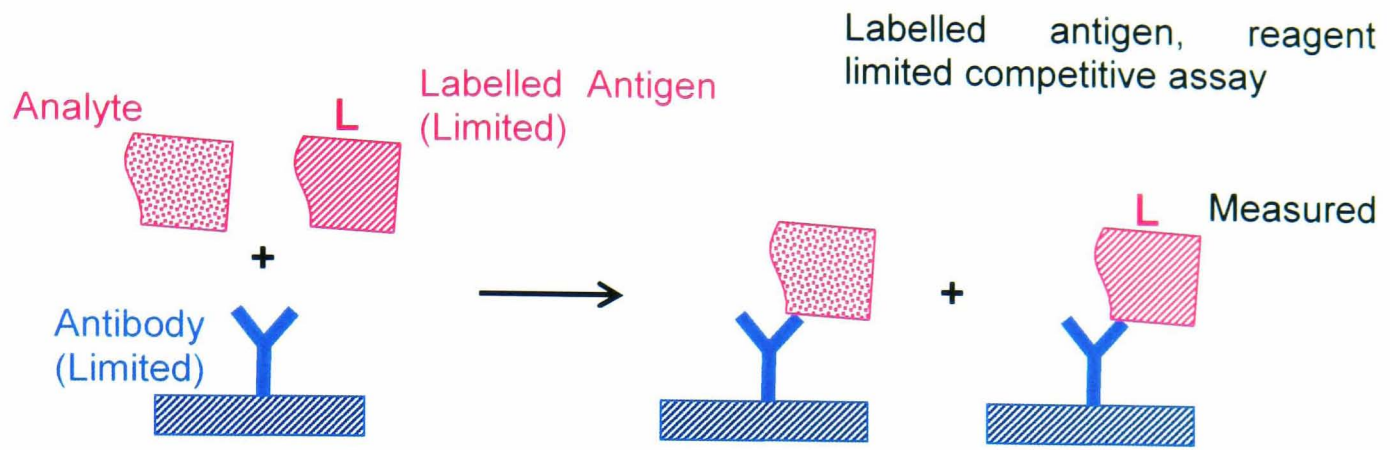
F. *Labelled antigen, reagent limited competitive assay where the antibody concentration is a constant limited concentration. The amount of label bound is inversely proportional to analyte concentration.*
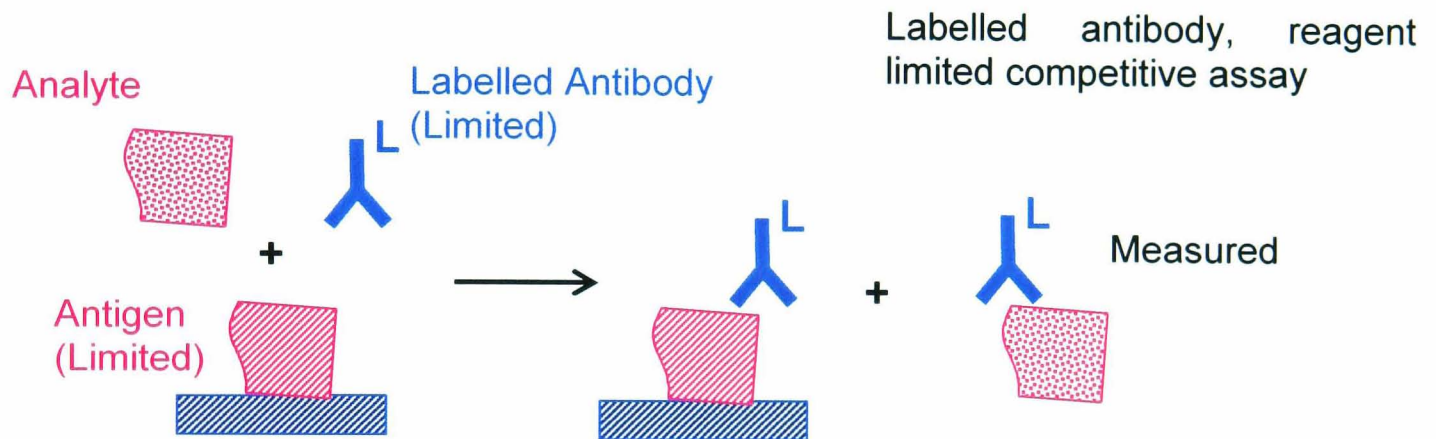
G. *Labelled antibody reagent limited competitive assay designed for antigen determination. Again, the amount of label bound is inversely proportional to analyte concentration.*

Homogeneous (separation free) immunoassays where the antibody and antigen are free in solution to interact are considered the optimal format for detection if the antibody-antigen complex can be directly detected. However, they can have poor accuracy and low sensitivity. Heterogeneous (separation) immunoassay whereby one reactant is immobilised onto a solid support provides a preconcentration step for the assay improving the sensitivity and is cost effective as the antibodies can be

regenerated and reused. When using a heterogeneous assay, there are several factors to consider, including the preservation of the structure and biological activity of the immobilised species. There should be sufficient attachment of the species to prevent loss of reactivity. The support should be inert to reduce non specific binding of interfering species to the support, and the reagent binding sites must be sufficiently away from the support in order for rapid and efficient interaction with the analyte to occur. [232, 233]

4.1.2.3 Antibody Labels

Labels and endpoints used in immunoassays for detection, as featured in figure 4.1, include radioisotopic, enzymatic, fluorescent or chemiluminescent molecules and are presented in table 4.2.[232, 233]

Indirect labelling can be applied by use of a labelled secondary antibody that conjugates to a specific primary antibody. The advantages of using this approach are for evaluating a number of anti-analyte antibodies, when there is a short supply of the anti-analyte antibody, and for investigating a range of assays. The disadvantage of this method is the development of non-specific binding, which can reduce sensitivity.

Table 4.2 Comparison of the different labels used in immunoassays: radioisotope, enzyme, fluorescent and chemiluminescent.

Label	Advantages	Disadvantages	Examples
Radioisotope	Simple labelling method Label unaffected by environmental factors	Hazardous Expensive (requirement of appropriate equipment and licensed facilities)	Iodine 125 (^{125}I) Tritium (^{3}H) Measured using scintillation counters
Enzyme	High Sensitivity (with fluorescence and luminescence methods) Relatively inexpensive Easy preparation labelled reagents Wide availability of necessary equipment Safe Commercially available	Produces a two step analysis (antibody-antigen binding and signal generation) which requires control, optimisation and reduced interference	Horseradish Peroxidase (HRP) Oxidised by hydrogen peroxide, then oxidises a second substrate – either a colorimetric, fluorometric or luminometric reagent Alkaline Phosphatase – catalyses ester hydrolysis of primary alcohols, phenols and amines
Fluorescent	Low Limits of Detection Stability of labelling Commercially available	Non-specific binding causes signal quenching. Disadvantage of photo-bleaching	Fluorescein-5-isothiocyanate (FITC)
Chemiluminescent	Low Limits of Detection	Requires preparation of labelled antibody	Luminol, isoluminol, and acridinium esters

Table 4.2 Labels used in Immunoassays.

Enzyme labels for immunoassays provide high sensitivity. A common enzyme employed in immunoassays is the horseradish peroxidase (HRP) enzyme. HRP can be used as a cooxidant in the luminol-hydrogen peroxide chemiluminescence reaction, previously investigated in chapter 3.

The HRP-Luminol Chemiluminescence Reaction

The reaction scheme for the HRP-luminol chemiluminescence reaction is generally accepted to be similar to the reaction with cobalt(II) as the cooxidant (see section 3.1.4). It involves the formation of a complex between the hydrogen peroxide and peroxidase which oxidises the luminol to produce a luminol radical, which then undergoes further reactions to produce the endoperoxide, which decomposes to yield 3-aminophthalate in the excited state. The multistep reaction creates areas in which the efficiency can be improved to increase light intensity. Examples of enhancers of the luminol-HRP-hydrogen peroxide reaction include 6-hydroxybenzathiole derivatives, phenolic compounds and naphthols and are outlined in table 4.3. *p*-Iodophenol is one of the most efficient enhancers of the HRP-luminol-hydrogen peroxide reaction.[214, 234-236]

The advantages of using an enhancer, besides increased light intensity and sensitivity include the fact that they are relatively specific.

Table 4.3 Summary of the compounds which enhance the emission intensity of the HRP-luminol chemiluminescence reaction.

Compounds	Examples	Reference
6-Hydroxybenzothiazole derivatives	Firefly *D*-luciferin Firefly *L*-luciferin 6-Hydroxybenzothiazole 2-Cyano-6-hydroxybenzothiazole	214, 237
Substituted phenols	*p*-Iodophenol *p*-Bromophenol *p*-Chlorophenol 2,4-Dichlorophenol *p*-Phenylphenol	214, 234-236, 238
Naphthols	1,6-Dibromonaphth-2-ol 1-Bromonaphth-2-ol 2-Naphthol 6-Bromonaphth-2-ol	214
Other enhancers	4-Biphenylboronic acid Sodium teraphenylborate	238

The reaction mechanism of the enhancement compounds is not fully understood, although evidence suggests that it is not the enhancers themselves that act as an emitter nor that the formation of more efficient chemiluminescence compounds takes place as they do not alter the emission spectra of the luminol reaction. The most likely explanation is that the enhancers either directly or indirectly increases the speed of one or more steps in the reaction pathway before emission takes place.[214]

Using an enhancer in the luminol hydrogen peroxide reaction provides a rapid sensitive assay for peroxidase, which can be used as a label in immunoassays.

Examples of HRP labels for immunoassays can be seen in table 4.4 in section 4.1.2.4.

4.1.2.4 Flow Immunoassay

Typical immunoassays are performed manually using 96 well microtitre plates. These are difficult to handle and time consuming and therefore it is preferable to automate the system. Automation incorporating microtitre plates is achievable and several systems are available, however the disadvantage to this technique is the expensive and complicated robotic equipment required. This has lead to the incorporation of immunoassay methodology into flowing systems. FIA systems have the advantage of simple instrumentation and can be easily automated. The sequential addition of reagents in immunoassays can easily be incorporated into a flowing system. Both homogeneous and heterogeneous immunoassays have been integrated into FIA. A heterogeneous immunoassay format is more amenable to FIA as it provides on-line separation and this is advantageous as it eliminates sample pre-treatment because the selective binding to the immunoreactor provides a preconcentration and clean up step. This approach requires a solid support, which allows the sample to be transported to the immobilised reagents for binding to occur, as opposed to passive diffusion in static systems. A disadvantage to this approach is the limited lifetime of the immunoreactor. Both competitive and non-competitive modes can be applied to flowing systems. Examples of flow injection immunoassays are given in table 4.4.

Table 4.4 Examples of Flow Injection Immunoassay Applications.

Application	Details	Detection	Limit of Detection/ Assay Time	Ref.
Aflatoxin B1	Competitive enzyme immunoassay with protein G capture column after formation of immunocomplex	Amperometric	11 ng L^{-1} (35 pmol L^{-1}) 6 samples/hour (triplicate)	239
Alpha-fetoprotein	Non- competitive enzyme immunoassay pre-incubation with column capture after formation of immunocomplex	Chemiluminescence (HRP label - luminol)	0.5 ng mL^{-1} 30 min	240
17 alpha-hydroxyprogester one and human chorionic gonadotropin	Non-competitive enzyme immunoassay	Chemiluminescence (ALP-cortisol-lucigenin)	1 x pmol L^{-1} (Assay time not available)	241
Carbaryl	Competitive heterogeneous (CPG) enzyme immunoassay	Fluorescence (HRP label with 3-(p-hydroxyphenyl)-propanoic acid (HPPA) substrate)	0.029 µg L^{-1} (0.1 nmol L^{-1}) 20 min	242
Carcinoembryoni c antigen (CEA)	Non- competitive enzyme immunoassay preincubation with column capture after formation of immunocomplex	Chemiluminescence (HRP label - luminol)	1 ng mL^{-1} 30 min	243
Digoxin	Competitive heterogeneous (hydroxysuccinimide activated metacrylate polymer) immunoassay with sequential injection	Chemiluminescence (Acridinium ester as label)	Low fmol range < 8 min	244

Digoxin	Competitive heterogeneous (CPG) immunoassay	Fluorescence (FITC label)	1.2 µg L^{-1} (1.5 nmol L^{-1}) 5 min	245
Okadaic acid in mussels	Competitive heterogeneous enzyme immunoassay using polyethersulfone membranes	Chemiluminescence (HRP label - luminol)	0.1 µg L^{-1} (0.1 nmol L^{-1}) 20 min	234
Theophylline	Competitive heterogeneous (CPG) enzyme immunoassay	Fluorescence	3 µg L^{-1} (17 nmol L^{-1}) 5 min	246
Environmental Pollutants: TNT, diuron and atrazine	Competitive enzyme heterogeneous immunoassay with antibody immobilised onto gold pyramidal structures in a single use chip	Chemiluminescence (HRP label - luminol)	0.1 µg L^{-1} (0.4 nmol L^{-1}) TNT 35-40 min	247
3,5,6-trichloro-2-pyridinol	Competitive heterogeneous (CPG) enzyme immunoassay	Fluorescence (HRP label with 3-(p-hydroxyphenyl)-propanoic acid (HPPA) substrate)	0.027 µg L^{-1} (0.1 nmol L^{-1}) 25 min	248
Triiodothyronine	Competitive heterogeneous (hydroxysuccinimide activated metacrylate polymer) immunoassay with sequential injection	Chemiluminescence (Acridinium ester as label)	0.44 ng mL^{-1} (0.9 pmol L^{-1}) 7-9 min	244
Vitellogin	Non-competitive heterogeneous (magnetic particles) enzyme immunoassay with sequential injection	Chemiluminescence (HRP label - luminol)	2 ng mL^{-1} 20 min	249

152

4.1.2.5 Current Research for the Determination of E. coli.

Several methods have been investigated for the determination of *E. coli* with the aim of improving the detection limits and analysis time in order to replace the traditional methods discussed in section 4.2. The majority of current research undertaken has been for the application of *E. coli* O157:H7 in food samples. These have also been documented as the methodology can also be applied to the analysis of *E. coli* in seawater. Common techniques applied to the analysis of *E. coli* include the use of biosensors and immunomagnetic separation techniques. Biosensors, specifically immunobiosensors, work using a molecular recognition process. Analysis is based on the specific antigen-antibody binding reaction at the surface of the sensor. Measurement is achieved *via* the signal-transfer process which detects the changes in an electrochemical or spectroscopic parameter of the sensor caused by the specific binding. Immunomagnetic separation techniques are based on the use of antibodies immobilised onto magnetic particles for species-specific identification and a magnetic field for separation.[250] The different approaches to *E. coli* analysis have been categorised by their detection methods.

4.1.2.5.1   Electrochemical Methods of Detection

Electrochemical methods of detection provide a simple, low powered, cost effective method of detection and have been used by several groups. LODs are reported as either cells mL^{-1}, or CFU mL^{-1} (Colony Forming Units per mL), CFU is a measure of viable bacterial numbers. A CFU number is not an exact measure of cells, as a colony-forming unit may contain more than one cell (pairs, chains or clusters).

Ruan *et al.* produced an impedance biosensor for *E. coli* O157:H7 detection. Impedance is the resistance of an alternating current and is measured with respect to an applied frequency and excitation signal. The main advantage of this technique is rapid data acquisition. The analysis utilised antibodies immobilised onto indium tin oxide electrodes using an epoxysilane monolayer with enzymatic catalysis precipitation of 5-bromo-4-chloro-3-indolyl phosphate by alkaline phosphatase for the electrochemical detection producing an LOD of 6 x 10^3 cells mL^{-1}.[251] A microimpedance biosensor was used by Radke *et al.* using a silicon microelectromechanical system consisting of *E. coli* specific antibodies immobilised onto gold electrodes allowing the impedance across the electrodes to be measured when *E. coli* was present. An extremely rapid analysis time of 5 min was reported, unfortunately the LOD was only 10^5 CFU mL^{-1} (colony forming units per mL), using a pure culture.[252]

Gau *et al.* demonstrated an amperometric detector for the detection of *E. coli*. The system integrated microelectromechanical systems (MEMS) to produce a multielectrode detector array with self assembled monolayers (SAMS) for the immobilisation of streptavidin onto a gold working electrode, which captures *E. coli* rRNA. ssDNA-rRNA hybridisation allowed for the specific detection of the bacteria and enzyme amplification using peroxidase allowed for very high sensitivity (LOD 1 x 10^3 *E. coli* cells). The analysis time was 40 min, a vast improvement on traditional methods.[253] An amperometric biosensor was also used by Ruan *et al.* in conjunction with immunomagnetic separation for *E. coli* O157:H7 analysis. The assay consisted of anti *E. coli* antibodies immobilised onto magnetic beads and a sandwich assay was adopted using alkaline phosphatase labelled anti *E. coli* antibodies. The alkaline

phosphatase was used to produce phenol from phenyl phosphate, the phenol was then detected using a tyrosinase-horseradish peroxidase amperometric biosensor. This assay gave a highly sensitive method with an LOD of 6 x 10^2 cells mL^{-1} in a reasonable assay time of 2 h.[254] Immunomagnetic separation and amperometric detection was also used by Perez *et al.* for the determination of *via*ble *E. coli* O157:H7. This approach gave a lower LOD of 10^5 cells mL^{-1} in a similar assay time of 2 h.[255]

Abdel-Hamid *et al.* developed a flow injection immunofiltration assay system with amperometric detection for *E. coli* and *Salmonella* in food, based on a disposable porous nylon membrane containing immobilised antibodies for a sandwich immunoassay. This produced a highly sensitive method with an LOD of 50 cells mL^{-1} for both bacteria with a fairly rapid assay time of 35 minutes.[256]

E. coli analysis can be achieved using β-galactosidase, a bacterial enzyme relatively specific to *E. coli*. Analysis time is fairly rapid, however one disadvantage to this approach is the occurrence of false positive and false negative results. A number of substrates can be utilised in the reaction for electrochemical detection. Boyaci *et al.* used β-galactosidase in conjunction with an amperometric detection system with immunomagnetic separation.[257] The paramagnetic microbeads are streptavidin functionalised with immobilised biotin-labelled capture antibodies for *E. coli*. This is incubated in a broth media containing isopropyl β-D-thiogalactopyranoside, which induces β-galactosidase. This converts *p*-aminophenyl beta-D-galactopyranoside into *p*-aminophenol, which is detected by amperometry. This technique gave a poor LOD of 2 x 10^6 CFU mL^{-1} for a 30 min incubation, which gave an analysis time of less than 1 h. The LOD could be improved to 20 CFU mL^{-1}, unfortunately this was

achieved by increasing the incubation time to 6-7 h. An amperometric enzyme biosensor with an antibody coated electrode was also developed for the electrochemical detection of β-galactosidase (p-amino-phenyl-beta-D-galactopyranoside as the substrate) for the determination of *E. coli* in water demonstrated by Mittleman *et al.* achieving a sensitive LOD of 1 x 10^3 CFU mL^{-1} within a reasonable 60-75 min assay time.[258]

Makenzo *et al.* used an immune labelling system, based on the formation of the immunocomplex of *E. coli* O157:H7 bacteria with alkaline phosphatase-labelled anti-*E. coli* O157:H7 polyclonal antibodies, which were filtered and the filter placed on a glassy carbon electrode which detected *p*-nitrophenol, the product of the alkaline phosphatase catalysis of *p*-nitrophenyl phosphate hydrolysis. This method gave a good LOD of 5 x 10^3 cells mL^{-1} in a rapid analysis time of 35 min in a small sample volume size of 100 µl.[259]

Ertl *et al.* employed a screen printed biosensor array with immobilised lectins for lectin-lipopolysaccharide recognition of microorganism. Lectins selectively bind to cell wall oligosaccharides to capture *E. coli* JM105 cells, detection was achieved electrochemically based on the oxidation of ferricyanide to generate chronocoulometric signals that could be analysed by principal component analysis (PCA) to identify *E. coli* subspecies in an analysis time of 40 min.[260]

Casimiri *et al.* developed an *E. coli* assay based on the measurement of the metabolite L-lactate produced by *E. coli* in media using L-lactate enzyme sensors (L-lactase oxidase immobilised on electrode). This approach achieved a small sample size of 1- 500 µl, however it gave a poor LOD of 5 x 10^5 cells mL^{-1}.[261]

An assay for *viable E. coli* O157:H7 in ground beef was presented by Guan *et al.* using immunomagnetic separation and PCR to produce an LOD of 0.7 CFU g^{-1} however it gave a lengthy analysis time of 6 h, although this is still an improvement on traditional methods.[262]

Electrochemical methods of detection for immunoassays provide a very rapid method of analysis compared with traditional methods of *E. coli* analysis. The main disadvantage of electrochemical techniques is electrode fouling as previously discussed in section 1.2.7.1.

4.1.2.5.2 Mass Sensitive Detection

Mass sensitive sensors work on the principle that a change in mass on the surface of the sensor occurs in the presence of analyte, which produces a change in resonance frequency and this can be measured and related to the analyte concentration.

A surface acoustic wave (SAW) biosensor was used by Howe *et al.* for the determination of *E. coli* and *Legionella* simultaneously utilising the immobilisation of the bacteria to the sensor before the addition of the antibody, this resulted in a detection system with a fairly poor LOD of 10^6 cells mL^{-1} in 3 h.[263] Pyun *et al.* developed a biosensor produced on an acousto-gravimetric flexural plate wave (FPW) transducer for the determination of *E. coli* K12 and *E. coli* J5 yielding an improved LOD of less than 10^3 cells in a fairly rapid analysis time of less than 30 min. Detection is based on the high sensitivity gravimetric transducers, which respond to mass changes at the membrane and in a layer of fluid exposed to the evanescent acoustic wave originating from the FPW on the membrane. The transducer membrane contains immobilised *E. coli* specific antibodies for specific

detection of the bacteria.[264] Ruan *et al.* also applied the enzymatic catalysis precipitation of 5-bromo-4-chloro-3-indolyl phosphate by alkaline phosphatase method to a mass sensitive magnetoelastic immunosensor, whereby the antibodies were immobilised onto the surface of a micrometer-scale magnetoelastic cantilever, with a very sensitive LOD of 10^2 *E. coli* O157:H7 cells mL^{-1}.[265]

Su *et al.* developed a piezoelectric immunosensor based on the immobilisation of antibodies onto a monolayer of 16-mercaptohexadecanoic acid (MHDA), attached to an AT-cut quartz crystal's gold electrode surface, bacteria binding causes a frequency shift which can be correlated to the concentration. This provided a good LOD of 10^3 *E. coli* O157:H7 cells mL^{-1} in a fairly rapid analysis time of < 50 min.[231]

Mass sensitive techniques have been developed, which provide rapid analysis times with good limits of detection. Problems associated with mass sensitive techniques include selectivity and the problem of non-specific binding, which can be overcome using immunological techniques.

4.1.2.5.3   Other Techniques

Other methods of analysis include proton NMR which can be applied to the identification of bacteria, including *E. coli*. The spectrum is based on the cell wall constituents of the bacteria and provides a method for fingerprint identity as demonstrated by Delpassand *et al.*.[266] NMR is a sensitive technique and useful for identification however it is not an appropriate method for portable detection systems.

Immunomagnetic separations with bacteriophage amplification prior to matrix-assisted laser desorption/ionisation mass spectrometry (MALDI-MS) has been used for the identification and detection of bacteria. An identification method was

achieved which could detect 5 x 10 ^{4} cells mL^{-1} of *E. coli* in broth in an analysis time of 2 h. [267] Again this technique is sensitive and useful for identification, but it is not amenable to portable systems.

4.1.2.5.4   Spectroscopic Methods of Detection

Absorbance

β-galactosidase (as previously discussed in section 4.1.2.5.1) can be detected using colourimetric detection using substrates including phenolphthalein-β-D-glucuronide, *p*-nitrophenol-β-D-glucuronide and indoxyl-β-D-glucuronide.[268]

Tu *et al.* used immunomagnetic beads with alkaline phosphatase-labelled anti-*E. coli* O157:H7 antibodies to sandwich the targeted bacteria. The enzyme catalysed the hydrolysis of *p*-nitrophenol phosphate to produce *p*-nitrophenol, which could be detected colourimetrically giving a good LOD of < 1 x 10^3 CFU mL^{-1}.[269]

Liu *et al.* used a capillary column containing immobilised anti-*E. coli* O157:H7 antibodies (glutaraldehyde and APTS) on the capillary walls for a sandwich assay with alkaline phosphatase-labelled anti-*E. coli* O157:H7 antibody that is used to catalyse *p*-nitrophenyl phosphate hydrolysis to give the product *p*-nitrophenol whose absorbance is detected post column. This gave a highly sensitive technique with an LOD of 5 x 10^2 CFU mL^{-1} in fairly rapid analysis time of less than 1.5 h.[270] Liu *et al.* also combined this detection method with immunomagnetic separation, this time with the anti-*E. coli* O157:H7 antibodies immobilised onto micromagnetic beads. This approach slightly improved the LOD to 3.2 x 10^2 CFU mL^{-1} but increased the analysis time to less than 2 h.[271]

A DNA fiber optic biosensor with PCR amplification was used by Tims *et al.* to detect 10^3 CFU mL^{-1}; however it gave a lengthy analysis time of less than 10 h.[272] An alternative faster approach to conventional DNA methods is the use of species-specific Peptide Nucleic Acid (PNA) oligonucleotide probe, which was directed against the V-1 region of the 16S rRNA molecule was produced for the detection of *E. coil* in water and reduced the analysis time to less than 3 h.[273]

Fluorescence

E. coli O157:H7 detection was achieved using a light addressable potentiometric sensor integrated with an immunoligand assay comprising of a sandwich assay based on biotinylated and fluoresceinated antibodies and using avidin–biotin interactions for the capture of immunocomplexed analyte by the biotinylated filter membranes. This offered a sensitive LOD of 2.5 x 10^4 cells mL^{-1} of live *E. coli* O157:H7 in a fairly rapid analysis time of 30 min.[274] Tu *et al.* also used a light addressable potentiometric sensor but with immunomagnetic capture and pre-concentration. The method comprised of magnetic beads with immobilised anti-*E. coli* O157:H7 antibodies, which captured and preconcentrated the analyte. This was then sandwiched with fluorescein-labelled anti *E. coli* antibody and urease-conjugated anti-fluorescein antibody for urease labelling, nitrocellulose or polycarbonate filters were used for filtration, the conjugated urease was then used to catalyse the formation of ammonia from urea. This method proved highly sensitive and could detect 1 *E. coli* O157:H7 CFU g^{-1} of hamburger meat, however it required a 6 h incubation time.[275, 276]

Bouvrette *et al.* developed a flow injection immunoanalysis (FIA) system for the determination of *E. coli* in food samples. Anti-*E. coli* antibodies were immobilised

160

onto porous aminopropyl glass beads using glutaraldehyde. β-D-glucuronidase in the bacteria was used to hydrolyse 4-methylumbelliferyl-beta-D-glucuronide to form the fluorescent compound 4-methylumbelliferone, which could be detected. This approach gave a poor LOD of 5×10^7 CFU mL^{-1} in an analysis time of 30 min.[277]

Yu *et al.* used an antibody-based immunomagnetic separation with microplate fluorescent immunoassay (FITC) for the determination of *E. coli* in environmental water samples. Using a microplate up to 96 samples can be analysed within an impressive 1 h, with good sensitivity (LOD of 2×10^3 cells).[278]

Song *et al.* presented a miniature biochip for the detection of *E. coli* O157:H7. The biochip consisted of an array of APTS/glutaraldehyde immobilised antibody capillary reactors as a sampling platform for an ELISA, with an integrated circuit detection system utilising complementary metal oxide semiconductors to fabricate the photodiode elements for fluorescence detection. Using alkaline phosphatase labelling and DDAO-phosphate for detection a very sensitive method was produced with an LOD of 3 cells and with a direct fluorescence label (Cy 5) an LOD of 230 cells was achieved. This also demonstrates the increased sensitivity of using enzyme labels.[279]

Chemiluminescence

Liu *et al.* developed a biosensor with immunomagnetic separation using horseradish peroxidase labelled anti-*E. coli* O157:H7 antibodies for the chemiluminescence detection using the luminol reaction. This technique was applied to real samples of ground beef, chicken carcass and lettuce, achieving a highly sensitive LOD of 3.2×10^2 CFU mL^{-1} (beef) in a fairly rapid analysis time of < 1.5 h. This highlights the

sensitivity of chemiluminescence as a detection technique, with improved analysis times compared with traditional techniques.[280] Ye *et al.* also utilised the luminol-HRP chemiluminescence detection and immunomagnetic separation for the determination of *E. coli* O157:H7. The chemiluminescence was measured *via* a reaction cell, a fiber-optic light guide, and a luminometer. A similar LOD of 1.8 x 10^2 CFU mL^{-1} and the same analysis time of 1.5 h were achieved.[281]

Tu *et al.* also used immunomagnetic beads but with a biochemiluminescence detection system. The method was based on lysing the cells to release cellular ATP, which could be detected using luciferin-luciferase bioluminescence. It produced a sensitive technique with detection of beef hamburgers spiked with less than one CFU mL^{-1} of the *E. coli* O157:H7 however this required a 6 h incubation time.[282]

Progress has been made into the development of rapid assays for *E. coli* detection, high sensitivity can be achieved but assay times are still greater than 30 minutes. One way to improve the assay time is by using microfluidic devices. As previously discussed in section 1.1, rapid analysis times can be achieved using microfluidic devices because of the reduction in transport lengths and improvement of mass transport for the chemical reaction within the channels.

4.1.2.6 Immunoassays within Microfluidic Devices

The use of immunoassays within a microfluidic device has been detailed by several groups, demonstrating the application of immunoassays used in conjunction with microfluidic devices. Homogeneous and heterogeneous immunoassays have been documented, utilising polymers and glass as device substrates, as well as the combination of immunomagnetic separation. The majority of applications detail the

use of fluorescence detection to achieve sensitivity. Units are in terms of g L^{-1} for larger non-bacterial pathogens e.g. hormones and antibodies which have been used for development work.

Cheng *et al.* presented a homogeneous immunoassay with affinity capillary electrophoresis and fluorescence detection for the simultaneous determination of ovalbumin and anti-estradiol within a multichannel microfluidic device. An LOD for anti-estradiol of 4.3 nmol L^{-1} was achieved in a rapid analysis time of 30 s for mixing, reaction and separation.[283] Roper *et al.* presented a homogeneous fluorescence immunoassay for the determination of insulin. Electrophoretic sampling of an anti-insulin antibody, fluorescein isothyocynate labelled insulin followed by electrophoretic separation enabled the on line assay of the insulin excreted from live cells with an LOD of 3 nmol L^{-1}.[284]

Cesaro-Tadic *et al.* demonstrated the determination of cytokine tumour necrosis factor alpha using a microfluidic device consisting of a PDMS layer precoated with capture antibodies for a fluorescence sandwich immunoassay. The device is made of a number of capillary systems containing a filling port, a microchannel and a capillary pump. Small sample volumes (600 nL) and an LOD of 20 pg mL^{-1} (1.14 pmol mL^{-1}) was achieved.[285] Dodge *et al.* detailed a heterogeneous immunoassay for rabbit immunoglobulin G with fluorescence detection (Cy 5) utilising electrokinetic pumping and protein A as a localised immobilised layer which has a high affinity for rabbit IgG. An LOD of 50 nmol L^{-1} and an assay time of 5 min was observed.[286] Gao *et al.* developed a PDMS/glass microfluidic device with electrokinetic pumping for a fluorescence (rhodamine) immunoassay for the detection of *Heliobacter pylori*. The bacterial protein antigen was immobilised onto the channel walls and an LOD of

1 ng μL^{-1} of was achieved within a 30 min analysis time.[287] Hofmann *et al.* present a 3d microfluidic device for a sample delivery and flow confinement system for heterogeneous immunoassays. The device consisted of a sample flow stream combining with a make up medium, this allowed the sample to be confined to a thin layer above the area of sensing.[288] The concept was verified using rabbit IgG immobilised on a silicon nitride waveguide combined in the microfluidic system for fluorescence detection (Cy 5) of anti rabbit IgG in an analysis time of 13 min. A phospholipid bilayer membrane on oxidised plasma PDMS microfluidic device was used by Phillips *et al.* for a fluorescence immunoassay for cholera toxin, achieving an LOD of 2 pmol L^{-1} in an assay time of 25 min.[289] Junker *et al.* detailed the concept of micromosaic immunoassays within microfluidic networks to detect cardiac markers, C-receptive protein (CRP), myoglobulin and cardiac troponin. A hydrophobic PDMS layer acts as the solid phase for the heterogeneous immunoassay. The LOD for CRP was 30 ng mL^{-1} for a sample size of 1 μl in an assay time of 10 min.[290]

Kim *et al.* described a PDMS microfluidic device for immunoassays using superparamagnetic nanoparticles and fluorescent polystyrene beads with immobilised antibody to form the sandwich. The complex is deflected and separated in a magnetic field for detection. The concept was demonstrated using rabbit IgG and mouse IgG with an LOD of 244 pg mL^{-1} and 6 ng mL^{-1} respectively.[291]

Hayes *et al.* demonstrated a heterogeneous fluorescence (FITC) immunoassay using paramagnetic particles within a microfluidic device for the analysis of parathyroid hormone (PTH) and interleukin-5 (IL-5) achieving LODs in the μg L^{-1} region.[292]

Bromberg *et al.* presented a competitive homogeneous immunoassay within a microfabricated capillary electrophoresis chip with fluorescence detection (FITC) for the analysis of TNT and six of its analogues. An LOD of 1 μg L^{-1} was achieved, although an incubation step of 45 min was included in the assay.[293]

Lin *et al.* used a gold nanoparticle label immunoassay within a microfluidic device for the detection of *Helicobacter pylori* and *E. coli* O157:H7. Detection was based on the scattering of the particles and visualised using a dark field stereomicroscope. Colourimetric quantification yielded results of 10 ng antigen.[294] Luo *et al.* also developed a microfluidic immunoassay using gold nanoparticles. Protein antigen coated gold nanoparticles are deposited in the presence of target antibodies on the microfluidic channel surface and detected with an optical microscope. An LOD for goat anti human IgG of 10 ng mL^{-1} was achieved.[295]

A microfluidic device for particle sizing and counting with laser light scattering detection was described by Pamme *et al.*. This was applied to a particle enhanced immunoassay for the determination of C-reactive protein (CRP) producing an LOD of 100 ng mL^{-1}.[296]

Yakovleva *et al.* utilized silicon microfluidic devices for the detection of atrazine using a competitive sandwich immunoassay with luminol chemiluminescence detection of a horseradish peroxidase (HRP) enzyme label. The antibodies were immobilised directly onto the surface of the channels, using surface modification and glutaraldehyde attachment. A rapid assay time of 10 min was achieved with an LOD of 0.8 ng L^{-1} with 3-glycidoxypropyltrimethoxysilane and branched polyethylenimine as the surface modifiers.[297] Yakovleva *et al.* developed this method

for atrazine detection by investigating protein A and protein G for antibody attachment to the channel walls. The assay time remained at 10 min and an LOD of 0.006 µg L^{-1} for polyethylenimine and dextran surface modification with protein G attachment.[298]

There is a need for a sensitive, accurate and rapid method of analysis for *E. coli* in the environment in order to determine faecal contamination. Immunological based methods of detection (immunoassays) have the advantage of high specificity and rapid analysis time. Microfluidic devices also have the benefit of rapid analysis times as well as portability, low reagent consumption, low waste production and small sample volumes. Chemiluminescence as a method of detection is highly sensitive with a simple instrumental set up. Combining all these advantages presents an ideal solution for determining *E. coli* in the environment. Therefore a flow immunoassay with chemiluminescence detection within a microfluidic device will be investigated and used in conjunction with the portable chemiluminescence detector discussed in section 2.1.2 in order to produce a portable method of detection for *E. coli* in seawater. This would allow high temporal and spatial resolution data to be obtained of contamination areas, as the rapid analysis would allow for a large number of measurements to be made.

4.2   Experimental

A non-competitive (reagent excess) heterogeneous two step sandwich immunoassay was selected as the most suitable immunoassay format (figure 4.3). This is because the reagent excess set up is more sensitive than the reagent limited (competitive) assay and the heterogeneous design allows for a preconcentration step which also

increases the sensitivity of the method as well as being more cost effective as the capture antibodies can be immobilised and regenerated. Antibodies will be immobilised onto CPG and packed into the microfluidic device detailed in section 2.3.3. The enzyme label, HRP, will be used with chemiluminescence detection (luminol-hydrogen peroxide chemiluminescence reaction) because it is a very sensitive technique. Suitable directly labelled HRP antibodies which are specific for *E. coli* are very expensive and therefore for development of the method an indirect labelling assay will be used, utilising a HRP labelled secondary antibody.
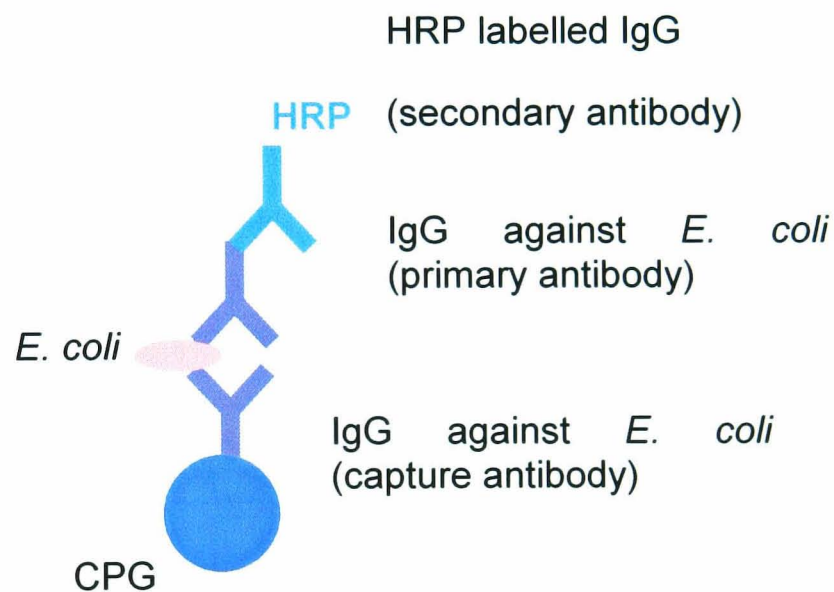
Figure 4.3 Schematic of sandwich immunoassay to be used in the determination of E. coli.

To investigate the immunoassay, the assay was separated into different steps and these were then considered individually:

- The chemiluminescence detection of HRP in solution with the luminol-hydrogen peroxide reaction was investigated in order to determine suitable parameters for the immunoassay detection.

- The immobilistation procedure was investigated in order to find a suitable loading of antibodies onto CPG.

- The commercially available antibody against *E. coli* was tested for its specificity against different isolates of *E. coli* using an ELISA (enzyme linked immunosorbent assay).

The stages were then combined to produce the non-competitive heterogeneous sandwich immunoassay for the determination of *E. coli*.

4.2.1 Reagents and Standards

All reagents were analytical grade and prepared from high purity deionised water (18 MΩcm resistivity, Elgastat UHQ PS, Elga, High Wycombe).

Chemiluminescence Determination of HRP

For the chemiluminescence reaction investigation, luminol, and 30% v/v hydrogen peroxide were purchased from Fluka (Gillingham, Dorset, UK). Trizma® hydrochloride (tris(hydroxymethyl)aminomethane hydrochloride), Trizma® base (tris(hydroxymethyl)aminomethane), horseradish peroxidase (HRP) (EC 1.11.1.7) and *p*-iodophenol were obtained from Sigma (Poole, Dorset, UK). The chemiluminescence buffer consisted of 0.1 mol L^{-1} tris-HCl, 140 mmol L^{-1} NaCl and 30 mmol L^{-1} KCl. The procedure is detailed in section 4.2.2.

ELISA and Immunoassay Protocol

For the ELISA and microfluidic immunoassay protocol, phosphate buffered saline (PBS) tablets were obtained from Invitrogen Ltd.. (Paisley, UK) and produced a

working solution of 0.01 mol L^{-1} PO_4^{3-}, 140 mmol L^{-1} NaCl, KCl 30 mmol L^{-1}, pH 7.45, which was sterilised (121°C, 15 psi, 15 min) before use. Monoclonal IgG *E. coli* specific antibody (mouse) was obtained from Oxford Biotechnology Ltd. (Kidlington, Oxfordshire, UK). Rabbit anti mouse IgG conjugated to HRP antibody was obtained from Serotec Ltd. (Kidlington, Oxfordshire, UK). Bovine serum albumin (BSA), and Tween 20 were purchased from Sigma (Poole, Dorset, UK). Marvel Non-fat dry bovine milk powder was obtained from Premier foods (Spalding, UK). A TMB (3,3',5,5'tetramethylbenzidine dihydrochloride) substrate kit for the colorimetric determination of peroxidase was purchased from Vector laboratories (Peterborough, UK) and prepared in agreement with the manufacturer's guidelines. Working solutions of the antibodies were prepared in sterile PBS. The washing buffer consisted of 0.01% Tween 20 in PBS. The blocking buffers investigated consisted of 1 % BSA and 2 % milk powder in PBS. The initial regeneration buffer investigated consisted of 0.2 mol L^{-1} glycine at pH 2.2. The *Escherichia coli* and *Psudemonas aeruginosa* cells were kindly provided by the Department of Biological Sciences, University of Hull. The cells were grown in sterile nutrient broth and re-suspended in sterile PBS. The total cell count for the sample was achieved using a haemocytometer. For cell staining, methylene blue was obtained from Fluka (Poole, Dorset UK) and a working solution of 0.3 g methylene blue in 30 mL ethanol and 100 mL water was used. The Syto®9 dye, a green fluorescent nucleic acid stain was obtained from Invitrogen Ltd. (Paisley, UK). The ELISA protocol is detailed in section 4.2.4 and the immunoassay procedure is given in section 4.2.5.

Additional reagents for the immobilisation of the monoclonal IgG *E. coli* specific antibody, including the controlled pore glass (CPG) (different specifications) and 3-aminopropyltriethoxysilane (APTS) were obtained from Sigma (Poole, Dorset UK). Ethanol and toluene were purchased from Fisher Scientific UK (Loughborough, UK). 1,1'-carbonyldiimidazole (CDI) was purchased from Fluka. The immobilisation procedure is outlined in section 4.3.3.1.

4.3 Results and Discussion

4.3.1 Investigation of the Luminol-HRP-Hydrogen Peroxide Chemiluminescence Reaction

The HRP-luminol chemiluminescence reaction was investigated in solution prior to its use as a label in the immunoassay in order to determine the optimal parameters for detection. The microfluidic manifold used in this investigation is shown in section 2.2.3 (figure 2.6) and consisted of a glass device with a serpentine manifold the length of which is 206 mm with a channel width of 200 μm and depth of 65 μm (Micro Chemical Systems, Hull). Reagents and sample were continuously introduced into the device (HRP in one inlet and the chemiluminescence reagent through the other) contained within the portable chemiluminescence detector detailed in section 2.1.2. Each sample was run for 5 minutes.

4.3.1.1 Optimisation of the Luminol Concentration and Hydrogen Peroxide Concentration for the Chemiluminescence Detection of HRP

To optimise the chemiluminescence reaction for the detection of HRP in solution, three variables were investigated: the concentration of luminol, the concentration of hydrogen peroxide and the pH. The optimal pH for the HRP-luminol reaction is well documented at pH 8.5, this is lower than the pH observed previously with Co(II) as the cooxidant. This is due to the compromise that needs to be made between the reduction in activity of the HRP at an increased pH and the decrease in luminol chemiluminescence intensity at a lower pH.[299] Therefore this value was adopted for the reaction. A buffer of 0.1 mol L^{-1} Tris-HCl buffer with 140 mmol L^{-1}NaCl and 30 mmol L^{-1} KCl for salinity conditions was used for the reaction.[234, 235, 237] A flow rate of 20 µL min^{-1} was used throughout as this was shown previously to be the optimal flow rate for the luminol reaction with Co(II) as the cooxidant in the device, see section 3.3.2. From the literature the optimum range for the luminol concentration was 0.1–9 mmol L^{-1} and for the hydrogen peroxide concentration the range was 0.1– 5 mmol L^{-1},[234, 235, 237] and these values were used in a design of experiment.[299] The experiments were carried out using a standard of 5.0 µg mL^{-1} HRP in a solution of Tris-HCl pH 7.0. The process for choosing the values in the design of experiment are shown in figure 4.4 and the chosen values are given in table 4.5.

Figure 4.4 Grid to show the selection of variables for the optimal determination of HRP design of experiment (set 1), using the luminol–hydrogen peroxide chemiluminescence reaction. The luminol concentration range was 0.1–9 mmol L^{-1} and the hydrogen peroxide concentration range was 0.1–5 mmol L^{-1}.

Table 4.5 Results table for the determination of HRP design of experiment (set 1), using the luminol – hydrogen peroxide chemiluminescence reaction.

Experiment	Concentration of Luminol (mmol L^{-1})	Concentration of Hydrogen Peroxide (mmol L^{-1})	Average Chemiluminescence Intensity (mV)	Standard Deviation	RSD (%)
1	0.1	0.1	1.4	0.01	0.70
2	0.1	2.6	20.7	0.07	0.33
3	0.1	5.0	31.3	0.10	0.33
4	2.5	1.3	69.6	0.14	0.20
5	2.5	3.8	155.3	0.56	0.36
6	5.0	0.1	1.7	0.01	0.84
7	5.0	2.6	192.3	1.05	0.54
8	5.0	5.0	331.5	2.40	0.73
9	7.6	1.3	60.5	0.62	1.03
10	7.6	3.8	127.0	0.84	0.66
11	9.0	0.1	1.0	0.01	0.53
12	9.0	2.6	96.8	0.21	0.22
13	9.0	5.0	246.50	1.63	0.66
14	5.0	2.6	170.3	1.57	0.92

Figure 4.5 Surface response plot for the determination of HRP design of experiment (set 1) values using the luminol – hydrogen peroxide chemiluminescece reaction. The luminol concentration range was 0.1 – 9 mmol L^{-1} and the hydrogen peroxide concentration range was 0.1 – 5 mmol L^{-1}.

From the results (figure 4.5) it can be seen the optimum value is in the range 4-6 mmol L^{-1} for luminol and around 5 mmol L^{-1} for hydrogen peroxide. Therefore a second design of experiment was carried out, altering the ranges for the concentration of luminol to 3-7 mmol L^{-1} and the concentration range for hydrogen peroxide to 3-7 mmol L^{-1}. The values were chosen according to the process given in figure 4.6. The results can be seen in table 4.6 and in figure 4.7.
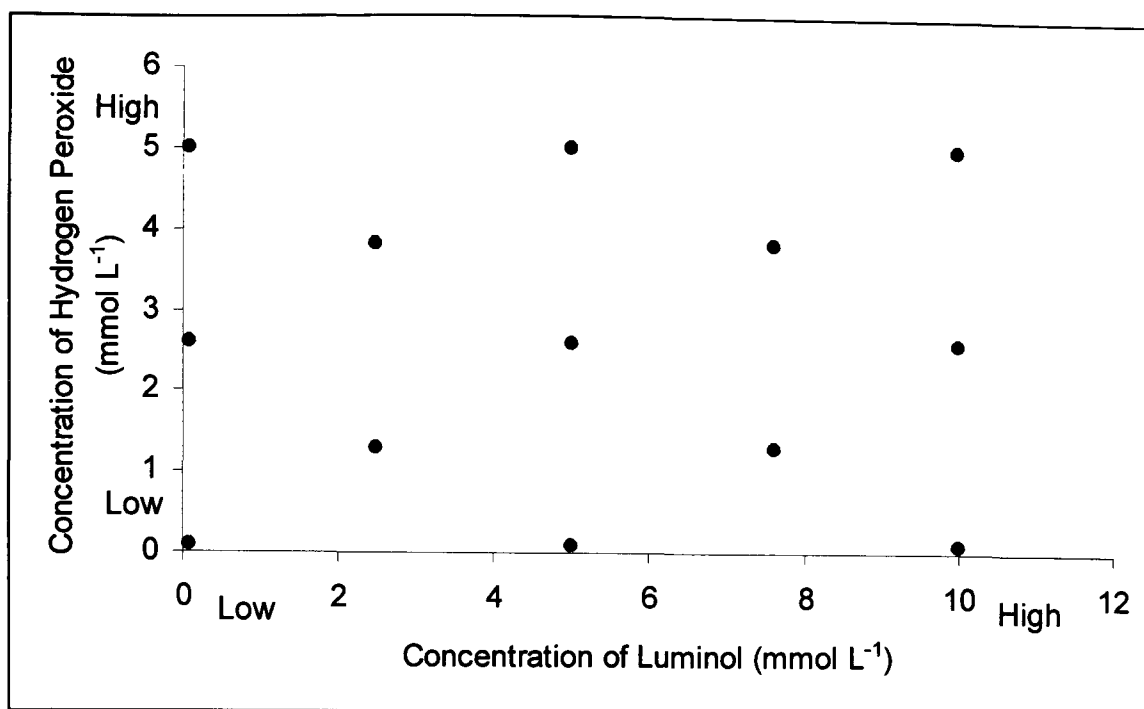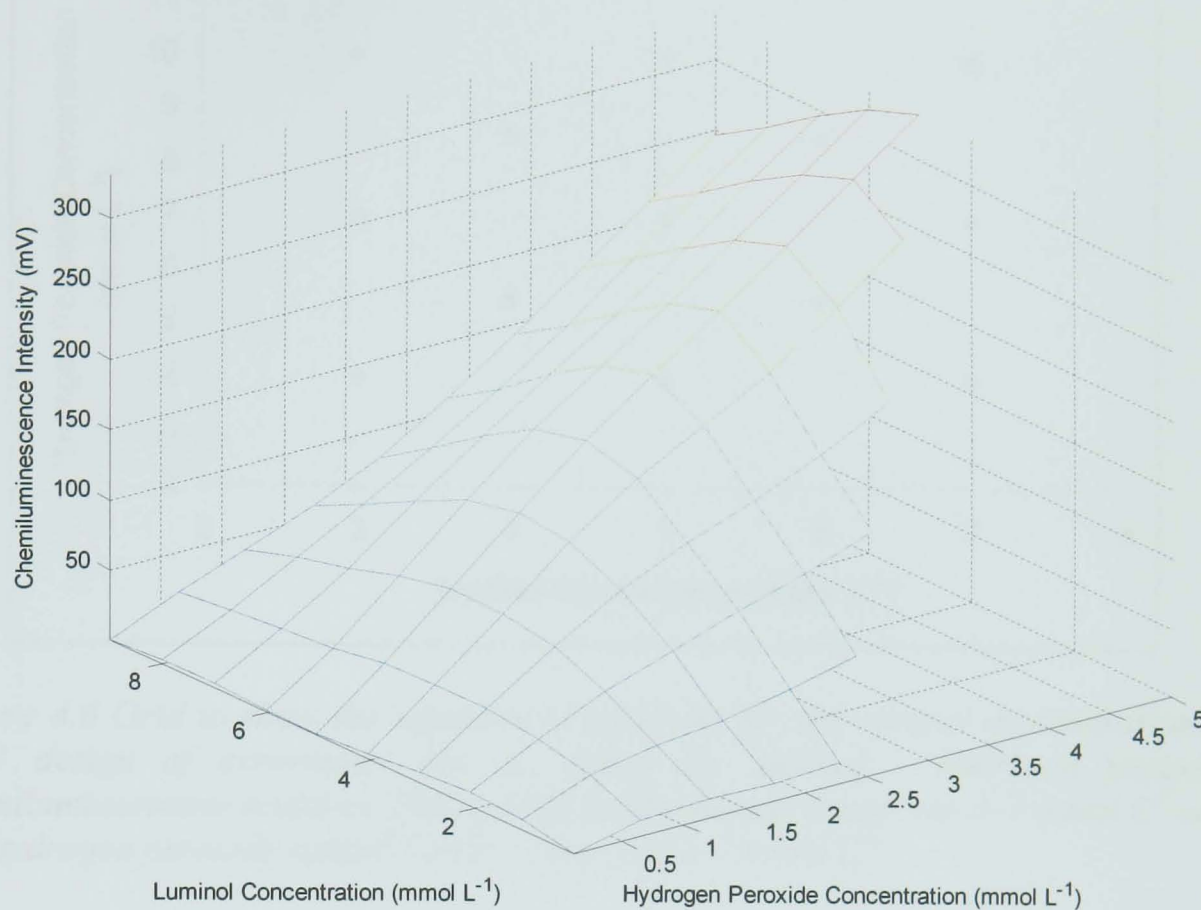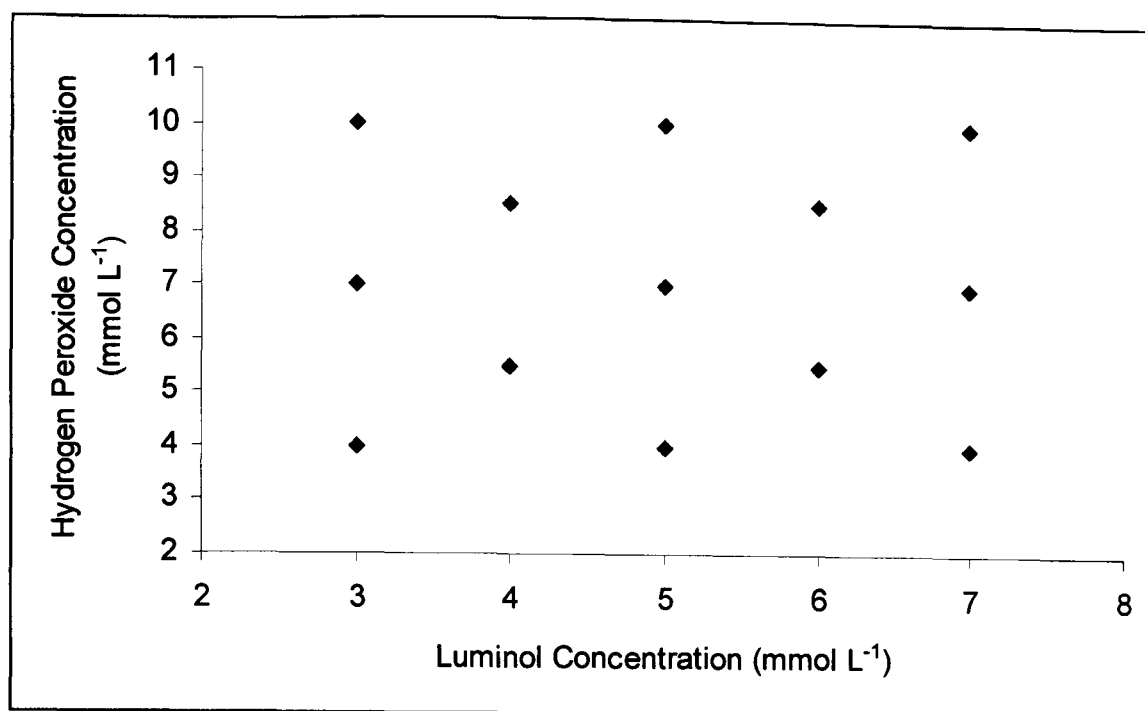
Figure 4.6 Grid to show the selection of variables for the optimal determination of HRP design of experiment (set 2), using the luminol – hydrogen peroxide chemiluminescence reaction. The luminol concentration range was 3–7 mmol L^{-1} and the hydrogen peroxide concentration range was 3–7 mmol L^{-1}.

Table 4.6 Results table for the determination of HRP design of experiment (set 2), using the luminol – hydrogen peroxide chemiluminescence reaction.

Experiment	Concentration of Luminol (mmol L^{-1})	Concentration of Hydorgen Peroxide (mmol L^{-1})	Average Chemiluminescnce Intensity (mV)	Standard Deviation	RSD (%)
1	3.0	4.0	112.4	0.93	0.82
2	3.0	7.0	145.9	0.34	0.23
3	3.0	10.0	160.5	0.52	0.33
4	4.0	5.5	152.8	1.69	1.11
5	4.0	8.5	111.0	1.44	1.30
6	5.0	4.0	119.5	1.03	0.86
7	5.0	7.0	158.8	0.99	0.62
8	5.0	10.0	156.4	0.93	0.59
9	6.0	5.5	142.3	0.71	0.50
10	6.0	8.5	142.8	0.71	0.50
11	7.0	4.0	130.6	0.77	0.59
12	7.0	7.0	218.9	2.55	1.17
13	7.0	10.0	183.0	1.35	0.74
14	5.0	7.0	154.3	1.35	0.88
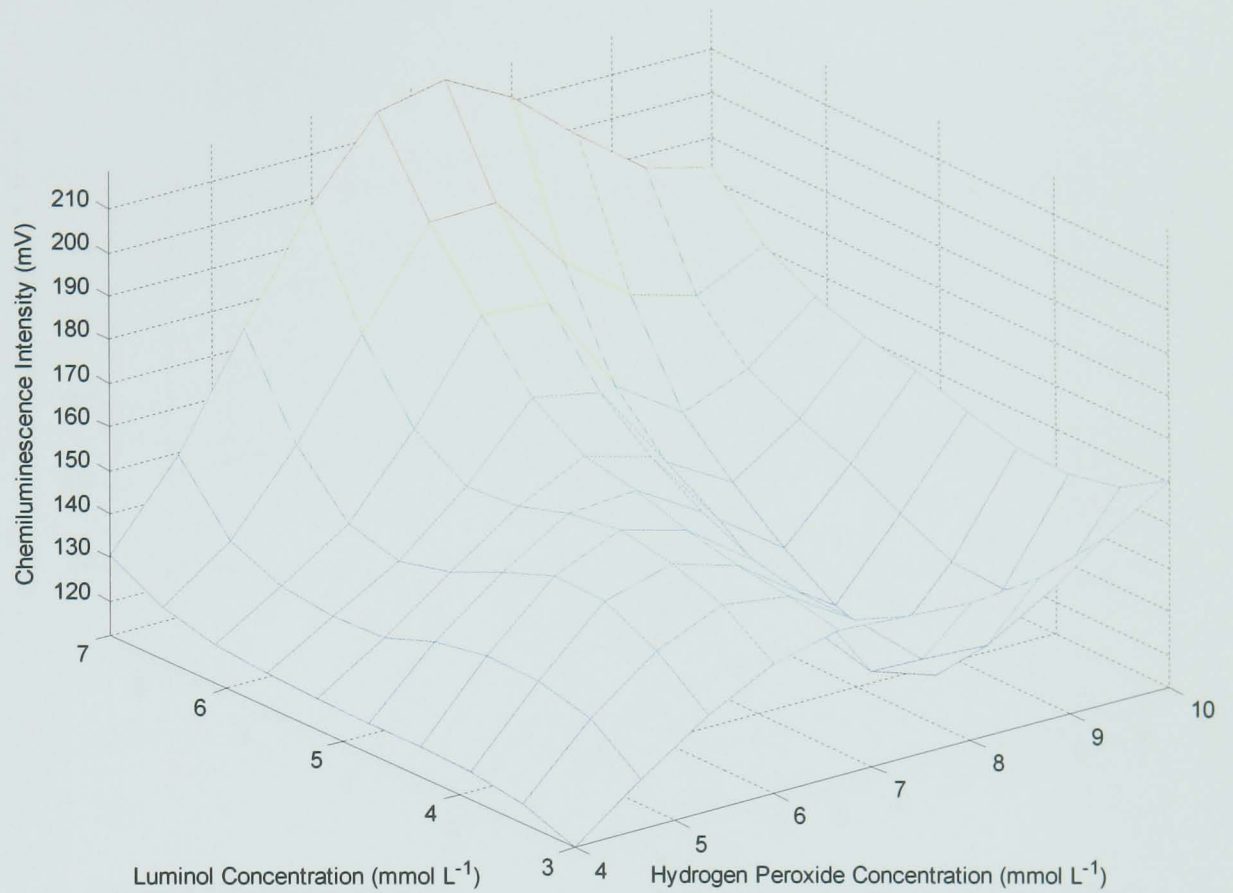
Figure 4.7 Surface response plot for the determination of HRP design of experiment (set 2) values using the luminol – hydrogen peroxide chemiluminescece reaction. The luminol concentration range was 3–7 mmol L^{-1} and the hydrogen peroxide concentration range was 3–7 mmol L^{-1}.

The two sets of design of experiment were then combined and can be seen in figure 4.8.
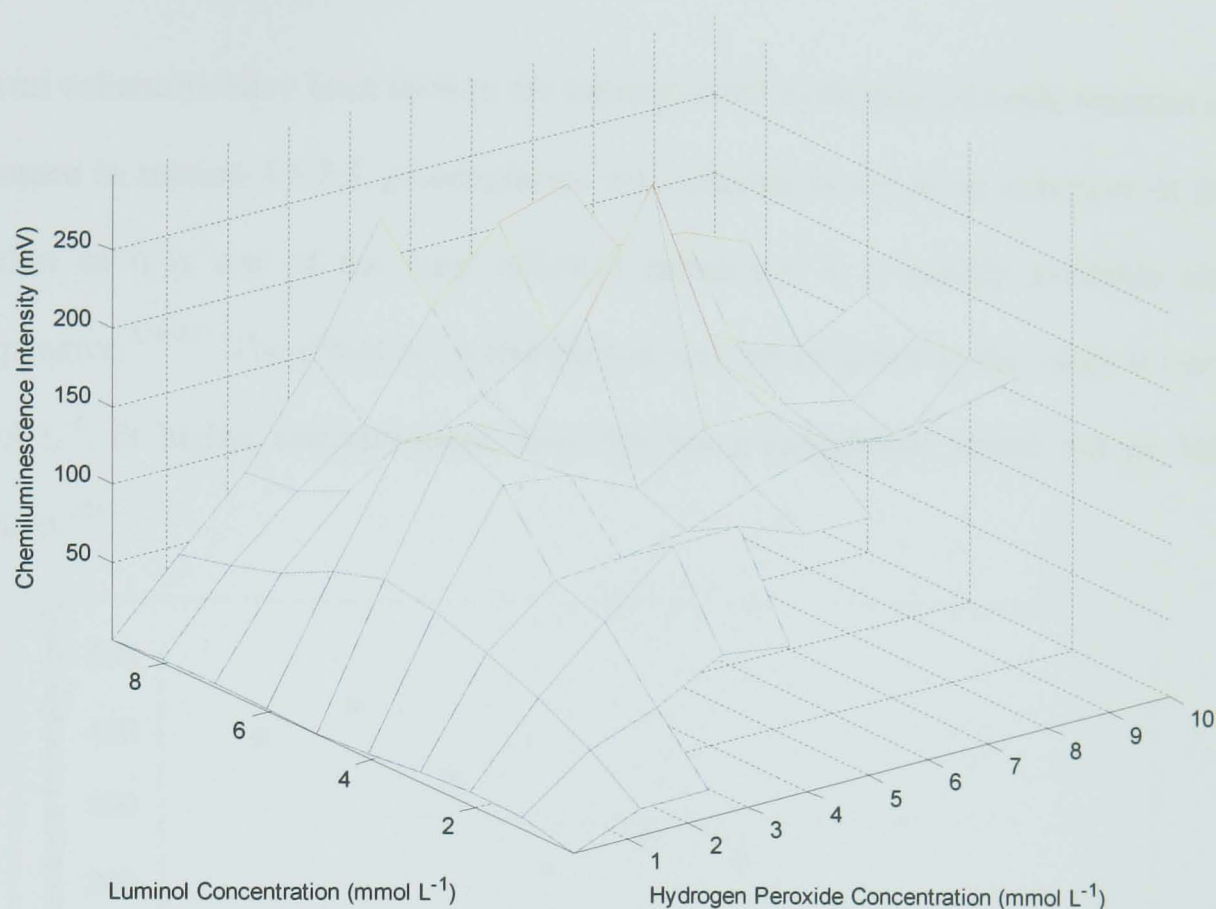
Figure 4.8 Surface response plot for the combined results of the determination of HRP design of experiments (set 1 and 2) using the luminol – hydrogen peroxide chemiluminescece reaction. An optimal chemiluminescence intensites observed at 5 mmol L^{-1} for luminol and 5.5 mmol L^{-1} for hydrogen peroxide.

From the data we can see the optimum values are around 5 mmol L^{-1} for luminol and 5.5 mmol L^{-1} for hydrogen peroxide and so these values have been selected for future work. These values are comparable with Mangru *et al.*.[235] but higher than those detailed by Whitehead *et al.*[237] and Marquette *et al.*.[234]

4.3.1.2 Effect of Enhancer

Several enhancers have been used in the luminol-HRP-hydrogen peroxide reaction as discussed in section 4.1.2.3. p-iodophenol was selected to use as an enhancer in the reaction as it is one of the most efficient enhancers, it is readily available and inexpensive.[234-237] The effect of p-iodophenol was investigated in the range 0.1-0.9 mmol L^{-1}, at higher concentrations than this the p-iodophenol would not go into solution.[236]
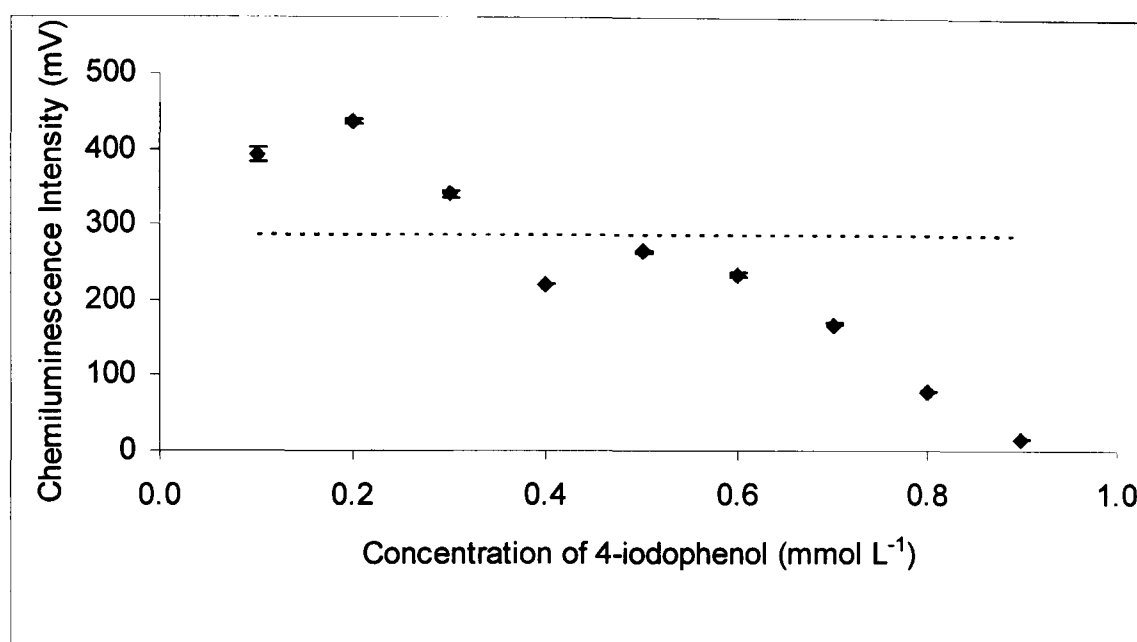
Figure 4.9 Effect of different concentrations of the enhancer 4-iodophenol on the determination of HRP (5.0 μg mL⁻¹) using the luminol-hydrogen peroxide chemiluminescence reaction. The dashed line represents the reponse of HRP in the absence of 4-iodophenol. Error bars: one standard deviation (n=3).

From the results (figure 4.9) it can be seen that a concentration of 0.2 mmol L^{-1} p-iodophenol gave the optimal enhancement of 1.5 fold (152%). At concentrations above this quenching of the chemiluminescence reaction was observed. This is consistent with the findings of Thorpe *et al.*[214]

4.3.1.3 Calibration

Using these optimal conditions, a calibration for HRP in solution was determined in the range 0.55-5.0 µg mL^{-1}. This can be seen in figure 4.10.
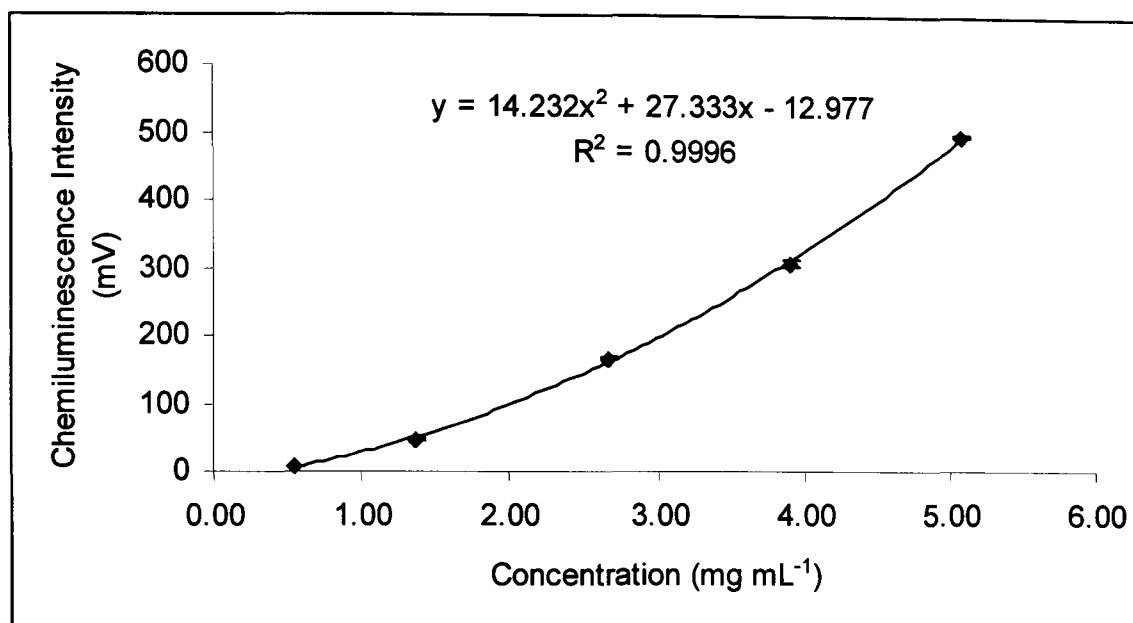
Figure 4.10 Calibration for the determination of HRP using the luminol-hydrogen peroxide chemiluminescence reaction. Error bars: one standard deviation (n=3).

A curved response was observed over this range (y = 14.232x^2 + 27.333x -12.977, R^2 = 0.9995). A plot of Log (Chemiluminescence Intensity (mV)) against Log (HRP Concentration (µg mL^{-1})) produces a linear response (y = 1.869x + 1.3953, R^2 = 0.9988). The limit of detection was calculated based on three times the deviation of the y-residuals using the linear portion of the curve,[225] and was determined to be 0.5 µg mL^{-1} for this manifold. From the results seen, the luminol reaction can be used for the detection of HRP within a microfluidic device and can be applied to a microfluidic HRP labelled immunoassay within the chemiluminescence detector.

4.3.2 Immobilisation of Antibodies

Several methods have been applied to the immobilisation of antibodies to solid phases. When using microfluidic devices it is important to maintain a high loading of the immobilised species to achieve the required sensitivity. One way to maintain this is to use controlled pore glass as a solid support and pack this within the microfluidic device (as previously discussed 2.3.2.2). For antibody immobilisation, covalent attachment is preferential in order to achieve increased sensitivity and robustness. Immobilisation is normally through free amino groups, the majority of which are available on lysine residues on the protein structure. Problems may occur when immobilisation occurs through residues near the active binding site.

Several approaches to immobilising antibodies to CPG have been documented. Fernandez *et al.* used APTS to silanise the CPG followed by periodate linking of an oxidised antibody achieving a loading of greater 1.28 µg mg^{-1}.[245] Franek *et al.* used aminopropyl CPG with avidin/biotin coupling of antibodies.[300] Functional groups and ligands can be used to influence the orientation of immobilisation of antibodies such as protein A and protein G. Protein A-CPG was used by Garcinuno *et al.* as Protein A has a high affinity for the antibody Fc region, which ensures the correct orientation of the immobilised antibody (i.e. immobilisation of the non active binding sites for antigen interactions). The disadvantage of this approach is the expense.[246] Glutaradehyde is one chemical to use for covalent attachment,[226, 277, 297] however this can produce low yields, poor retention of the original activity and is difficult to control.[226] Another approach for achieving antibody immobilisation is by using a carboiimide attachment (e.g. 1,1'-carbonyldiimidazole (CDI)).[238, 301-303] As an initial immobilisation protocol, CDI was selected as the chemical attachment for antibodies

onto CPG, the attachment is through a carboxylic acid group on the protein (figure 4.11). Using this immobilisation approach should enable attachment through the COOH terminus of the Fc portion of the antibody, away from the active binding site, which will preserve the activity of the antibody.

4.3.2.1 Immobilisation Procedure

The immobilisation was carried out in batch prior to packing within the microfluidic device. For the immobilisation procedure, CPG (0.1 g) was boiled in 5% nitric acid (30 min), filtered, washed with deionised water and dried (100 °C). The cleaned CPG was immersed in 10% APTS in toluene with shaking overnight, filtered, washed with ethanol and water and dried (100 °C). The CPG was then immersed in CDI (4 mg mL^{-1}) in Tris-HCl buffer (pH 7.0), degassed and shaken for 30 min, the antibody (Monoclonal IgG *E. coli* specific antibody (mouse)) of differing concentrations was added and kept at 4°C for a specified period of time.[226, 238] The CPG was then washed with PBS and stored in PBS at 4°C. The amount of antibody immobilised was monitored before and after contact with the CPG using UV spectroscopy (Perkin Elmer UV/VIS spectrometer, Lambda Bio 10). Absorption maxima should be observed around 280 and 200 nm for proteins in solution. The 280 nm peak is due to amino acids containing aromatic rings and the peak around 200 nm is primarily due to peptide bonds. From the experimental data, no peak was observed at 280 nm, only a peak maximum was seen at 202 nm. Due to interference from the CDI present in the supernatant a calibration could not be used as the CDI also absorbs at around 200 nm and is present in the supernatant before and after immobilisation. The concentration of the immobilised antibody was based on the known absorbance of the initial concentration of the antibody in the supernatant (concentration of the CDI

interference will also decrease linearly as it is also being immobilised at the same rate as the antibody). The loading was calculated according to equation 4.1. This method only gives you an inferential loading, true loadings can be evaluated using the immunoassay, as the maximum number of cells detected is directly related to the available immobilised antibodies.

$$L = \frac{(CL_B - CL_A) \times V}{m}$$

Where L is the loading of the antibody on the solid support (mol g^{-1}), CL$_B$ is the concentration of antibody before immobilisation (mol L^{-1}), CL$_A$ is the concentration of antibody after immobilisation (mol L^{-1}), V is the volume of solution used in the immobilisation and m is the mass of the solid support used in the immobilisation (g).
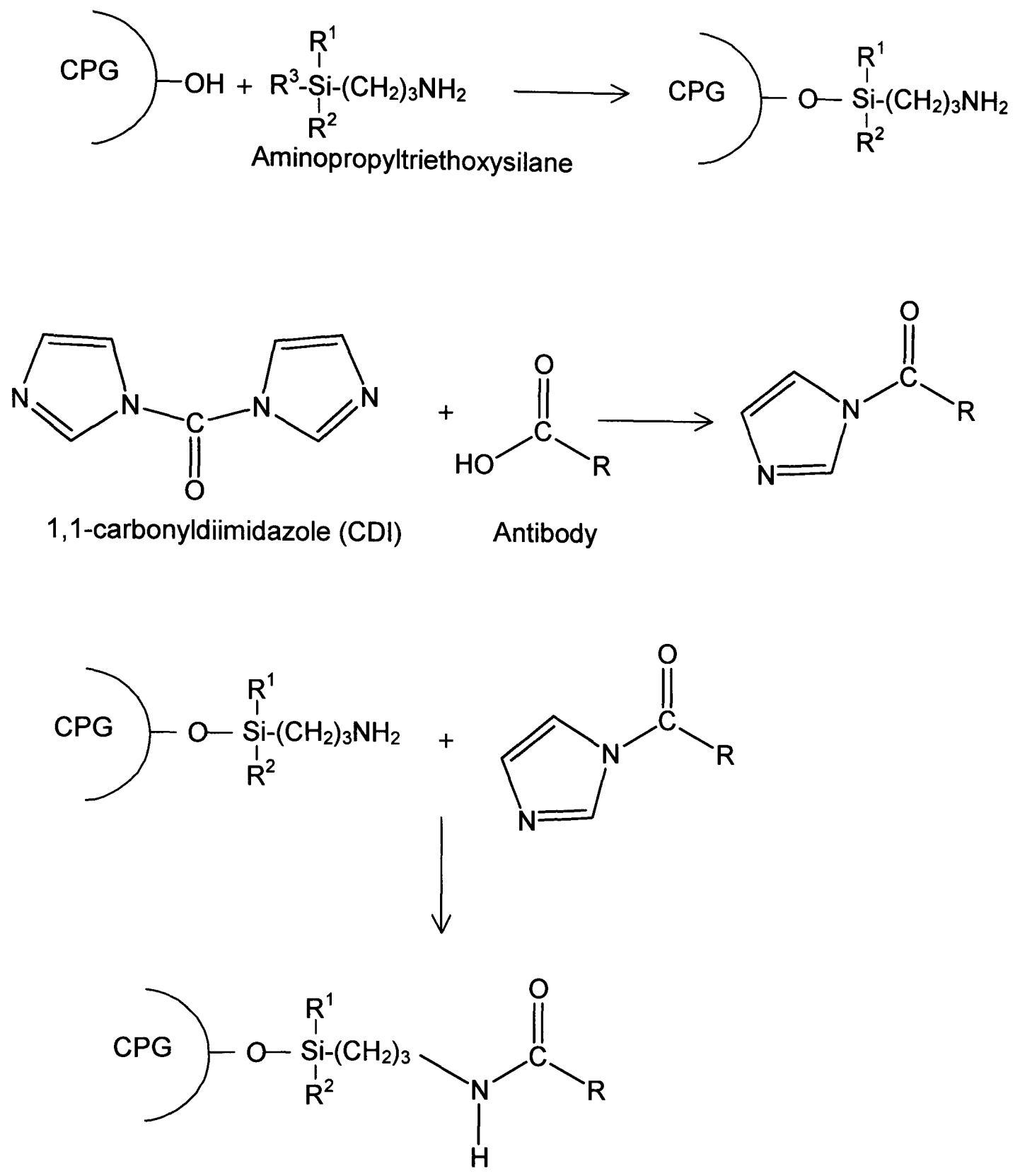
Figure 4.11 Procedure for immobilising antibodies onto CPG using APTS and CDI.

4.3.2.2 Determination of Optimal Parameters for the Immobilisation Procedure.

Selection of Controlled Pore Glass

The first variable under investigation was the specification of CPG to be used as the solid support. Two different particle sizes were investigated (200–400 mesh (37– 74 μm) and 120-200 mesh (74-125 μm)) this was limited to their compatibility with packing into a microfluidic device (see section 2.3.3). Within these particle sizes different porosities were investigated (240 – 1010 Å). An antibody concentration of 0.5 μg mL^{-1} was used and the antibody was left overnight. The results of this can be seen in figure 4.12.
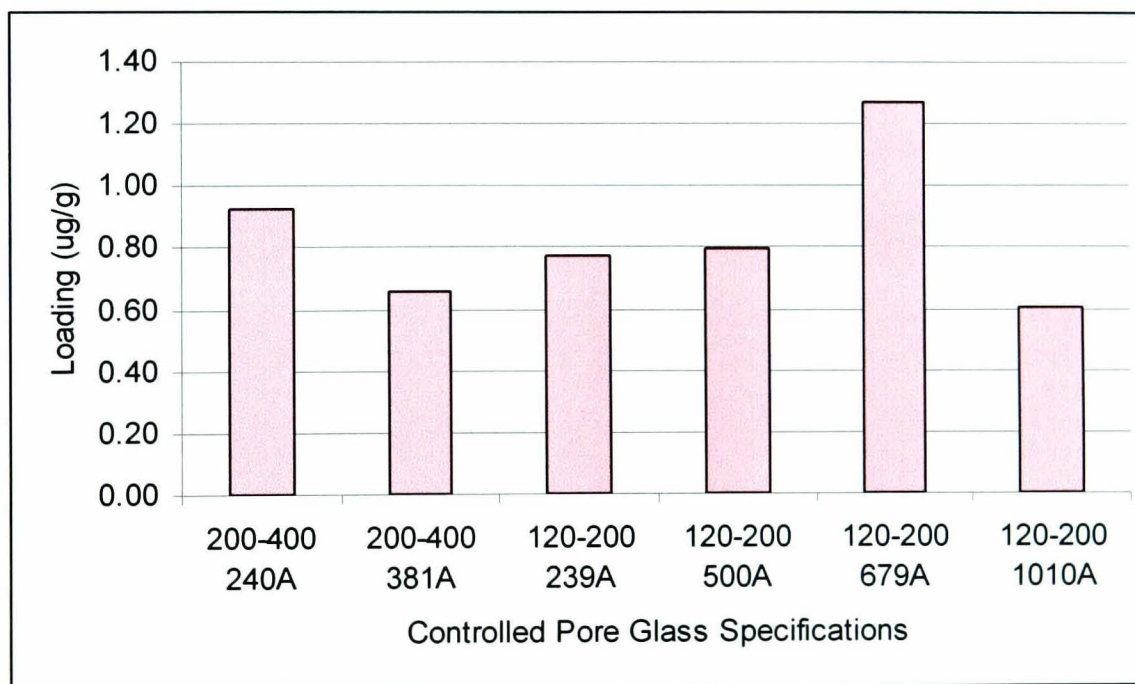
Figure 4.12 Determination of the optimal particle and pore size of the CPG used as the solid support for the immobilisation of E. coli specific antibodies. The antibody concentration was 0.5 μg mL^{-1} and the immobilisation reaction was left overnight. Error bars: one standard deviation (n=2).

The optimal specification of CPG was found to be 120-200 mesh (74-125 μm) with a pore size of 679Å. However it must be noted that the optimal loading does not necessarily give the optimal response to the assay due to steric hindrance of the antibodies and thus has to be evaluated using the immunoassay protocol.

Effect of Antibody Concentration

It was necessary to determine the optimal concentration of the capture antibody to be immobilised because at high concentrations of antibody in solution the antibody can agglomerate, therefore reducing the amount of available sites for covalent attachment. Three concentrations of antibody were investigated: 0.2, 0.5 and 1.0 μg mL^{-1}. The antibody was left overnight for immobilisation and the CPG used was 120-200 mesh (74-125 μm), 679 Å pore size.
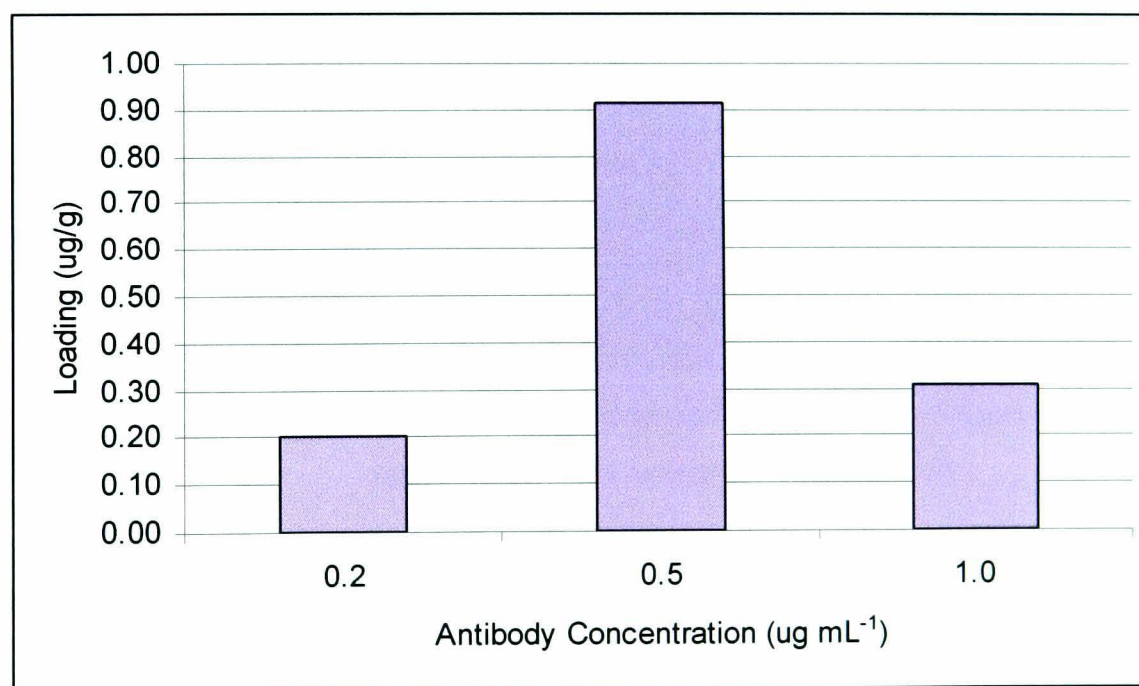
Figure 4.13 Determination of the optimal concentrion of E. coli specific antibody used for the immobilisation of the E. coli specific antibodies onto CPG. The CPG used was 120-200 mesh (74-125 μm) particle size and 679 Å pore size. The immobilsation reaction was left overnight. Error bars: one standard deviation (n=2).

The optimal concentration for the concentrations investigated was found to be 0.5 µg mL^{-1}. Again, this may not give the optimal response to the assay as the full binding activity towards the *E. coli* of the immobilised capture antibody may have been hindered and has to be evaluated using the immunoassay protocol.

Effect of Time on Antibody Immobilisation

The effect the length of time the capture antibody was left to immobilise was investigated and variables of 1 hour, overnight and 2 days were selected. The CPG used was 120-200 mesh (74-125 µm), 679 Å pore size with an antibody concentration of 0.5 µg mL^{-1}. The results can be seen in figure 4.14.
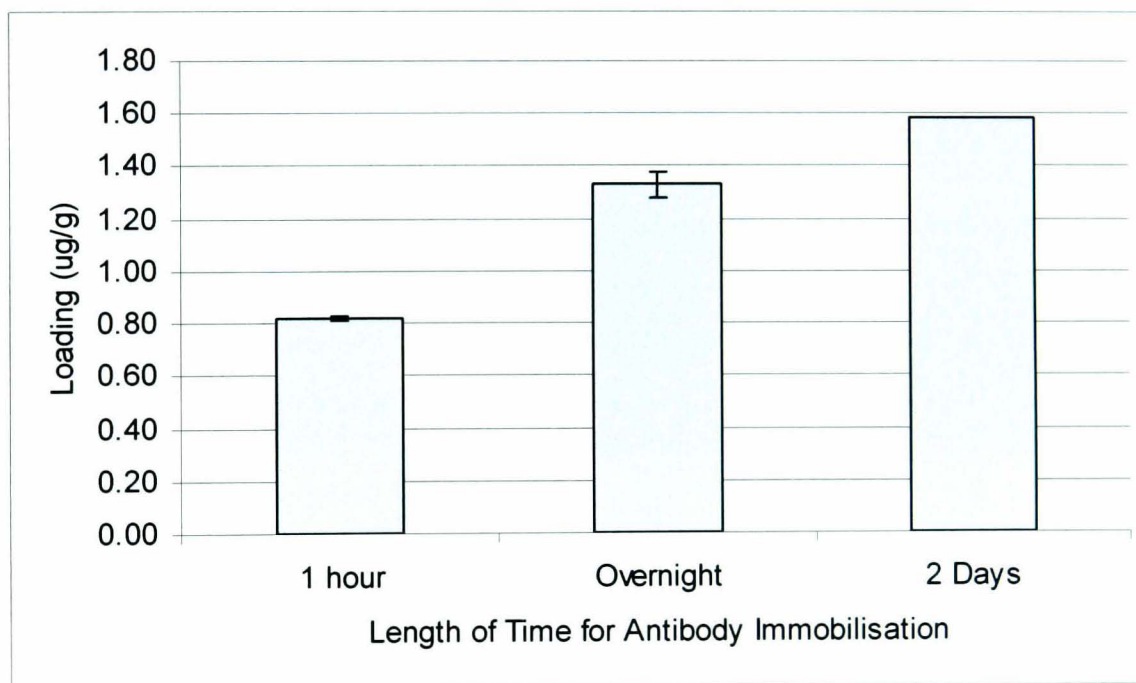
Figure 4.14 Determination of the optimal length of time for the immobilisation of E. coli specific antibodies onto CPG to take place. The antibody concentration was 0.5 µg mL^{-1} and the CPG used was 120-200 mesh (74-125 µm) particle size and 679 Å pore size. Error bars: one standard deviation (n=2).

The longer the antibody was left for immobilisation the higher the loading of the capture antibody onto the solid phase. The antibody was not left for longer than 2 days as longer working times are not practical.

Batch Reproducibility

Three batches were compared to investigate the between run reproducibility using a CPG specification of 120-200 mesh (74-125 μm), 679 Å pore size and an antibody concentration of 0.5 μg mL^{-1} which was left overnight for antibody immobilisation. The results of this can be seen in figure 4.15.
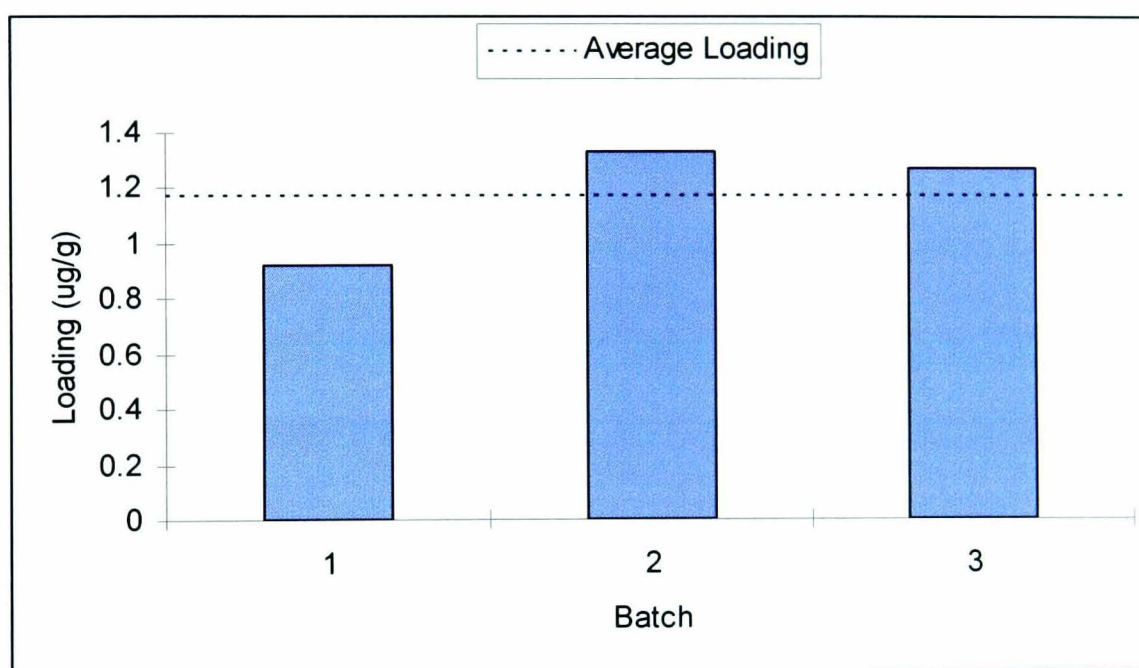
Figure 4.15 Graph to show the difference in batch reproducibility for the immobilisation of E. coli specific antibodies onto CPG. The CPG used was 120-200 mesh (74-125 μm) particle size and 679 Å pore size, an antibody concentration of 0.5 μg mL^{-1} was used and the reaction was left overnight for immobilisation to take place. The dashed line shows the average loading of E. coli specific antibody onto CPG (1.2 μg g^{-1}). Error bars: one standard deviation (n=2).

The average loading of the batches was 1.2 μg g^{-1}, although a poor reproducibility was observed (RSD 18.9%). However, only a tiny amount (20 mg) of the CPG is required to pack the microfluidic device and so reproducibility between the packed devices from one immobilised batch is consistent.

The most effective immobilisation procedure for the capture antibody consisted of CPG of specification 120-200 mesh (74-125 μm), 679 Å pore size, a working antibody concentration of 0.5 μg mL^{-1}, and a period of two days for immobilisation. This produced a loading of approximately 1.5 μg g^{-1}. This was not necessarily the optimal procedure for the assay due to problems with steric hindrance, which limits the antigen accessing the antibody, as well as retaining the activity of the antibody. This has to be evaluated later using the immunoassay protocol. In comparison with other methods, Fernandez *et al.* reported loadings of greater 1.28 μg mg^{-1} using a periodate linkage of an oxidised antibody to silanised CPG, which is significantly higher than that achieved using the CDI method and so this will be considered when evaluating the immunoassay protocol.

4.3.2.3 Validity of the Immobilisation Procedure.

To ensure covalent attachment of the antibodies was occurring as opposed to the antibodies adsorbing to the CPG, a series of control experiments were carried out (table 4.7) by using the immobilisation procedure to immobilise antibodies to microscope slides. *E. coli* cells were then bound to the antibodies and visualised using methylene blue. Methylene blue (3,7-bis(dimethlamino)-phenazathionium chloride) is a basic dye (cationic) which is attracted to the slightly negatively charged cytoplasm of the *E. coli* bacterial cell, thus staining it blue.

Table 4.7 Control conditions for the immobilisation of E. coli specific antibodies onto microscope slides. A green tick indicates the presence of the condition and a red cross indicates the absence of a condition.

Experiment	Conditions Present		
	APTS	CDI	Antibody
1	✓	✓	✓
2	✓	✗	✓
3	✓	✓	✗
4	✗	✓	✓
5	✗	✗	✓

Procedure

200 μL of cell suspension in PBS (10^8 cells mL^{-1}) were added to each slide and left for 30 minutes after which time it was washed with PBS. The methylene blue dye was added to the slide and left for 30 minutes and finally washed with PBS. The stained *E. coli* cells were visualised using a microscope (Nikon Eclipse E400). An example of this is given in figure 4.16.
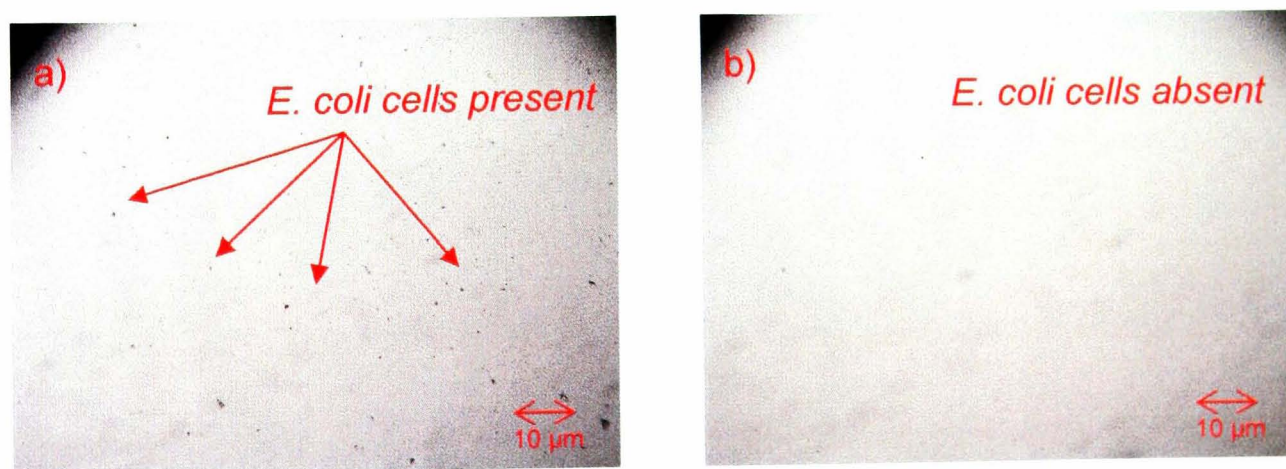
Figure 4.16 E. coli cells stained with methylene blue binding to a) immobilised antibodies on a microscope slide and b) no immobilised antibodies on microscope slide (x 40). E. coli cells are only present when E. coli specific antibodies are immobilised onto the microscope slides using APTS and CDI.

From the results it was seen that only *E. coli* cells were present when all of the immobilisation procedure is followed, showing no unwanted adsorption of the antibodies (figure 4.16). However, very few cells are observed, indicating a low loading, which may produce problems for the assay.

The immobilisation process was also investigated using Syto®9 dye, a green fluorescent nucleic acid stain. The dye is taken up by bacteria cells and binds to DNA/RNA, which enhances fluorescence. 200 μL cells in PBS (10^8 cells mL^{-1}) were added to 33.4 μmol L^{-1} of the Syto®9 dye (in accordance with the manufacturers guidelines). This was left in the dark for 30 minutes to develop. To investigate the immobilisation of the antibodies onto the CPG, the beads were packed into a borosilicate glass column (500 μm (i.d.) x 30 mm length, sealed into place with glass wool. The cells were flowed for 2 minutes at a flow rate of 5 μL min^{-1}, using a syringe pump, and washed with PBS by using a 2 minute flow time at 5 μL min^{-1}. A blank packed column was also used consisting of CPG with nothing immobilised. The columns were observed using a fluorescence microscope (Leica, Germany). This can be seen in figure 4.17.
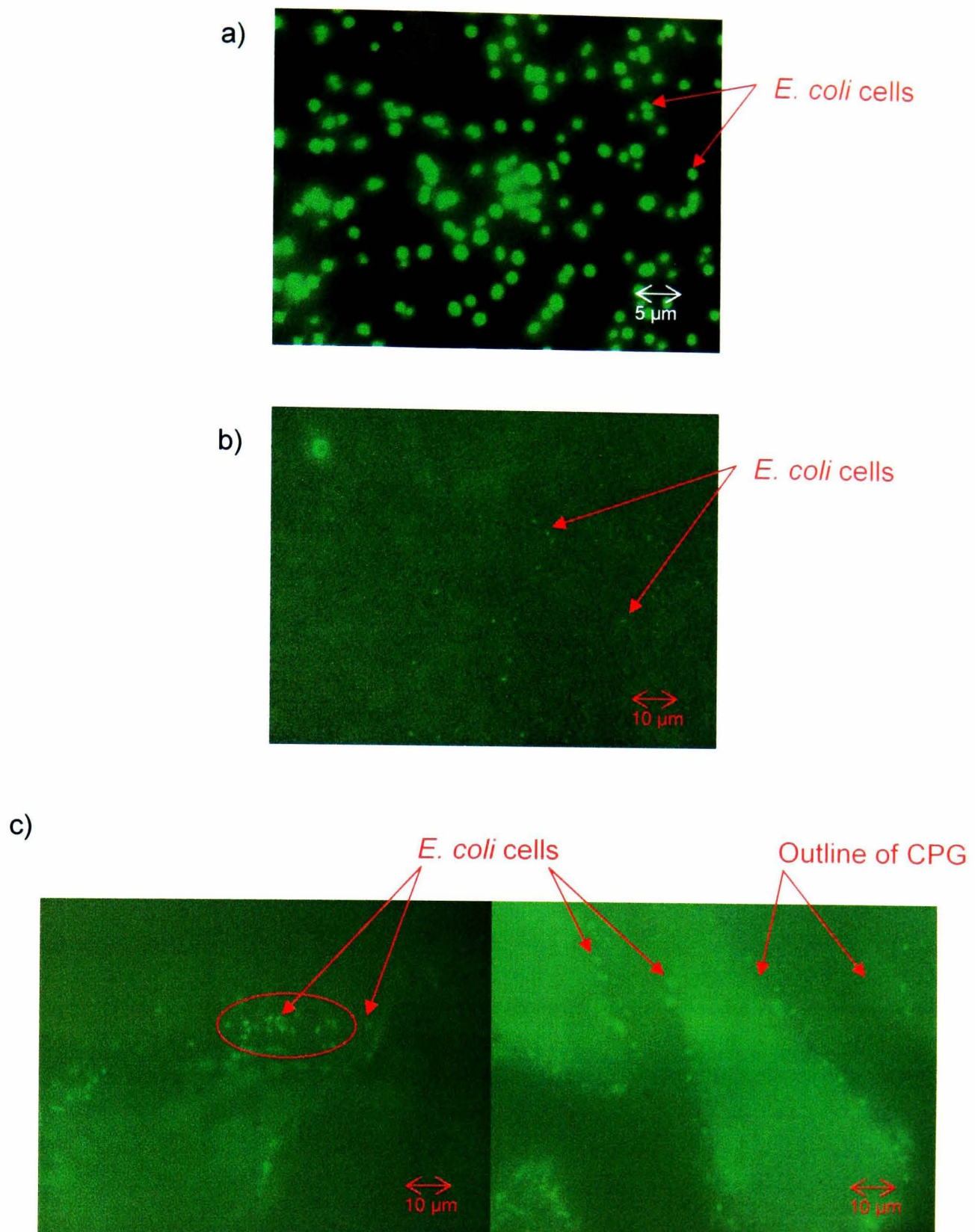
Figure 4.17 Fluorescence images of E. coli cells stained with Syto®9 dye a) in PBS solution b) binding to antibodies immobilised onto a glass microscope slide and c) binding to antibodies immobilised onto CPG.

It can be seen from figure 4.17 that the antibodies have immobilised to the glass beads and that they are binding to the *E. coli* cells, showing that rapid and efficient interaction of the antibodies and antigens is taking place. The cells were also observed to be moving in a small circular pattern, indicating the anchoring of the

antibodies. This shows the immobilisation protocol chosen is suitable to allow access for the cells to the antibodies.

To conclude, an immobilisation method using APTS and CDI was investigated for the covalent attachment of antibodies to CPG. Optimal parameters were selected to give a loading of 1.5 μg g^{-1}.

4.3.3 Specificity of Antibodies

4.3.3.1 Development of an ELISA Method for E. coli Detection

An ELISA was developed to investigate the specificity of the commercially available antibodies for different isolates of *E. coli* over other pathogens. This is necessary because selective identification of *E. coli* is required as there may be low numbers of them coexisting with large numbers of different bacteria in the seawater sample and if the different bacteria interact with the antibodies a false positive result will be observed. An ELISA was developed as it enabled the antibody-antigen recognition part of the immunoassay to be studied as a single process, i.e. the interaction between the *E. coli* and the primary IgG *E. coli* specific antibody and the secondary rabbit anti mouse IgG conjugated to HRP antibody.

Two key variables to investigate for the ELISA are the use of blocking agents and detergents. Blocking agents are used to block non-specific sites, common substances include bovine serum albumin and non-fat dry bovine milk. Detergents are also used in immunoassays to remove any non-specific bound biomolecules from the surface. Tween 20 (non ionic) is a commonly employed detergent. It removes non-specific binding by disrupting hydrophobic bonds formed between biomolecules and

surfaces. It also acts as a blocking agent by covering any exposed hydrophobic patches.

A series of control experiments were carried out to determine the most suitable blocking and washing procedures used for the ELISA. TMB (3,3',5,5'tetramethylbenzidine dihydrochloride) was used for the colorimetric determination of HRP. The absorbance of the individual wells of the microtitre plate was measured using a plate reader (Dynex Technologies MRX II, Dynex Technologies Ltd., Worthing, UK). NUNC immuno maxisorp 96 well polystyrene microtitre plates (flat bottomed) obtained from Fischer Scientific UK (Loughborough, UK) were employed for the ELISA protocol. Polystyrene is a hydrophobic polymer and allows for the adsorption of cells.

The control experiments consisted of a positive control of a well containing *E. coli* cells, the monoclonal IgG *E. coli* specific antibody (primary antibody) and the rabbit Anti mouse IgG conjugated to HRP antibody (secondary antibody). The other controls for comparison consisted of a) a well containing only *E. coli* cells and the secondary antibody b) a well containing *E. coli* cells, a different primary antibody and the secondary antibody c) a well containing no *E. coli* cells and the primary and secondary antibody. The control experiments were carried out on two different isolates of *E. coli* (clinical and environmental) and with *Psudemonas aeruginosa* (a gram negative bacteria found in coastal marine habitats).

Different protocols were employed for the adhesion of the cells to the flat bottomed microtitre plate. This included the use of plain plates, poly – 1 –lysine coated plates and methanol fixing. Poly – 1 –lysine coated plates resulted in the unwanted adhesion of antibody and therefore interfered in the assay. This was observed because no

response was seen for the *Pseudomonas aeruginosa* cells as expected, but a response was seen for the other negative controls, which should have given no response. *Pseudomonas aeruginosa* cells are larger than *E. coli* cells (0.5-0.8 μm width, 1.5-3.0 μm length), indicating that they were blocking the poly-l-lysine from the antibodies. Methanol fixing proved insufficient and no cells were retained on the flat bottomed plates. Therefore conical shaped well microtitre plates were employed for the assay.

The optimum washing procedures and blocking procedures determined are presented in the working ELISA protocol (table 4.8) (using a primary IgG *E. coli* specific antibody (mouse) concentration of 0.5 μg mL^{-1} and a secondary rabbit anti mouse IgG conjugated to HRP antibody concentration of 0.1 μg mL^{-1}). The results of the control experiments can be seen in figure 4.15 (which used a longer substrate development time of 30 mins) (n=3)).

Table 4.6 Procedures for the ELISA method for the determination of E. coli. A two site immunoassay is used within a 96 well microtitre plate with colourimetric detection of the HRP labelled secondary antibody.

Step	Procedure
1	Grow fresh bacterial cultures to exponential phase, wash twice in PBS and re-suspended in PBS. Cells are counted using a haemocytometer.
2	Add 100 µl cells to designated well and centrifuge (5min).
3	Replace PBS with 100 µl 1% BSA (in PBS) and 100 µl 2% milk powder (in PBS) and incubate at room temperature for 30 min.
4	Wash twice with PBS.
5	Add 100 µL/well of test antibody in 1% BSA (in PBS), incubate for 1 h at room temperature with rocking.
6	Wash once with PBS, once with 0.05% Tween 20 (in PBS) and once again with PBS.
7	Add 100 µL/well of relevant secondary antibody in 1% BSA (in PBS) incubate for 1 h at room temperature with rocking.
8	Wash twice with 0.05% Tween 20 (in PBS) and once with PBS.
9	Add TMB substrate, as prepared according to kit, leave colour to develop in dark for 10-30 min.
10	Add 50 µL 1N sulphuric acid.
11	Read absorbance (450 nm).
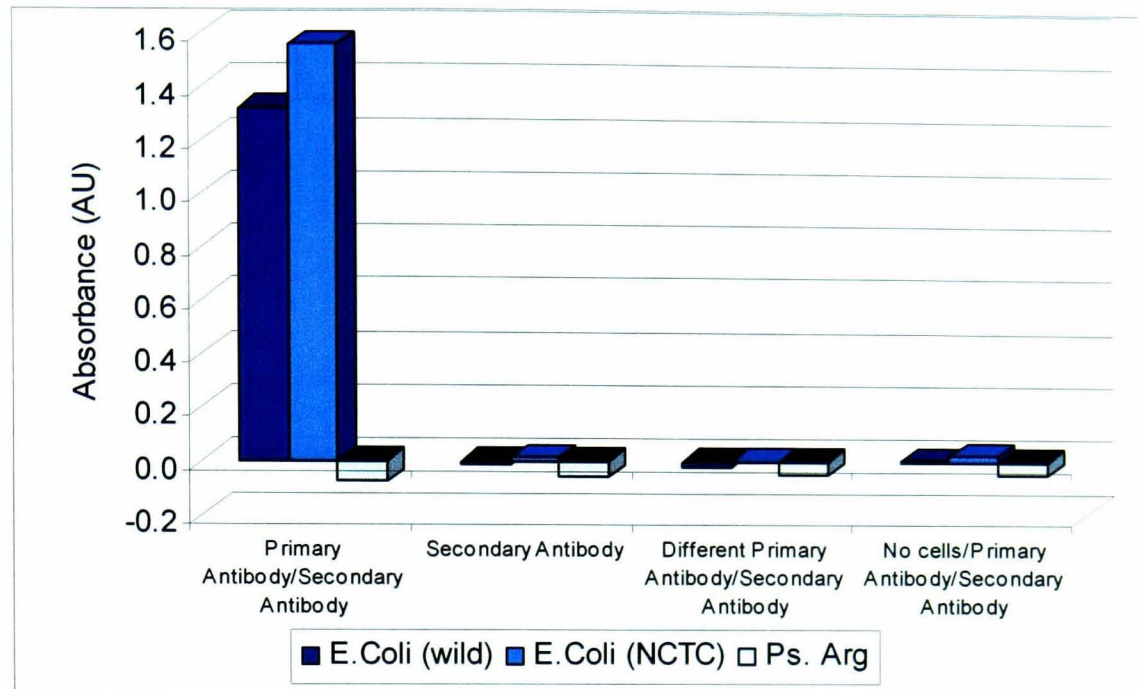
Figure 4.18 Graph to show the results of the antibody specificity experiment for the determination of E. coli using an ELISA with colourimetric detection of the HRP label using TMB. A positive result for E. coli (wild and clinical strain) is only achieved in the presence of the E. coli specific primary antibody and HRP labelled secondary antibody (n=3). No response is observed for Psudemonas aeruginosa.

To conclude, from the control experiments a working ELISA protocol was developed, which demonstrated the antibody specificity for *E. coli* bacteria over the gram negative bacteria *Psudemonas aeruginosa*.

4.3.3.2 Optimisation of the ELISA Method for E. coli Detection

A design of experiment was carried out using the ELISA to determine the optimum concentration of the primary IgG *E. coli* specific antibody (mouse) and the secondary rabbit anti mouse IgG conjugated to HRP antibody. The working ranges for the antibodies were 0.2-1.0 μg mL^{-1} for the primary antibody and 0.05-0.2 μg mL^{-1} for the secondary antibody (supplied with antibody specifications from manufacturers). Each one analysed in triplicate. This can be seen in figure 4.19.
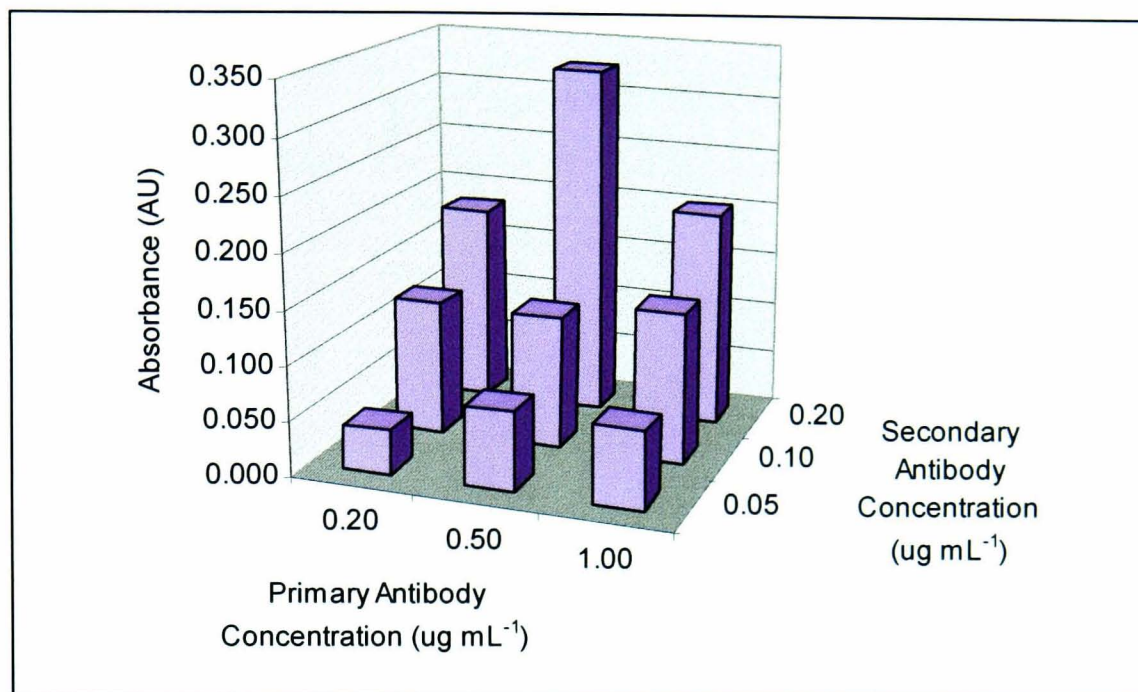
Figure 4.19 Graph to show the results for the optimal primary (E. coli specific) and secondary (HRP labelled) antibody concentrations used in the determination of E. coli using an ELISA with colourimetric detection of the HRP label using TMB.

An optimum primary IgG *E. coli* specific antibody (mouse) concentration of 0.5 μg mL^{-1} and an optimum secondary rabbit anti mouse IgG conjugated to HRP antibody concentration of 0.2 μg mL^{-1} was observed and used for subsequent experiments.

4.3.3.3 Calibration for E. coli Detection Using the ELISA Protocol

A calibration was constructed out using the ELISA over the range $1.4 \times 10^8 - 5.6 \times 10^8$ cells mL^{-1} in order to investigate linearity of the antibody-antigen binding. This can be seen in figure 4.20.
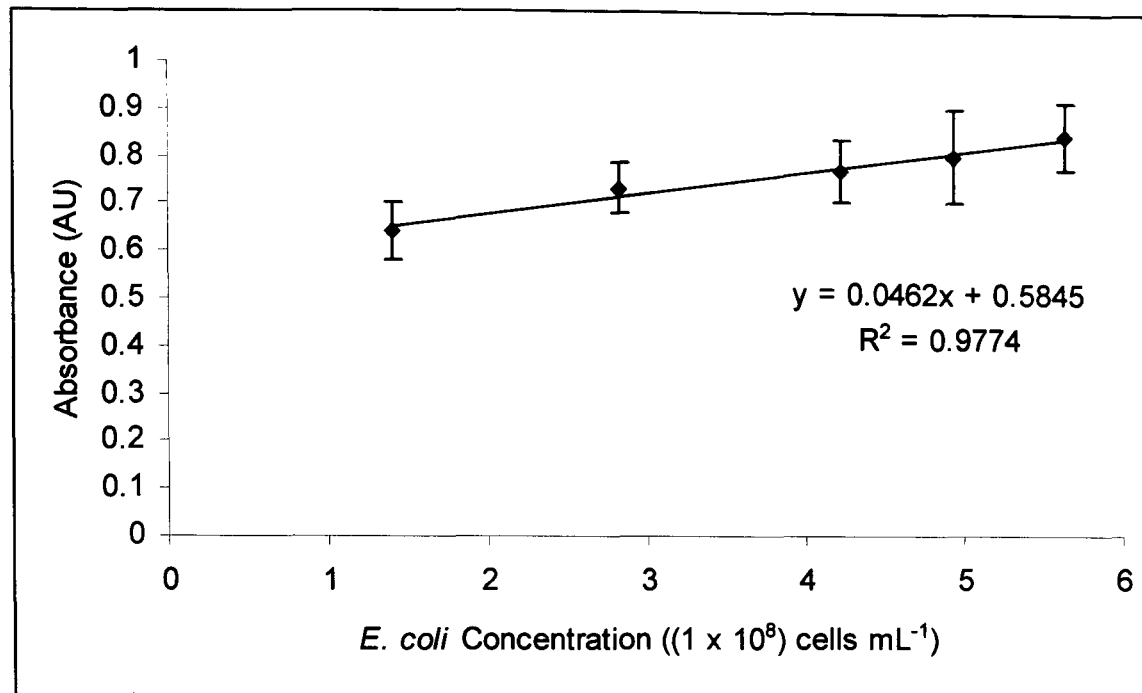
Figure 4.20 *Calibration for the determination of E. coli using using an ELISA with colourimetric detection of the HRP label using TMB. Error bars: one standard deviation (n=3).*

A linear plot was observed over the range and the limit of detection was calculated based on three times the deviation of the y-residuals,[225] and was determined to be 7.6 $\times$ 10^7 cells mL^{-1}, a fairly poor LOD. The reproducibility was also relatively poor (RSD 8-12%, n=3). However the ELISA provided a method for screening different *E. coli* isolates in order to investigate the specificity of the IgG *E. coli* specific antibody.

4.3.3.4 Screening of Different Isolates of E. coli Using the ELISA Protocol

A number of different isolates of *E. coli* bacteria will be present in the environment; therefore it was necessary to investigate how specific the antibodies were towards different isolates of *E. coli*. If the antibodies are too specific this will reduce the sensitivity and accuracy of the method.

A number of *E. coli* isolates supplied by the Department of Biological Sciences, University of Hull and were investigated to see if the primary IgG *E. coli* specific antibody would recognise different isolates of *E. coli*. Sixteen different isolates from environmental sources (A) and five from clinical sources were screened using the ELISA protocol for this purpose. The results from this can be seen in figure 4.21.
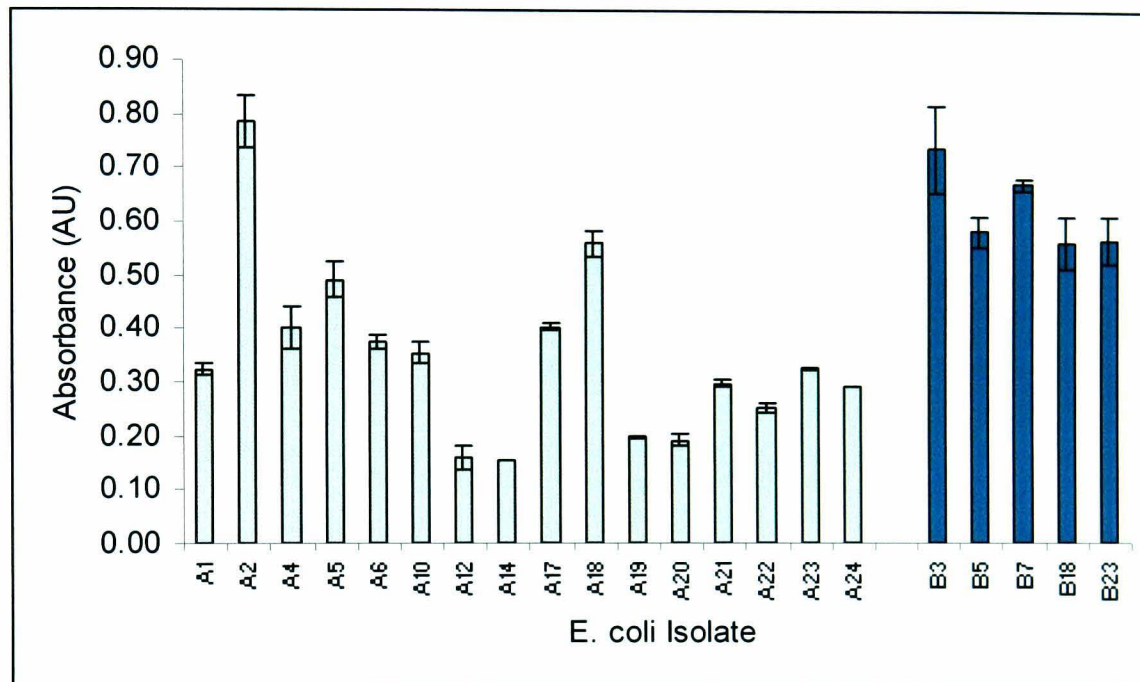
Figure 4.21 Determination of different isolates of E. coli using using an ELISA with colourimetric detection of the HRP label using TMB, where A are environmental samples and B are clinical samples. Error bars: one standard deviation (n=3).

The ELISA showed that the antibody gave a response to the different isolates of *E. coli* demonstrating that the commercially available IgG *E. coli* specific antibody is suitable to be used in an immunoassay for the determination of *E. coli* in seawater (the difference in absorbance for each isolate is due to the varying concentration of the cells used in the experiment).

To conclude, an ELISA has been developed to evaluate the specificity of antibodies towards there antigens. The ELISA is a lengthy analysis (6 h), which is complicated

and requires expertise. However, it does allow for the investigation into the antibody-antigen interactions.

4.3.4 Microfluidic Immunoassay for the Determination of *E. coli*

The capture IgG *E. coli* specific antibodies immobilised onto CPG discussed in section 4.2.3 (120-200 mesh (74-125 µm), 679 Å pore size, loading 1.5 µg g^{-1}) were packed into the microfluidic device described in section 2.3.3. The flow immunoassay protocol was based on the working ELISA detailed in section 4.2.4.1 and is given in table 4.7. A standard was prepared of 5 x 10^7 *E. coli* cells mL^{-1} and was used throughout the microfluidic immunoassay experiments. The initial primary IgG *E. coli* specific antibody (mouse) concentration used was 0.5 µg mL^{-1} and the secondary rabbit anti mouse IgG conjugated to HRP antibody concentration used was 0.2 µg mL^{-1}, as used in the ELSIA protocol (see section 4.3.3.2), prepared in 1% BSA in PBS. The chemiluminescence reagent consisted of 5 mmol L^{-1} luminol, 5.5 mmol L^{-1} hydrogen peroxide and 0.2 mmol L^{-1} *p*-iodophenol in 0.1 mol L^{-1} Tris-HCl buffer, pH 8.5 (140 mmol L^{-1}NaCl and 30 mmol L^{-1} KCl) as previously discussed in section 4.3.1. Each reagent was changed manually. An initial flow rate of 10 µl min^{-1} was used as this was the slowest flow rate compatible with the device and pump, and as discussed in section 1.2.6, a slow flow rate is required for mixing which would indicate a slow rate is required for antigen-antibody interactions. An initial time of 1 min for each reagent passing through the packed reactor was selected in order to keep analysis times down.

Table 4.7 Procedures for the microfluidic non-competitive (reagent excess) heterogeneous two step sandwich immunoassay. The microfluidic device is packed with CPG containing immobilised E. coli specific antibodies and each step signifies the reagent and flow rate to be passed through the packed microchannel.

Step	Flow rate (μl min^{-1})	Time (min)	Solution
1	10	1	PBS
2	10	1	Blocking buffer (1% BSA in PBS)
3	10	1	Sample
4	10	1	Blocking buffer (1% BSA in PBS)
5	10	1	PBS
6	10	1	Primary antibody (IgG *E. coli* specific antibody (mouse))
7	10	1	PBS
8	10	1	Secondary antibody (Rabbit anti mouse IgG conjugated to HRP)
9	10	1	PBS
10	10	2	Chemiluminescence reagent
11	10	2[a]	Regeneration buffer

[a]Length of time the regeneration is needed to regenerate the antibody column investigated separately see section 4.3.4.1.

4.3.4.1 Regeneration of Immobilised Antibodies

Antibody-antigen interactions are due to intermolecular forces and are therefore reversible. The antigens can therefore be removed from the immobilised antibodies after the detection stage of the immunoassay. This enables the immunoreactor to be regenerated and recycled, increasing its lifetime and achieving a greater sample throughput. A common regeneration buffer used in heterogeneous immunoassays to remove the antigen from the immobilised antibodies is 0.2 mol L^{-1} glycine buffer, pH

2.2.[238, 300] This buffer was employed in the microfluidic immunoassay to investigate immunoreactor regeneration (see figure 4.22). The gycine buffer was passed through the microfluidic device after chemiluminescence detection had occurred for 5 minutes.
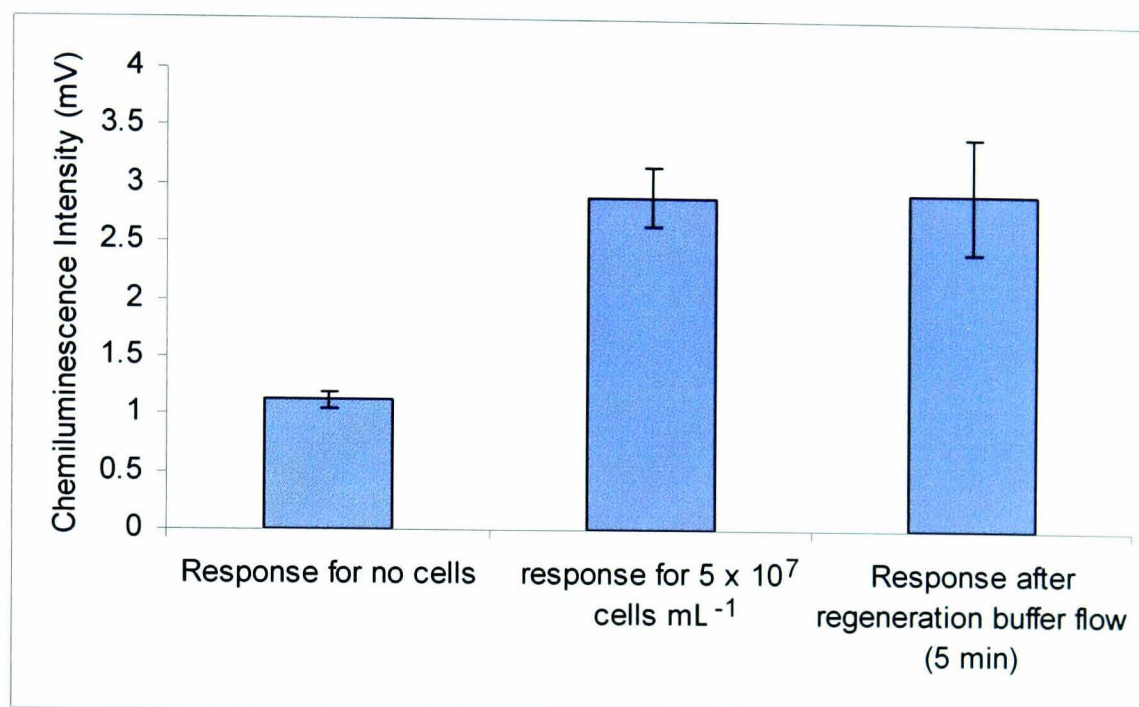
Figure 4.22 Results to show the response for no cells, 5 x 10^7 E. coli cells mL^{-1} and after 5 minutes of the 0.2 mol L^{-1} glycine regeneration buffer (pH 2.2), using the luminol – hydrogen peroxide reaction. A chemiluminescence response is still observed after regeneration. Error bars: one standard deviation (n=3).

From figure 4.22 it can be seen that the glycine regeneration buffer is not regenerating the immunoreactor as after 5 minutes of flowing the regeneration buffer a chemiluminescence signal is still observed at the same intensity to that seen for the *E. coli* sample. It has been discussed by Franek *et al.* that regeneration conditions found for individual immunoreactors were not necessarily compatible with different immunoreactors.[300] This is because of the kinetics and thermodynamics of the antigen–antibody interactions. Therefore the regeneration of the antibodies must be investigated separately. Another regeneration buffer investigated by Franek *et al.*

was 0.5 mol L^{-1} sodium hydroxide, and so this was also investigated for the regeneration of the immunoreactor (figure 4.23).
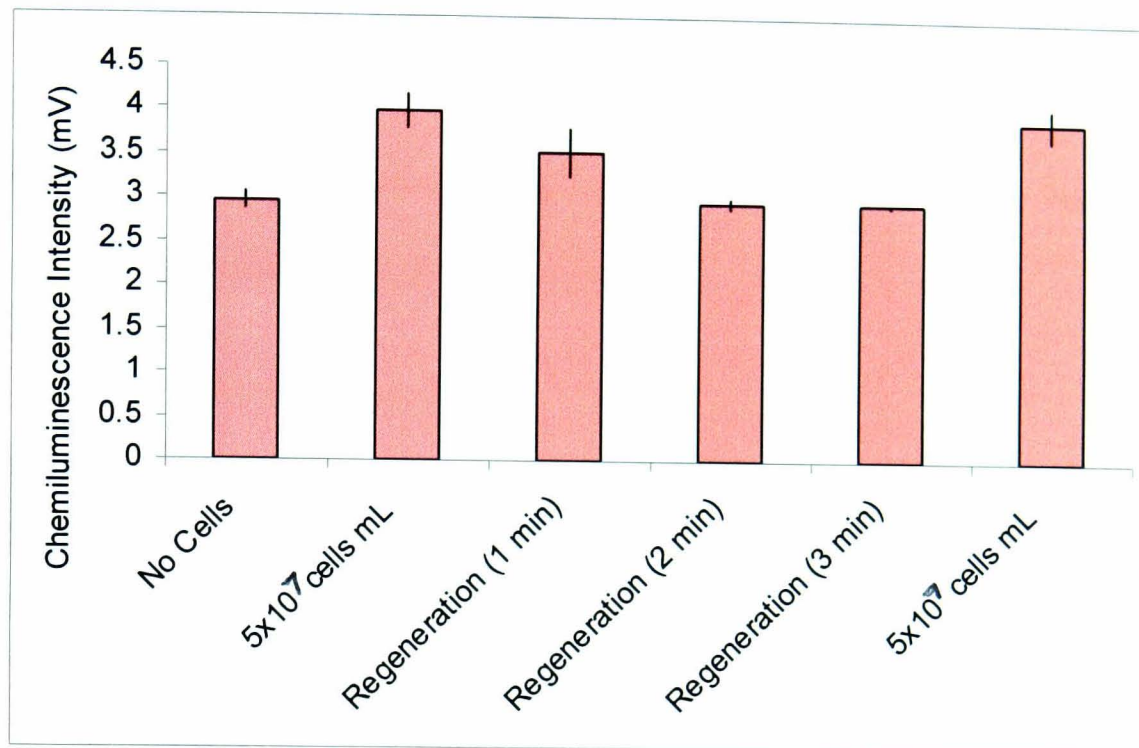
Figure 4.23 Results to show the chemiluminescence response for no cells, 5 x 10^7 E. coli cells mL^{-1} and after 1, 2 and 3 minutes of the 0.5 mol L^{-1} sodium hydroxide regeneration buffer, using the luminol-hydrogen peroxide reaction. A chemiluminescence response higher than the blank is still observed after regeneration for 1 mintue, but after 2 minutes the chemiluminescence response due to no cells was observed, indicating that the immunoreactor has been successfully regenerated. Error bars: one standard deviation (n=3).

A chemiluminescence response higher than the blank signal (no cells) was still observed for the immunoreactor after the sodium hydroxide regeneration buffer was passed over the immobilised antibodies for 1 mintue. After 2 minutes of regeneration buffer flow the chemiluminescence response decreased and was equal to the response of the blank (no cells). This demonstrated that the immunoreactor was successfully regenerated and could be used again for further *E. coli* samples.

202

Using this set-up a complete microfluidic immunoassay could be achieved in a total assay time of 13 minutes. A high background is observed in the presence of no cells in the sample, this is due to the HRP conjugated secondary antibody binding to unorientated immobilised *E. coli* antibody on the CPG. To decrease this high background signal it would be preferable to use a directly labelled *E. coli* specific antibody instead of the indirect labelling technique. This would decrease the background signal and reduce the assay time.

4.3.4.2 Investigation into Assay Time

In order to reduce the assay time a flow through time of 30 s for the reagents and sample at each stage of the immuoassay protocol was investigated (see table 4.7 for immunoassay protocol). The results are presented in figure 4.24.
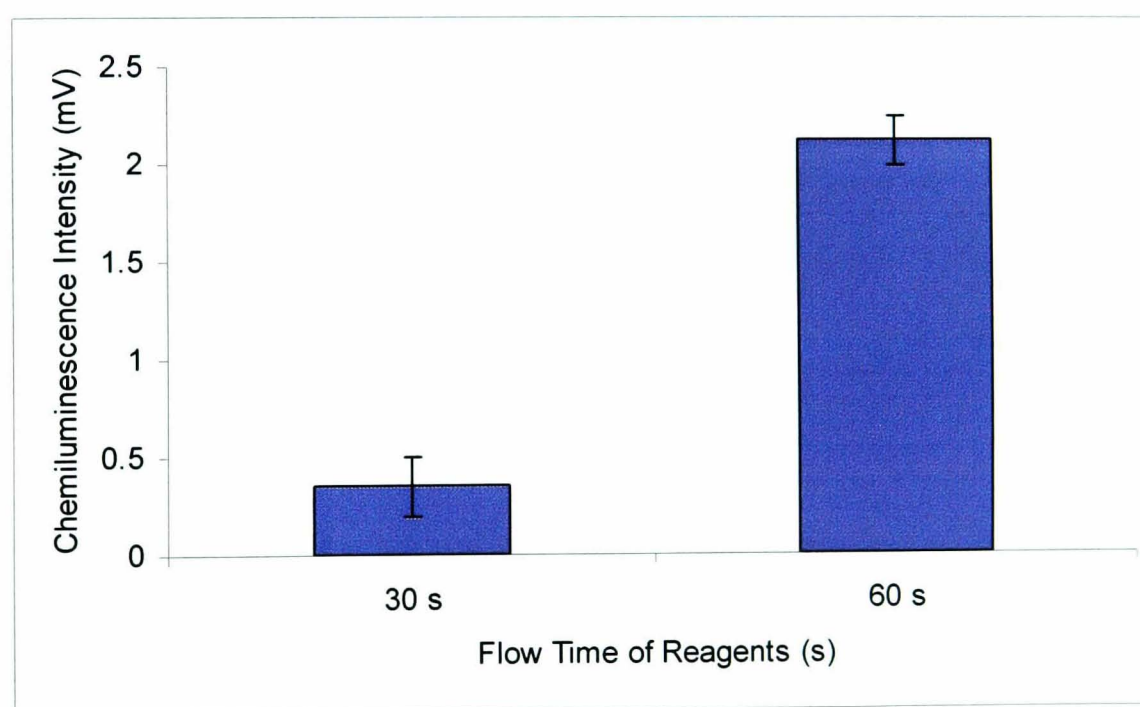
Figure 4.24 23 Results to show the chemiluminescence response for a sample of 5 x 10⁷ E. coli cells mL⁻¹ passed over the immunoreactor for different lengths of time (30 s and 60 s), using the luminol-hydrogen peroxide chemiluminescence reaction. Error bars: one standard deviation (n=3).

It can be seen from figure 4.24 that by reducing the assay time there is a significant decrease in the chemiluminescence intensity and therefore sensitivity of the assay, so a 1 minute flow through time was adopted.

4.3.4.3 Design of Experiment for Optimal Antibody Concentrations for the Assay

A poor signal was observed using the concentrations obtained from the ELISA experiments for the primary and secondary antibodies. Therefore a separate design of experiment was carried out for the microfluidic immunoassay to determine the optimal concentration of the primary and secondary antibody (see figure 4.25).
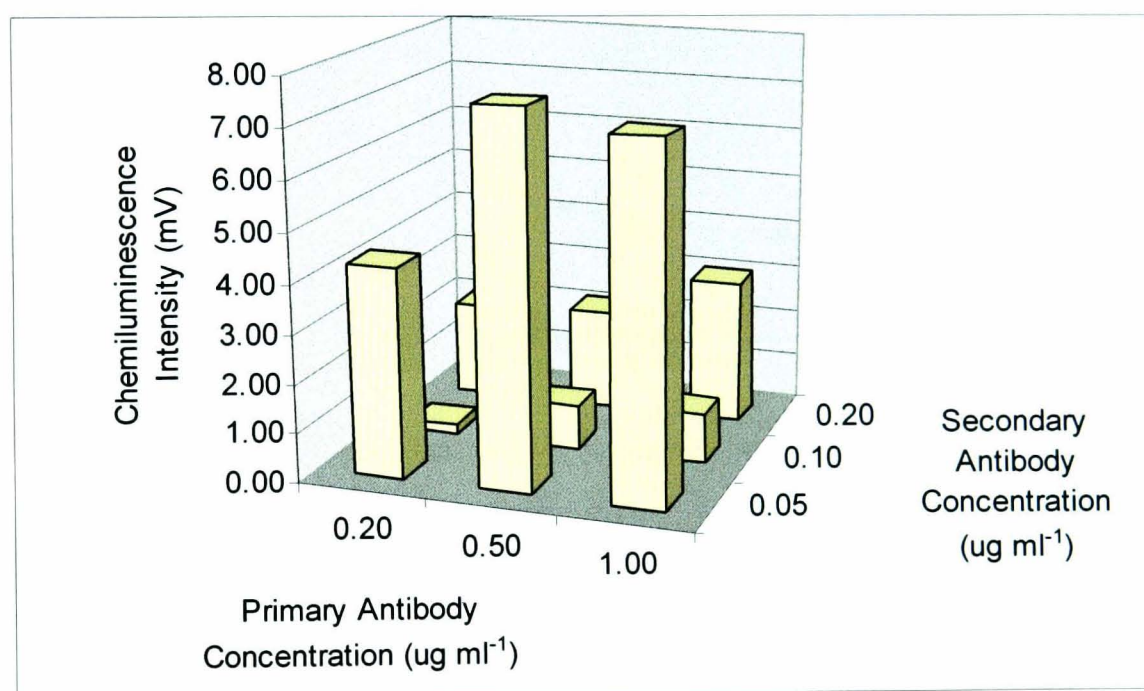
Figure 4.25 Graph to show the results for the optimal primary (E. coli specific) and secondary (HRP labelled) antibody concentrations used in the determination of E. coli (5 x 10^7 cells mL^{-1}) using the microfluidic immunoassay with detection of the HRP label by the luminol-hydrogen peroxide reaction.

The design of experiment for the microfluidic immunoassay produces different results to those observed for the ELISA. This is attributed to the different fluid properties in the microfluidic device to those in the bulk solution used in the ELISA.

Within the microfluidic device there is an increase in the efficiency of mass transport of the species, allowing greater accessibility of the antigen to interact with the antibody. The optimal primary IgG *E. coli* specific antibody (mouse) concentration used was 0.5 µg mL^{-1} and the secondary rabbit anti mouse IgG conjugated to HRP antibody concentration used was 0.05 µg mL^{-1}.

4.3.4.4 Effect of Flow Rate of the Immunoassay

The effect on the flow rate of the reagents within the microfluidic device was investigated in the range 9 – 22 µL min^{-1} (figure 4.26).
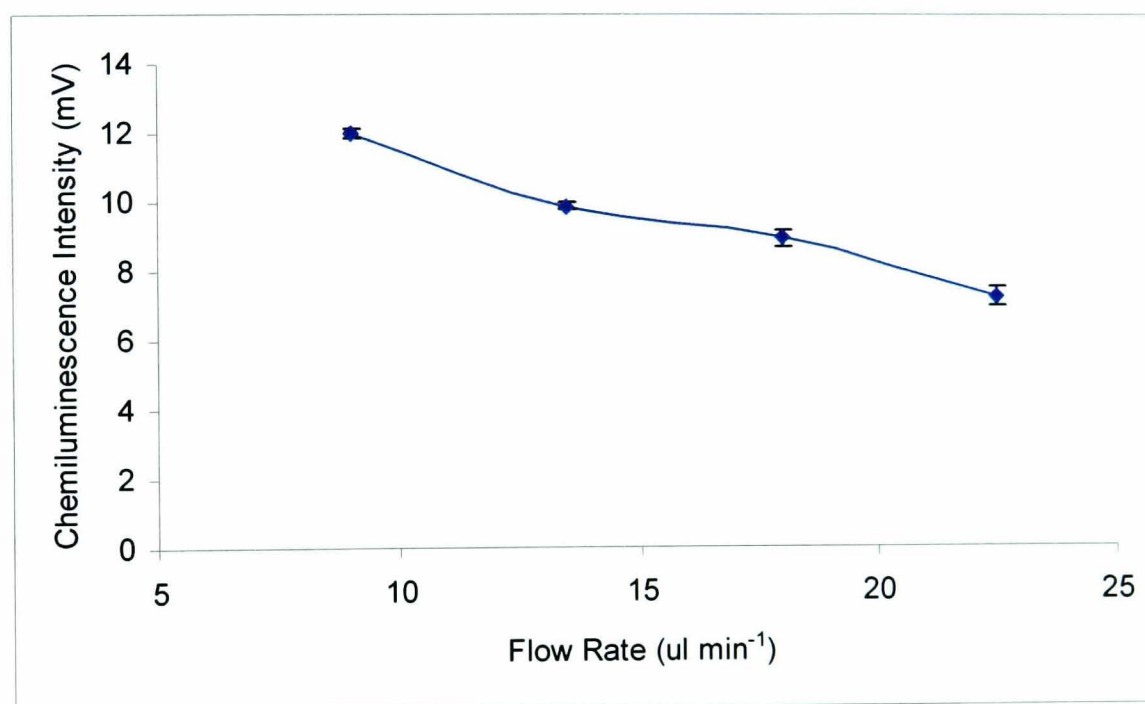
Figure 4.26 Effect of the flow rate of the reagents and sample during the immunoassay protocol on the determination of E. coli (5 x 10^7 cells mL^{-1}) using the luminol – hydrogen peroxide chemiluminescence reaction. Error bars: one standard deviation (n=3).

An increased response is observed for a low flow rate. At a lower flow rate, diffusion of the species to the immobilised components of the immunoassay is more efficient. The low flow rate also enables lower amounts of reagents to be used during the

assay, only 10 μL of primary antibody and 10 μL of secondary antibody is required per assay, which is ten times less than that required for the ELISA.

To conclude, a working microfluidic immunoassay protocol has been developed for the determination of *E. coli*. A rapid analysis time of 13 minutes was demonstrated, however the key issue was the sensitivity of the method, which is more sensitive than the ELISA but not nearly sensitive enough to measure *E. coli* in the environment. The sensitivity problems are attributed to the poor loading of the immobilised antibodies and the fact that the same antibody is used for the capture and detection of the *E. coli*. There may not be enough available binding sites for the sandwich immunoassay, using a different *E. coli* specific antibody in the detection step of the assay may improve this.

4.4 Conclusions and Future Work

A rapid method for the determination of *E. coli* in seawater has been developed. This was achieved using a non-competitive (reagent excess) heterogeneous two step sandwich immunoassay with a HRP enzyme label that was detected using the luminol-hydrogen peroxide chemiluminescence reaction within a microfluidic situated in the portable chemiluminescence detector.

The luminol-hydrogen peroxide chemiluminescence detection of HRP was investigated independently in solution within a microfluidic device and *p*-iodophenol was selected as an enhancer for the reaction which provided a sensitive method for the determination of HRP. *E. coli* specific antibodies were immobilised onto CPG *via* covalent attachment with APTS and CDI to produce a heterogeneous immunoassay format. The optimal loading of antibody on the CPG achieved was 1.5

$\mu g\ g^{-1}$. An ELISA method was utilised to ensure the correct antibody-antigen interactions were occurring between the *E. coli* specific antibody and *E. coli* bacteria. The ELISA was also used to screen the commercially available antibody for its specificity towards different isolates of *E. coli*. The *E. coli* specific antibody showed high specificity for *E. coli* over other bacteria and could detect a range of *E. coli* isolates found in the environment. A miniaturised immunoassay was presented using the immobilised *E. coli* specific antibodies packed within a microfluidic device. Using this format a rapid analysis time of 13 min was achieved, with low reagent consumption and waste production. A successful regeneration protocol of the immobilised antibodies using 0.5 mol L^{-1} sodium hydroxide was established enabling the packed microfluidic device to be reused for more than one sample.

High sensitivity was not achieved in the required range and future work would include resolving this problem by looking at different ways to covalently attach the capture antibodies onto CPG in order to increase the antibody loading. Different *E. coli* specific antibodies could be used for the capture stage and detection stage as this would increase the potential binding sites available on the bacteria for antibody interactions and improve the sensitivity of the assay. Another problem encountered was a high background and this could be overcome by using a direct labelling format, whereby the *E. coli* antibody is labelled with the HRP, as opposed to using an indirectly labelled technique with HRP labelled onto a secondary conjugate antibody.

The system was not fully field deployable and to achieve this, the next step will be to fully automate the system, this is discussed in section 3.4.

Chapter 5

Conclusions

5. Conclusions

The intrinsic advantages of microfluidic devices provide an advantageous approach to the development of portable methods of analysis for environmental monitoring. These include the advantages of low reagent consumption, small sample volumes, low waste production, faster analysis times and portability.

The selected detection method is very important to achieve the sensitivity required. Although electrochemical and spectrophotometric detection for microfluidic devices have both been demonstrated for environmental applications using microfluidic devices, chemiluminescence detection has the benefits of high sensitivity and simple instrumentation.

A portable battery operated chemiluminescence detection system was developed to provide a detection system for chemiluminescence reactions within a microfluidic device. A miniaturised peristaltic pump is used to continuously introduce samples and reagents into a microfluidic device situated above a miniaturised PMT, protected by a shutter. This is all contained within a light tight housing to prevent interference from external light.

Photolithography and wet etching were discussed as the fabrication process used for channel etching of the microfluidic devices supplied for the work and thermal bonding is described as the procedure for bonding the glass plates. Investigation into mixing showed a serpentine manifold gave improved mixing over a T-shape design.

Immobilisation techniques were assessed for the purpose of developing a reagentless assay. Covalent bonding was identified as a suitable immobilisation technique, which

lead to the investigation of solid supports for their compatibility with microfluidic devices in order to increase the surface area and therefore the loading of the immobilised species. Packed beads provide an inexpensive method of increasing the surface area within the channels, based on this a device was designed and fabricated utilising a tapered design to use the keystone effect to pack the beads within the device. Laser ablation was used to deepen part of the packing area to 120 µm in order to improve packing. This provided a working device which could be used with reagents immobilised onto beads

A portable, sensitive method of analysis for the determination of real time hydrogen peroxide levels in rainwater during a rainfall event was presented. This was accomplished using the luminol–cobalt(II) chemiluminescence reaction within a microfluidic device situated in the portable chemiluminescence detection system.

The chemiluminescence signal was enhanced by 132.3% using the mirror reaction to directly apply a reflective surface to the top of the microfluidic device, this enabled the sensitivity of the method to be achieved in the desired micromolar range. The limit of detection was determined to be 4.7 nmol L^{-1}. A small sample volume size of 10 µL min^{-1}, reagent consumption size (1.2 mL per hour) and waste production size (2.4 mL per hour) was also achieved. Immobilisation techniques for immobilising luminol onto a solid support were investigated, however poor sensitivity was observed and this approach was not progressed.

The system was used to analyse two rainfall events and the desired sampling rate of every 5 minutes was achieved. The results showed the hydrogen peroxide levels in the rain varied from 0.1-3.2 µmol L^{-1}. The system was also used to analyse snow

samples. The results showed the hydrogen peroxide levels in the snow samples collected from ground level varied from 0.2-0.5 μmol L^{-1}.

The system was not fully field deployable and to achieve this, the system needs to be fully automated and integrated with a rainwater sample collector and a portable data collecting device.

Once a straightforward chemical application had been demonstrated the approach was extended for biochemical applications. A need for a rapid and sensitive method for the determination of *E. coli* in seawater was identified. A rapid method for the detection of *E. coli* in seawater was developed using a non-competitive (reagent excess) heterogeneous two step sandwich immunoassay with a HRP enzyme label that was detected using the luminol -hydrogen peroxide chemiluminescence reaction within a microfluidic situated in the portable chemiluminescence detector.

The chemiluminescence detection of HRP, the enzyme label used for the immunoassay was investigated individually within a microfluidic device, the detection was optimised and *p*-iodophenol was selected as an enhancer. This produced a sensitive method for the determination of HRP. The immobilisation of the *E. coli* specific antibody onto CPG was investigated and an optimal loading of 1.5 μg g^{-1} was achieved. An ELISA was developed in order to screen the antibody for their specificity towards different isolates of *E. coli*. Finally, a microfluidic immunoassay was presented. Regeneration of the immobilised antibodies was achieved using 0.5 mol L^{-1} sodium hydroxide. A rapid analysis time of 13 min was demonstrated for a much simpler technique than the ELISA and which allowed for a low reagent consumption and waste production. The rapid testing of a number of

small samples enables the provision of high temporal and spatial resolution data. The immunoassay did not provide enough sensitivity for the determination of *E. coli* in seawater, ways to overcome this problem have been discussed.

Further work on the *E. coli* in seawater application includes the development of an alternative immobilisation procedure for the covalent attachment of the capture antibodies onto CPG. This is in order to find a method which will increase the antibody loading and therefore improve the sensitivity of the assay. Alternative *E. coli* specific antibodies need to be identified which will enable different antibodies to be used for the capture stage and for the detection stage of the assay. This may also improve the sensitivity of the assay as it increases the available sites that can be used in the antibody-antigen interactions during the two different stages. Direct labelling of the *E. coli* specific antibody with HRP, which is used in the detection step of the assay, needs to be investigated in order to reduce the background signal.

Chapter 6

References

6. References

1   A. Manz, N. Graber, and H. M. Widmer, *Sensors and Actuators B: Chemical*, 1990, **1**, 244.
2   G. Hanrahan, S. Ussher, M. Gledhill, E. P. Achterberg, and P. J. Worsfold, *Trac-Trends in Analytical Chemistry*, 2002, **21**, 233.
3   J. Ruzicka and E. H. Hansen, *Analytica Chimica Acta*, 1975, **78**, 145.
4   S. J. Haswell, *Analyst*, 1997, **122**, R1.
5   N. W. Barnett, C. E. Lenehan, and S. W. Lewis, *Trac-Trends in Analytical Chemistry*, 1999, **18**, 346.
6   C. E. Lenehan, N. W. Barnett, and S. W. Lewis, *Analyst*, 2002, **127**, 997.
7   D. R. Reyes, D. Iossifidis, P. A. Auroux, and A. Manz, *Analytical Chemistry*, 2002, **74**, 2623.
8   A. E. Guber, M. Heckele, D. Herrmann, A. Muslija, V. Saile, L. Eichhorn, T. Gietzelt, W. Hoffmann, P. C. Hauser, J. Tanyanyiwa, A. Gerlach, N. Gottschlich, and G. Knebel, *Chemical Engineering Journal*, 2004, **101**, 447.
9   M. Sequeira, M. Bowden, E. Minogue, and D. Diamond, *Talanta*, 2002, **56**, 355.
10   P. A. Greenwood and G. M. Greenway, *Trac-Trends In Analytical Chemistry*, 2002, **21**, 726.
11   T. McCreedy, *Trac-Trends in Analytical Chemistry*, 2000, **19**, 396.
12   T. McCreedy, *Analytica Chimica Acta*, 2001, **427**, 39.
13   M. Bowden, O. Geschke, J. P. Kutter, and D. Diamond, *Lab On A Chip*, 2003, **3**, 221.
14   J. Rossier, F. Reymond, and P. E. Michel, *Electrophoresis*, 2002, **23**, 858.
15   C. K. Malek and V. Saile, *Microelectronics Journal*, 2004, **35**, 131.
16   M. Worgull and M. Heckele, *Microsystem Technologies-Micro-And Nanosystems-Information Storage And Processing Systems*, 2004, **10**, 432.
17   M. Heckele and W. K. Schomburg, *Journal Of Micromechanics And Microengineering*, 2004, **14**, R1.
18   J. Narasimhan and I. Papautsky, *Journal Of Micromechanics And Microengineering*, 2004, **14**, 96.
19   T. Vilkner, D. Janasek, and A. Manz, *Analytical Chemistry*, 2004, **76**, 3373.
20   P. D. Grossman and J. C. Colburn, 'Capillary Electrophoresis: Theory and Practice.' Academic Press, San Diego, 1992.
21   D. J. Laser and J. G. Santiago, *Journal Of Micromechanics And Microengineering*, 2004, **14**, R35.
22   G. M. Greenway, S. J. Haswell, and P. H. Petsul, *Analytica Chimica Acta*, 1999, **387**, 1.
23   P. D. Christensen, S. W. P. Johnson, T. McCreedy, V. Skelton, and N. G. Wilson, *Analytical Communications*, 1998, **35**, 341.
24   M. Koch, N. Harris, A. G. R. Evans, N. M. White, and A. Brunnschweiler, *Sensors And Actuators A-Physical*, 1998, **70**, 98.
25   M. Richter, R. Linnemann, and P. Woias, *Sensors And Actuators A-Physical*, 1998, **68**, 480.
26   M. J. Bloxham, M. H. Depledge, and P. J. Worsfold, *Laboratory Robotics and Automation*, 1997, **9**, 175.

27   H. Andersson, W. van der Wijngaart, P. Nilsson, P. Enoksson, and G. Stemme, *Sensors And Actuators B-Chemical*, 2001, **72**, 259.

28   A. Wego and L. Pagel, *Sensors And Actuators A-Physical*, 2001, **88**, 220.

29   O. C. Jeong and S. S. Yang, *Sensors And Actuators A-Physical*, 2000, **83**, 249.

30   M. A. Unger, H. P. Chou, T. Thorsen, A. Scherer, and S. R. Quake, *Science*, 2000, **288**, 113.

31   J. Dopper, M. Clemens, W. Ehrfeld, S. Jung, K. P. Kamper, and H. Lehr, *Journal Of Micromechanics And Microengineering*, 1997, 7, 230.

32   N. R. Tas, J. W. Berenschot, T. S. J. Lammerink, M. Elwenspoek, and A. van den Berg, *Analytical Chemistry*, 2002, **74**, 2224.

33   A. V. Lemoff and A. P. Lee, *Sensors And Actuators B-Chemical*, 2000, **63**, 178.

34   A. V. Lemoff and A. P. Lee, *Biomedical Microdevices*, 2003, **5**, 55.

35   L. Huang, W. Wang, M. C. Murphy, K. Lian, and Z. G. Ling, *Microsystem Technologies-Micro-And Nanosystems-Information Storage And Processing Systems*, 2000, **6**, 235.

36   E. S. Roddy, H. W. Xu, and A. G. Ewing, *Electrophoresis*, 2004, **25**, 229.

37   L. M. Fu, R. J. Yang, G. B. Lee, and H. H. Liu, *Analytical Chemistry*, 2002, **74**, 5084.

38   L. M. Fu, R. J. Yang, and G. B. Lee, *Analytical Chemistry*, 2003, **75**, 1905.

39   R. J. Yang, L. M. Fu, and G. B. Lee, *Journal Of Separation Science*, 2002, **25**, 996.

40   S. J. Baldock, P. R. Fielden, N. J. Goddard, H. R. Kretschmer, J. E. Prest, and B. J. T. Brown, *Journal Of Chromatography A*, 2004, **1042**, 181.

41   N. Y. Lee, M. Yamada, and M. Seki, *Analytical Sciences*, 2005, **21**, 465.

42   A. P. O'Neill, P. O'Brien, J. Alderman, D. Hoffman, M. McEnery, J. Murrihy, and J. D. Glennon, *Journal Of Chromatography A*, 2001, **924**, 259.

43   D. Solignac and M. A. M. Gijs, *Analytical Chemistry*, 2003, **75**, 1652.

44   H. W. Gai, L. F. Yu, Z. P. Dai, Y. F. Ma, and B. C. Lin, *Electrophoresis*, 2004, **25**, 1888.

45   U. Backofen, F. M. Matysik, and C. E. Lunte, *Analytical Chemistry*, 2002, **74**, 4054.

46   X. X. Bai, H. J. Lee, J. S. Rossier, F. Reymond, H. Schafer, M. Wossner, and H. H. Girault, *Lab On A Chip*, 2002, **2**, 45.

47   H. W. Xu and A. G. Ewing, *Analytical And Bioanalytical Chemistry*, 2004, **378**, 1710.

48   H. W. Xu, E. S. Roddy, T. P. Roddy, J. A. Lapos, and A. G. Ewing, *Journal Of Separation Science*, 2004, **27**, 7.

49   X. M. Xu, T. P. Roddy, J. A. Lapos, and A. G. Ewing, *Analytical Chemistry*, 2002, **74**, 5517.

50   J. L. Pittman, A. I. Terekhov, S. W. Suljak, and S. D. Gilman, *Analytica Chimica Acta*, 2003, **496**, 195.

51   E. S. Roddy, J. A. Lapos, and A. G. Ewing, *Journal Of Chromatography A*, 2003, **1004**, 217.

52   J. A. Lapos and A. G. Ewing, *Analytical Chemistry*, 2000, **72**, 4598.

53   D. Kaniansky, M. Masar, R. Bodor, M. Zuborova, E. Olvecka, M. Johnck, and B. Stanislawski, *Electrophoresis*, 2003, **24**, 2208.

54   J. E. Prest, S. J. Baldock, P. R. Fielden, N. J. Goddard, and B. J. T. Brown, *Analytical and Bioanalytical Chemistry*, 2003, **376**, 78.

55   J. E. Prest, S. J. Baldock, P. R. Fielden, N. J. Goddard, and B. J. T. Brown, *Journal of Chromatography A*, 2003, **990**, 325.

56   W. N. Vreeland, S. J. Williams, A. E. Barron, and A. P. Sassi, *Analytical Chemistry*, 2003, **75**, 3059.

57   T. B. Stachowiak, T. Rohr, E. F. Hilder, D. S. Peterson, M. Q. Yi, F. Svec, and J. M. J. Frechet, *Electrophoresis*, 2003, **24**, 3689.

58   E. Verpoorte, *Lab On A Chip*, 2003, **3**, 60N.

59   P. A. Auroux, D. Iossifidis, D. R. Reyes, and A. Manz, *Analytical Chemistry*, 2002, **74**, 2637.

60   R. J. Emrich, 'Fluid dynamics ', Methods of experimental physics, Volume 18 A, Academic Press, New York, 1981.

61   K. J. Laidler and J. H. Meiser, 'Physical Chemistry', Houghton Mifflin, 1999.

62   N. T. Nguyen and Z. G. Wu, *Journal Of Micromechanics And Microengineering*, 2005, **15**, R1.

63   P. Hinsmann, J. Frank, P. Svasek, M. Harasek, and B. Lendl, *Lab On A Chip*, 2001, **1**, 16.

64   M. Koch, H. Witt, A. G. R. Evans, and A. Brunnschweiler, *Journal Of Micromechanics And Microengineering*, 1999, **9**, 156.

65   F. G. Bessoth, A. J. deMello, and A. Manz, *Analytical Communications*, 1999, **36**, 213.

66   S. C. Jacobson, T. E. McKnight, and J. M. Ramsey, *Analytical Chemistry*, 1999, **71**, 4455.

67   M. Kakuta, F. G. Bessoth, and A. Manz, *Chemical Record*, 2001, **1**, 395.

68   K. Jensen, *Nature*, 1998, **393**, 735.

69   J. B. Knight, A. Vishwanath, J. P. Brody, and R. H. Austin, *Physical Review Letters*, 1998, **80**, 3863.

70   G. M. Walker, M. S. Ozers, and D. J. Beebe, *Sensors And Actuators B-Chemical*, 2004, **98**, 347.

71   B. L. Gray, D. Jaeggi, N. J. Mourlas, B. P. van Drieenhuizen, K. R. Williams, N. I. Maluf, and G. T. A. Kovacs, *Sensors And Actuators A-Physical*, 1999, **77**, 57.

72   M. S. Munson and P. Yager, *Analytica Chimica Acta*, 2004, **507**, 63.

73   B. He, B. J. Burke, X. Zhang, R. Zhang, and F. E. Regnier, *Analytical Chemistry*, 2001, **73**, 1942.

74   J. Melin, G. Gimenez, N. Roxhed, W. van der Wijngaart, and G. Stemme, *Lab On A Chip*, 2004, **4**, 214.

75   K. Handique and M. A. Burns, *Journal Of Micromechanics And Microengineering*, 2001, **11**, 548.

76   P. Paik, V. K. Pamula, and R. B. Fair, *Lab On A Chip*, 2003, **3**, 253.

77   J. D. Tice, H. Song, A. D. Lyon, and R. F. Ismagilov, *Langmuir*, 2003, **19**, 9127.

78   C. P. Jen, C. Y. Wu, Y. C. Lin, and C. Y. Wu, *Lab On A Chip*, 2003, **3**, 77.

79   Y. Mizuno and M. Funakoshi, *Fluid Dynamics Research*, 2002, **31**, 129.

80   S. J. Park, J. K. Kim, J. Park, S. Chung, C. Chung, and J. K. Chang, *Journal Of Micromechanics And Microengineering*, 2004, **14**, 6.

81   H. Chen and J. C. Meiners, *Applied Physics Letters*, 2004, **84**, 2193.

82   R. A. Vijayendran, K. M. Motsegood, D. J. Beebe, and D. E. Leckband, *Langmuir*, 2003, **19**, 1824.

83   C. C. Hong, J. W. Choi, and C. H. Ahn, *Lab On A Chip*, 2004, **4**, 109.

84   V. Mengeaud, J. Josserand, and H. H. Girault, *Analytical Chemistry*, 2002, **74**, 4279.

85   Y. H. Lin, G. B. Lee, C. W. Li, G. R. Huang, and S. H. Chen, *Journal Of Chromatography A*, 2001, **937**, 115.

86   H. Z. Wang, P. Iovenitti, E. Harvey, and S. Masood, *Smart Materials & Structures*, 2002, **11**, 662.

87   T. J. Johnson, D. Ross, and L. E. Locascio, *Analytical Chemistry*, 2002, **74**, 45.

88   A. D. Stroock, S. K. W. Dertinger, A. Ajdari, I. Mezic, H. A. Stone, and G. M. Whitesides, *Science*, 2002, **295**, 647.

89   H. Z. Wang, P. Iovenitti, E. Harvey, and S. Masood, *Journal Of Micromechanics And Microengineering*, 2003, **13**, 801.

90   T. Fujii, Y. Sando, K. Higashino, and Y. Fujii, *Lab On A Chip*, 2003, **3**, 193.

91   I. Glasgow and N. Aubry, *Lab On A Chip*, 2003, **3**, 114.

92   L. H. Lu, K. S. Ryu, and C. Liu, *Journal Of Microelectromechanical Systems*, 2002, **11**, 462.

93   A. O. El Moctar, N. Aubry, and J. Batton, *Lab On A Chip*, 2003, **3**, 273.

94   M. H. Oddy, J. G. Santiago, and J. C. Mikkelsen, *Analytical Chemistry*, 2001, **73**, 5822.

95   Z. L. Tang, S. B. Hong, D. Djukic, V. Modi, A. C. West, J. Yardley, and R. M. Osgood, *Journal Of Micromechanics And Microengineering*, 2002, **12**, 870.

96   H. H. Bau, J. H. Zhong, and M. Q. Yi, *Sensors And Actuators B-Chemical*, 2001, **79**, 207.

97   J. C. Rife, M. I. Bell, J. S. Horwitz, M. N. Kabler, R. C. Y. Auyeung, and W. J. Kim, *Sensors And Actuators A-Physical*, 2000, **86**, 135.

98   Z. Yang, H. Goto, M. Matsumoto, and R. Maeda, *Electrophoresis*, 2000, **21**, 116.

99   Z. Yang, S. Matsumoto, H. Goto, M. Matsumoto, and R. Maeda, *Sensors And Actuators A-Physical*, 2001, **93**, 266.

100   G. G. Yaralioglu, I. O. Wygant, T. C. Marentis, and B. T. Khuri-Yakub, *Analytical Chemistry*, 2004, **76**, 3694.

101   R. H. Liu, J. N. Yang, M. Z. Pindera, M. Athavale, and P. Grodzinski, *Lab On A Chip*, 2002, **2**, 151.

102   H. B. Mao, T. L. Yang, and P. S. Cremer, *Journal Of The American Chemical Society*, 2002, **124**, 4432.

103   J. Khandurina and A. Guttman, *Journal of Chromatography A*, 2002, **943**, 159.

104   K. Huikko, R. Kostiainen, and T. Kotiaho, *European Journal of Pharmaceutical Sciences*, 2003, **20**, 149.

105   L. J. Kricka, *Journal of Clinical Ligand Assay*, 2002, **25**, 317.

106   J. Metzger, M. Blobner, and P. B. Luppa, *Clinical Chemistry and Laboratory Medicine*, 2001, **39**, 514.

107   C. L. Colyer, T. Tang, N. Chiem, and D. J. Harrison, *Electrophoresis*, 1997, **18**, 1733.

108   E. Verpoorte, *Electrophoresis*, 2002, **23**, 677.

109 Y. Liu, C. D. Garcia, and C. S. Henry, *Analyst*, 2003, **128**, 1002.
110 P. D. I. Fletcher, S. J. Haswell, E. Pombo-Villar, B. H. Warrington, P. Watts, S. Y. F. Wong, and X. Zhang, *Tetrahedron*, 2002, **58**, 4735.
111 X. Z. Feng, S. J. Haswell, and P. Watts, *Current Topics In Medicinal Chemistry*, 2004, **4**, 707.
112 S. J. Haswell and P. Watts, *Green Chemistry*, 2003, **5**, 240.
113 M. A. Schwarz and P. C. Hauser, *Lab on a chip*, 2001, **1**, 1.
114 J. Wang, *Trac-Trends in Analytical Chemistry*, 2002, **21**, 226.
115 J. Wang, *Talanta*, 2002, **56**, 223.
116 J. J. Xu, N. Bao, X. H. Xia, Y. Peng, and H. Y. Chen, *Analytical Chemistry*, 2004, **76**, 6902.
117 J. Wang, A. Escarpa, M. Pumera, and J. Feldman, *Journal of Chromatography A*, 2002, **952**, 249.
118 J. Wang, M. P. Chatrathi, B. M. Tian, and R. Polsky, *Electroanalysis*, 2000, **12**, 691.
119 J. Wang, M. P. Chatrathi, and B. M. Tian, *Analytica Chimica Acta*, 2000, **416**, 9.
120 J. Wang, M. P. Chatrathi, A. Mulchandani, and W. Chen, *Analytical Chemistry*, 2001, **73**, 1804.
121 J. Wang, M. P. Chatrathi, and B. M. Tian, *Analytical Chemistry*, 2000, **72**, 5774.
122 A. Hilmi and J. H. T. Luong, *Analytical Chemistry*, 2000, **72**, 4677.
123 A. Hilmi and J. H. T. Luong, *Environmental Science & Technology*, 2000, **34**, 3046.
124 O. T. Guenat, G. C. Fiaccabrino, W. E. Morf, M. Koudelka-Hep, and N. F. de Rooij, *Chimia*, 1999, **53**, 87.
125 J. Lichtenberg, N. F. de Rooij, and E. Verpoorte, *Talanta*, 2002, **56**, 233.
126 T. Becker, S. Muhlberger, C. Bosch-von Braunmuhl, G. Muller, T. Ziemann, and K. V. Hechtenberg, *Sensors and Actuators B-Chemical*, 2000, **69**, 108.
127 T. Becker, S. Muhlberger, C. Bosch-vonBraunmuhl, G. Muller, A. Meckes, and W. Benecke, *Journal of Microelectromechanical Systems*, 2000, **9**, 478.
128 B. H. Timmer, K. M. van Delft, R. P. Otjes, W. Olthuis, and A. van den Berg, *Analytica Chimica Acta*, 2004, **507**, 137.
129 S. I. Ohira, K. Toda, S. I. Ikebe, and P. K. Dasgupta, *Analytical Chemistry*, 2002, **74**, 5890.
130 T. Korenaga, T. Odake, Y. Ono, and L. Rong, *Bunseki Kagaku*, 2000, **49**, 423.
131 D. C. Harris, 'Quantitative chemical analysis ', W.H. Freeman, New York, 1999, 5th ed.
132 R. N. C. Daykin and S. J. Haswell, *Analytica Chimica Acta*, 1995, **313**, 155.
133 G. N. Doku and S. J. Haswell, *Analytica Chimica Acta*, 1999, **382**, 1.
134 P. H. Petsul, G. M. Greenway, and S. J. Haswell, *Analytica Chimica Acta*, 2001, **428**, 155.
135 A. Daridon, M. Sequeira, G. Pennarun-Thomas, H. Dirac, J. P. Krog, P. Gravesen, J. Lichtenberg, D. Diamond, E. Verpoorte, and N. F. de Rooij, *Sensors and Actuators B-Chemical*, 2001, **76**, 235.
136 M. Sequeira and D. Diamond, *Trac-Trends in Analytical Chemistry*, 2002, **21**, 816.

137 A. Bowden and D. Diamond, *Sensors and Actuators B-Chemical*, 2003, **90**, 170.

138 M. Bowden, M. Sequeira, J. P. Krog, P. Gravesen, and D. Diamond, *Analyst*, 2002, **127**, 1.

139 M. Bowden, M. Sequiera, J. P. Krog, P. Gravesen, and D. Diamond, *Journal of Environmental Monitoring*, 2002, **4**, 767.

140 Q. Lu, G. E. Collins, M. Smith, and J. Wang, *Analytica Chimica Acta*, 2002, **469**, 253.

141 Y. Ueno, K. Ajito, and Y. Y. Maruo, *Physical Chemistry Chemical Physics*, 2002, **4**, 2341.

142 Y. Ueno, K. Ajito, Y. Yamada, Y. Maruo, O. Niwa, K. Torimitsu, and T. Ichino, *Applied Spectroscopy*, 2001, **55**, 1151.

143 Y. Ueno, T. Horiuchi, T. Morimoto, and O. Niwa, *Analytical Chemistry*, 2001, **73**, 4688.

144 Y. Ueno, T. Horiuchi, and O. Niwa, *Analytical Chemistry*, 2002, **74**, 1712.

145 Y. Ueno, T. Horiuchi, O. Niwa, H. S. Zhou, T. Yamada, and I. Honma, *Sensors and Actuators B-Chemical*, 2003, **95**, 282.

146 Y. Ueno, T. Horiuchi, M. Tomita, O. Niwa, H. S. Zhou, T. Yamada, and I. Honma, *Analytical Chemistry*, 2002, **74**, 5257.

147 B. S. Broyles, S. C. Jacobson, and J. M. Ramsey, *Analytical Chemistry*, 2003, **75**, 2761.

148 L. J. Nelstrop, P. A. Greenwood, and G. M. Greenway, *Lab on a Chip*, 2001, **1**, 138.

149 R. G. Su, J. M. Lin, Q. Feng, Y. H. Gao, and Z. F. Chen, *Acta Chimica Sinica*, 2003, **61**, 885.

150 Y. C. Xu, B. Vaidya, A. B. Patel, S. M. Ford, R. L. McCarley, and S. A. Soper, *Analytical Chemistry*, 2003, **75**, 2975.

151 B. F. Liu, M. Ozaki, Y. Utsumi, T. Hattori, and S. Terabe, *Analytical Chemistry*, 2003, **75**, 36.

152 X. J. Huang, Q. S. Pu, and Z. L. Fang, *Analyst*, 2001, **126**, 281.

153 X. Y. Huang, J. N. Wang, L. Chen, and J. C. Ren, *Chinese Chemical Letters*, 2004, **15**, 683.

154 E. Tyrrell, C. Gibson, B. D. MacCraith, D. Gray, P. Byrne, N. Kent, C. Burke, and B. Paull, *Lab On A Chip*, 2004, **4**, 384.

155 A. M. Jorgensen, K. B. Mogensen, J. P. Kutter, and O. Geschke, *Sensors and Actuators B-Chemical*, 2003, **90**, 15.

156 A. M. Garcia-Campana and W. R. G. Baeyens, 'Chemiluminescence in Analytical Chemistry', Marcel Dekker, 2001

157 A. M. Garcia-Campana, W. R. G. Baeyens, L. Cuadros-Rodriguez, F. A. Barrero, J. M. Bosque-Sendra, and L. Gamiz-Gracia, *Current Organic Chemistry*, 2002, **6**, 1.

158 H. O. Albrecht, *Zeitschrift für Physikalische Chemie*, 1928, **136**, 321.

159 R. G. Su, J. M. Lin, F. Qu, Z. F. Chen, Y. H. Gao, and M. Yamada, *Analytica Chimica Acta*, 2004, **508**, 11.

160 M. Hashimoto, K. Tsukagoshi, R. Nakajima, K. Kondo, and A. Arai, *Journal of Chromatography A*, 2000, **867**, 271.

161 P. A. Greenwood, C. Merrin, T. McCreedy, and G. M. Greenway, *Talanta*, 2002, **56**, 539.

162 Z. R. Xu and Z. L. Fang, *Analytica Chimica Acta*, 2004, **507**, 129.

163 Y. Lv, Z. J. Zhang, and F. A. Chen, *Talanta*, 2003, **59**, 571.

164 Y. Lv, Z. J. Zhang, and F. N. Chen, *Analyst*, 2002, **127**, 1176.

165 A. K. Campbell, 'Chemiluminescence. Principles and Applications in Biology and Medicine', Ellis Horwood/CVH, Chichester, 1998.

166 *For more information see www.Hamamatsu.com.*

167 P. Fletcher, K. N. Andrew, A. C. Calokerinos, S. Forbes, and P. J. Worsfold, *Luminescence*, 2001, **16**, 1.

168 A. S. Carretero, J. R. Fernandez, A. R. Bowie, and P. J. Worsfold, *Analyst*, 2000, **125**, 387.

169 *For more information see www.Hull.ac.uk/chemistry/microfabrication.*

170 'Immobilized biomolecules in analysis : a practical approach', T. Cass and F. S. Ligler, Oxford University Press, Oxford, UK, 1998.

171 H. Andersson, W. van der Wijngaart, P. Enoksson, and G. Stemme, *Sensors And Actuators B-Chemical*, 2000, **67**, 203.

172 K. Sato, M. Tokeshi, T. Odake, H. Kimura, T. Ooi, M. Nakao, and T. Kitamori, *Analytical Chemistry*, 2000, **72**, 1144.

173 T. Richter, L. L. Shultz-Lockyear, R. D. Oleschuk, U. Bilitewski, and D. J. Harrison, *Sensors and Actuators B-Chemical*, 2002, **81**, 369.

174 L. Ceriotti, N. F. de Rooij, and E. Verpoorte, *Analytical Chemistry*, 2002, **74**, 639.

175 H. Andersson, C. Jonsson, C. Moberg, and G. Stemme, *Talanta*, 2002, **56**, 301.

176 H. Nakamura, R. Yamazaki, T. Shirai, H. Sano, Y. Nakami, K. Ikebukuro, K. Yano, Y. Nomura, Y. Arikawa, Y. Hasebe, Y. Masuda, and I. Karube, *Analytica Chimica Acta*, 2004, **518**, 45.

177 F. Xiang, Y. H. Lin, J. Wen, D. W. Matson, and R. D. Smith, *Analytical Chemistry*, 1999, **71**, 1485.

178 S. S. Park, S. I. Cho, M. S. Kim, Y. K. Kim, and B. G. Kim, *Electrophoresis*, 2003, **24**, 200.

179 B. He, N. Tait, and F. Regnier, *Analytical Chemistry*, 1998, **70**, 3790.

180 W. Zhan, G. H. Seong, and R. M. Crooks, *Analytical Chemistry*, 2002, **74**, 4647.

181 G. H. Seong, J. Heo, and R. M. Crooks, *Analytical Chemistry*, 2003, **75**, 3161.

182 N. Kiba, T. Tokizawa, S. Kato, M. Tachibana, K. Tani, H. Koizumi, M. Edo, and E. Yonezawa, *Analytical Sciences: The International Journal Of The Japan Society For Analytical Chemistry*, 2003, **19**, 823.

183 A. M. Tan, S. Benetton, and J. D. Henion, *Analytical Chemistry*, 2003, **75**, 5504.

184 T. Rohr, C. Yu, M. H. Davey, F. Svec, and J. M. J. Frechet, *Electrophoresis*, 2001, **22**, 3959.

185 D. J. Throckmorton, T. J. Shepodd, and A. K. Singh, *Analytical Chemistry*, 2002, **74**, 784.

186 J. G. Calvert, Lazarus, A., Kok, G.L., Heikes, B.G., Walega, J.G., Lind, J. and Cantrell, C.A., *Nature*, 1985, **317**, 27.

187 J. G. Calvert and W. R. Stockwell, *Environmental Science and Technology*, 1983, **17**, 428.

188 Y. W. Deng and Y. G. Zuo, *Atmospheric Environment*, 1999, **33**, 1469.

189 D. W. Gunz and M. R. Hoffmann, *Atmospheric Environment Part A-General Topics*, 1990, **24**, 1601.

190 D. Price, P. J. Worsfold, and R. F. C. Mantoura, *Trac-Trends In Analytical Chemistry*, 1992, **11**, 379.

191 V. Ortiz, M. A. Rubio, and E. A. Lissi, *Atmospheric Environment*, 2000, **34**, 1139.

192 P. A. Tanner and A. Y. S. Wong, *Analytica Chimica Acta*, 1998, **370**, 279.

193 V. Lvovich and A. Scheeline, *Analytical Chemistry*, 1997, **69**, 454.

194 L. S. Zhang and G. T. F. Wong, *Talanta*, 1994, **41**, 1853.

195 D. Price, R. Fauzi, C. Mantoura, and P. J. Worsfold, *Analytica Chimica Acta*, 1998, **377**, 145.

196 D. Price, R. Fauzi, C. Mantoura, and P. J. Worsfold, *Analytica Chimica Acta*, 1998, **371**, 205.

197 D. Price, P. J. Worsfold, and R. F. C. Mantoura, *Analytica Chimica Acta*, 1994, **298**, 121.

198 J. C. Yuan and A. M. Shiller, *Analytical Chemistry*, 1999, **71**, 1975.

199 J. C. Yuan and A. M. Shiller, *Atmospheric Environment*, 2000, **34**, 3973.

200 R. Escobar, S. Garcia-Dominguez, A. Guiraum, O. Montes, F. Galvan, and F. F. de la Rosa, *Luminescence*, 2000, **15**, 131.

201 Y. Zhou, T. Nagaoka, F. Li, and G. Zhu, *Talanta*, 1999, **48**, 461.

202 Q. L. Ma, H. M. Ma, Z. H. Wang, M. H. Su, H. Z. Xiao, and S. C. Liang, *Talanta*, 2001, **53**, 983.

203 J.-M. Lin, H. Arakawa, and M. Yamada, *Analytica Chimica Acta*, 1998, **371**, 171.

204 D. Janasek, U. Spohn, and D. Beckmann, *Sensors and Actuators B-Chemical*, 1998, **51**, 107.

205 W. Qin, Z. J. Zhang, and H. H. Chen, *International Journal of Environmental Analytical Chemistry*, 1997, **66**, 191.

206 W. Qin, Z. J. Zhang, B. X. Li, and S. N. Liu, *Analytica Chimica Acta*, 1998, **372**, 357.

207 S. Hanaoka, J. M. Lin, and M. Yamada, *Analytica Chimica Acta*, 2001, **426**, 57.

208 A. N. Diaz, M. C. R. Peinado, and M. C. T. Minguez, *Analytica Chimica Acta*, 1998, **363**, 221.

209 B. X. Li, Z. J. Zhang, and Y. Jin, *Sensors and Actuators B-Chemical*, 2001, **72**, 115.

210 G. J. Zhou, G. Wang, J. J. Xu, and H. Y. Chen, *Sensors and Actuators B-Chemical*, 2002, **81**, 334.

211 K. Hool and T. A. Nieman, *Analytical Chemistry*, 1987, **59**, 869.

212 K. Hool and T. A. Nieman, *Analytical Chemistry*, 1988, **60**, 834.

213 N. M. Rao, K. Hool, and T. A. Nieman, *Analytica Chimica Acta*, 1992, **266**, 279.

214 K. E. Sawcer, A. T. Bodley-Tickell, S. E. Kitchen, A. P. Sturdee, and G. H. G. Thorpe, *Water Environment Research*, 2000, **72**, 22.

215 E. H. White and M. M. Bursey, *Journal of the American Chemical Society*, 1964, **86**, 941.

216 E. H. White, O. C. Zafiriou, H. H. Kagi, and J. H. M. Hill, *Journal of the American Chemical Society*, 1964, **86**, 940.

217 G. Merenyi and J. S. Lind, *Journal Of The American Chemical Society*, 1980. **102**, 5830.

218 G. Merenyi, J. Lind, and T. E. Eriksen, *Journal Of Physical Chemistry*, 1984, **88**, 2320.

219 G. Merenyi, J. Lind, and T. E. Eriksen, *Photochemistry and Photobiology*, 1985, **41**, 203.

220 G. Merenyi and J. Lind, *Journal of Bioluminescence and Chemiluminescence*, 1988, **2**, 234.

221 G. Merenyi, J. Lind, and T. E. Eriksen, *Journal of Bioluminescence and Chemiluminescence*, 1990, **5**, 53.

222 W. Quintero-Betancourt, E. R. Peele, and J. B. Rose, *Journal of Microbiological Methods*, 2002, **49**, 209.

223 A. I. Vogel, 'Textbook of quantitative chemical analysis', Longman, Harlow, 1989, 5.

224 Y. Saito, J. J. Wang, D. N. Batchelder, and D. A. Smith, *Langmuir*, 2003, **19**, 6857.

225 J. C. Guo, J. N. Miller, M. Evans, and D. A. Palmer, *Analyst*, 2000, **125**, 1707.

226 L. C. Shriver-Lake, W. B. Gammeter, S. S. Bang, and M. Pazirandeh, *Analytica Chimica Acta*, 2002, **470**, 71.

227 R. M. Maier, I. L. Pepper, and C. P. Gerba, 'Environmetal Microbiology', Academic Press, San Diego, USA, 2000.

228 *For more information see www.environment-agency.gov.uk.*

229 K. Geissler, M. Manafi, I. Amoros, and J. L. Alonso, *Journal Of Applied Microbiology*, 2000, **88**, 280.

230 G. R. Campbell, J. Prosser, A. Glover, and K. Killham, *Journal Of Applied Microbiology*, 2001, **91**, 1004.

231 X. L. Su and Y. B. Li, *Biosensors & Bioelectronics*, 2004, **19**, 563.

232 'Immunoassays : a practical approach', J. P. Gosling, Oxford University Press, Oxford, 2000.

233 I. Roitt, J. Brostoff, and D. Male, 'Immunology', Mosby, Edinburgh, 2001, 6.

234 C. A. Marquette, P. R. Coulet, and L. J. Blum, *Analytica Chimica Acta*, 1999, **398**, 173.

235 S. D. Mangru and D. J. Harrison, *Electrophoresis*, 1998, **19**, 2301.

236 A. N. Diaz, F. G. Sanchez, and J. A. G. Garcia, *Analytica Chimica Acta*, 1996, **327**, 161.

237 T. P. Whitehead, G. H. G. Thorpe, T. J. N. Carter, C. Groucutt, and L. J. Kricka, *Nature*, 1983, **305**, 158.

238 J. X. Luo and X. C. Yang, *Analytica Chimica Acta*, 2003, **485**, 57.

239 M. Badea, L. Micheli, M. C. Messia, T. Candigliota, E. Marconi, T. Mottram, M. Velasco-Garcia, D. Moscone, and G. Palleschi, *Analytica Chimica Acta*, 2004, **520**, 141.

240 J. H. Lin, F. Yan, and H. X. Ju, *Applied Biochemistry And Biotechnology*, 2004, **117**, 93.

241 J. M. Lin, A. Tsuji, and M. Maeda, *Analytica Chimica Acta*, 1997, **339**, 139.

242 M. A. GonzalezMartinez, S. Morais, R. Puchades, A. Maquieira, A. Abad, and A. Montoya, *Analytica Chimica Acta*, 1997. **347**, 199.

243 J. H. Lin, F. Yan, and H. X. Ju, *Clinica Chimica Acta*, 2004, **341**. 109.

244 D. Dreveny, J. Michalowski, R. Seidl, G. Gubitz, and Analyst, 1998, **123**, 2271.

245 P. Fernandez, J. S. Durand, C. Perez-Conde, and G. Paniagua, *Analytical and Bioanalytical Chemistry*, 2003, **375**, 1020.

246 R. M. Garcinuno, P. Fernandez, C. Perez-Conde, A. M. Gutierrez, and C. Camara, *Talanta*, 2000, **52**, 825.

247 I. M. Ciumasu, P. M. Kramer, C. M. Weber, G. Kolb, D. Tiemann, S. Windisch, I. Frese, and A. A. Kettrup, *Biosensors & Bioelectronics*, 2005, **21**, 354.

248 M. A. Gonzalez-Martinez, R. Puchades, and A. Maquieira, *Trac-Trends in Analytical Chemistry*, 1999, **18**, 204.

249 N. Soh, H. Nishiyama, Y. Asano, T. Imato, T. Masadome, and Y. Kurokawa, *Talanta*, 2004, **64**, 1160.

250 I. Safarik and M. Safarikova, *Journal Of Chromatography B*, 1999, **722**, 33.

251 C. M. Ruan, L. J. Yang, and Y. B. Li, *Analytical Chemistry*, 2002, **74**, 4814.

252 S. M. Radke and E. C. Alocilja, *Ieee Sensors Journal*, 2004, **4**, 434.

253 J. J. Gau, E. H. Lan, B. Dunn, C. M. Ho, and J. C. S. Woo, *Biosensors & Bioelectronics*, 2001, **16**, 745.

254 C. Ruan, H. Wang, and Y. Li, *Transactions Of The Asae*, 2002, **45**, 249.

255 F. G. Perez, M. Mascini, I. E. Tothill, and A. P. F. Turner, *Analytical Chemistry*, 1998, **70**, 2380.

256 I. Abdel-Hamid, D. Ivnitski, P. Atanasov, and E. Wilkins, *Analytica Chimica Acta*, 1999, **399**, 99.

257 I. H. Boyaci, Z. P. Aguilar, M. Hossain, H. B. Halsall, C. J. Seliskar, and W. R. Heineman, *Analytical And Bioanalytical Chemistry*, 2005, **382**, 1234.

258 A. S. Mittelmann, E. Z. Ron, and J. Rishpon, *Analytical Chemistry*, 2002, **74**, 903.

259 R. S. Mazenko, F. Rieders, and J. D. Brewster, *Journal of Microbiological Methods*, 1999, **36**, 157.

260 P. Ertl and S. R. Mikkelsen, *Analytical Chemistry*, 2001, **73**, 4241.

261 V. Casimiri and C. Burstein, *Analytica Chimica Acta*, 1998, **361**, 45.

262 J. Guan and R. E. Levin, *Food Biotechnology*, 2002, **16**, 135.

263 E. Howe and G. Harding, *Biosensors & Bioelectronics*, 2000, **15**, 641.

264 J. C. Pyun, H. Beutel, J. U. Meyer, and H. H. Ruf, *Biosensors & Bioelectronics*, 1998, **13**, 839.

265 C. M. Ruan, K. F. Zeng, O. K. Varghese, and C. A. Grimes, *Analytical Chemistry*, 2003, **75**, 6494.

266 E. S. Delpassand, M. V. Chari, C. E. Stager, J. D. Morrisett, J. J. Ford, and M. Romazi, *Journal Of Clinical Microbiology*, 1995, **33**, 1258.

267 A. J. Madonna, S. Van Cuyk, and K. J. Voorhees, *Rapid Communications In Mass Spectrometry*, 2003, **17**, 257.

268 E. W. Frampton and L. Restaino, *Journal of Applied Bacteriology*, 1993, **74**, 223.

269 D. L. Stokes, G. D. Griffin, and V. D. Tuan, *Fresenius Journal of Analytical Chemistry*, 2001, **369**, 295.

270 Y. C. Liu, C. M. Wang, and K. P. Hsiung, *Analytical Biochemistry*, 2001, **299**, 130.

271 Y. C. Liu and Y. B. Li, *Journal Of Microbiological Methods*, 2002, **51**, 369.

272   T. B. Tims and D. V. Lim, *Journal Of Microbiological Methods*, 2003, **55**, 141.

273   A. M. Prescott and C. R. Fricker, *Molecular And Cellular Probes*, 1999, **13**, 261.

274   A. G. Gehring, D. L. Patterson, and S. I. Tu, *Analytical Biochemistry*, 1998, **258**, 293.

275   S. I. Tu, J. Uknalis, and A. Gehring, *Journal Of Rapid Methods And Automation In Microbiology*, 1999, **7**, 69.

276   S. I. Tu, J. Uknalis, M. Gore, and P. Irwin, *Journal of Rapid Methods and Automation in Microbiology*, 2002, **10**, 185.

277   P. Bouvrette, J. H. T. Luong, and I. J. o. F. Microbiology, 1995, **27**, 129.

278   H. Yu, *Analytica Chimica Acta*, 1998, **376**, 77.

279   J. M. Song and T. Vo-Dinh, *Analytica Chimica Acta*, 2004, **507**, 115.

280   Y. C. Liu, J. M. Ye, and Y. B. Li, *Journal Of Food Protection*, 2003, **66**, 512.

281   J. Ye, Y. Liu, and Y. Li, *Transactions of the Asae*, 2002, **45**, 473.

282   S. I. Tu, D. Patterson, J. Uknalis, and P. Irwin, *Food Research International*, 2000, **33**, 375.

283   C. C. Wang, W. S. Li, S. K. Cheng, C. Y. Chen, and J. F. Kuo, *Journal of Applied Polymer Science*, 2001, **82**, 3248.

284   M. G. Roper, J. G. Shackman, G. M. Dahlgren, and R. T. Kennedy, *Analytical Chemistry*, 2003, **75**, 4711.

285   S. Cesaro-Tadic, G. Dernick, D. Juncker, G. Buurman, H. Kropshofer, B. Michel, C. Fattinger, and E. Delamarche, *Lab On A Chip*, 2004, **4**, 563.

286   A. Dodge, K. Fluri, E. Verpoorte, and N. F. de Rooij, *Analytical Chemistry*, 2001, **73**, 3400.

287   Y. L. Gao, F. Y. Lin, G. Q. Hu, P. A. Sherman, and D. Q. Li, *Analytica Chimica Acta*, 2005, **543**, 109.

288   O. Hofmann, G. Voirin, P. Niedermann, and A. Manz, *Analytical Chemistry*, 2002, **74**, 5243.

289   K. S. Phillips and Q. Cheng, *Analytical Chemistry*, 2005, **77**, 327.

290   D. Juncker, B. Michel, P. Hunziker, and E. Delamarche, *Biosensors & Bioelectronics*, 2004, **19**, 1193.

291   K. S. Kim and J. K. Park, *Lab On A Chip*, 2005, **5**, 657.

292   M. A. Hayes, N. A. Polson, A. N. Phayre, and A. A. Garcia, *Analytical Chemistry*, 2001, **73**, 5896.

293   A. Bromberg and R. A. Mathies, *Analytical Chemistry*, 2003, **75**, 1188.

294   F. Y. H. Lin, M. Sabri, D. Erickson, J. Alirezaie, D. Q. Li, and P. M. Sherman, *Analyst*, 2004, **129**, 823.

295   C. X. Luo, Q. Fu, H. Li, L. P. Xu, M. H. Sun, Q. Ouyang, Y. Chen, and H. Ji, *Lab On A Chip*, 2005, **5**, 726.

296   N. Pamme, R. Koyama, and A. Manz, *Lab On A Chip*, 2003, **3**, 187.

297   J. Yakovleva, R. Davidsson, A. Lobanova, M. Bengtsson, S. Eremin, T. Laurell, and J. Emneus, *Analytical Chemistry*, 2002, **74**, 2994.

298   J. Yakovleva, R. Davidsson, M. Bengtsson, T. Laurell, and J. Emneus, *Biosensors & Bioelectronics*, 2003, **19**, 21.

299   'Encyclopedia of analytical science', A. Townshend, Academic Press, London, 1995.

300   M. Franek, A. P. Deng, V. Kolar, and A. C. Acta, 2000, **412**, 19.

301   P. A. Chapman and R. Ashton, *International Journal of Food Microbiology*, 2003, **87**, 279.

302   M. T. W. Hearn, G. S. Bethell, J. S. Ayers, and W. S. Hancock, *Journal Of Chromatography*, 1979, **185**, 463.

303   I. H. Lee and M. E. Meyerhoff, *Analytica Chimica Acta*, 1990, **229**, 47.

Appendix I

APPENDIX 1

Publications

Leanne Marle and Gillian M. Greenway, "Microfluidic devices for environmental monitoring." *TrAC Trends in Analytical Chemistry*, 2005, **24**, 795.

Leanne Marle and Gillian M. Greenway, "Determination of hydrogen peroxide in rainwater in a miniaturised analytical system." *Analytica Chimica Acta*, 2005, **548**, 20.

Presentations

Poster: *"Chemiluminescence for environmental monitoring"*, Analytical Research Forum, Royal Society of Chemistry, University of Sunderland, July 2003.

Poster: *"Portable microfluidic systems for water monitoring"*, Analytical Research Forum, Royal Society of Chemistry, University of Central Lancashire, Preston, July 2004.

Poster: *"Miniaturised portable devices for water monitoring"*, "PITTCON", The Pittsburgh Conference on Analytical Chemistry and Applied Spectroscopy, Spectroscopy Society of Pittsburgh (SSP) and the Society for Analytical Chemists of Pittsburgh (SACP), Orange County Convention Center, Orlando, Florida, February 2005.

Poster: *"Miniaturised portable devices for water monitoring"*, Analytical Research Forum, Royal Society of Chemistry, University of Plymouth, July 2005.